Enzymology of Isolated Functional Domains from Iterative Fungal Polyketide Synthases

Von der Naturwissenschaftlichen Fakultät der Gottfried Wilhelm Leibniz Universität Hannover

zur Erlangung des Grades

Doktor der Naturwissenschaften (Dr. rer. nat.)

genehmigte Dissertation von

Christoph Bartel, M. Sc.

[2017]

Referent: Professor Russell J. Cox, PhD.

Korefferent: Professor Dr. Andreas Kirschning

Tag der Promotion: 24.05.2017

Kurzzusammenfassung

Enzymatische Untersuchungen von isolierten funktionellen Domänen aus iterativen Pilz-Polyketidsynthasen

Der von Pilzen hergestellte Naturstoff Squalestatin S1 wird von zwei verschiedenen iterativen Polyketidsynthasen erzeugt, einer Hexaketidsynthase (SQHKS) und einer Tetraketidsynthase (SQTKS).

Der Fokus dieser Arbeit liegt auf der chemischen und biologischen Untersuchung der isolierten Dehydratase (DH) und Enoylreduktase (ER) von SQTKS. Die Untersuchungen der ER konzentrierte sich auf eine mögliche Programmierung des Enzyms. Hierzu wurden verschiedene Moleküle synthetisiert, mit denen das Enzym untersucht wurde. Es wurde erwartet, dass diese Programmierung von anderen katalytischen Domänen, die in SQTKS involviert sind, unabhängig ist. Um diese Hypothese zu prüfen wurden mehrere Pantetheinverbindungen synthetisiert und in *in vitro* Versuchen getestet. Die Pantethein-verbindungen imitierten verschiedene Zwischenprodukte der ER und das Endprodukt von SQTKS. In dieser Untersuchung war es möglich, Informationen über die Selektivität und Inhibierung des Enzyms zu erhalten. Für die Messung von kinetischen Daten wurde eine neue Analysemethode entwickelt.

Für die Untersuchung der DH von SQTKS wurde das erste natürliche Substrat als Pantetheinverbindung synthetisiert und ebenfalls in einem *in vitro* Versuch bezüglich seiner Aktivität und Kinetik getestet. Für analytische und kinetische Messungen wurden die Methoden LCMS und UV-Spektroskopie verwendet. Eine mögliche Inhibierung der DH wurde ebenfalls getestet und analysiert.

In einem weiteren Projekt wurde die mögliche Interaktion der isolierten ER und DH untersucht. Hierzu wurden verschiedene Methoden (SPR, ITC) verwendet. Außerdem wurden Wechselwirkungen mit Substraten geprüft, die Zwischenprodukte anderer Domänen von SQTKS nachahmten. Die Oberfläche von SPR-Chips wurde mit diesen Substraten modifiziert und mit den isolierten Enzymen gespült. Auf diese Weise konnten Interaktionen von verschiedenen Substraten mit der ER oder der DH gemessen werden.

Im letzten Projekt wurde die Selektivität einer Acyl-Transferase (AT) untersucht, die im letzten Schritt der Squalestatinbiosynthese aktiv ist. Hierzu wurden verschiedene Vorstufen von Squalestatin S1, sowie verschiedene Reaktionspartner hydrolysiert. Die enzymatische Untersuchung und die Synthese von neuen Squalestatinderivaten bilden den Abschluss dieser Doktorarbeit.

Abstract

Enzymology of Isolated Functional Domains from Iterative Fungal Polyketide Synthases

The fungal secondary metabolite Squalestin S1 is produced by two different highly reducing iterative polyketide synthases (HR-iPKS), a hexaketide (SQHKS) and a tetraketide (SQTKS) synthase. The main investigation of this thesis is focussed on the chemical selectivity of the isolated dehydratase (DH) and enoyl reductase (ER) domains of SQTKS. The isolation of these domains was performed in previous work.

Investigations of the ER domain focused on possible mechanisms of programming. This programming was expected to be independent of other catalytic domains involved in SQTKS. To test this hypothesis several pantetheine substrates were synthesized and tested *in vitro*. Pantetheine substrates should mimic intermediates and the final product, squalestatin tetraketide, of SQTKS. In this investigation, it was possible to get information about the selectivity and inhibition of the enzyme. A new analysis method was developed to measure kinetic data.

In further investigation the DH domain of SQTKS was investigated. The first natural substrate was synthesized as a pantetheine compound and activity of the enzyme was tested *in vitro*. Analysis methods by LCMS and UV were performed to measure kinetic data. Inhibition assays of the DH domain similar to the ER domain were tested and analysed.

In the next project interactions of the isolated ER domain and DH domain with each other were tested. Also, interactions with substrates that mimic intermediates of other domains of SQTKS were investigated. A synthesis was developed to create pantetheine glycine substrates which were used to modify analytical chips for use in surface plasmon resonance (SPR) to develop a standard protocol to measure protein-substrate interactions. The results of this investigation showed that the DH and ER domain are not specifiic to the known chemical motifs and can also interact with other chemical motifs which are substrates for keto-reductase (KR) or C-methyltransferase (*C*-MeT) domains.

Finally the selectivity of an acyl transferase (AT) enzyme which acts as the last step of squalestatin biosynthesis was investigated using various squalestatin precursors synthesised by degradation of squalestatin S1 itself. This allowed the synthesis of new squalestatin analogues.

Schlagwörter:

1. Enzymkinetik
2. Pantetheinsubstrate
3. Isolierte Enzyme
4. Enzymology
5. Kinetic Investigation
6. Surface Plasmon Resonance Spectroscopy

Contents

Abbrevations and Units

ACP	Acyl carrier protein
AT	Acyl-transferase
BSA	Bovine serum albumin
CDI	*N, N'*-carbonyldiimidazole
DCM	Dichloromethane
C-MeT	*C*-Methyltrasferase
CoA	Coenzyme A
COSY	Correlation spectroscopy
Da	Dalton
DH	Dehydratase
DMAP	4-Dimethylaminopyridine
DTT	Dithiothreitol
EDCI	1-Ethyl-3-(3-dimethylaminopropyl) carbodiimide
ER	Enoyl reductase
FAS	Fatty acid synthase
His-tag	Histidine tag
HMBC	Heteronuclear multiple bond correlation
HSQC	Heteronuclear single quantum correlation
HPLC	High performance liquid chromatography
HRMS	High resolution mass spectrometry
IPTG	Isopropyl β-D-1-thiogalactopyranoside
K_M	Michaelis-Menten constant
KR	β-Ketoacyl reductase
KS	Ketosynthase
LC	Liquid chromatography
LCMS	Liquid chromatography mass spectrometry
MS	Mass spectrometry
NAC	*N*-Acetylcysteamine
NADPH	Nicotinamide adenine dinucleotide phosphate
NMR	Nuclear magnetic resonance
PANT	Pantetheine
PCC	Pyridinium chlorochromate
PCR	Polymerase chain reaction

PKS	Polyketide synthase
ppm	Parts per million
SNAC	S-*N*-acetyl cysteamine
SQTKS	Squalestatin tetraketide synthase
TE	Thiolesterase
TFA	Trifluoro acetic acid
THF	Tetrahydrofuran
UV	Ultra violet
V_{Max}	Maximum rate of a reaction

1. Introduction

Polyketides are one of the major groups of natural products. They are not essential for their producers and classified as secondary metabolites. Producers of polyketides are bacteria, fungi and plants.[1] The functions of many of these compounds are currently unknown. However, since polyketides occur widely it is assumed that they give their hosts some advantage. It is hypothesised that these compounds are used for defence against other organisms or as signal substances for communication with other organisms. They might have an advantage as effect to get new living environment for example.[1]

Polyketides have a high structural diversity. They include aliphatic, cyclic, acyclic, and aromatic compounds and macrocyclic lactones. The structural diversity of these compounds is the reason for their biological activity. Representative examples are tetracycline **1** and erythromycin B **2** (Figure 1).[1-2]
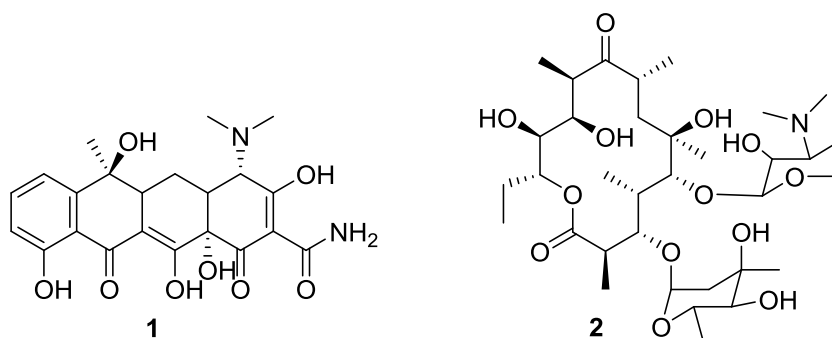
Figure 1: Structure of tetracycline **1** and erythromycin B **2**.

1 is an antibiotic isolated from *Streptomyces aureofaciens* that is used against Gram negative and Gram positive bacteria.[3-5] **2** was first isolated from *Streptomyces erythreus*. In contrast to **1**, **2** is only active against Gram positive bacteria. It is used against bacteria that have a resistance against β-lactam antibiotics and is used as a replacement for penicillin.[6] Other polyketides are known that are candidates for use as antiparasitic, antifungal and cholesterol lowering drugs.[7-8]

The reason for the diversity of polyketides is their different functionalization. Despite their chemical diversity all polyketides are produced by enzymes known as polyketide synthases (PKS). The PKS are encoded by genes, and usually PKS genes are found clustered in the genome with genes which encode enzymes which perform post-PKS modification of the polyketide.[9,10] These are known as *tailoring* steps.

1.1 Biosynthesis of Polyketides

Polyketides and fatty acids are biosynthesised in the same way. Both are built by megasynthases composed of several different catalytic enzymes. The structural diversity of polyketides is a result of the programming of the megasynthases. A polyketide is formed by a PKS, which is responsible for forming a backbone of carbon atoms. The starter unit in most cases is acetyl CoA **3**, although other starter units are known. More uncommon starter units are propionyl CoA **4** and benzoyl CoA **5** (Figure 2).[11,12,13]
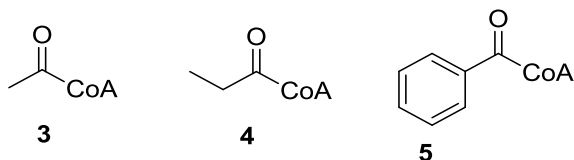
Figure 2: Starter units of a PKS.

PKS consists of several catalytic enzymes or domains.[11,12,13] Most PKS have an acyl transferase (AT), a ketosynthase (KS) and an acyl carrier protein (ACP). The KS performs the key carbon-carbon bond-forming reaction and is essential for all FAS and PKS. The process starts with the loading of a starter unit onto the KS domain (Scheme 1). For this the AT catalyses the reaction with an activated acyl unit, which is usually a CoA thiolester. The ACP has a phosphopantetheine group which is covalently bound to a strictly conserved serine residue. Acyl groups are bound as thiolesters to the terminal thiol of the phosphopantetheine.[11,12,13]
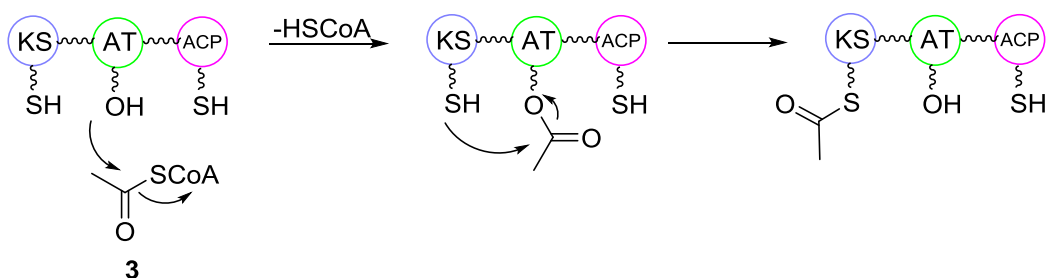
Scheme 1: Loading of the KS domain with the starter unit.

For elongation of the carbon chain, an extender unit is loaded onto the ACP. A typical extender unit for a PKS or FAS is malonyl CoA **6**. This process is also catalysed by the AT domain. The starter unit and the extender unit then react in a condensation reaction similar to a Claisen condensation by loss of carbon dioxide (Scheme 2).[14] This formation of the carbon-carbon bond is catalysed by the KS domain.[15,16]

The extension is performed with an inversion of the configuration at the malonyl carbon. In most cases this inversion is not directly observed since the extender unit is without substituent in the α-position (Scheme 2).[15,16]
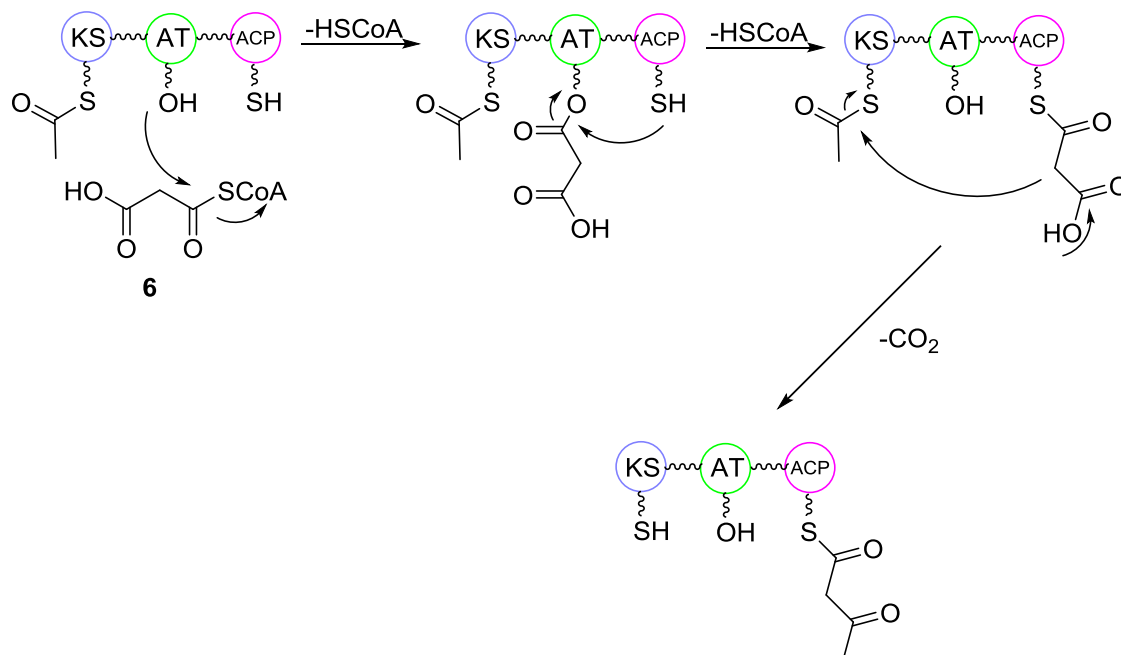
Scheme 2: Extension of the carbon chain without any modification.

After the chain extension it is now possible to modify the ACP-bound molecule by enzymatic reactions at the β-carbonyl. A different catalytic domain is responsible for each modification step. The modifying domains are the *C*-methyl transferase (*C*-MeT, not present in FAS), ketoreductase (KR), dehydratase (DH) and the enoyl reductase (ER, Scheme 3).[15] These reactions are known as the β-modification cycle. In FAS the cycle is always completed to give a β-methylene; but in PKS the cycle can be shortened.
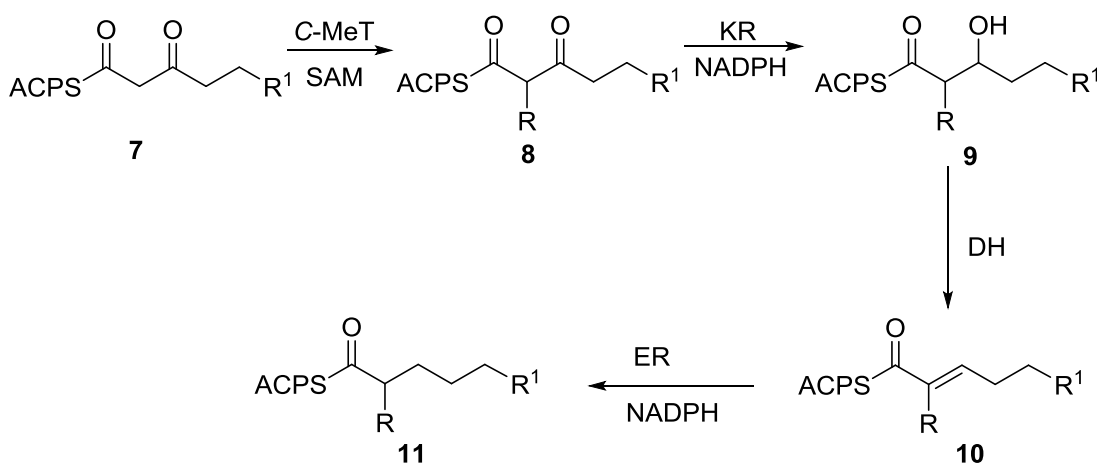
R= Me or H

Scheme 3: The β-modification cycle.

Nearly every functionalization requires a cofactor. In some fungal PKS the first modification of the carbon chain is catalysed by the *C*-methyltransferase (*C*-MeT). The *C*-MeT can transfer a methyl group to the acidic α-position of the polyketide. A deprotonation of this position results in an enolate, and a nucleophilic S_N2 reaction follows in which the α-carbon attacks the methyl group of *S*-adenosyl methionine (SAM) **12** (Figure 3). At the methylation stage, and in the two subsequent reductions, new stereocenters are formed, therefore *R*- and *S*-isomers of the different PKS intermediates are possible. The absolute configurations of the stereogenic centers are in some cases predicted by different amino acid residues of the active site of the protein.[17]

12
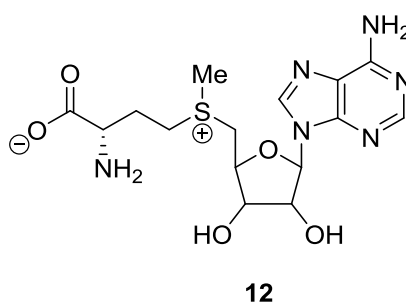
Figure 3: Known cofactor for methylation reactions: *S*-adenosyl methionine **12**.

The KR domain acts after the *C*-MeT and reduces the β-carbonyl moiety to a β-hydroxy intermediate. Cofactors that are used during this process are nicotinamide adenine dinucleotide (NADH) and nicotinamide adenine dinucleotide phosphate (NADPH) **13** (Figure 4). Both are known for a hydride transfer and can be used in the reduction step.[17]
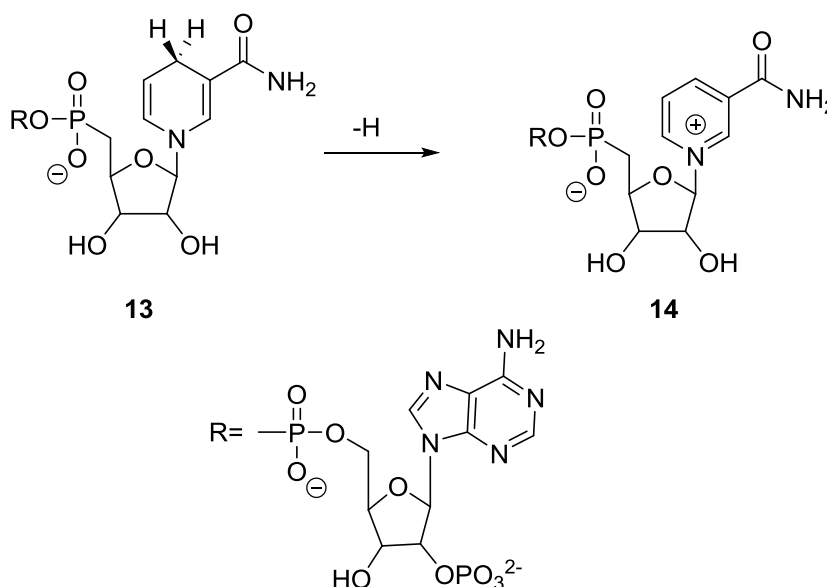
Figure 4: Essential structural part of NADH and NADPH **13**.

During the reduction two stereocenters are predicted by the KR domain; the carbonyl can be reduced stereoselectively to L-β-hydroxyl- or D-β-hydroxyl groups. The stereochemistry of substituents in the α-position is determined by the domain after the reduction. In total four different stereochemical outcomes are possible.[18,19,20]

The next modification step is performed by the DH domain which eliminates the β-hydroxyl group. Both configurations (*cis* and *trans*) of the resulting double bond are known. The stereochemical information that was introduced in the previous (KR) step is lost by this elimination.[21,22] Finally, reduction of the α–β olefin is catalysed by the ER domain. The carbon-carbon double bond is reduced in the presence of the cofactor NADPH **13**. The enzyme can introduce two new stereocenters similar to the KR domain.[22]

After each β-modification cycle the newly functionalised chain is passed back to the KS for further extension. Extensions and β-modifications are continued until the chain reaches its predetermined length. Finally, the elongated carbon chain is cleaved from the PKS. This is usually achieved by a thiolesterase (TE), although other types of release mechanisms, including reductive methods, are also known.[23,24] Intramolecular macrocyclisation is a common release mechanism. In this release an internal hydroxyl group or amino group performs the nucleophilic attack.[24] Examples are 10-deoxymethynolide **15** and narbonolide **16** (Figure 5) which are the precursors of the antibiotics methymycin and pikromycin respectively.[25,26]
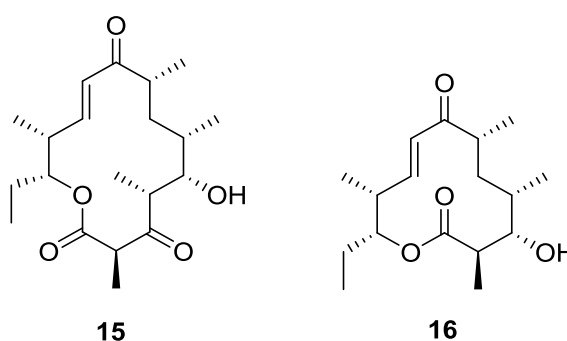
Figure 5: Structures of 10-deoxymethynolide **15** and narbonolide **16**.

The mechanism of TEs involves initial transfer of the polyketide to a catalytic serine residue to form an intermediate ester. This is then attacked either by water (to form a carboxylic acid), or by an internal nucleophile to form a macrocycle (Scheme 4).[26,27]
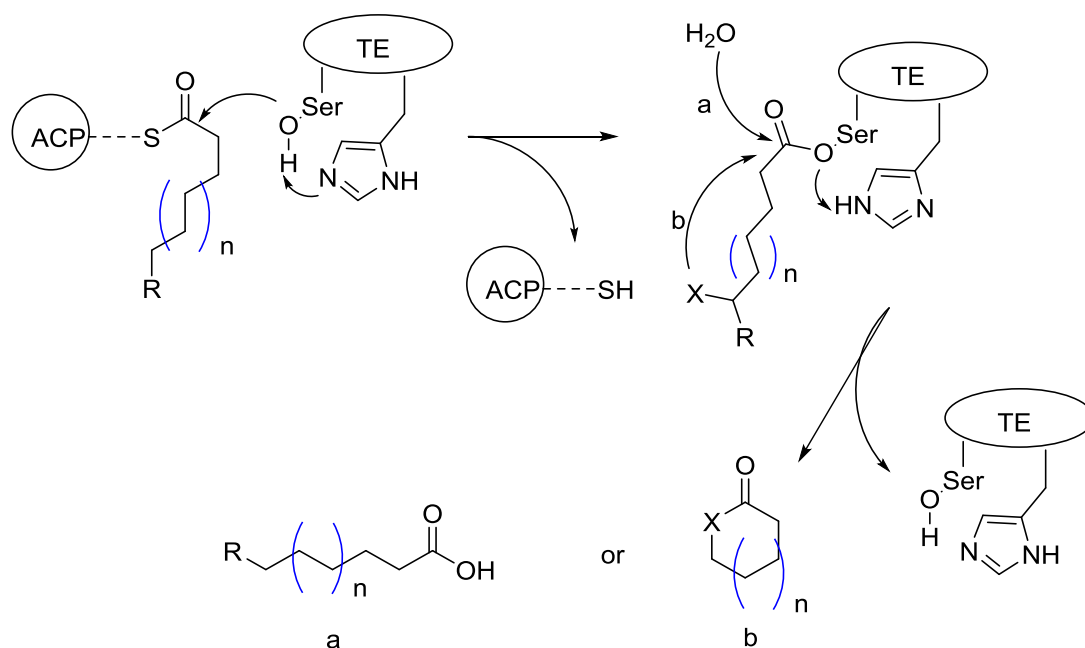
Scheme 4: Proposed mechanism of the thiolesterase.[27]

1.2   Architectures of FAS and PKS

The architecture of FAS is well studied, and some FAS molecules have been fully crystallized and investigated. Two architectures of FAS are known, and these are classified as Type I and Type II systems. In Type I systems the catalytic domains are covalently linked to form one or two very large single molecules. In Type II systems the catalytic domains are separate proteins, but it is very likely that they assemble via non-covalent interactions to form functional complexes which are similar to the Type I systems.[28]

Investigations of PKS structures are further behind the studies of FAS. It has not yet been possible to crystallize a complete PKS. Some single domains have been successfully crystallized and investigated. Compared with FAS the same domains, active residues, and cofactors are observed, and PKS are classified in the same way as FAS, into Type I and II systems.[21,28,29]

Type I PKS are found in bacteria and fungi. They consist of large multi domain megasynthases. The domains are covalently bound together.[1,30] Type I PKS usually form dimers. Type I PKS are further subdivided into iterative and modular types (see below for details). The iterative Type I PKS are further sub-divided into non reducing (NR-PKS), partially reducing (PR-PKS) and highly reducing PKS (HR-PKS) types. Modular Type I PKS can be broadly divided into *cis*-AT and *trans*-AT types.[2,11,31]

Type II PKS are mono domain enzymes that come together and form a non-covalent complex which functions iteratively. This complex consists of five to ten individual enzymes. The synthesized polyketides normally have a chain length of 16 to 24 carbons. In most cases the chain length is controlled by the KS domain. Different amino acid residues seem to be important for chain length control. Type II PKS have only been found in bacteria, to date.[32,33,34] A typical compound produced by a Type II PKS is actinorhodin **17** (Figure 6).[11]
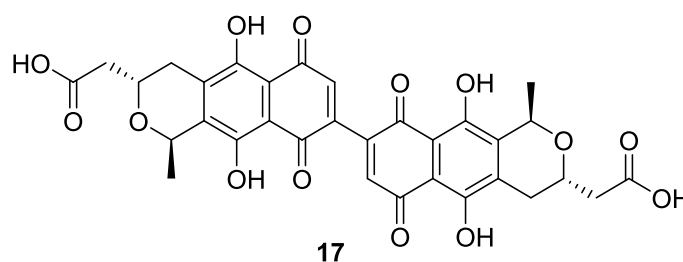
Figure 6: Structure of actinorhodin **17**.

Type III PKS are simple enzymes, an example is the chalcone synthase. Structurally this Type of PKS is completely independent from the other two forms. They are simple homodimers of ketosynthases that do not use an ACP or AT. They react directly with CoA-bound substrates in a decarboxylative Claisen condensation. Usually aromatic compounds like *p*-coumaroyl-CoA **18** are the starter units, but malonyl-CoA **6** can also be used as a starter unit. Type III PKS enzymes act in an iterative way and produce small aromatic metabolites like the chalcone **19** (Scheme 5) by a PKS Type III.[11,35,36]
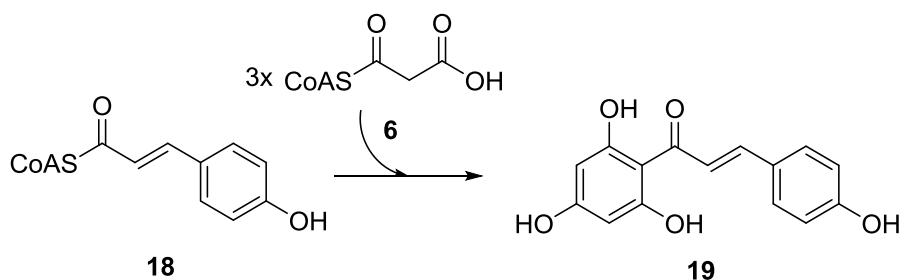
Scheme 5: Extension of like *p*-coumaroyl-CoA **18** by **6**.[36]

1.2.1 Modular Type I Polyketide Synthase

Modular PKS form an assembly line with several active *modules* (Scheme 6). A module contains all required extension and β-processing domains for a single round of biosynthesis. It is possible to read these mPKS like a book and to get all information about the several extension and reducing steps. One of the most investigated synthases

is the PKS of 6-Deoxyerythronolide B **20** (DEBS), the backbone of erythromycin B **2**.[37,38,39] DEBS has three large proteins (DEBS1- DEBS3) that can each be divided into two or three modules.
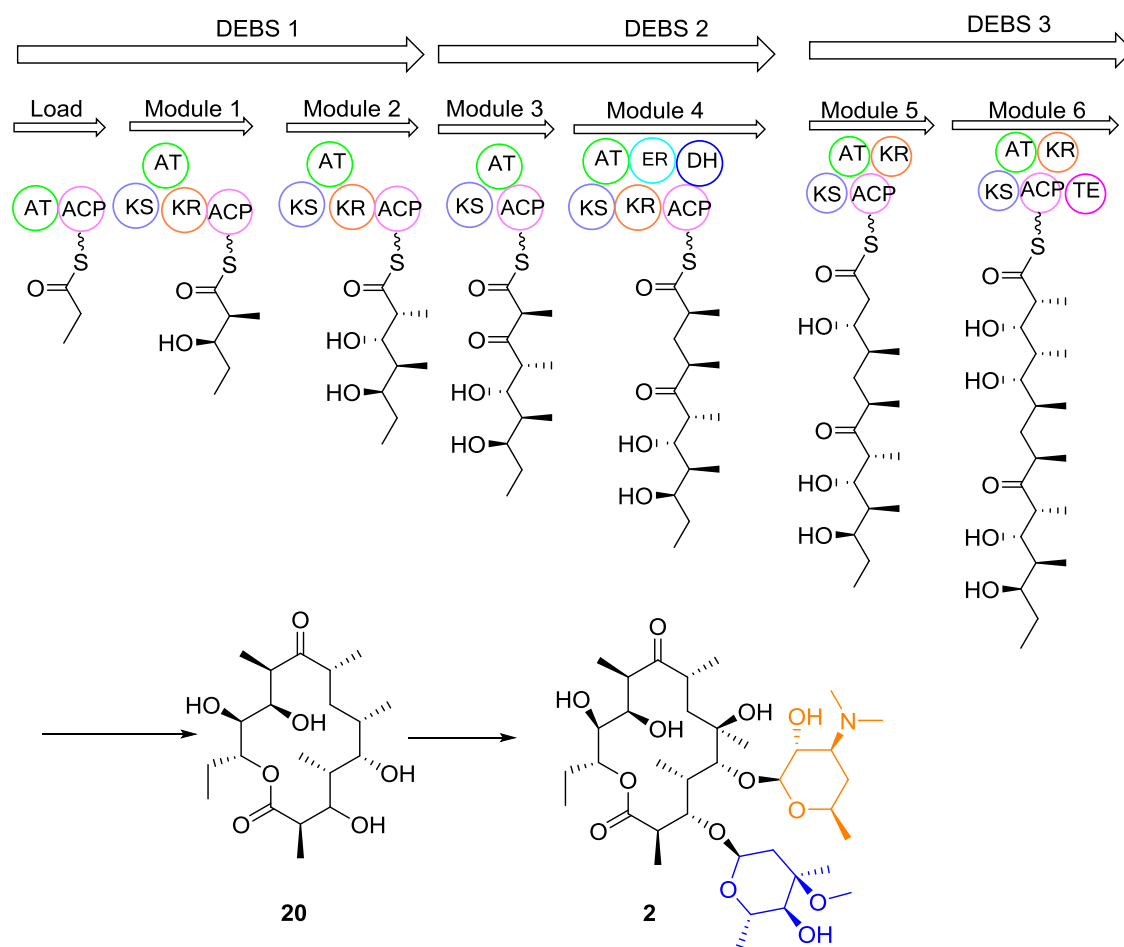
Scheme 6: Biosynthesis of 6-Deoxyerythronolid B **20** and erythromycin B **2**.

Each module has a certain set of domains that are responsible for the catalytic reactions. The starter unit propionyl CoA **4** is loaded onto the synthase by a specialised AT-ACP didomain which makes up the initial *loading module*. This is passed on to module 1 which loads a methyl malonyl extender unit (AT), catalyses carbon-carbon bond formation (KS) and then reduces the β-ketone (KR). As is usual, the intermediates are attached to the ACP.[37,38,39] The programming of β-processing is controlled by the presence or absence of β-processing domains in each module. Only DEBS module 4 has a complete set of domains to reduce the keto function to a methylene. The final module containes a thiolesterase which catalyses the release of the polyketide by formation of a macrocycle.[37,38,39] The observation that each module catalyses a single round of extension and β-processing which corresponds to a single 'ketide unit' of the product is known as the *colinearity rule*.[40]

After the polyketide is released from the PKS, post-PKS-modifications take place by hydroxylases, methyl-transferases and glycosyl transferases to form the final compound **2** which is an important member of the class of macrolide antibiotics.[41]

There are some modular PKS known that do not follow the co-linearity rule. For example the iterative use of modules during chain extension is known. Another form of mPKS uses *trans*-AT domains. In contrast to the integrated AT domains (Scheme 6) the AT domain is free standing (Scheme 7).[42,43]

"*cis*"-AT PKS   "*trans*"-AT PKS
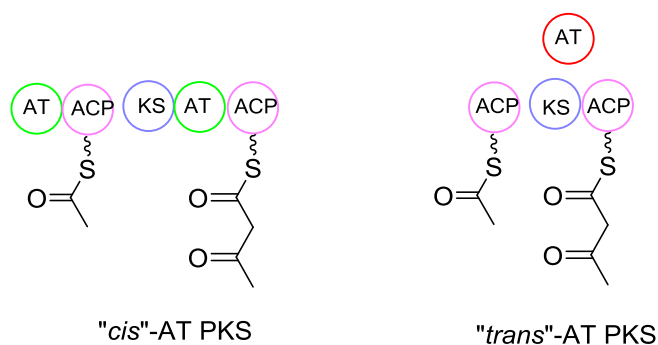
Scheme 7: Modular arrangement of *trans*- and *cis*- AT domains.[43]

1.2.2 Iterative Type I Polyketide Synthases

In contrast to modular PKS, iterative Type I PKS only have a single set of catalytic domains. These domains are used in different combinations during the β-modification cycle and the extent of β-modification can have a large variation between the different extensions. This makes it much more difficult to predict the chemical programme of the PKS. Which protein components control this diversity is still unknown. Iterative Type I PKS are often found in fungi and rarely in bacteria.[44,45]

Iterative Type I PKS are divided into different subclasses based on the domains present in the enzyme, and the overall chemistry carried out. The simplest systems are known as *non-reducing* PKS (NR-PKS) and these perform no reductive modifications during chain construction; slightly more complex are the *partially reducing* PKS (PR-PKS) which usually perform a single programmed reduction; and the most complex are known as *highly reducing* PKS (HR-PKS).[46] Currently there are no reported structures of complete fungal iterative Type I PKS systems.

1.2.3 Non Reducing PKS (NR-PKS)

Non reducing PKS have no reducing domains that are involved in the β-processing of the polyketide - they lack KR and ER domains. Starter units are transferred to the PKS by an *N*-terminal *starter unit acyl-carrier transacylase* (SAT) domain which is unique to this class of PKS. The KS, AT and ACP are responsible for forming a poly-β-keto acyl ACP (Scheme 8) in the usual way. The cyclisation of the chain appears to be controlled by another unique domain known as a *product template* (PT) domain.[47,48] PT domains are required because poly-β-keto intermediates have acidic protons and keto functions that make the polyketide intermediate very unstable. Spontaneous cyclisations are possible, and the PT domain some-how prevents these reactions. In most cases backbone cyclisations, as well as the chain length of the product, are controlled by the PT domain.[47,48]
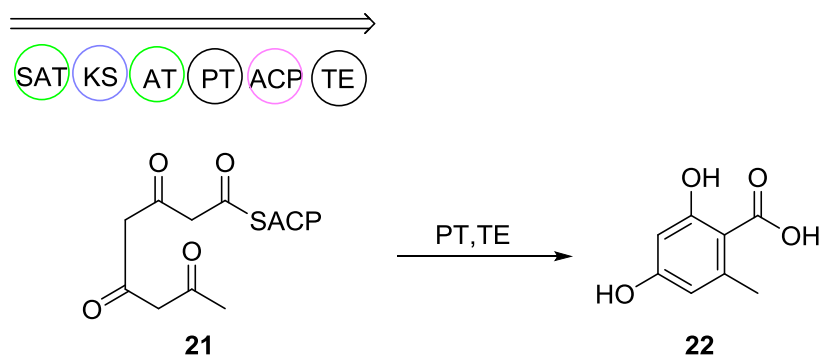
Scheme 8: NR-PKS of orsellinic acid **22**.[49]

A typical example of a NR-PKS is that involved in orsellinic acid **22** biosynthesis (Scheme 8). Sequence analysis of the orsellinic acid PKS (orsellinic acid synthase, OAS) shows the expected domains SAT, KS, AT, PT and ACP.[50]

A variety of different domains are known to be present downstream of the ACP in NR-PKS. For example in OAS there is a thiolesterase (TE) which releases the mature polyketide from the PKS.
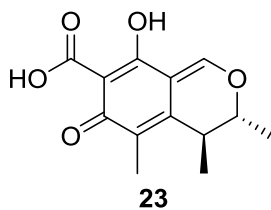
Figure 7: Structure of citrinin **23**.

For some products of NR-PKS a *C*-MeT can also be found at this position. The production of citrinin **23** involves, for example, the addition of two methyl groups to the growing carbon chain (Figure 7).[51] Final release of the PKS products can be catalysed by several different domains. Currently reductive releases (R domains), TE domains or Claisen cyclases (CLC) are known.[52]

1.2.4 Partially Reducing PKS (PR-PKS)

Partially reducing PKS are known in bacteria and fungi. The PKS consists of KS, AT, KR, and ACP domains. Known examples of PR-PKS produce mellein **25** and 6-methyl salicylic acid. In comparison to NR-PKS some functionalization of the polyketide chain is possible by PR-PKS. Diversity in the chain-length of the produced polyketide can be attributed to the C-C-bond forming catalytic domains. In most cases the chain length is controlled by the substrate-binding pocket of the KS domain. Cyclisation, (Scheme 9), is not catalysed like the ones in the NR-PKS by PT domains, but the positions of the keto and hydroxyl groups determine the cyclisation pattern. The reducing step is clearly programmed because not every keto functionalization gets reduced.[50,53,54,55,56]
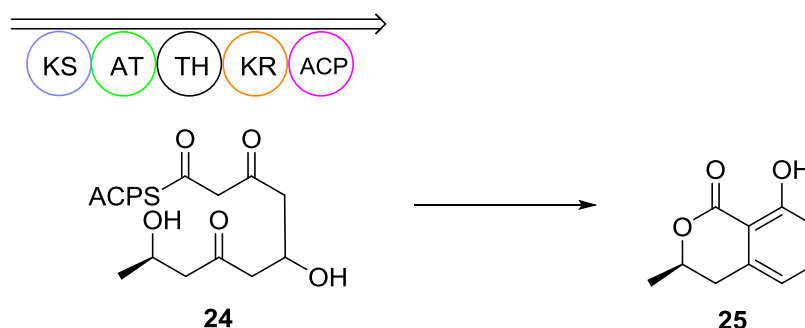
Scheme 9: Mellein biosynthesis.

1.2.5 Highly Reducing PKS (HR-PKS)

HR-PKS are an enigmatic group of multidomain enzymes that can control chain-length and β-processing reactions in a programmed way. How this programming works, however, is unclear.[44,45,57] HR-PKS are large multifunctional enzymes which act in an iterative way. The domain set is the same as mammalian FAS (mFAS, section 1.3) with KS, AT, DH, *C*-MeT, ER, KR and ACP domains. The KS, AT and ACP must be active in each extension cycle, but the other domains can be active or inactive during each cycle of β-processing. Different combinations of the β-processing domains are active after each different extension cycle, and this results in structurally complex compounds.[57] The use of HR-PKS is known mostly in fungi and rarely in bacteria.[57]

The biosynthesis of the fungal metabolite lovastatin **26** is a good example of HR-PKS, and also illustrates two different classes of HR-PKS. In the lovastatin diketide synthase (LDKS) the ER domain plays an essential role as it is present and active during biosynthesis. For the lovastatin nonaketide synthase (LNKS) the original ER domain that is found in the PKS is inactive. In this system a *trans*-acting ER performs the reduction of the olefin during β-processing. This ER is encoded by a separate gene and works in addition to the PKS (Figure 8).[58]
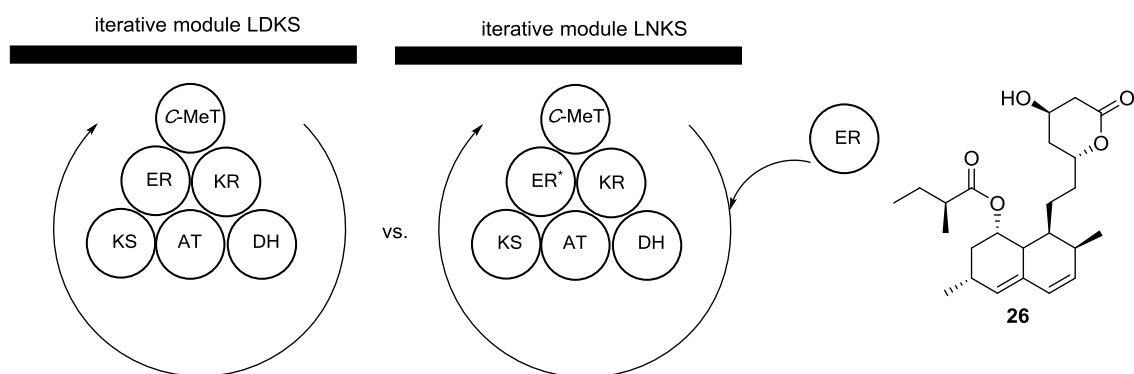
Figure 8: Iterative modules of LDKS and LNKS. ER* is inactive.

Brefeldin A **28** is an antibiotic isolated from the fungus *Eupenicillium brefeldianum* and is also the product of a HR-PKS. It is used as protein-transport inhibitor and has antiviral, antifungal and antitumor activities. **28** probably arises from the highly functionalised C_{16} precursor **27** and shows the high level of programming possessed by HR-PKS (Scheme 10).[59,60]
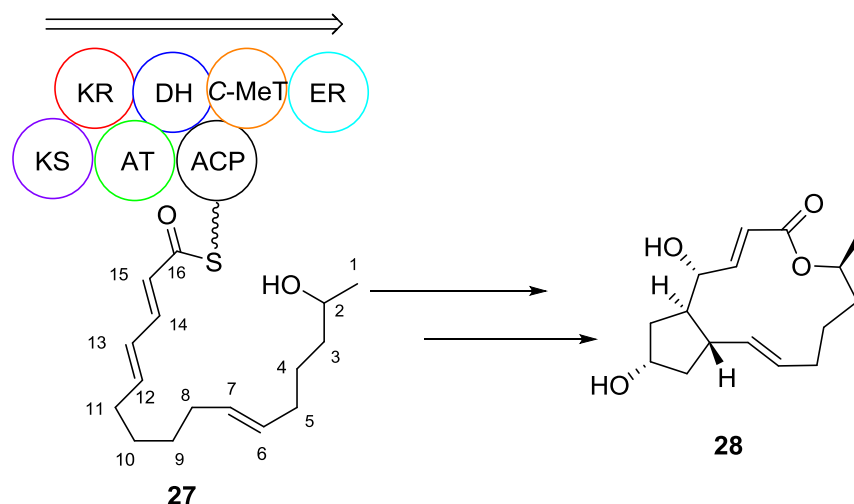
Scheme 10: Structure of brefeldin A **28** and its likely biosynthesis from a C_{16} hydroxy triene product of an HR-PKS.

The switching between active and inactive domains during β-processing is shown in the contrast between full reduction (position 4) and partial reduction (position 2). The DH appears to be inactive during the first cycle, but active elsewhere, and the ER appears to be inactive during cycles 3, 6 and 7, but active in cycles 2, 4 and 5.[59]

1.3   Structure of mammalian FAS

Currently there are very few crystal structures of isolated PKS modules available. However, PKS (especially HR-PKS) have strong end-to-end sequence similarity to mammalian fatty acid synthases (mFAS) and it is hypothesized that they are similar and have closely related structures. The structure of mFAS has been elucidated by crystallization studies (Figure 9).[61]

mFAS is a homodimer with a roughly anthropomorphic shape. The central body is determined by the KS, DH and ER domains. The arms and legs are shown by AT and KR. Two non enzymatic domains are attached at the top of mFAS. One of these domains is homologous to the methyltransferase family and is called a pseudo-methyltransferase (ΨMeT). The other non-functional domain dimerizes with the catalytic active KR domain, and is named pseudo-ketoreductase (ΨKR).[61] Unfortunately the mFAS structure does not show the position of the ACP, or of its terminal TE domain.
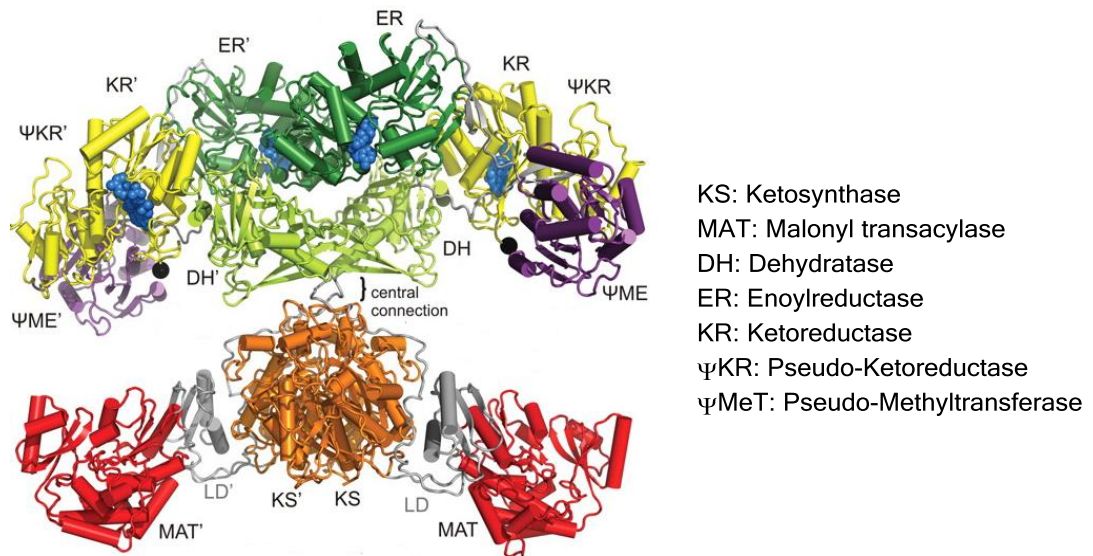
Figure 9: Structure of mFAS.[61]

KS: Ketosynthase
MAT: Malonyl transacylase
DH: Dehydratase
ER: Enoylreductase
KR: Ketoreductase
ΨKR: Pseudo-Ketoreductase
ΨMeT: Pseudo-Methyltransferase

Two sets of every catalytic domain are found in the dimeric structure. It can be divided into the elongation and in the β-processing part. The elongation section is determined by the domains of the KS and MAT. Both are important for the extension steps (Figure 10). The remaining domains are used for the β-modification cycle. The crystal structure of mFAS is very highly organized with only 9% of the whole sequence being linker region.[61]

KS: Ketosynthase
AT: Acyltransferase
DH: Dehydratase
ER: Enoylreductase
KR: Ketoreductase
ΨKR: Pseudo-Ketoreductase
CMeT: Methyltransferase
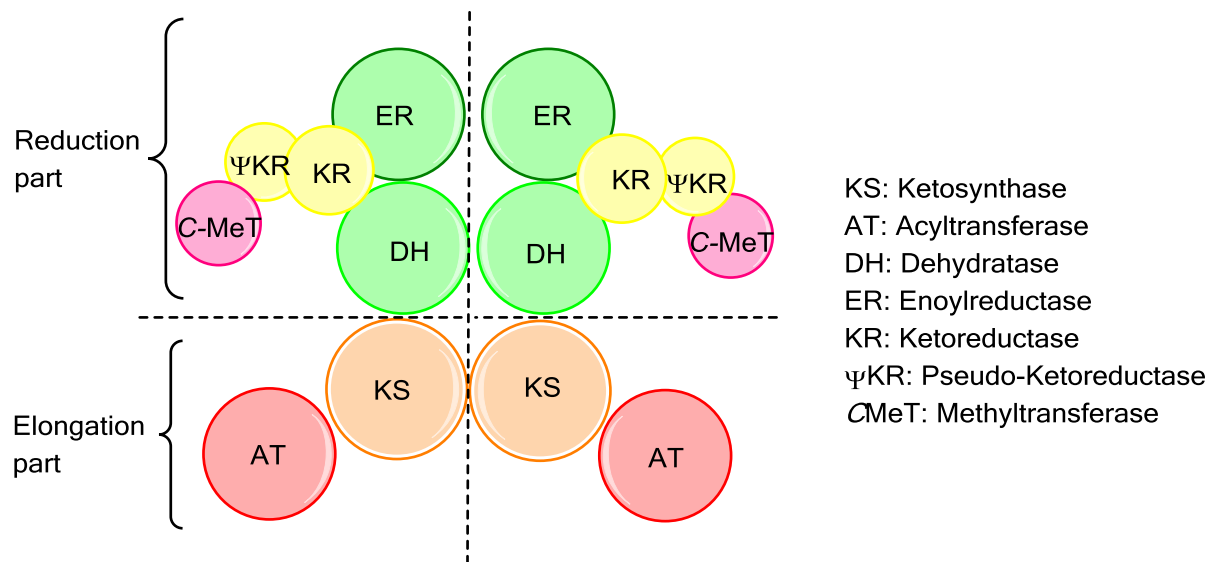
Figure 10: Different parts of Type I FAS and PKS.

1.3.1 Intersubunit and Interdomain Connections of mFAS

The dimerized mFAS polypeptides have an interface which is created by the contacts between the different domains. In total an interface of 5400 Å^2 exists. Nearly 150 amino acid residues are involved at these interfaces.[28] Most of the interfaces are contributed by the homodimers of KS and ER domains (2600 Å and 1600 Å/ 74 and 47 amino acids respectively). Other contacts are formed by the DH domains (800 Å/ 27 amino acids) and smaller contacts between MAT, DH and KS domains (400 Å).[62,63]

The elongation and β-modification parts of mFAS are connected by a small linker (20 amino acid residues). Due to the fact that mFAS and fungal HR-PKS show end-to-end sequence homology it seems highly likely that HR-PKS are structurally similar to mFAS. Thus the structure of mFAS gives information about how the protein structure of an HR-PKS could be.[61]

KS and MAT domains make up the elongation part. The KS domain exists as a homodimer with an interface of the two monomers and is located in the centre. This dimer is surrounded by the DH and MAT domains. The KS and MAT domains are connected by a linker, which is built up of 70 amino acids. Direct interactions of KS and MAT domain are prevented by α-helices and β-sheets. Also a connection between MAT and DH domain is known. A linker connects the KS domain with the DH domain and thus elongation and modification part.[61,62,63]

The β-modification part of the protein is formed by five domains. DH, ER, KR, ΨKR and (Ψ)C-MeT domains are involved in the different modification steps. In mFAS the DH domain exists as a homodimer. It shows weak connections to the ER domain, which also exists as a homodimer. An interface between the subdomain of the DH and KR domain of 800 Å was found. The second hot dog subdomain of the DH is the part that interacts with the KR.[61]

The KR domain is the central domain of the modifying part and has an interface to all modifying and noncatalytic domains (DH, ER, ΨKR and ΨMeT). KR and ΨKR form the main interface. This interface has a size of 1100 Å^2. The size of the interface between KR, ΨKR and ΨMeT is 200 Å^2.[61]

Analysis of the non-catalytic domains shows some special structural modifications. The ΨKR is half the size of the active KR domain, but it forms an important structure which supports the catalytically active KR.[61] The second non-catalytic domain of mFAS, the ΨMeT, is a relic of an S-adenosyl-methionine dependent

methyltransferase. Its inactivity is due to the loss of the binding motif for the cofactor SAM **12**, as well as several peptide deletions when compared to active *C*-MeT domains, for example those of HR-PKS.[64]
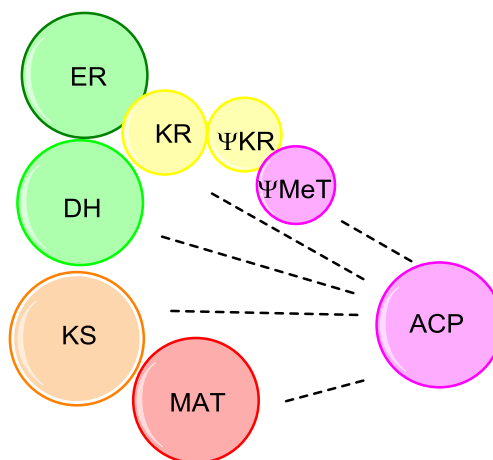
Figure 11: Possible position for ACP domain for interaction with elongation and modification part.

The final important domain is the ACP. It was not possible to crystallize the ACP as a part of the FAS structure. This could be explained by the high flexibility of the domain. However it is observed that the entries to the active sites of the catalitc domains appear to line the large cavity formed by the MAT, KS, DH, KR and ΨMeT domains. The anchor point for the ACP may lie in the center of this modification area. Structurally the ACP consists of a four helix bundle. This is the usually found structure for ACPs. One of the helices is very important for the docking process to the different domains. The docking process leads to electrostatic interactions (Figure 11).[61,65]

1.3.2 Structural Relationship of mFAS and PKS

At the moment very few structures of mPKS have been reported. Production of crystals of a complete PKS is usually not possible because of instability of the enzymes.[63] However, progress has been made in crystallising isolated domains and didomains of PKS enzymes. Several crystallisation experiments of isolated mPKS fragments were successful.

KS-AT-didomain

Tang and coworkers reported the isolation and crystallisation of a KS-AT fragment of the DEBS5 module.[62] It has a size of 194 kDa and is homodimeric. The full length of

KS and AT domains and additional linkers were crystallised. The orientation and organisation of KS and AT domains were very similar to mFAS. Homodimeric KS domains seems to be centered on a 2-fold rotational axis. AT domains are located at the edge of the KS domains. The active sites of both domains have a distance of 80 Å (Figure 12).[62]
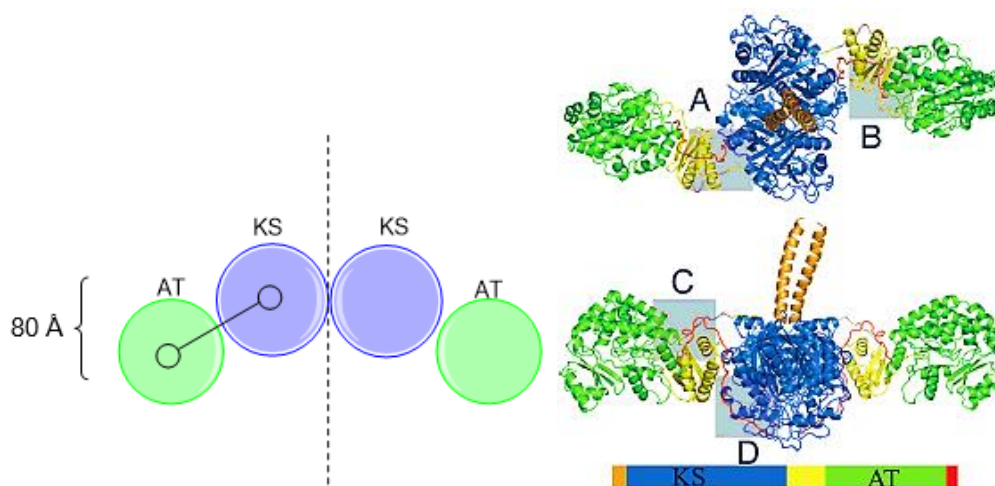
Figure 12: Orientation and organisation of KS-AT didomain of DEBS5.[62]

Comparison of the linker regions of mPKS and mFAS also shows similarities. Linker of KS to AT regions fits well. A contrast was recognized for an *N*-terminal linker. This could be reasoned to the transfer of the growing polyketide chain that is transferred by this linker. However, the linker is missing in the mFAS sequence.[61,62,63]

KR domains

Other domains that have been investigated very frequently are KR domains from modular PKS. Two examples are EryKR1 and TylKR1. Both are structurally related to the KR domain of mFAS. Interfaces of this domain were found with ER- and DH domain. In agreement to the structure of mFAS is that the isolated KR domains are monomeric.[61,66] The catalytic KR domain consists of two structural subdomains. One contains the known Rossman fold which forms the cofactor binding site, the other one (known as ΨKR) is a subdomain that has lost the dinucleotide binding site and its main role is the stabilization of the KR domain.[66,67]

DH domains

Crystal structures of several isolated DH domains of modular PKS are available. All reported structures shows that the DH domain exists as a dimer. This is similar to the reported structure of mFAS. Also for mPKS only a small interface is observed.[68-70]

The DH domain of DEBS DH4 is similar to the mFAS DH and is composed of two subdomains, each is a *hot dog* fold. The "bun" is formed by a seven-stranded antiparallel β-sheet. A central helix is orientated in this fold and makes up the "sausage" of the "hot-dog" (Figure 13).
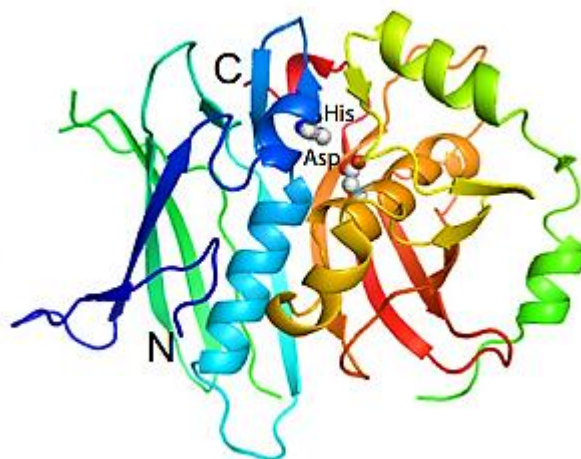
Figure 13: Structure of the *hot dog* fold of cur F.[71]

Several catalytic residues are conserved between the mFAS and DEBS DH4. In particular, the HXXXGXXXXP motif is distinctive for DH domains. The glycine is necessary to allow a turn in the structure. Several other motifs that are conserved are "GYXYGPXF" and "LPFXW". More detail is discussed in section 3.5.[68-70]

The proposed mechanism of DH starts with a deprotonation at the α-position by a histidine residue (section 3.5). Elimination of water occurs *via* an E1cb mechanism, with overall *syn* stereochemistry. Further details of the mechanism are discussed in section 3.5.[68-70]

ER domains

Different structures of ER domains from modular PKS are known. For example the structure of the ER-KR didomain of Spn2 from the spinosyn mPKS has been reported. The ER domain of Spn2 belongs to the medium-chain dehydrogenase/reductase family. Two subdomains are found for this class (section 2.2). In contrast to mFAS the ER

domains of the PKS do not exists as dimers. In the case of the *trans*-acting ER domain a loop prevents the dimerisation.[70]
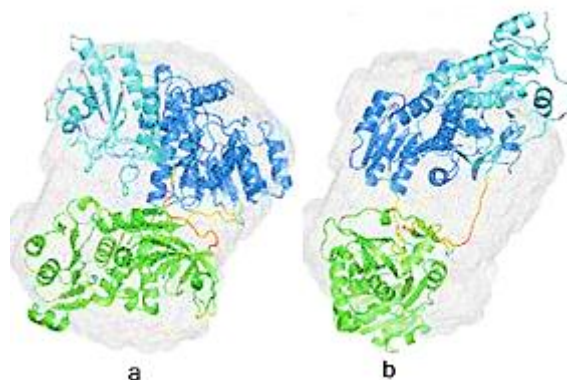
Figure 14: Orientation of ER-KR domains in Spn2 (a) and mFAS (b).[72]

Crystallisation of the ER-KR didomain fragment of the spynosyn synthase module 2 shows an interface of both domains. This interface is larger than the known one of mFAS. Nonconserved hydrophilic residues in the subdomain (KR) and substrate binding domain (ER) seems to be responsible for this interaction. Additional linkers increase this interface (Figure 14).[72] This is in contrast to mFAS. [61]

Types of proposed protein structures of modular PKS

Zheng *et al.* proposed, based on several crystallisation experiments, a different possible structure for modular PKS. This structure has a similar elongation part to mFAS but a differently organised β-processing part. Differences are shown by the organisation of the domains.[72]
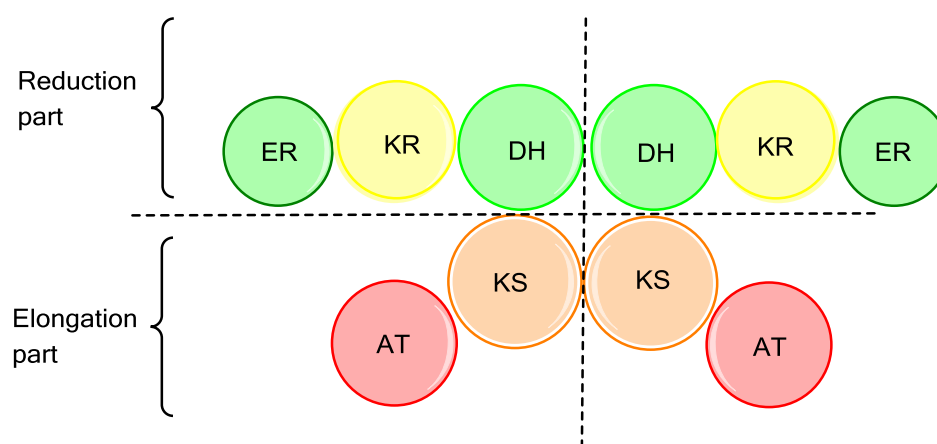
Figure 15: Proposed domain organisation by Zheng et. al.

Difference between the mPKS and mFAS exists in this model in the β-processing part. The organisation of DH, KR and ER shows a monomeric behaviour for the ER domain. Zheng *et al*. showed the structural relation between ER domain and KR domain by the crystallisation of the didomain of the modular PKS Spn2. In contrast to mFAS the ER domain is not located in the center of the protein. The result is a more open structure of the protein (Figure 15).[61,72]

Since it was not possible to create a complete crystal structure of a PKS other methods for structural analysis have been developed. One of these is cryo electron microscopy. Dutta and coworkers worked with this method to visualize module 5 of the pikromycin modular PKS which consists of KS, AT, KR, ACP domains. A completely different domain organisation was found in contrast to mFAS.[61,73,74] The domains are shaped like an arch. The KS domain exists in this architecture as a homodimer. An additional connection to the AT domains is observed. The AT domain is connected on the other side to the KR domain. Positions for the ACPs were found near to the AT and KR domains in a reaction chamber which is faced by the KR and AT (Figure 16).[73]
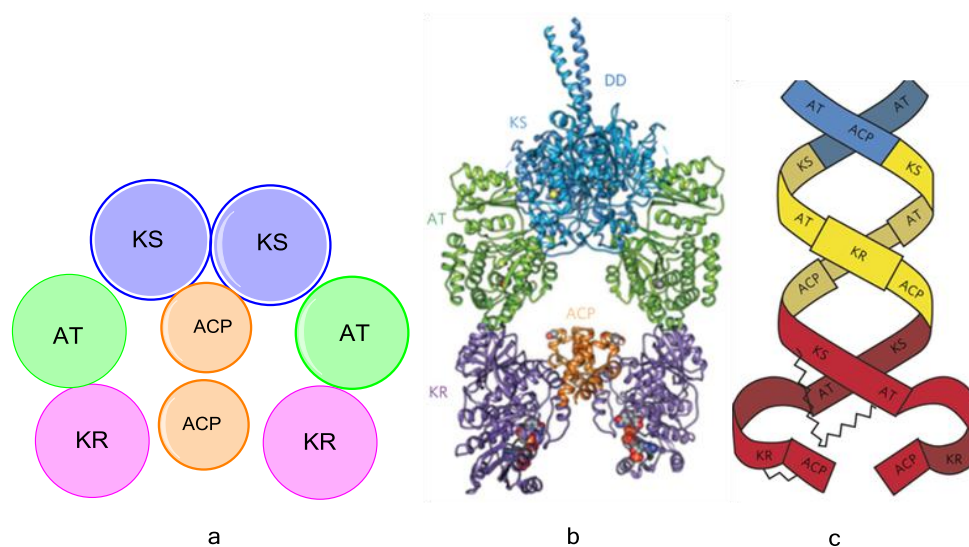
Figure 16: Domain organisation of PikAIII (a and b).[74]

This configuration is very near to the one that was proposed by Staunton *et al*. (Figure 16, Structure c)),[75] Structural relationship to KS-AT didomains or mFAS do not exist.[62,73] Every AT domain in PikAIII is rotated by 120° in comparison to mFAS. An interface between KS and AT domains is observed. In mFAS the connection between both domains exists by a linker.[61] This orientation of the AT forms, in connection with the KR a reaction chamber in the center of PikAIII.[75]

Fungal HR-PKS

No structures of any of the core components of a fungal HR-PKS, either as single domains or as multidomains, are known. However there is overall end-to-end sequence homology between mFAS and HR-PKS, with active sites located in the same positions and showing very high levels of amino acid conservation. This includes both active and inactive domains, and even includes the inactive *C*-MeT domain of mFAS, which is active in many HR-PKS. It is therefore hypothesised that the mFAS structure is likley to be a good model for that of HR-PKS.

1.4   Programming in Fungal HR-PKS

The programming in highly reducing iterative polyketide synthases has been rarely investigated. One of the biggest problems is that in an iterative PKS the extension steps are cryptic. The structure of the polyketide cannot be predicted by sequence analysis. How is the chain length determined? Where does a methylation take place? Which reductive domains are active? So far very little information has been gathered about how these programming steps are controlled. However, the biosynthesis of a few polyketides has been investigated in considerable detail and some information is beginning to be discovered. In particular the cases of lovastatin **26** and tenellin **47** have revealed key information about programming.

1.4.1 Biosynthesis of Lovastatin

One of the most investigated and understood highly-reduced polyketides is the cholesterol lowering drug lovastatin **26** (Figure 17) obtained from the filamentous fungus *Aspergillus terreus* and also identified in *Monascus ruber* as Monacolin K.[76-78] Due to inhibition of (3*S*)-hydroxy-3-methylglutaryl-coenzyme A (HMG-CoA) **26** is used as a cholesterol lowering drug, and also for the inspiration for the development of many semi-synthetic analogues.[77-80]
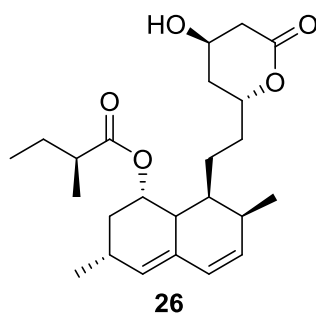
Figure 17: Structure of lovastatin **26**.

Lovastatin **26** is built up by two different iterative polyketide synthases. The polyketides are linked together by an acyl transferase to form an ester linkage. The lovastatin nonaketide synthase (LNKS / *lovB*) is responsible for the production of the lovastatin precursor dihydromonacolin L **29** (Figure 18). This PKS contains KS, AT, DH, *C*-MeT, ΨKR, ER*, KR, ACP, C domains. The terminal C (condensation) domain is a relic from a now inactive NRPS module - the C domain is thought to be inactive.[79]
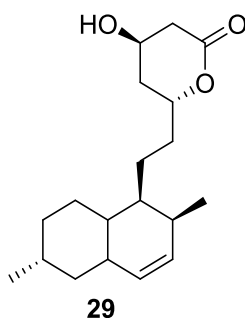
Figure 18: Structure of precursor dihydromonacolin L **29**.

In vitro studies showed that LovB as a stand alone synthase is not able to produce **29** since its ER domain is inactive (demnoted ER*). During the production of **29** the required ER is encoded by *lovC*. This ER is a separate protein and is known as a *trans*-acting ER.[77-80]

The side chain of **26** is synthesized by a second PKS known as Lovastatin diketide synthase (LDKS/ *lovF*) which shows the following domain organisation KS, AT, DH, *C*-MeT, ΨKR, ER, KR, ACP. No release domain was found and further investigations showed that the offloading of this domain is performed by protein-protein interactions with LovF and LovD (AT domain involved in the transfer of LDK to LNK).[77-80]
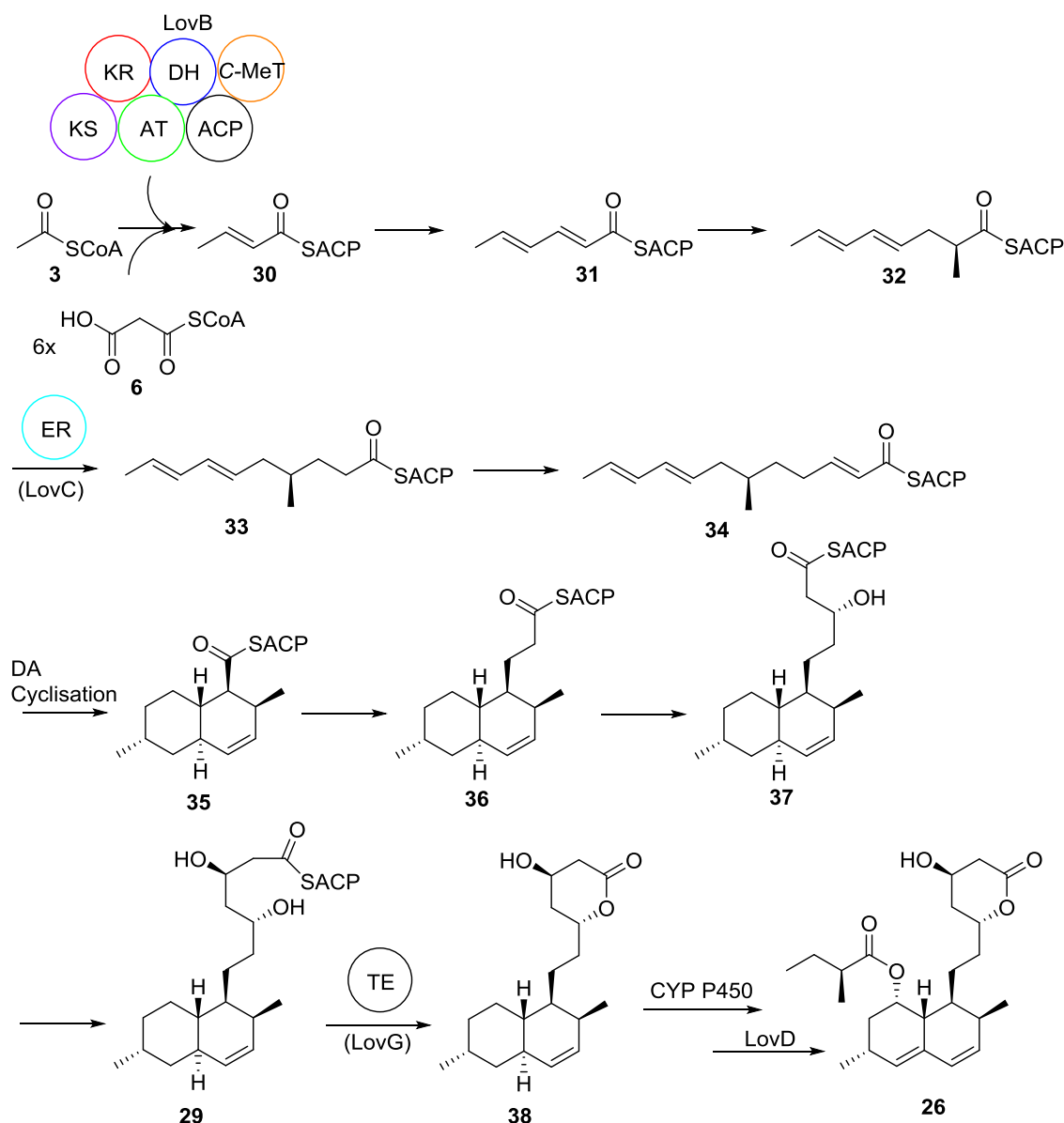
Scheme 11: Biosynthesis of lovastatin **26**.

Several intermediates of the biosynthesis of **26** are known (Scheme 11). The synthase starts with acetyl CoA **3** which is elongated by malonyl CoA **6**. After the first two elongations only the KR and DH modification enzymes are active (intermediates **30** and **31**). After the third elongation all domains are active, including the *C*-MeT and *trans*-acting ER with consequent full reduction to form compound **32**. Similar modifications operate during the fourth step, but without methylation to give **33**. After another elongation with active KS, KR and DH domains, the formed hexaketide **34** is transferred into the bycyclic compound **34** by a Diels Alder reaction.[77-80] After further elongation to **36**, **37** and then **29** the carbon chain is cleaved by a thiolesterase (TE/LovG) to release **38** as the first enzyme-free intermediate.

By later modifications the precursor **38** is oxidized twice by a P450 enzyme (LovA) to introduce the second olefin and a hydroxyl group. In the last modification step the AT domain encoded by *lovD* forms **26** with the addition of α-*S*-methylbutyrate that was produced by LDKS. Further details of LovD activity are discussed in chapter 5.1.[77-80]

Tang and coworkers showed another example of programming in iterative PKS in 2015. Specifially the methyltransferase domain of lovastatin was investigated.[85] After the third elongation, the *C*-MeT works directly after the ketosynthase, and it is the only time the *C*-MeT domain is active. This methylation is important because without it, it is not possible for the ER domain to work. The substrate cannot be recognized (Scheme 12).[81]
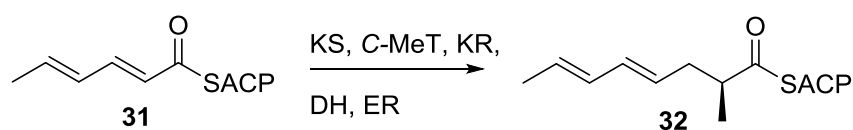
Scheme 12: Third elongation step of LNKS.

To investigate the behaviour of the *C*-MeT domain several SNAC-substrates were synthesized, which were different in chain length. The first four elongation substrates of LNKS were synthesized with an SNAC-residue. For enzyme assays the iterative enzyme LovB was expressed and a mutation in the DH was introduced to stop further modifications (designated LovB*, Scheme 13).[81]
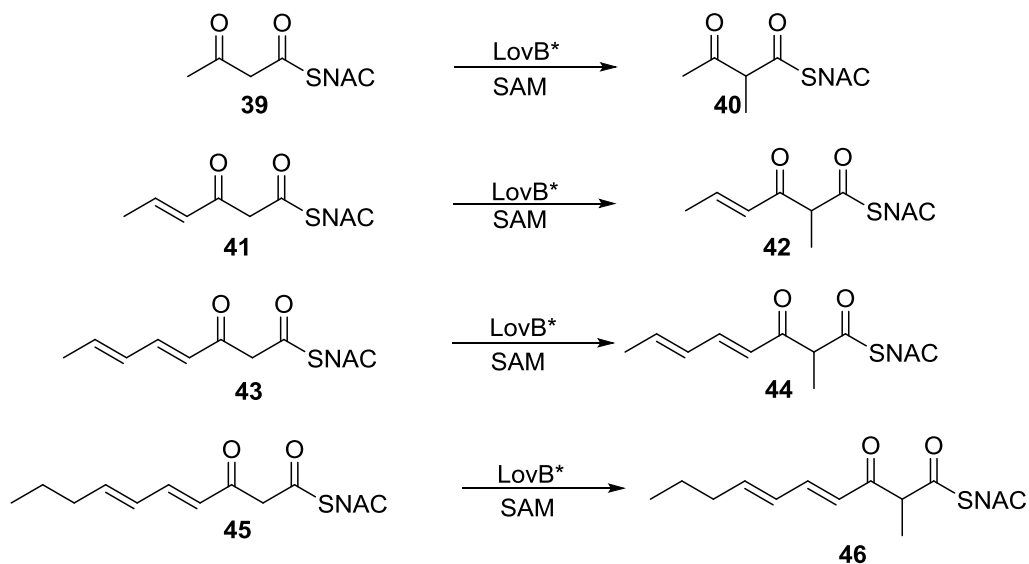
Scheme 13: Enzyme assays of several β-keto-acyl-SNACs.

Different enzyme assays were set up. First the natural tetraketide substrate **43** was assayed with LovB* in the presence of SAM. The activity of the enzyme with this

substrate was observed by LCMS. Also the diketide, triketide and pentaketide mimics were analysed but the diketide and pentaketide were not substrates, and the triketide was methylated very slowly (Scheme 13).[81]

Comparing the kinetic results of the tetraketide with the triketide analogue the catalytic efficiency slows down by a factor 2500, also the k_{cat} and K_M each change by a factor of 50. Additional substrates based on tri- and tetraketides, that had saturated carbon chains showed slow activity with LovB, but again an increase of K_M was detected, which shows the high substrate specificity of the lovB C-MeT domain for its natural substrate.[81]

After analysing the C-MeT assays, the same investigations were performed with the KR domain. Since the KR is active in every extension, in contrast to the C-MeT, a much higher spectrum of different substrates would be expected to be processed. In the evaluation of the different assays of tri- and tetraketides it seemed not to have an effect to the enzyme if a methyl group is added to the β-keto-ester or not. Also the chain length does not affect the KR domain.[81]

In final competitive assays of lovB* in the presence of the corresponding cofactors **12** and **13**, different substrates were tested with the DH-mutated enzyme (Scheme 14). The assays showed clearly that the triketide has a higher affinity to the KR than the C-MeT. Only a small amount of the methylated version was found in the LCMS chromatogram.[81]
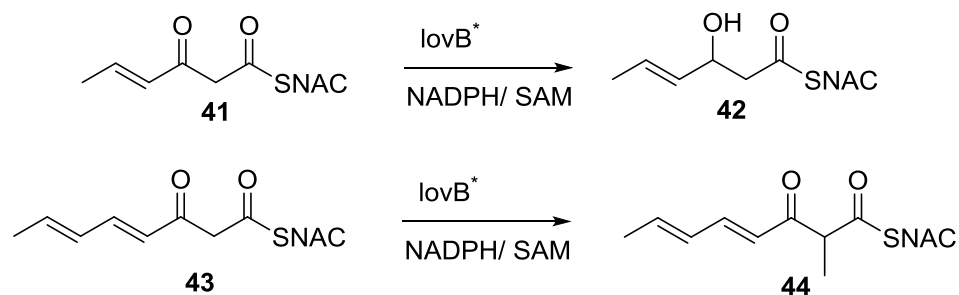
Scheme 14: Competitive enzyme assays of KR and C-MeT domains.

The competitive assay of the tetraketide showed a high affinity to the C-MeT. No reduced product of the KR was observed. This shows again the much higher catalytic efficiency of the C-MeT to the natural tetraketide. Since there is not much control by the KR domain, the substrate specificity of the C-MeT seems to be important for the programming and the synthesis of the correct substrate, which are necessary in the following elongation steps.

The programming of the second extension step is programmed in a competitive step of *C*-MeT and KR. Both enzymes compete for the release product of the KS domain. In every elongation without the second one, the KR is favour against the *C*-MeT. The second elongation in contrast to the other ones shows the high selectivity of the *C*-MeT to the tetraketide.[81]

After the sixth elongation step a bicyclic system is formed via a biological Diels Alder reaction. LNKS catalyses an intramolecular *endo* cyclisation. It seems likely that LNKS controls the conformation of **34** so as to bring the atoms to the correct distance for the cyclisation (Scheme 15) but it is still not known exactly how this is achieved.[82-83]

34   **35**
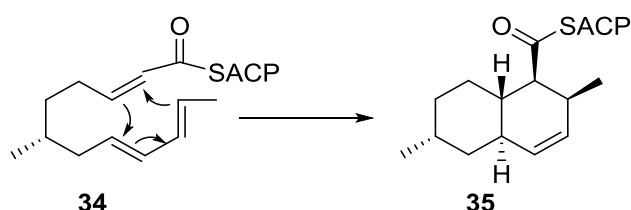
Scheme 15: Diels-Alder reaction after the sixth elongation.

1.4.2 Biosynthesis of Tenellin and Desmethylbassianin

The fungal metabolites tenellin **47** and desmethylbassianin (DMB) **48** are biosynthesized by hybrid PKS-NRPS systems, and have also been investigated to determine the origin of PKS programming. The PKS is a HR-PKS and the NRPS adds a tyrosine to the resultant polyketide chain and catalyses a Dieckmann cyclisation. For both compounds a *trans*-acting ER domain is used (Figure 19). Tenellin **47** is built up by four different proteins: the iterative HR-PKS (TenS) which works with the *trans*-acting enoyl reductase (TenC) and two cytochrome P450 mono oxygenases (TenA and TenB).[84,85]

47   **48**
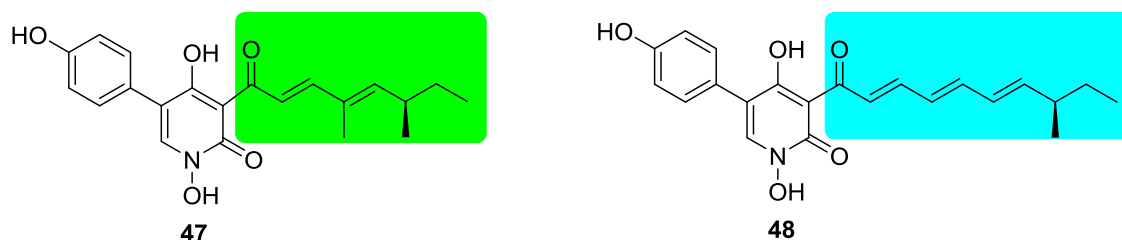
Figure 19: Structure of tenellin **47** and desmethylbassianin **48**.

The biosynthesis of **47** starts with acetyl CoA **3** which is elongated four times with malonyl CoA **6**. After the first elongation all β-processing enzymes are active. Complete reduction is performed by the TenC *trans* ER domain. This *trans* ER domain is inactive after the next elongation cycles so an unsaturated carbon chain is formed. The methyl transferase only works after the first two cycles and is then silent. The KR is functional after the first three rounds of extension, but inactive after the fourth. After the fourth extension the polyketide is fused with a tyrosine residue to form pretenellin A **49** (Scheme 16). The two P450 oxidases work in a post PKS modification to form **47**.[84,85]
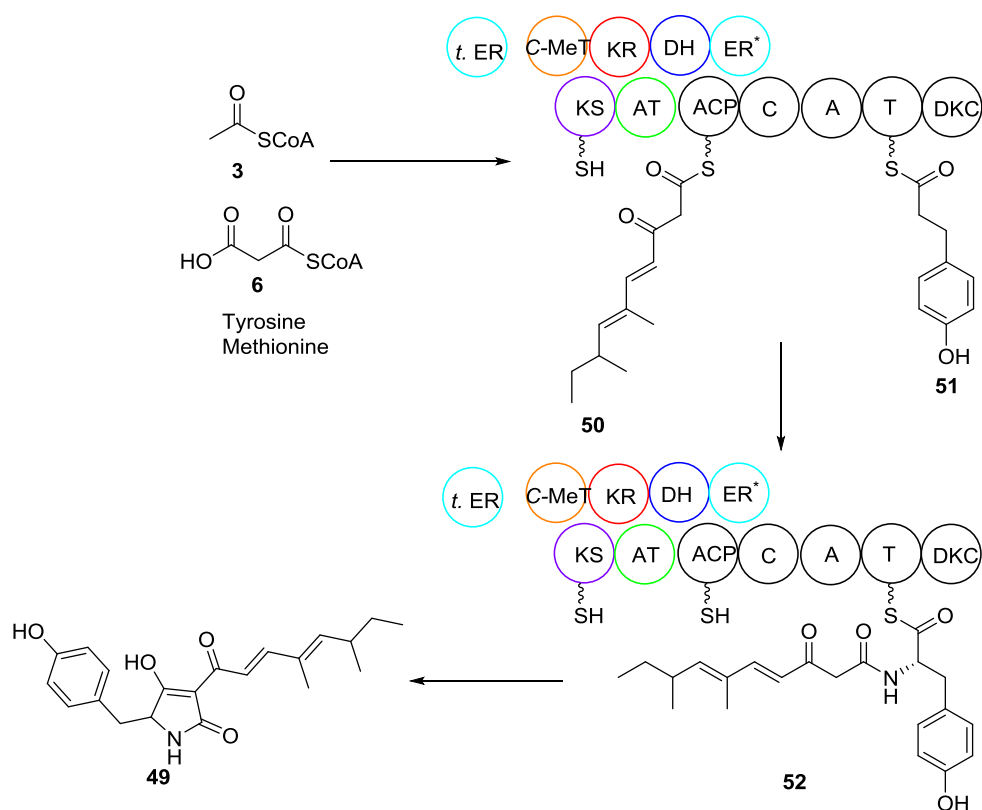
Scheme 16: Biosynthesis of tenellin precursor pretenellin A **49**.

DMB **48** is similar to **47** and is also built by a PKS-NRPS known as DMBS which requires a *trans* ER (DmbC). Examination of the structure of **48** indicates that it has one more extension cycle than **47**. In contrast to **47, 48** has one less methylation. To investigate a possible role of programming the *trans* ER domains were investigated. The *trans*-ER proteins of **47** and **48** biosynthesis were interchanged but this did not show any significant changes or possible reprogramming by these proteins.[84,85]

Comparison of the two biosynthesic gene clusters shows very high homology between the different genes and proteins. The two clusters have a 90% sequence identity of the genes and also the same orientation of the open reading frames. The very

high level of protein similarity allowed fusion proteins to be formed by genetic engineering in which different domains from DMBS are inserted into TENS (Scheme 17).[86-88]
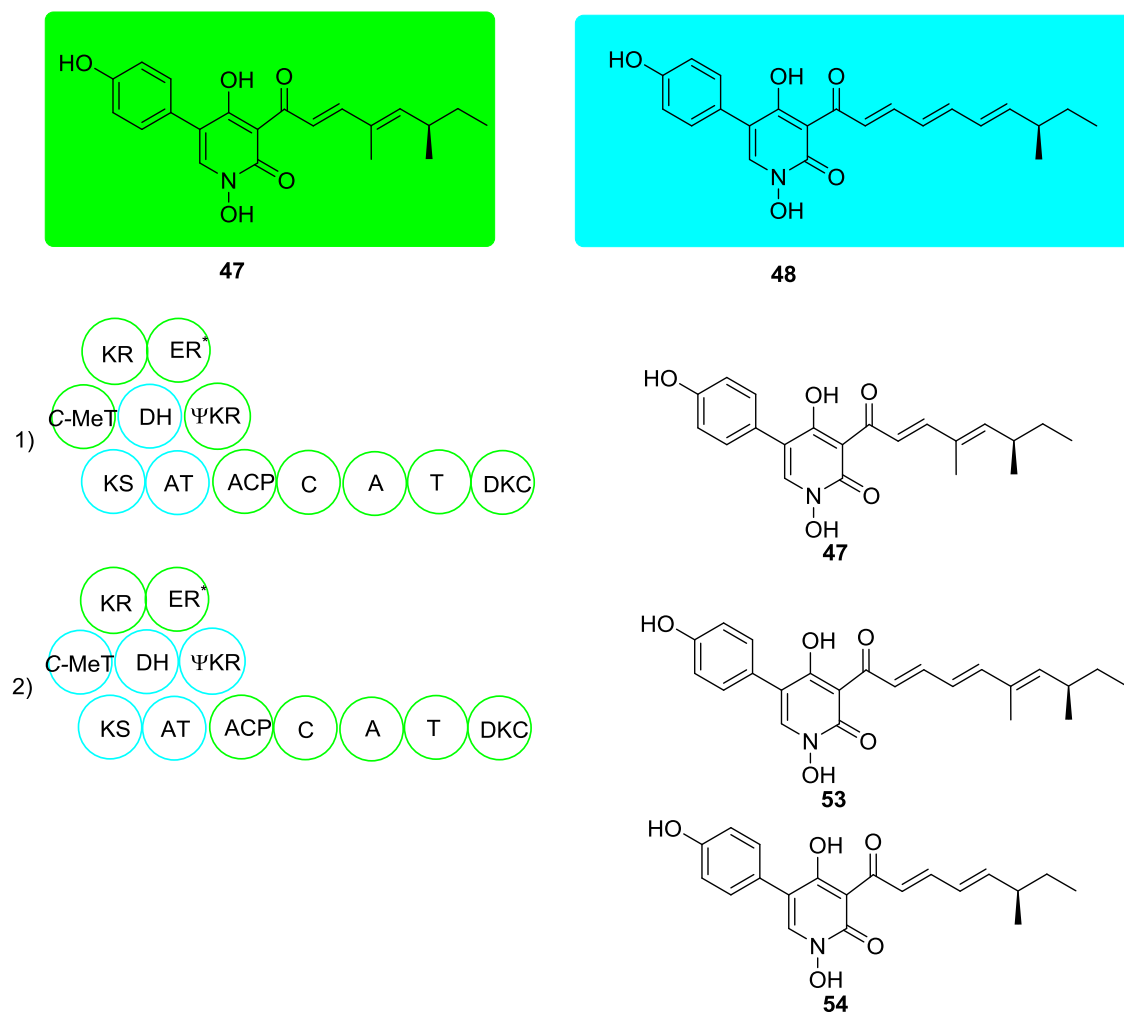
Scheme 17: Fused chimaeras of DMBS and TenS.

Interestingly after replacing the elongation part and the dehydratase (KS, AT, DH) of TENS with the ones of DMBS no change in the polyketide chain was observed. The product was still **47**. This means that the chain length cannot be programmed by these three domains. In the next experiment *C*-MeT and ΨKR from DMBS were swapped into TenS. With this fusion two new products were observed. Desmethyl-pretenellin A **53** and prebassianin **54** were isolated as major and minor products. The methylation pattern changed for the major product to a double methylated compound, but has the same chain length as **48**. For the minor product the chain length was the same as **47**. In contrast to this, the methylation pattern was this time different. Only one methylation was observed which corresponds to the side chain of **48**.[86-88]

Including in the next domain swap the keto reductase of DMBS, changes the product proportion to the predesmethylbassianin A **55**. More precise swaps of DMBS (*C*-MeT-ΨKR) showed a high titer of **54**. Also a small amount of **47** was detected. These results suggest that the methylation pattern is controlled by the *C*-MeT-ΨKR (Figure 20).[88] It seems, that the *C*-MeT must be programmed on its own. The DMBS *C*-MeT seems only to recognize diketides, but the TenS *C*-MeT can recognise both diketides and triketides.[88]
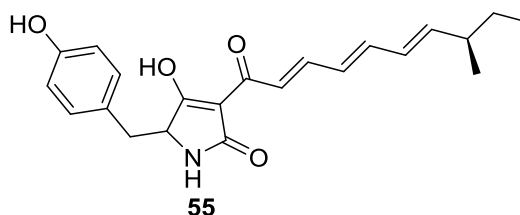
Figure 20: Structure of predesmethylbassianin A **55**.

The use of domain swaps became a useful tool and was also used in further investigations of NR-PKS. An exchange of the SAT domain in NR-PKS showed that it is possible to control/ influence the chain length of the final products.[89]

1.5   Squalestatin S1

Squalestatin S1 **56** (SQS1), also known as zaragozic acid A, is produced by *Phoma* species of fungi.[90-95] It is an inhibitor of mammalian squalene synthase and thus a potential inhibitor of cholesterol biosynthesis. SQS1 **56** was discovered in the early 1990s and investigated independently by Glaxo and Merck and is potentially a lead structure for the development of a cholesterol lowering drug.[90-95]

There are several derivatives of the squalestatins/ zaragozic acids known (e.g. **57** and **58**). All compounds have a very polar 4,8-dioxabicyclo[3.2.1]octane core which is the result of post polyketide modifications (Figure 21).

At position 6 of the core of **56** is attached a tetraketide side chain (Side chain B in Figure 21). This position can be substituted by many different side chains.[93-100] The side chains have a high diversity in the chain length, methylation pattern and methylation positions. Also the reduction pattern of the side chains can differ. This diversity could be an indication of a broad substrate tolerance of an acyl transferase which combines both polyketides. The origin of the heavy atoms of **56** was elucidated by feeding experiments using ^{13}C, ^{2}H and ^{18}O labelled precursors.[93,96,97]
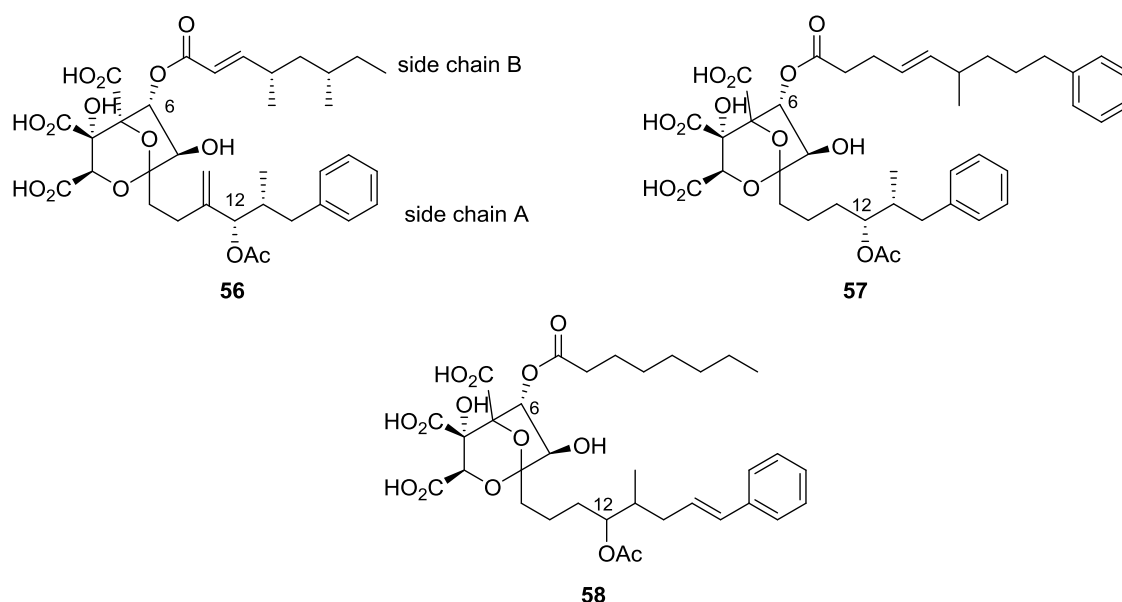
Figure 21: Structure of target compound squalestatin S1 **56** and known derivatives.[92]

SQS1 **56** is is built up by two different polyketide synthases similar to lovastatin **26** biosynthesis. The core of **56** and side chain A are synthesized by a hexaketide synthase (known as squalestatin hexaketide synthase, SQHKS) and the very uncommon benzoate **5** starter unit. This starter unit is extended five times by malonyl CoA **6**. The different methyl groups are derived from SAM **12**. Four oxygens (O*) are derived from atmospheric oxygen **59**.[97]
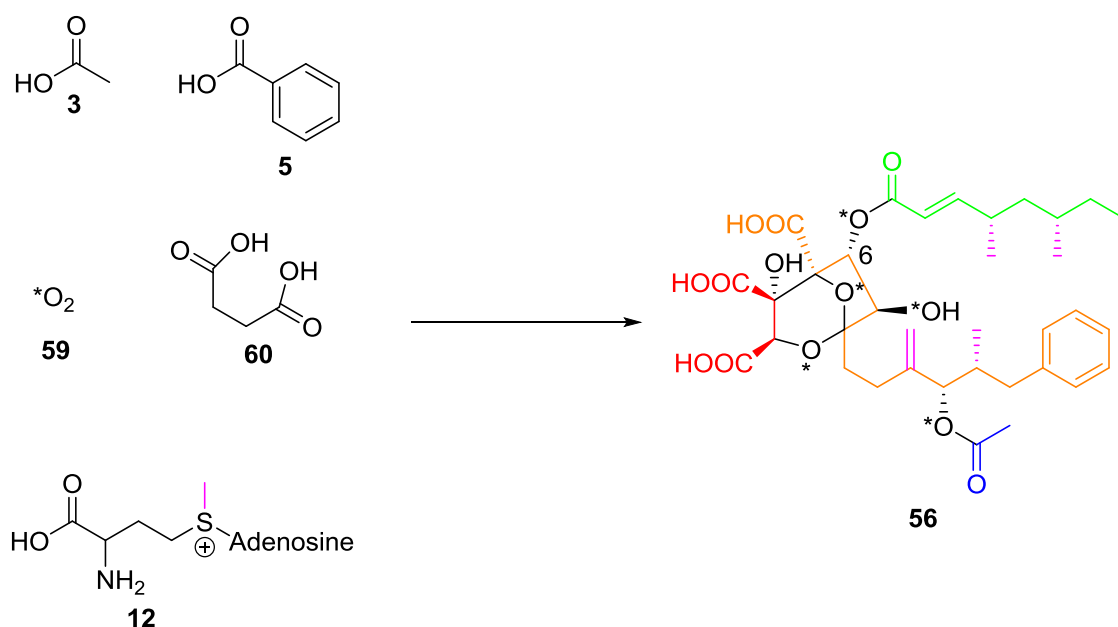
Scheme 18: Biosynthase of **56** with corresponding starter units.

After that, several modifications take place to form the final 4,8-dioxabicyclo[3.2.1]octane core. Four carbon atoms are derived from citric acid **60** and attached by condensation reactions at the hexaketide chain. The gene cluster encoding SQS1 biosynthesis was identified using full genome sequencing by Beate Bonsch (Scheme 18), but the exact chemical steps leading to the formation of the 4,8-dioxabicyclo[3.2.1]octane core are still unknown.[97]

Knockout experiments of the identified tetraketide synthase gene (*phpks1*) showed the loss of **56**, but formation of **56** lacking the B side chain **61** suggested that the tetraketide is probably added late during the biosynthesis.[98]

The squalestatin tetraketide **61** is constructed by the squalestatin tetraketide synthase (SQTKS, Scheme 19). Cox *et al.* found the 8 Kb gene (*phpks1*) that encodes SQTKS in 2004. SQTKS consists of KS, AT, *C*-MeT, ΨKR, KR, DH, ER, and ACP domains. Alignments with mFAS and LDKS showed 26% and 59% similarity respectively.[98]
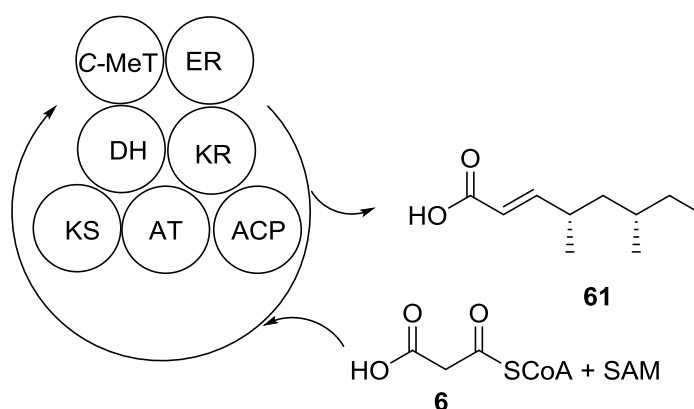
Scheme 19: Iterative module producing SQTK.

The biosynthesis of **61** starts with the starter unit acetyl CoA **3**. **61** and is elongated in three extensions with malonyl CoA **6**. In the first two cycles all domains are active. The PKS chain is methylated and fully reduced at the β-keto moiety to a methylene. After the final extension step the *C*-MeT and ER are inactive. The methyl group in the α-position is missing (Scheme 19). Also a double bond in the α-position of **61** exists. Finally the tetraketide gets released from the PKS. As there is no TE domain contained within SQTKS it is currently unknown how **61** is released from the PKS. Possibly another gene in the gene cluster is responsible for this step.[98]

Finally both individual side chains are combined by an acyl transferase (AT) to build up the target compound **56**. For **56** it was proposed that two different ATs work separately and individually.[97]

31

1.6   Aims of the Projects

The tetraketide side chain of squalestatin S1 **56** is produced by SQTKS, but the programming mechanisms of the PKS is unknown. Analysis of **61** shows that the ER and *C*-MeT domains of SQTKS are inactive after the last extension. The crucial questions of the project are how is **61** formed, how is its biosynthesis programmed and what is the mechanism for controlling the programme?
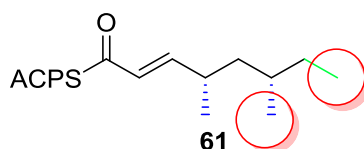
Figure 22: Possible points that can control the programming of SQTKS.

The programming could be performed either by substrate-recognition or by kinetic selection, but this is unclear. Previous investigations have shown that some domains, such as *C*-MeT, appear to be individually programmed.[88] Programming of recognition could be connected to the methylation pattern, methylation position but also to the chain length of each indicidual substrate (Figure 22). However, other domains such as KR control chain-length and this is counter-intuitive.

Previous work in the Cox group has succeeded in isolating several domains of SQTKS which are involved in the synthesis of **61**. An individual analysis of single domains could be performed.[100,101] In the following thesis, the focus is on the investigation of the ER and DH domains of SQTKS. These domains appear to have contrasting programming: the DH works after all three rounds of extension; but the ER does not work after the second round of extension. Previous work (Doug Roberts in the Cox group, unpublished) also showed that the isolated SQTKS-ER domain cannot properly control the stereoselectivity of the reduction - it releases racemic products in contrast to complete SQTKS which releases enantiopure products.[100] A problem could be the expressed protein but also the reaction rate could be too slow. Protonation could be completed by water. Also in the previous work acyl substrates were based on SNAC compounds and only a small part of the ACP was mimicked in that way.[100]
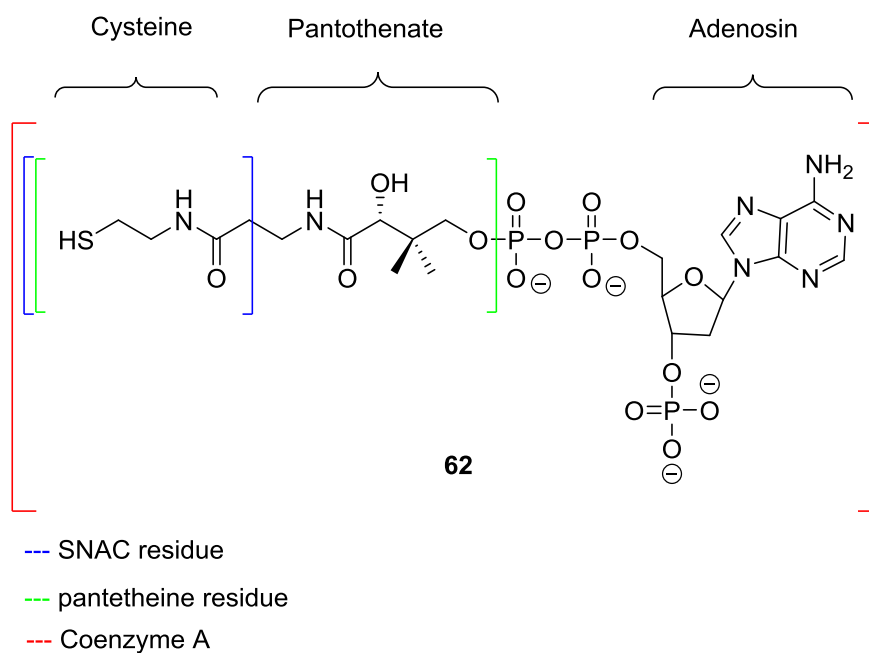
Figure 23: Structure of Coenzyme A **62**.

The current project is based on the use of pantetheine substrates which mimic more of the acyl ACP natural substrate of PKS domains (Figure 23). This longer chain should result in more interactions between the domain under study and its acyl substrate. A higher reaction rate should be observed in the reduction process. Possible interactions of the DH and ER domains will also be analysed by biophysical methods such as surface plasmon resonce (SPR) and isothermal calorimetry (ITC).

Finally, acyl transfer of squalestatin tetraketide **61** to the squalestatin core will be investigated. Possible precursors are necessary for the enzymatic investigation. The focus will be on the synthesis of three possible candidates that could be involved in the biosynthesis. The counterparts to the squalestatin cores will also be prepared. Substrates with pantetheine and CoA residues will be synthesized. Possible differences between these substrates will be investigated and analysed.

2.0   Project 1: Investigation of the Programming of the Isolated ER Domain of the Squalestatin Tetraketide Synthase

Fungal iterative HR-PKS show distinct and often complex programming. It is clear that systems such as SQTKS can build polyketides which possess a similar level of structural complexity to those synthesised by modular PKS, but the use of a single iterative PKS module makes the fungal PKS highly efficient. However, the mechanisms of programming of these types of PKS are not clear. For modular systems the programme is controlled by: the number of modules (*i.e.* chain length); the presence or absence of β-processing domains within modules (*i.e.* extent of functionalisation at each β-position); and individual domain selectivity, for example by the AT domains, which controls the selection of extender units (*i.e.* the methylation pattern). Furthermore, modular PKS can control the stereochemistry of each α- and β-position, and this is usually controlled by the selectivity of the KR domain (β-hydroxyl positions) and the ER domain (α-alkyl positions).

The only one of these programming methods which is available to fungal PKS is individual domain selectivity. Some evidence has been collected to-date to support the idea that the individual domains might control their own programming. For example the Cox group have shown through *in vivo* domain swaps that the tenellin PKS *C*-MeT domain appears to control its own 'programme' (section 1.5); while the Vederas group have shown that isolated catalytic domains of LNKS also have distinct selectivity preferences for different polyketide intermediates (section 1.5). Since SQTKS itself is too large to express as a single protein, we planned to use *in vitro* studies of isolated domains from SQTKS to determine their substrate- and stereo-selectivities.

The chemical programme of SQTKS can be inferred from the structure of squalestatin tetraketide **61** itself (Scheme 20). All β-processing domains are functional after the first two extension cycles, but the *C*-MeT and ER are inactive after the third extension, and the KS also does not act again after the third extension. There must also be a cryptic off-loading step which removes the polyketide from SQTKS at the end of biosynthesis, but it is not known how this happens.

Since the ER also sets the stereochemistry of the two asymmetric centres of SQTK **61** we decided to start our studies by investigating it, and we thus planned to produce the isolated ER domain and study its interaction with various substrates. In addition we planned to investigate its setereoselectivity.
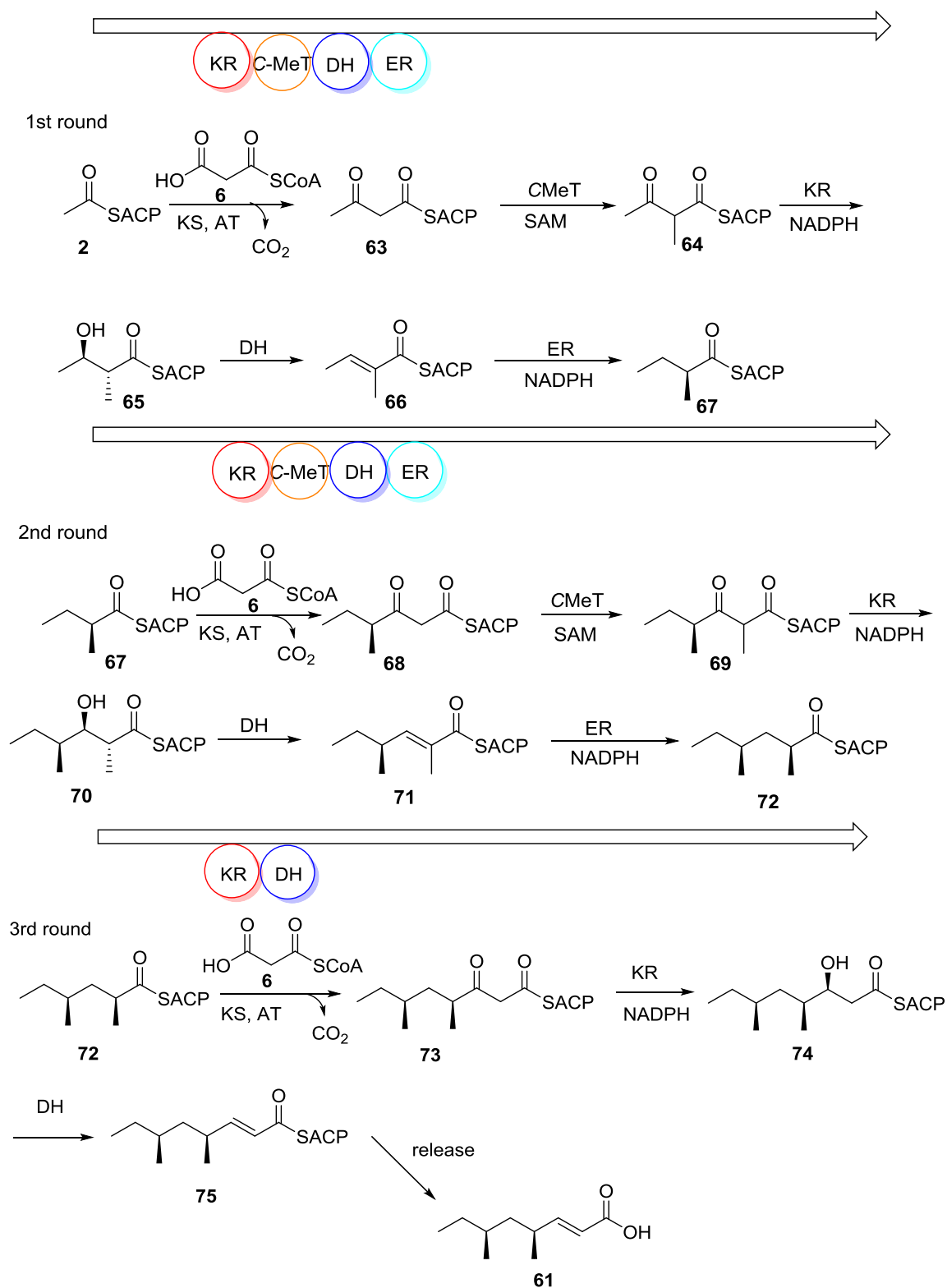
Scheme 20: Different extension steps of the squalestatin tetraketide synthase (SQTKS).[98]

2.1   Previous Studies of ER domains from FAS and PKS

The ER domain is the final enzyme of the modification set of enzymes that can be active in the β-processing cycle of a polyketide synthase. It belongs to the medium chain NADPH-dependent dehydrogenase/ reductase family (MDR). The enzyme is built of two structural subdomains: a substrate binding and a co-factor binding domain combined by a linker region. The stereochemistry of the α-position is determined by this enzyme *e.g.* the 2*R* or 2*S* configuration (Figure 23). The stereochemistry is controlled by the face-selectivity of the reprotonation at the α-position. Which amino acid residues are necessary or important is currently unclear.[22,101,102]
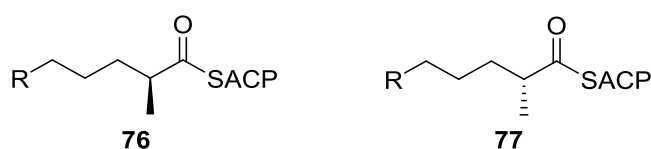
Figure 23: Possible stereochemical outcomes of the ER domain.

Only a few studies have been performed to determine the possible catalytic residues in the active site of an ER domain. The mechanism most likely involves transfer of a hydride to the β-position of the reacting substrate, to create an intermediate enol(ate) **78**.
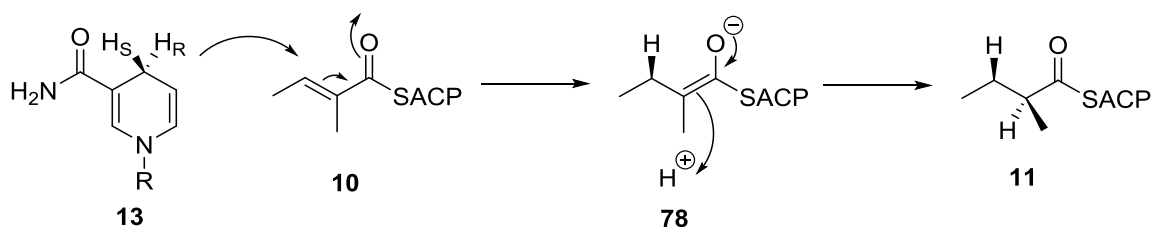
Scheme 21: Proposed mechanism of the ER domain.

The collapse of **78** and its reprotonation at the α-carbon sets the stereochemistry, but residues involved in activating and orienting the substrate, and in stabilising the intermediate and actively reprotonating **78** have not been conclusively identified (Scheme 21).[103]
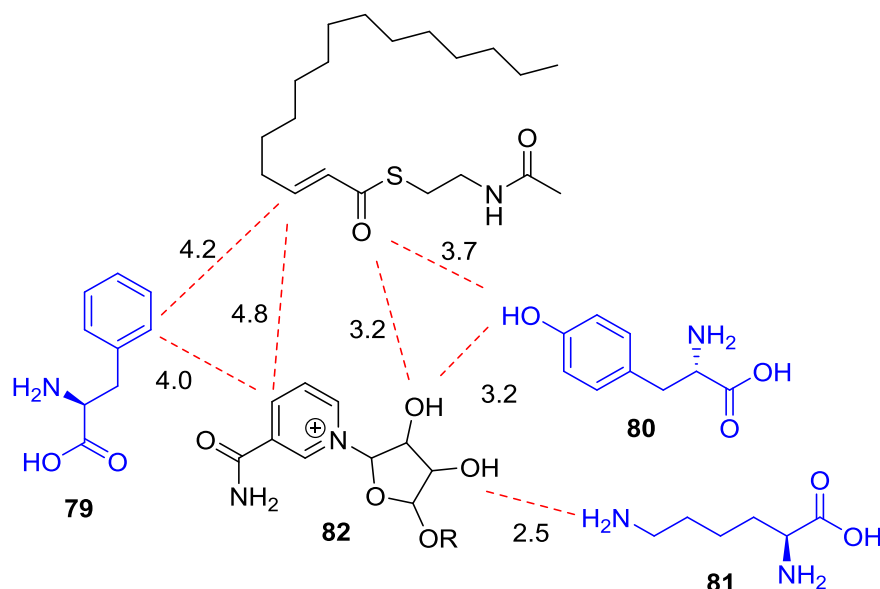
Figure 24: Proposed catalytical triad involved in the reduction process. Distances in Å.[104]

The crystal structure of the *Mycobacterium tuberculosis* FAS ER-ACP didomain was obtained in complex with NAD^{+} **82** and an acyl-substrate (Figure 24). The *trans* double bond is positioned near to the nicotinamide (4.8 Å). The *p*-hydroxyl of a tyrosine residue **80** can interact by hydrogen-bonding with the substrate carbonyl oxygen (3.7 Å). It is proposed that this interaction stabilizes the enolate during the reducing step. NAD^{+} **82** interacts with two other amino acids. It is speculated that phenylalanine **79** is involved to ensure that the hydride for the transfer is in the correct distance to the β-carbon of the substrate. How the final reprotonation works is unclear, and residues possibly responsible for this step are not identified.[104]

Further investigations were performed using mPKS ERs by Leadlay's group in Cambridge. To elucidate important residues that predict the stereochemistry of the final product, mPKS were sequenced and divided into two groups that produce *R* and *S* products. ER domains of the fourth module of erythromycin (Ery-4) and module 13 of rapamycin (Rap-13) were used in recombinant model PKSs. The modules were inserted into DEBS1 and combined with the TE domain of DEBS3 and to produce triketides.[105]

These chimeric PKSs produced a 2-methyl triketide lactone that is completely reduced at C-3. Studies showed that for the erythromycin hybrid the 2*S*-methyl product **83** is observed and for the rapamycin hybrid PKS the 2*R*-product **84** is produced (Scheme 22).[103,107-108]
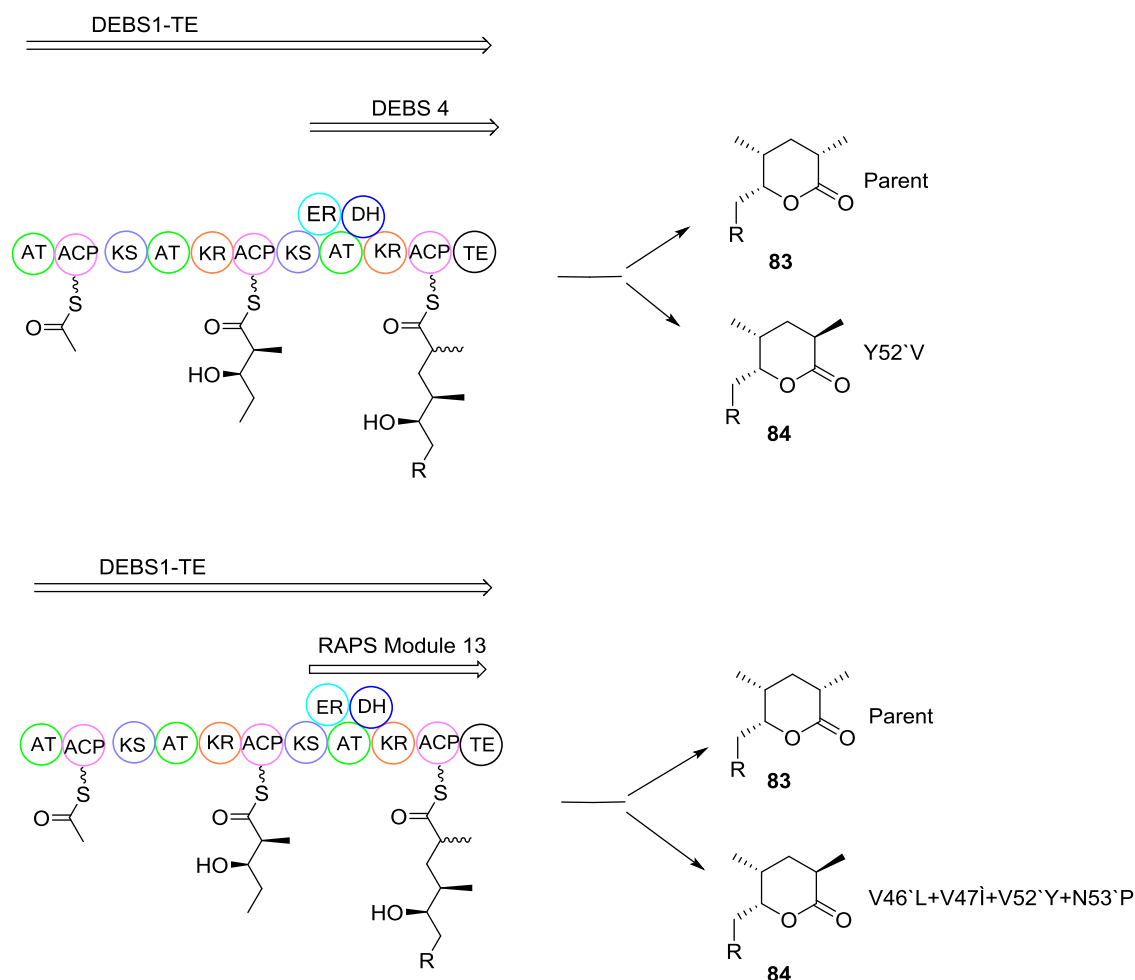
Scheme 22: Chimeric PKS of DEBS1-TE with DEBS 4 or RAPs 13.

It was found that one single amino acid shows good correlations with the configuration of the polyketide product. For *S*-configuration a tyrosine at position 52 (Tyr52) seems to play an essential role. If this residue is not present, the *R*-configured product is found (Scheme 22). For the *R*-configuration the three amino acids valine, alanine or phenylalanine were found at position 52. Module-4 of DEBS has a tyrosine at position 52, which is missing in module-13 of RAPS and replaced with valine. Replacing tyrosine by valine in the erythromycin module resulted in a 2*R*-configured final product **84**.[103,107-108]

In a later study Leadlay and coworkers then replaced the valine in the rapamycin module by tyrosine, but surprisingly this resulted in no change in the final product. Compound **84** was still produced. Position 52 seems to be an important point in the active site but there must be some additional residues that are involved in controlling the α-position stereochemistry.[103,107-108]

Further analysis showed that ER positions 46, 47, 52 and 53 are possible key residues for predicting the stereochemistry of the α-position. In the ER which produces the 2*S*-configured triketide lactone **83**, positions 46 and 47 contain leucine or isoleucine; proline is present at position 53. The 2*R*-configured product **84** is produced by an ER which has valine (46, 47) and proline (53) residues in these positions. Mutations of RAPS module-13 at these positions produces a small proportion of the 2*S*-methyltriketide lactone **83** (Scheme 22).[103,107-108]
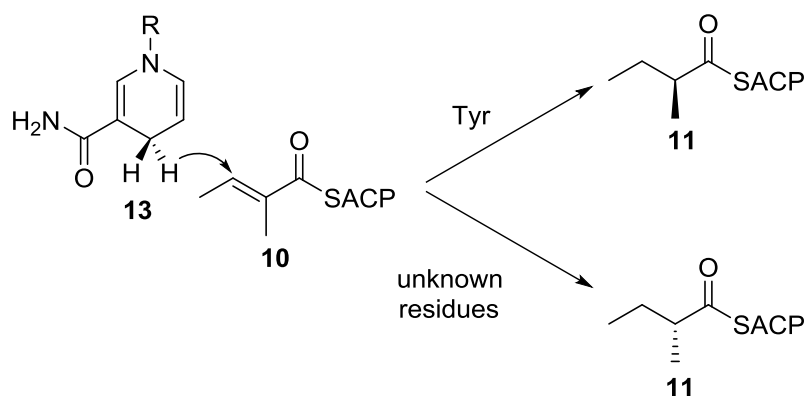
Scheme 23: Prediction of chemical outcomes of the ER domains.

A possible explanation is as follows: The hydride of NADPH **13** attacks the β-position of the double bond forming an enolate intermediate. After that a protonation at the α-position takes place either at the *re-* or *si* face. The results of Leadlay and co-workers showed that often a tyrosine residue is the proton source in the *re-* face that yields in an *S*-α-substituent. In the absence of this tyrosine the protonation occurs from the other side which results in a *R*-α-substituent. Which residue is the source of the proton in this case is unclear (Scheme 23).

Another example of these essential amino acid residues in ER enzymes was published by Erb and coworkers who also highlighted a tyrosine residue at position 79 as the cryptic proton donor. In contrast to Leadlay, Erb investigated a yeast mitochondria reductase which was a *pro*-2-*R* specific ER domain. A replacement of the tyrosine and a tryptophan residue was performed. A redesigning of the active site was expected to change the stereochemistry. These residues were replaced with phenylalanine and glutamic acid respectively. A pro-2-*S* specific ER was generated by the mutation. This was in contrast to the original active site.[109]

Whether these investigations by Kwan, Leadlay and Erb can be transfered from modular to iterative PKS enzymes is not clear. The SQTKS-ER could also use residues like tyrosine in the active site that act as a proton donor. Sequence alignments between SQTKS-ER and EryER4 and RapER13 showed more than 35% identity to the PKS ER domain. Comparison of the yeast sequence with the modular PKS enzymes showed at position 79 always a tyrosine. This position in the SQTKS-ER is occupied by leucine and the other specific residues from Leadlay's study show no similarity to those in the ER of SQTKS.

There are several tyrosine residues in the sequence of SQTKS-ER but only the amino acids around the tyrosine at position 152 showed some identity in SQTKS, RapER13 and EryER4 (Figure 25). This tyrosine residue is placed in the binding site of NADPH.
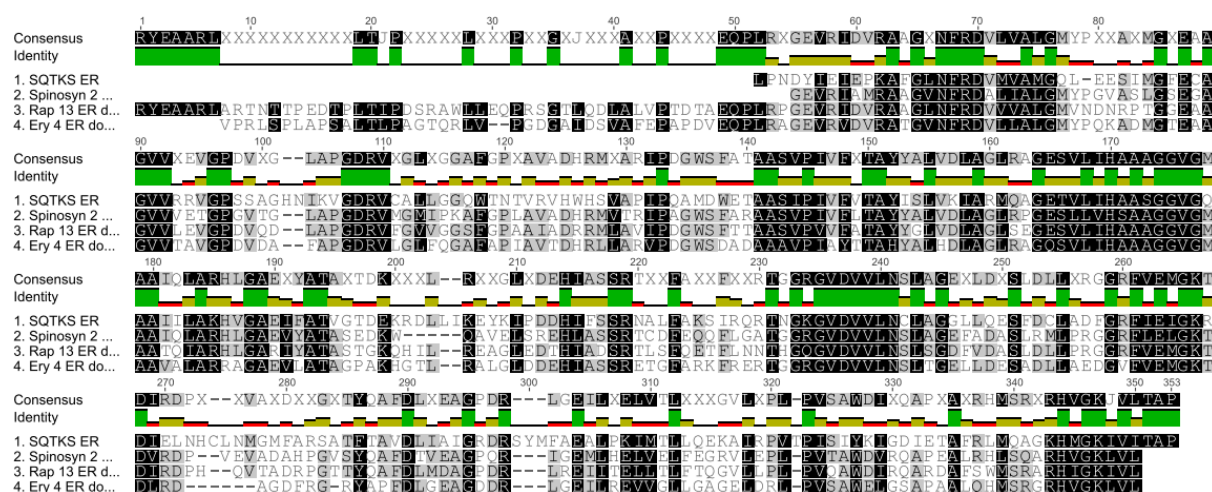
Figure 25: Sequence alignment of SQTKS, RapER13 and EryER4.

Other parts where a high similarity is shown between the three ER domains is within the amino acids from 57 to 76. These amino acids are a part of the substrate binding site. Position 56 has a tyrosine residue in SQTKS but it seems very unlikely that this residue is important for the stereochemical outcome. This residue is far away from the reduction position in the model of SQTKS-ER (section 2.4).

None of the tyrosine residues found in SQTKS-ER align with the tyrosine residues of EryER4 (position 78) and the valine residue of RapER13 (position 78) that are (possibly partly) responsible for the stereochemical outcome of their PKS enzymes. In the sequence of SQTKS-ER a leucine residue is placed at this position. If tyrosine is the important residue, in SQTKS-ER the amino acids should be similar to the one of

other PKS enzymes. If the tyrosine is not the essential residue, there must be other residues responsible for the stereochemical outcome. They must be positioned on the other site of NADPH and near to the double bond. Arginine and aspartic acid are two possible candidates for this protonation.

In contrast to most modular polyketides the spinosyn PKS module two (SpnER2) has an ER domain that acts as a monomer, confirmed by size exclusion chromatography. This is in contrast to the experimental analysis of SQTKS-ER. Sequence alignment of SpnER2 and the SQTKS-ER shows an identity of 34%.[72] The crystal structure of SpnER2 shows the residues lysine (position 264) and aspartic acid (position 288). They are possible candidates for stabilizing the reduction intermediates or directly involved as proton source. Both residues are found in the active site at a distance of 6 Å away from the nicotinamide hydride. These residues are potential candidates for taking part in the protonation and stabilizing the substrate or possible intermediates. The alignment of the sequences show that for the SQTKS-ER both residues are available, only separated by 22 amino acids. The distance to the highly conserved pyrophosphate binding motif (GGVGMA) is 84 amino acids. This is similar to the distance based on the crystal structure of SpnER2.[72]

2.2   Aims of the project

To get more information about the programming of iPKS, investigations of the isolated ER domain of SQTKS were performed. The focus of the investigation was the stereocontrol and the substrate selectivity of the isolated protein. The ER domain should be programmed since it sets two stereocenters in the final tetraketide **61** and cannot reduce the teraketide intermediate.

Programming could be controlled by substrate recognition,[100,101] and this could be tested by small molecules that vary in chain length, methylation pattern or the geometry of the double bond. Testing the programming using acyl-ACP substrates would be very difficult, due to the size of the ACP. Historically the ACP was mimicked by SNAC substrates[100], but since investigations of the isolated ER with these substrates gave poor results in previous studies it was decided to produce pantetheine substrates here. The pantetheine substrates mimic more of the phosphopantetheine link to the ACP. We hoped that they may interact more strongly with the isolated ER

domain. If this is the fact, then the double bond should be reduced faster than in the equivalent SNAC compounds.

The synthesis of structurally different pantetheine substrates is the first aim of this project. The substrate library will be include compounds with different chain length, methylation patterns and the geometries of the double bond. The second aim is the enzymatic investigation of the isolated ER domain with these pantetheine substrates. A stable kinetic enzyme assay has to be develop to analyse the different acyl pantetheine substrates. The third aim is the investigation of pantetheine substrates in the presence of **61**. Is there any influence of **61** on the isolated ER domain and is the effect of **61** in enzyme assays detectable. It is possible that **61** may act as an inhibitor of the ER.

2.3   Results

2.3.1 Isolation of the Single ER Domain of SQTKS

In order to investigate the programming of the ER domains from SQTKS the *phpks1* gene was reconstructed using cDNA and optimised for *E.* coli expression. The reconstructed gene was used as a template for PCR so that several single domains coding regions could be isolated. A separate investigation by David Ivison led to the production of 22 different soluble protein constructs, including single domains. David Ivison produced soluble protein of 22 different constructs.[100,101]

The generation of soluble protein was achieved by heterologous expression of a plasmid contributing the domain coding region of interest. The expression plasmid was transformed in *E. coli* Rosetta II cells. The expression vector pET28a(+)_ER was constructed (Figure 26) in previous work by David Ivison to express the ER domain in *E. coli*.[100,101]
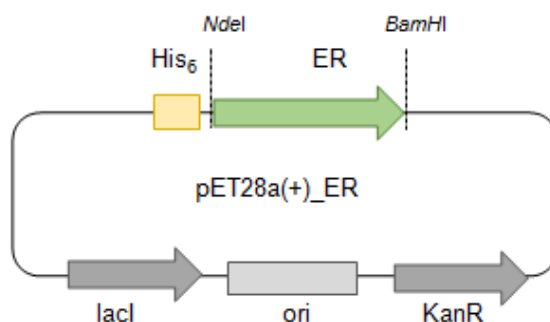
Figure 26: Plasmid in pET28a(+)_ER which was transferred in *E. coli.*

In this project pET28a(+)_ER was transformed into the bacterial producer strain *E. coli* BL21. A successful transformation of the plasmid into *E. coli* was confirmed by colony PCR amplifying the DNA insert coding for the ER domain. A PCR product of 906 bp was generated, which is the same size as the PCR product from SQTKS producer *Phoma* sp. (Figure 27).
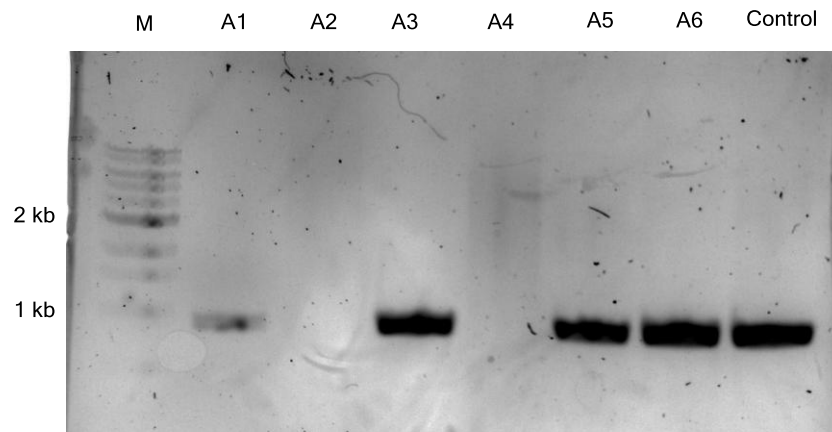
Figure 27: Colony PCR control of the fresh transformed cells. Lanes A1, A3 and also A5 and A6 show in comparison to the control the successfull transfer. The size of 1 kb confirms the expected result.

Strains positive for the SQTKS-ER domain were grown in a starter culture of 2TY-medium. This starter culture was incubated over night. After that it was diluted 1:100 in 2TY-medium (1-2-litre). The protein production was induced with *iso*-propyl β-D-1-thiogalactopyranoside (IPTG) at an OD_{600} of 0.6 and at 16 °C. After incubation over night the cells were harvested by centrifugation. The cells were broken by sonification and the resulting lysate was purified by a Nickel NTA column. The final protein was expressed as a His_6-tagged fusion protein and isolated by affinity column in the first step.
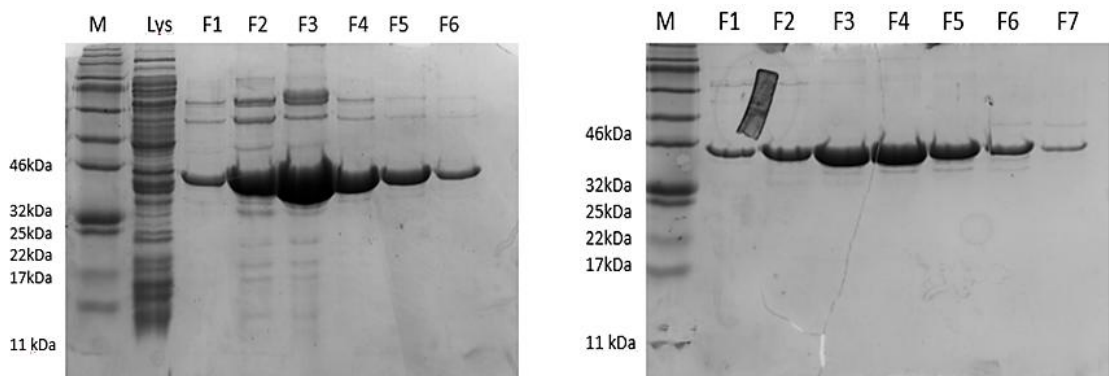
Figure 28: SDS-page of NiNTA and gelfiltration purification of the ER domain.

In the second step of the protein purification, the protein was purified by gel filtration to remove final impurities. Finally the resulting protein was analysed by SDS page (Figure 28). The purified protein matched the expected size (38.7 kDa). Isolation of 20 to 25 mg of protein (Bradford) per expression was typical.[101]

The ER domain forms a discrete dimeric protein when analysed by calibrated gel filtration (Figure 29). This is consistent with the structure of mFAS in which the ER domain appaers to have a large dimerisation surface.[61] This contrasts to some other PKS ER domains, such as from the spinosyn modular PKS, which show monomeric behaviour.[72]
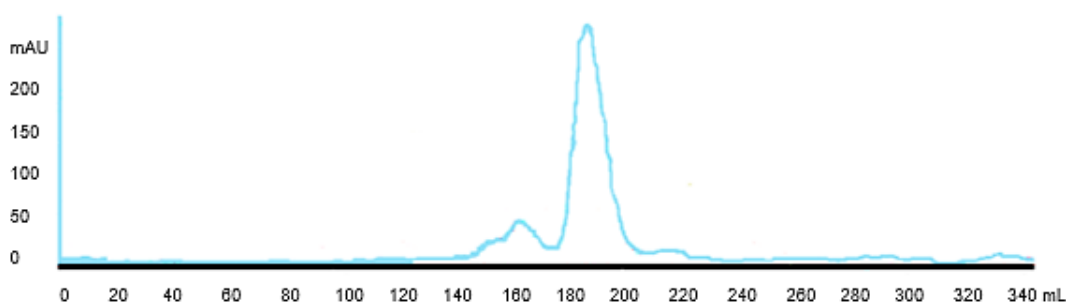
Figure 29: Purification chromatogram of ER domain.

For the calibration of the gel filtration column the three enzymes, Carbonic anhydrase (28 kDa, **3**), BSA (66 kDa, **2**) and Apoferritin (443 kDa, **1**), were used. The resulting UV FPLC run of the calibration is shown (Figure 30). This calibration made it possible to investigate the isolated enzyme between their behaviour about oligomerization. The calibration run was performed in the same buffer as the size exclusion purification of SQTKS-ER.
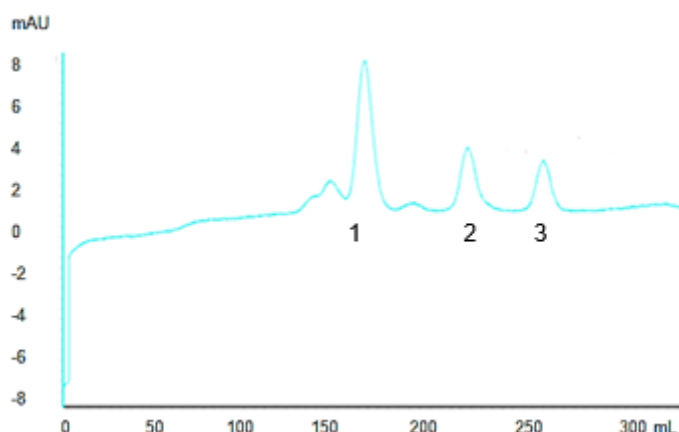
Figure 30: Size-exclusion chromatogram of calibration enzymes.

2.3.2 Investigation of Programming by holo-ACP Mimics

To determine the programming rules within the ER domain, a substrate library of several ER substrates was synthesized. Since ER proteins usually process ACP-bound substrates, perfect synthetic substrates should be ACP-bound. Some examples are known from the literature of the use of acyl-ACP substrates in kinetic assays.[110] However since ACP-substrates are hard to produce and analyse, we decided to use acyl pantetheines and acyl SNACs (Figure 31) which are widely used as acyl-ACP mimics.[111,112]
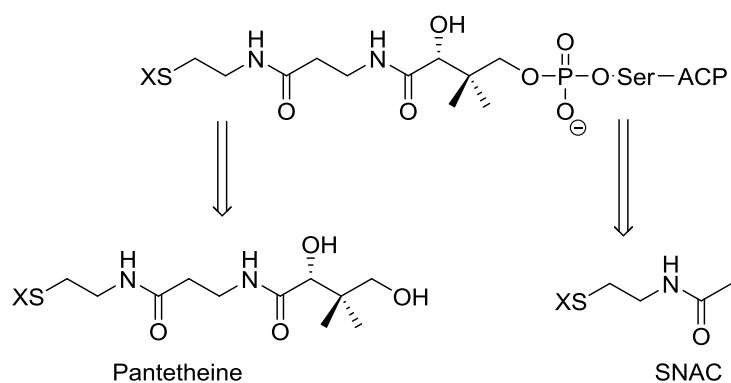
Figure 31: Structures of used substrate residues.

In addition to the natural substrates (**85**, **93** and **102**), this library includes a broad range of unnatural substrates, *e.g.* with modifications in chain length; methylation pattern; methylation position; olefin stereochemistry; and even ethyl-substitution (Figure 32).

We also included compound pairs such as **93/94** and **102/104** to test whether the ER is sensitive to stereocentres further away from the reaction centre. Previous investigations by Doug Roberts were made with SNAC compounds.[100]
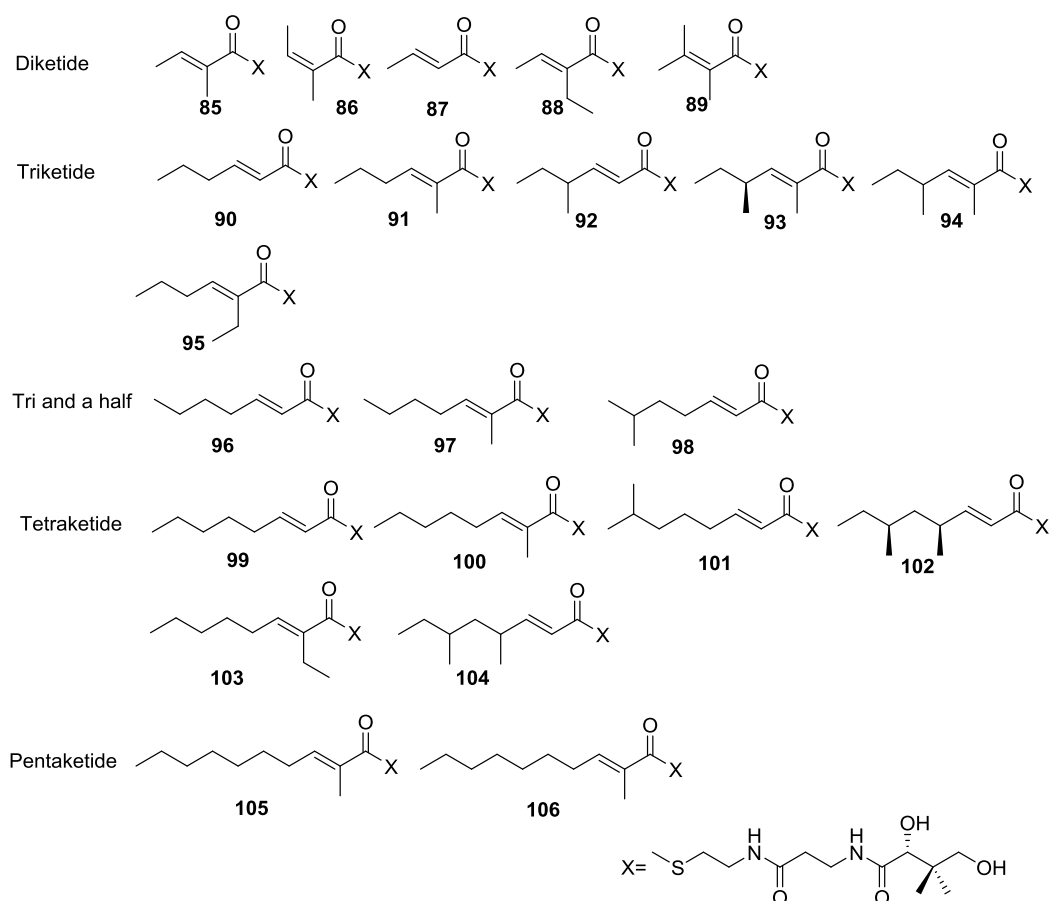
Figure 32: Table of synthesized pantetheine substrates.

In early work in this project SNAC and pantetheine substrates were directly compared using purified ER protein. Assays were set up which contained the ER protein, the SNAC or pantetheine substrate at identical concentration, and NADPH **13** which is the ER's preferred cofactor. As substrate is reduced, **13** is oxidised and this is observed spectro-photometrically at 340 nm. The rate of consumption of **13** is thus directly related to the reduction of the substrate. A similar method was developed by Kapoor *et al.*[113]

The reduction of tigloylpantetheine **85** and tigloyl SNAC **107** were directly compared (Figure 33). To observe significant data in the SNAC assay, five times more enzyme was required than for the pantetheine to get comparable data. The pantetheine substrate is reduced twelve times faster than the SNAC substrate. The differences in the assays are caused by the structure of the two substrates. It seems that the pantetheine must interact with the active site of the ER domain. Based on this early assay we decided to use only acyl pantetheines as substrates.
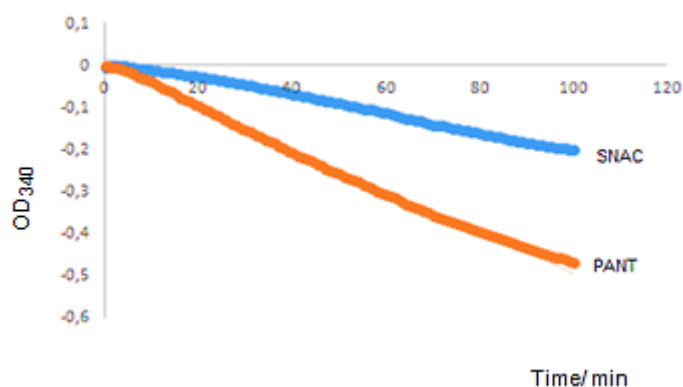
Figure 33: Enzyme assay of tigloylpantetheine 85 and tigloyl SNAC 107.

Preliminary experiments in previous work showed that it is possible to synthesize small pantetheine compounds. For this, commercially available pantethine dimer was cleaved with DTT to give the free thiol, and addition of acyl chlorides 108-111 generated the corresponding pantetheine thiolesters 113, which were then purified by HPLC (Scheme 24).[72]
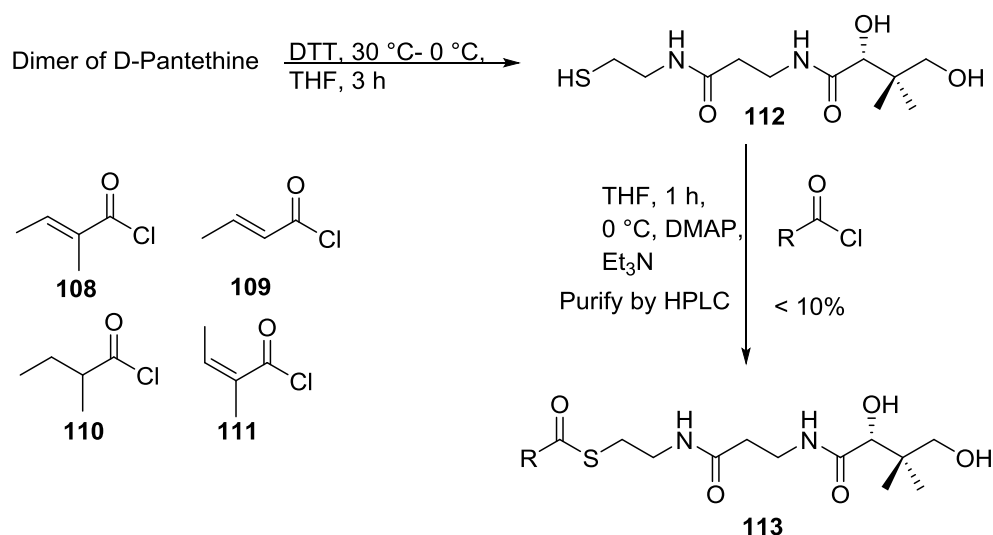
Scheme 24: First method for synthesis of pantetheine substrates.

For diketides this reaction worked well, but for longer substrates it was not effective. One problem was the low solubility of the pantetheine dimer in organic solvents which limited possible acyl coupling reactions. Small acids and acid chlorides were commercially available and were used directly as shown in scheme 24.

2.3.3 Synthetic Route of Pantetheine Substrates

For longer and modified substrates an alternative synthetic route was developed. This starts with carboxylic acids that are coupled to a protected pantetheine residue which can be easily handled in organic solvents and purified. The final step is deprotection and purification by mass-directed HPLC.

The required acids were created in the following different ways. Knoevenagel reactions were used for unmethylated α-unsaturated acids (Scheme 25). For this reaction, different aldehydes **114** were dissolved in pyridine in the presence of malonic acid. The elongated intermediate of the reaction was then decarboxylated in an additional reflux reaction at 115 °C. Finally, acidification and extraction resulted in the formation of products in high purity (>95%) and acceptable yield (40 to 50%). In this way it was possible to create 2-hexenoic- **116**, 2-heptenoic- **117**, 2-octenoic- **118** and 2-decenoic **119** acids.[115,116]
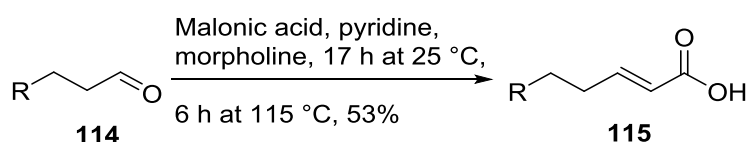
Scheme 25: Knoevenagel reaction of different carboxylic acids.

Wittig reactions were used to create the α-methylated unsaturated carboxylic acids. Aldehyde **114** was used as the starting material for elongation by Wittig salts. Both starting materials were stirred in CH_2Cl_2 at RT for 18 hours and were finally purified by flash column chromatography. The corresponding esters **120** were cleaved by potassium hydroxide in a mixture of ethanol and water. After three hours under reflux the mixture was acidified and extracted to isolate the final α-methyl-unsaturated acids **121**. The produced substrates imitated tri-, tetra- and pentaketides (Scheme 26).[116,117]
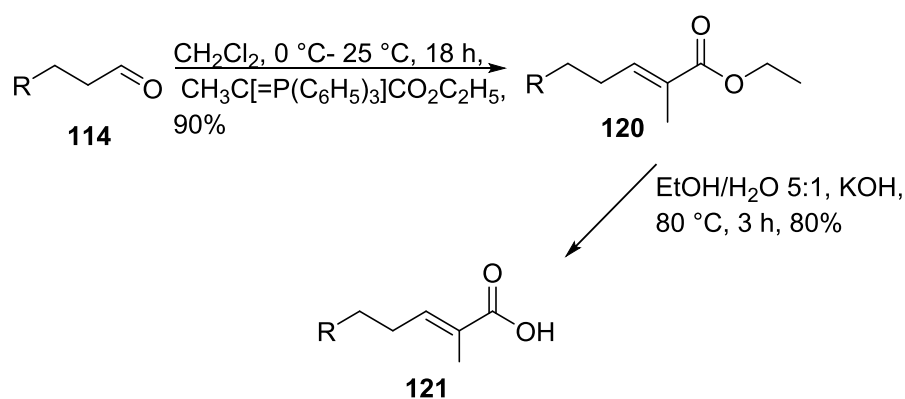
Scheme 26: Synthesis route of α-methylated carboxylic acids.

In the third method a reaction route was developed to synthesize α-ethylated carboxylic acids. Triethyl-2-phosphonobutyrate **122** was deprotonated by potassium *tert*-butoxide in THF at 0 °C and then **114** was added to give the corresponding ethyl esters **123** and **124**. In this reaction both geometries of the double bond (*E* and *Z* ratio 2:1) were synthesized. Finally, the esters were cleaved again with potassium hydroxide to the corresponding carboxylic acids **125**, **126**. Ethylated hex-2-enoic **127**, hept-2-enoic **128** and oct-2-enoic **129** carboxylic acids were created using this method. The *E*- and *Z*-isomers were then coupled to pantetheine resdues and used in the enzyme assays without separation (Scheme 27).[118]
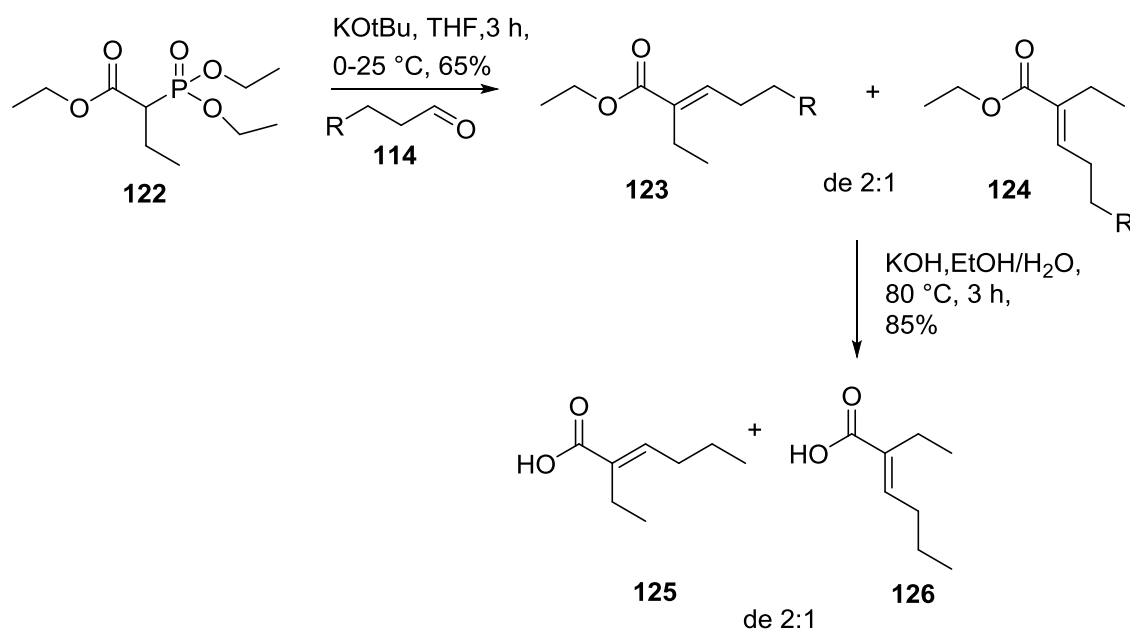
Scheme 27: Synthesis route of α-ethylated carboxylic acids.

Several different carboxylic acids were prepared using a fourth route. A one pot reaction is shown for this synthesis in literature that combines oxidation and olefination.[119] An example is the synthesis of 7-methyloct-2-enoic acid **132** and 6-methylhept-2-enoic acid **135** (Scheme 28). 4-methylpentanol **130**, 5-methylhexanol **133** were oxidised (PCC) to form the corresponding aldehydes in a one pot reaction, which was followed by TLC. The aldehyde was then treated *in situ* with a Wittig salt to give the corresponding methyl esters **131** and **134**. The addition of celite and magnesium sulphate was used to bind the reduced chromium salts and aid removal by filtration.[119,120] After purification by flash column chromatography the resulted esters can be cleaved on the usual way. The acids could be isolated in a yield around 70%.[118,121]
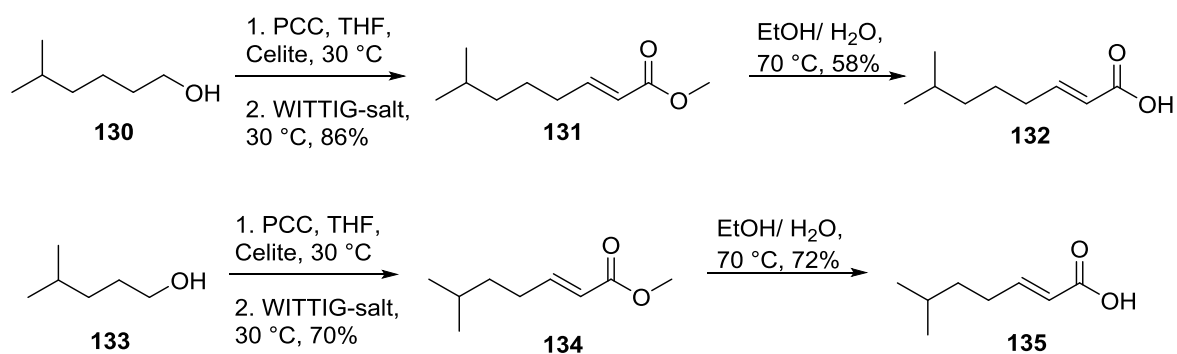
Scheme 28: Synthesis of 7-methyloctenoic acid **132** and 6-methylheptenoic acid **135**.

A racemic version of SQTK **136** was synthesised (Scheme 29). This began with racemic 2-methylbutyraldehyde **137**. A Wittig-reduction-Wittig strategy was used to obtain **142** as a racemic mixture of diastereomers. At the starting point of the investigation, no enantiopure version of SQTK was available. Parts of this synthesis were performed by Adeline Kongtso during the supervision of her Masters Thesis.[122,123,124]
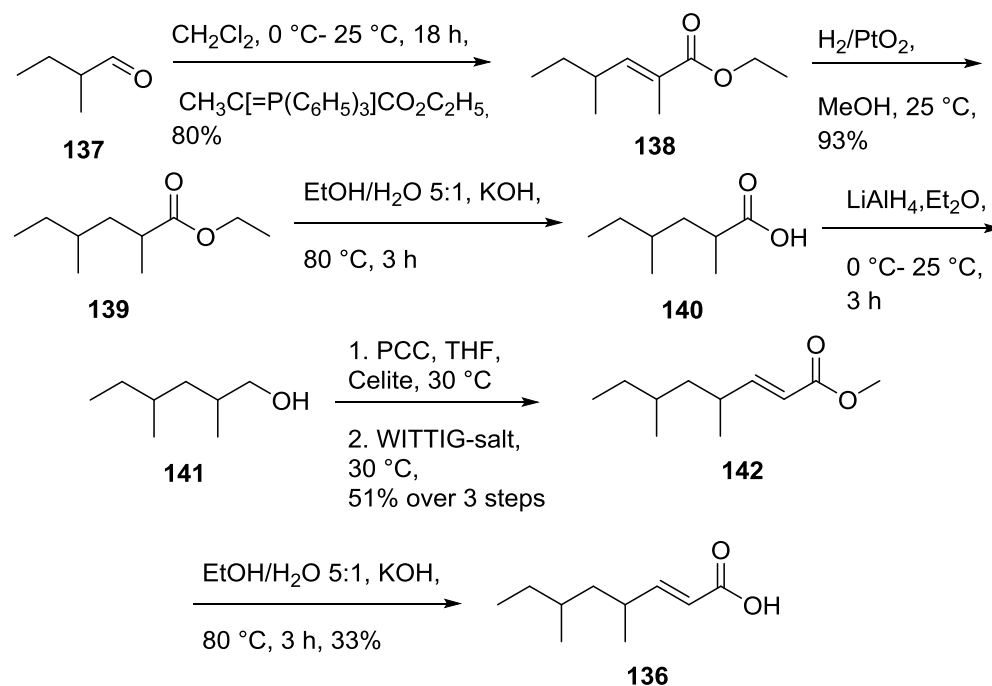
Scheme 29: Synthesis of racemic version of SQTK **136**.

The enantiopure tetraketide **61** was synthesized using Squalestatin S1 **56** as starting material. **56** was cleaved with potassium hydroxide. The final solution was extracted at pH 11 with sodium hydrogencarbonate. After that it was acidified to pH 1 and extracted with ethyl acetate. Compound **61** was obtained without by-products in a yield of 86% (Scheme 30).[118]
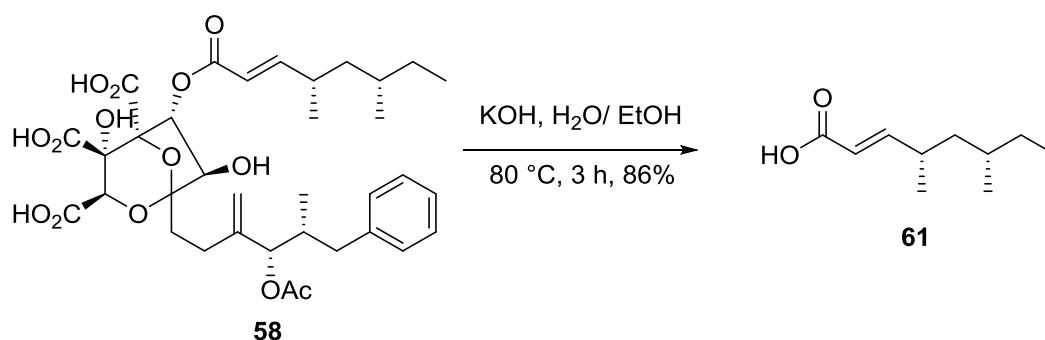
Scheme 30: Synthesis of enantiopure SQTK **61**.

Once the carboxylic acids had been synthesised we then set out to find good methods to couple them to pantetheine. Townsend and coworkers published a method to synthesize a possible precursor for pantetheine in 2013. First pantothenic acid hemi-calcium salt **143** was protected in actone at 25 °C in the presence of *p*-toluensulfonic acid to give the acetal **144**. After that, a coupling with CDI and cysteamine in THF was used to generate the pantetheine dimethyl ketal **145**. The yields of 84% for **145** are similar to the ones described by Townsend *et al*.[49]
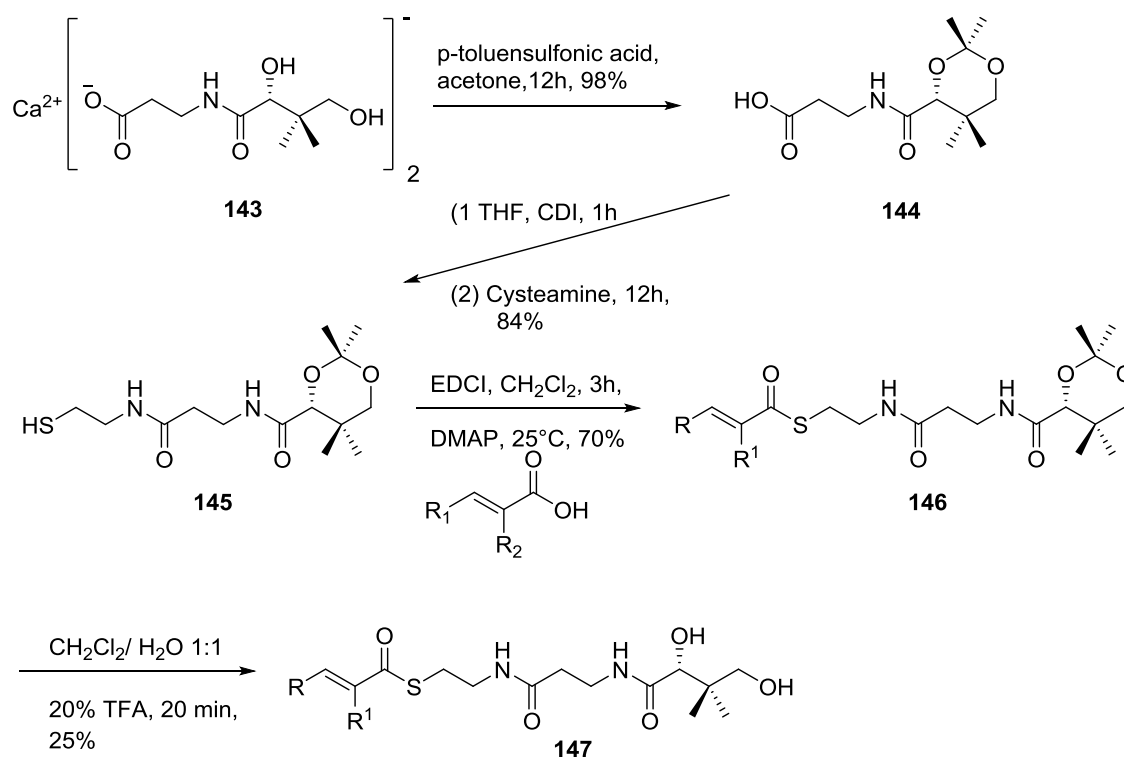
Scheme 31: Synthesis route of pantetheine substrates.

The protection changes the solubility of the pantetheine so that **145** is soluble in CH_2Cl_2, EtOAc and MeCN. It was now possible to do an EDCI coupling, followed by deprotection and purification by HPLC, to get the final pantetheine substrates **147**

(Scheme 31). In total, it was possible to synthesize twenty two pantetheine substrates which had differences in the methylation pattern, chain length, the isomerization of the double bond, and the methylation position. Yields and purity of the pantetheine dimethyl ketal substrates are not described in literature. Compared with other EDCI reactions for example the procedure of Carroll *et al.* that was used in the previous work by Doug Roberts the yield of 70 to 80% is in the expected area.[100,125] Several advantages are known in contrast to the synthetic route that was performed by Zheng *et al.* (section 2.3.2, Scheme 24). The pantetheine dimer and monomer are highly hydroscopic. A sticky oil is formed on air. In contrast to the pantetheine dimethyl ketal it is also only soluble in water, THF, methanol, and acetonitrile.[72,100]

The pantetheine substrates included the three natural substrates and 19 different unnatural substrates designed to probe the selectivity of the ER. For example, an ethyl group in the α-position should give information about the size of the ER active site at this position. This substrate library of diketides, triketides, tri and a half ketides, tetraketides and pentaketides completes the chemical part of the project.

2.3.4 Enzymatic Investigation and Substrate Selectivity

Kinetic investigation of the synthesized substrates described in section 2.3, should give further information about the selectivity of the ER and we hoped to be able to link this to the observed programming of the ER during the biosynthesis of squalestatin tetraketide **102**. We planned to measure V_{Max}/K_M values (known as the specificity constant) for each of the different substrates. In that way a quantitative, detailed comparison of the different substrates and the enzyme selectivity should be possible. Differences in the selectivity of the enzyme should be revealed by different substrate structures of the compounds.

Several early experiments were conducted to show that the reduction of the double bond can in fact be catalysed by the isoltated SQTKS-ER domain. These assays involved incubation of the ER enzyme with an SNAC or pantetheine substrate, such as **85**, and NADPH **13** in buffer at 25 ˚C. The reactions were followed by HPLC and the product **148** is clearly produced (Figure 34). However *discontinuous* HPLC-based assays are not convenient for measuring kinetic parameters. In order to obtain good initial rate data a

continuous assay is required. We developed a method based on the wavelength of the used cofactor **13** (340 nm). During the reaction the concentration of **13** decreases and this can be observed continuously at 340 nm.[100,113]
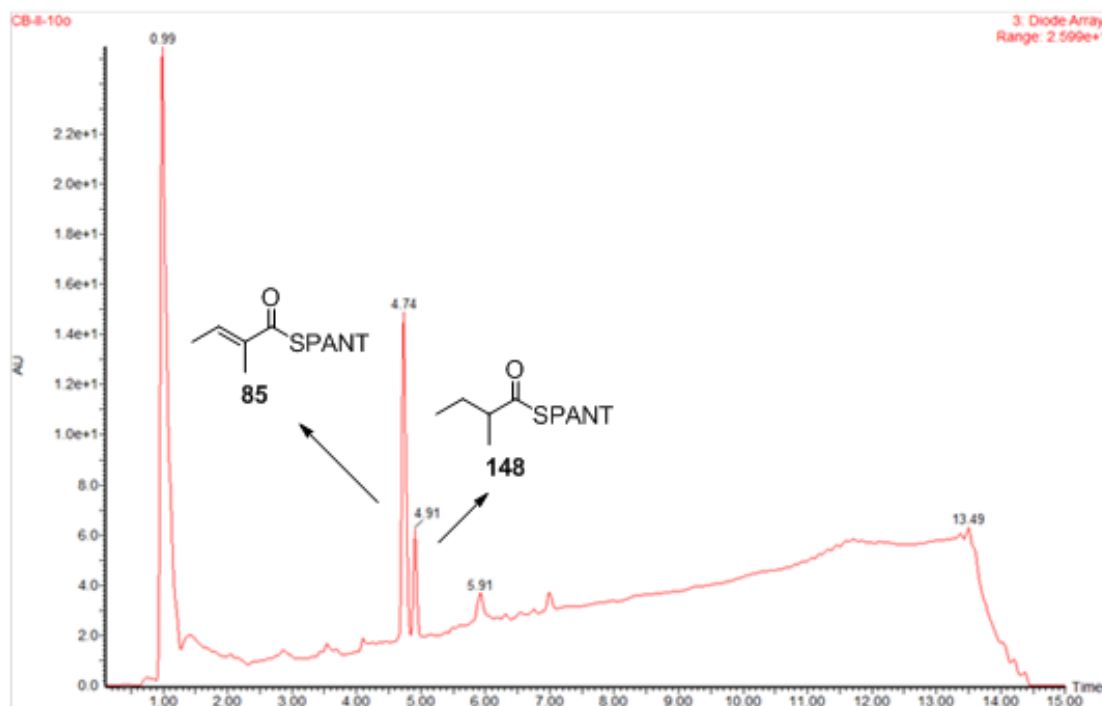
Figure 34: Analytical enzyme assay of tigloylpantetheine **85**.

We first tried to set up *in vitro* UV assays at 200 μL scale using 96 well plates.[100] However, no reproducible data was obtained.[100] The formation of air bubbles was observed in the wells, which severely influenced the absorbtion. Absorption gets measured from the bottom to the top in the instrument. Changing the buffer conditions to reduce the amount of glycerol did not show a significant effect. Much better data was obtained when the enzyme assays were performed in cuvettes. The volume was scaled up from 200 μL to 400 μL to reach the minimum required volume. The absorption was measured from the side so that formation of air bubbles was limited or had no effect on the assay. It was possible to collect reproducible data. Assays were performed with 50 mmol TRIS, 150 mmol NaCl and 20% glycerol buffer (Figure 35).

X= Pantetheine
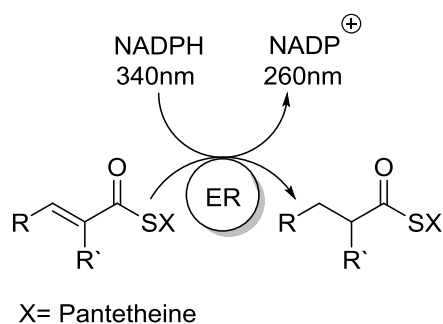
Figure 35: Reaction of the enoyl reductase in the present of NADPH **13**.

The enzyme requires the cofactor NADPH **13** to function, so this was added to the buffer in a 0.25 mmol concentration. Detection of NADH was not successful and showed no turn-over. Every substrate was measured in three technical replicates in substrate concentrations from 0.0625 to 0.625 μM (Figure 36).
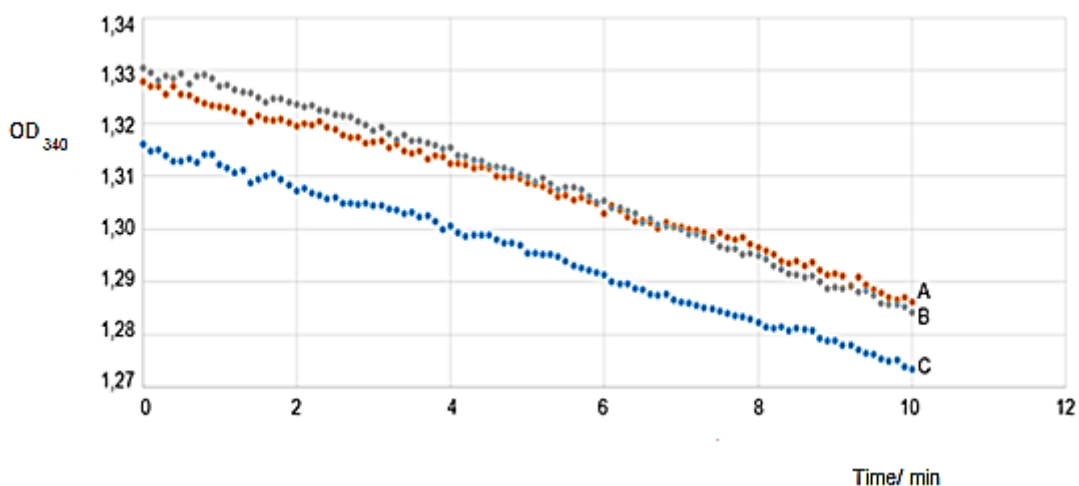
Figure 36: Absorption curves (A,B,C) of the three replicates of tigloylpantetheine **85** at 0.0625 μM.

Enzyme activity was standardised under constant conditions using ethyl-hex-2-enoyl pantetheine **95**, so that in every assay the same activity of the enzyme was used (SQTKS-ER, 0.08 U/μl). In the assays the absorption curve of consumed **13** was followed. After calculating the initial rates of the different substrates by Microsoft EXCEL the rate data were plotted with the software *Curve Expert*. In that way, it was possible to generate a nonlinear fit of initial rates in triplicate by direct fit to the Michaelis Menten equation (Figure 37).

Finally the curve gives information about the Michaelis Menten Constant K_M and the rate V_{Max}, and these values allow the comparison of the different substrates with each other. Although separate values can be obtained the value of V_{Max}/K_M (the

specificity constant) is the best way to directly compare the different substrates (Figure 38).
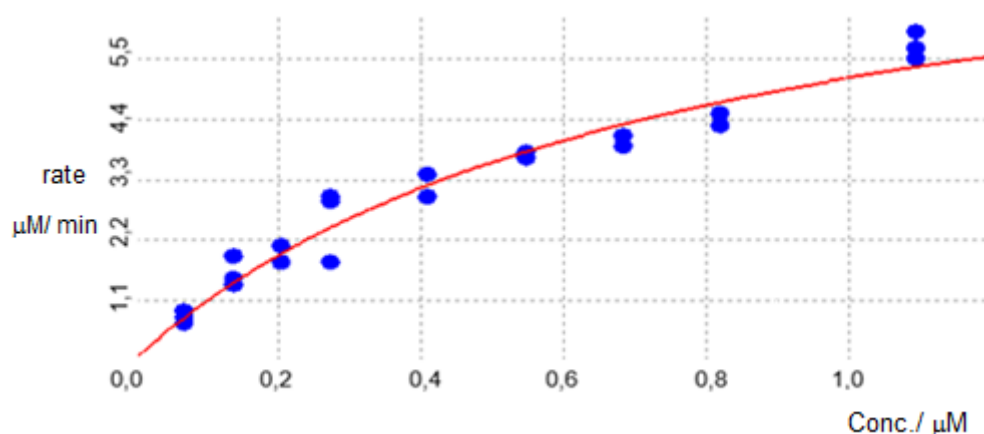
Figure 37: Michaelis Menten curve of **85**, substrate concentration against the rate.

The comparison of the different values shows that a methyl or ethyl group in the α-position seems to fit very well in the active site and be reduced very fast. This is visible for example by the results of compound **91** and **95**. It seems that at this position the shape of the active site has enough space to accept several different substituents in the γ- or ε-position. If the methylation is present at another position in longer carbon chains, the initial rates and V_{Max}/K_M values are much lower in comparison to α-methylated or α-ethylated substrates (compounds **92**, **93**, **94**). It was also possible to show that both *E*- and *Z*-isomers of the diketides **85** and **86** could be reduced successfully.

The fact that *Z*-olefins could be reduced by the enzyme is another indication of a broad substrate specifity. This shows that the ER domain is not selectively programmed to *E*-isomers, which are the naturally expected substrates.

The chain length of the substrates has some influence as well. For the diketides the substrates **85** to **88** could be reduced. Only the tetra-substituted form **89** shows no conversion to the reduced product. Triketides seems to be good substrates for the ER domain, which results in higher V_{Max}/K_M values (compounds **90**- **95**). The kinetic results of the tri and a half- and the tetraketides (**96**- **104**) show a smaller V_{Max}/K_M value than the di- and triketides. Also surprising are the enzyme assays of the pentaketides **105** and **106** that shows that they can be reduced by the ER domain.
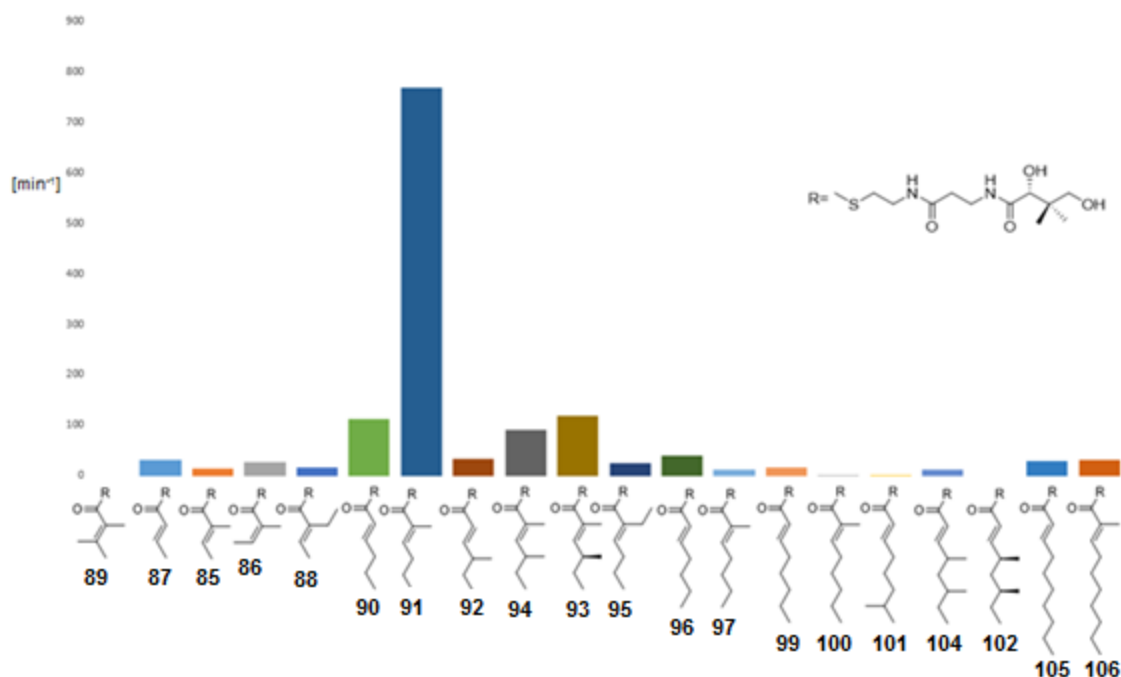
Figure 38: V_{Max}/K_M values of the different pantetheine substrates.

Interestingly, the result of the 4S-2-dimethylhex-2-enoyl pantetheine **93** showed a higher rate of conversion to the reduced product than the racemic version of this substrate **104**. From this result, it is not clear what effect the stereocenter at the γ-position plays, which is in one assay clear determined and in the other assay in a racemic form. The role of this position cannot be confirmed without testing the pure 4R-substrate **149** (Figure 39). In comparison with the racemic version, the assay using compound **93** ran 1.5 times faster. Therefore it might be expected that **149** should work similarly to an inhibitor and block the active site. Whether blocking is reversible or irreversible is not known at this time and needs to be further investigated. If this position is important, it should also be recognized in the enzyme assay of a stereo controlled 4S-methylated triketide.

149
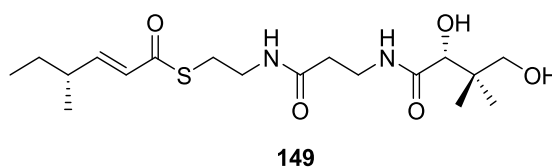
Figure 39: Structure of 4R-methylhex-2-enoyl pantetheine **149**.

Another example of the influence of the stereochemistry is the natural 4S,6S – tetraketide **102**, which is not measurably reduced by the ER in our kinetic studies. However the 4RS,6RS mixture of stereoisomers did show measureable reduction, so at least one stereoisomer of the tetraketide must be recognised and reduced.
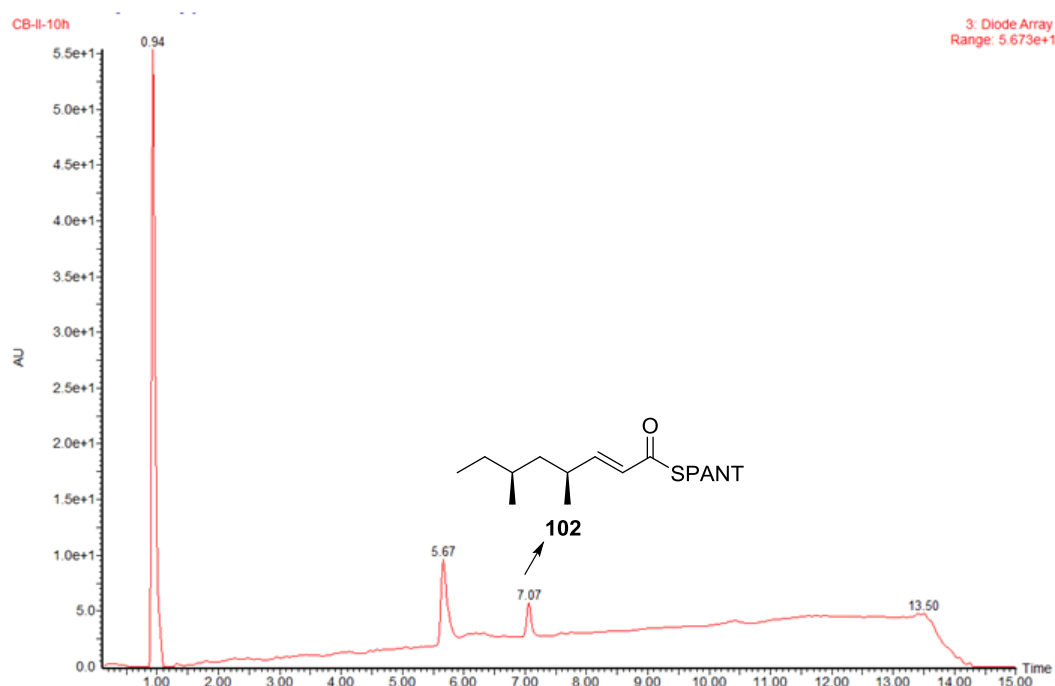
Figure 40: Enzyme assay of 4*S*-6*S*-dimethyloct-2-enoyl pantetheine **102**.

It seems that the ER domain is sensitive against 4*S*,6*S* dimethyloct-2-enoyl pantetheine **102**. Which of the three other stereoisomers can be reduced was not further investigated. Since the kinetic assay runs only for a time period of twenty minutes we tested in an analytical assay over a time period of 24 hours a possible conversion of **102** into the reduced product. Also in this assay no conversion was obtained (Figure 40).

2.3.5 Inhibition Test of SQTK

The kinetic results suggested that some compounds could not be reduced, but do not show if this is because the compounds cannot access the active site at all, or if they can enter the active site but not form a productive conformation for reaction. We tested these possibilities by setting up inhibition assays. If compounds can act as inhibitors it means that they can enter the active site.

The substrate **85** was incubated with the ER enzyme in the presence of different concentrations of **102** under same conditions as used previously. The rate of the reaction of **85** is lower (Figure 41) in the presence of the tetraketide **102**. It can be concluded that the tetraketide **102** can enter the active site of the ER domain but cannot be reduced, presumably because it cannot reach a productive conformation.

57
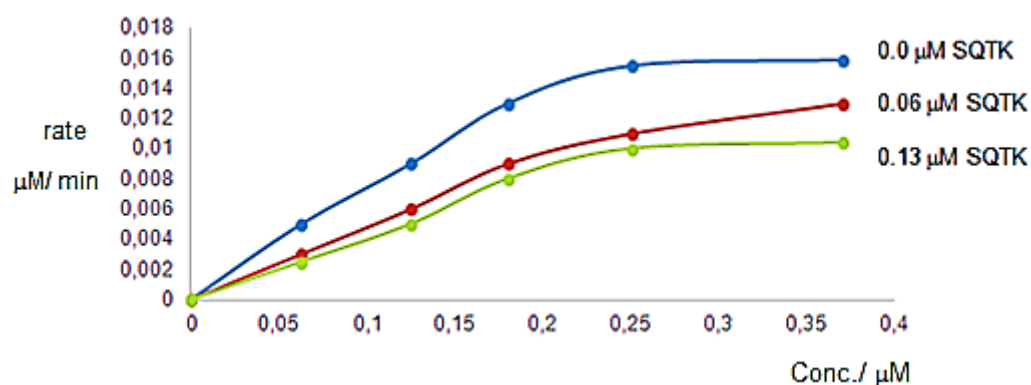
Figure 41: Enzyme assay of **85** in the present of different **102** concentrations.

Since there is still a reduction process of **85**, a reversible inhibition must take place. The fact that longer unmethylated pantetheine substrates can be reduced, as well as other stereoisomers of **102** shows that the ER is very sensitive to the methylation position and stereochemistry, and this presumably is the reason why **102** cannot be reduced by SQTKS *in vivo*.

2.3.6 Stereoselectivity of the Isolated ER Domain

The reduction of the double bond by NADPH **13** been studied in several investigations reported in the literature. In general, the 4-*pro-R* hydride of **13** is transferred and few exceptions are known. During the reduction four stereochemical outcomes are possible for the substrate and all of them are known in ERs from different FAS systems. Previous investigations were performed by isotope labeling experiments. By specific known dehydrogenases the position of the isotopic label was decided (Scheme 32).[126-128]
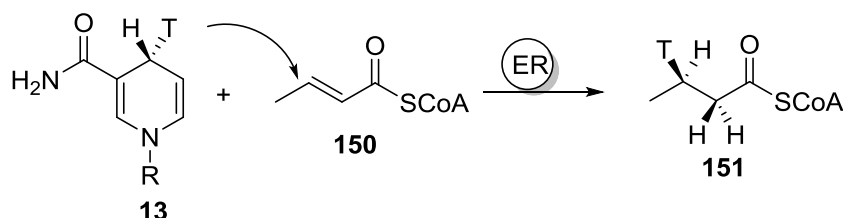
Scheme 32: Investigation of the hydride transfer of **13** to **150**.

The final product of SQTKS is released as 4*S*,6*S* dimethyl oct-2-enoic acid **61**. Since the ER catalyses the last β-modification step of the synthase, it must be responsible for the determination of the stereochemistry in the molecule. In addition to position C-2

also the hydride transfer of **13** to C-3 could be investigated. The two possible hydrides of **13** are available for this process.

The stereoselectivity of the isolated SQTKS-ER domain was investigated in previous work by Doug Roberts using Parker`s *in situ* NMR method for the determination of chirality of α-substituted carboxylic acids. The ER product 2-methylbutyric acid **151** was used. By adding 1*R*,2*R*-1,2-diphenylethylenediamine **152** to the NMR sample, resonances for the methyl groups of **151** are shifted enantioselectively, meaning the *R* and *S* enantiomers of **151** are resolved in the ^{1}H NMR spectrum (Scheme 33).[129,130]
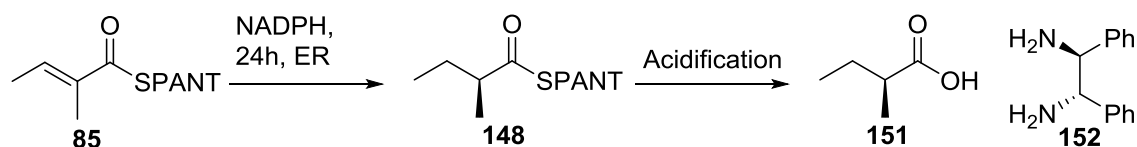
Scheme 33: Stereoselective investigation of C2-position.

If a single enantiopure compound was generated from the ER reactions, only a single set of resonances for 2*S*-2-methylbutyric acid **151** would be expected. Tigloyl-pantetheine **85** was incubated with the ER domain and **13** for 24 hours. Then the reaction product was isolated and hydrolysed. After that the mixture was acidified and extracted into CDCl$_3$ and two equivalents of **152** were added. It was shown that both product stereoisomers are formed and thus the isolated ER is not able to control the stereochemistry of the substrates in the α-position.[99,129,130]

It was possible to show the transfer of the 4'-*pro-R*-hydride of **13** to the substrate **85**. The transfer of the hydride was elucidated by several isotope labelling experiments using stereoselectively deuteriated NADPD. The different forms of NADPD (4'-*R* and 4'-*S*) were synthesized by known enzymatic procedures.[130] Both forms were incubated overnight with the ER domain and **85**. After incubation of the ER domain with both isomers of NADPD and **85**, the hydride transfer were analysed by LCMS.[129]
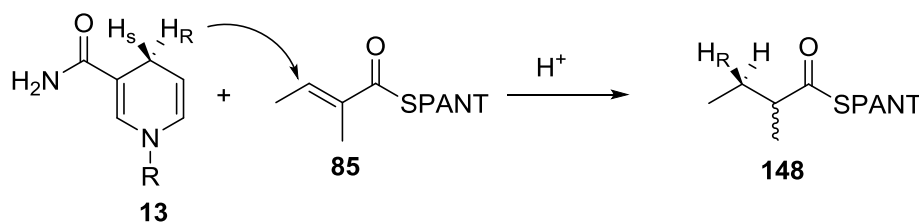
Scheme 34: Enzymatic reaction of **13** with a pantetheine substrate to determine the stereocontrol of the β-position.

In the corresponding assays it was clearly determined that the 4'-*pro-R*-hydride is transferred. The rate of reaction using the labelled 4'*R*-NADPD was slower than the rate of the 4'*S*-NADPD reaction, presumably due to a primary kinetic isotope effect.[129]
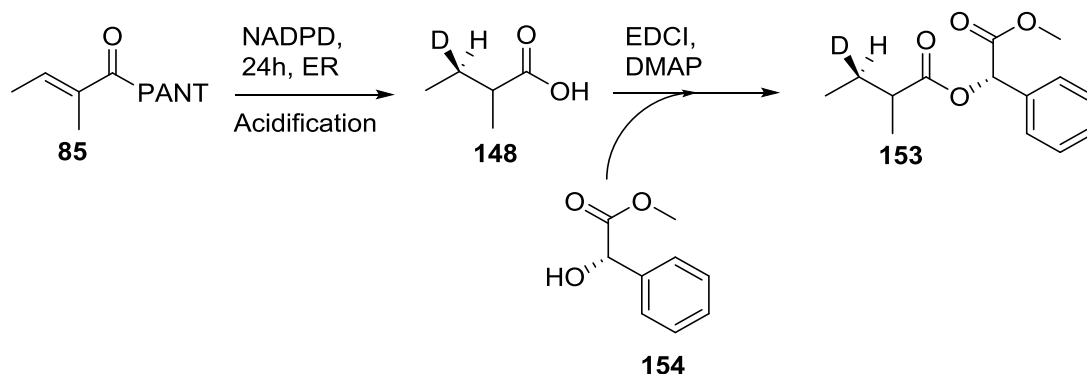
Scheme 35: Synthesis of corresponding *S*-mandelate esters to investigate the stereoselectivity of the β-position.

The resulting deuterated products from the enzyme assays were hydrolysed and coupled to *S*-methylmandelate **148** and analysed by NMR and LCMS. The results of these assays again confirmed that the products were racemic at the α-position. However transfer of deuterium from 4'-*R*-NADPD was highly stereoselective at the β-position (Scheme 35).[129]

2.4   Discussion

To investigate the programming of the ER domain a library of different pantetheine substrates was created. Several different methods had to be developed for the synthesis of the carboxylic acids. These acids were then converted successfully to the corresponding pantetheine thiolesters. The pantetheine synthesis was also significantly improved by using the acetal-protected pantetheine reported by Townsend for the coupling reactions.[49] Pantetheine substrates showed a much better solubility and reproducibility in the final *in vitro* enzyme assays than the previously investigated SNAC substrates. The successfully synthesized library included substrates with different structural features to test the selectivity and programming of the isolated ER domain.

Comparing the different SNAC and PANT substrates with each other showed the different results. For SNAC substrates the best diketide is tigloyl- followed by angelic- and crotonyl- SNAC. For PANT substrates the order is crotonyl- **87**, angelic- **86**, tigloylpantetheine **85**. Other variations of diketides were not synthesized as SNAC substrates. The best substrates are the triketides: **91** and the natural substrate **93** (**93** was not made as an SNAC). A substituent in the α-position seems to increase the rate of the reaction. Possibly the methyl group favours the orientation of the double bond to the catalytic residues of the active site. After that the unmethylated triketide follows which can rotate more freely in the active site. At least the racemic 4-2-dimethylhex-2-enoyl substrate **94** follows. The additional methyl groups decreases the rate. This is for PANT and SNAC residues the same. The 4(*S*)-2-dimethylhex-2-enoyl substrate **93** is in contrast to **94** enantiopure. It shows a higher V_{Max}/K_M value than **94**. This is in agreement with the expected results, since **93** is the natural precursor of the tetraketide **102**. Unfortunately the second enantiopure compound **149** could not be synthesized but it is expected that its V_{Max}/K_M should be lower than that of **94**.[100]

Other important information was elucidated for the tetraketides. The best tetraketide is the α-methylated form **100**, followed by **99** and **104**. This is surprising since the SNAC version of **104** showed no conversion to the fully reduced compound. Possibly the reduction process is too slow for the SNAC version. Enantiopure compound **102** as the PANT substrate showed no conversion in contrast to **104**. Longer carbon chained SNAC compounds showed a low water solubility (8-10 carbon atoms). Addition of DMSO was necessary to ensure their solubility. The use of PANT substrates had no limits for longer substrates containing this number of carbon atoms. Also different methylation patterns had no significant effect to the solubility. For both residues a reduction of mimicked pentaketides could be measured.[100]

In comparison to the previous results of SQTKS-ER with SNAC compounds, a faster reduction was observed. Large errors were measured for the reduction of the SNAC substrates, also was it difficult to tell if a reduction happen for the slowest substrates or not. The faster determination of the kinetic data with the pantetheine substrates prevents the enzyme from precipitation. A typical enzyme assay of a PANT substrate took 10 to 15 min. Enzyme assays for SNAC substrates required nearly a day. For the PANT substrates three replicates of measurements were performed to minimize the errors.[100]

The ER domain of SQTKS shows broad substrate selectivity as a stand-alone enzyme. It was possible to reduce almost all the synthetic pantetheines. Another investigation of programming of iPKS by Tang (section 1.4) showed, in contrast to this, the high selectivity of the C-MeT domain of LNKS. This enzyme is highly selective to one compound which was shown in competition assays with the KR domain of LNKS. In contrast to the performed investigation of the ER domain of SQTKS, the C-MeT domain was investigated by SNAC compounds. The analytical method that was used was different. Tang et al. analysed their enzyme assays by LCMS.[81] This method was not possible to establish for the ER domain of SQTKS. Another difference is the used enzyme. In the case of SQTKS we used an isolated ER domain excised from the complete PKS, while Tang et al. used a mutated version of the complete LNKS PKS protein. A mutation in the DH domain of LNKS stopped the reaction after the KR reaction. In that way the information of the stereochemistry of the first two β-processing steps was determined.

The isolated ER domain seems not to control the stereochemistry in the α-position. The problem of the racemisation at the α-position could not be solved by changing from SNAC to pantetheine substrates. First, it was speculated that possibly the low reaction rate of SNAC compounds was the reason so that a protonation by water could take place.

A catalytically active form of the ER domain was expressed but the loss of stereoselectivity at the α-position was thought to be due to a problem with protein folding. It is also possible that the fragment of the ER domain is catalytical active but some essential amino acid residues are not included in the expressed protein.[129] Taillorin et al. published a theory that could influence the stereochemical outcome of the ER domain in our investigations. The paper focussed on the interactions of the ACP with the isolated ER domain. The target of the investigation was the inhibition of the Escherichia coli Type II FAS ER domain (FabI).[131] It seems possible that a part of the ACP is necessary for the closing process of the ER's active site. Another possibility is the interaction with other PKS domains around the ER.

In contrast to the α-position, the stereochemistry of the β-position could be elucidated by Doug Roberts. The hydride transfer of NADPH to the substrate is controlled.[129]

2.5 Conclusion

The tested structural factors with the subtrates synthesized in section 2.3.2 showed several information about the programming of the ER domain. Use of acyl PANT substrates gave useful kinetic data in combination with the isolated ER domain. Two analytical methods could be established. One that showed the reduction process by UV, the other one by LCMS.

The *in vitro* assays were also significantly improved. The change of the system from 96 well plates to cuvettes gave significant improvements. The different substrates were measured in triplicate for each concentration, and this gave consistent data sets with low variation. The rate data was then used to create the Michaelis-Menten curves that were used to create the V_{Max}/K_M values for each substrate.

The results show that the isolated ER domain of SQTKS has remarkably broad substrate selectivity, with almost all synthesised substrates showing measurable activity. The substrates included assumed intermediates as well as others which are unlikely intermediates (the *Z*-isomers) and those which cannot be intermediates (*e.g.* ethyl-substituted, incorrectly methylated, and compounds with odd carbon chain-lengths). This suggests that the active site of the SQTKS-ER domain must be quite large and flexible. Another information that could be required is the relation between the *C*-MeT and ER domain. Further investigations showed that SQTKS-ER exists as dimer. Since there is a high end to end homology between vFAS and the fungal HR-PKS this confirmed the expected data.[61,101]

In vitro assays showed that the isolated ER domain is not possible to predict the stereochemistry of the α-position. All substrates were produced as racemates. None of the enantiomers was preferred. This position is very rare investigated in mPKS and iPKS. Some investigations of this position are mentioned in section 2.1. Catalytic residues were highlighted but none of these informations could be transferred to SQTKS. It is possible that the ACP is involved in the process, but this can not yet be confirmed as the SQTKS-ACP has not yet been cloned and expressed. Catalytical activity was shown without the ACP but maybe the active site needs to be docked by the ACP. Otherwise it could be flooded by water. An uncontrolled protonation could result in the entrance of water.

In contrast to this the stereochemical investigation of substrate-position C-3 was successfull. The transfer of the hydride could be investigated. It seems that the

orientation of the substrate in relation to the cofactor may be more important. Investigation of possible protein structural features that could be important is necessary to further investigate this point. The production of protein crystals was attempted by previous workers, but this was not successful.[100]

However previous workers were able to generate a structural model of the isolated ER domain, based on the crystal structure of the vertebrate fatty acid synthase (2vz9) as template.[129] The three main features of the model are the *N*-terminus, which forms a globular domain, the middle section, which forms a cofactor binding domain containing a Rossmann fold and finally the *C*-terminus that forms part of the active site around the cofactor and substrate binding regions.[129]

A tunnel is indicated by the model that shows the active site with the possible entry of the substrate and the underlying cofactor. The active hydrides of the cofactor are positioned at the end of the tunnel (Figure 42).
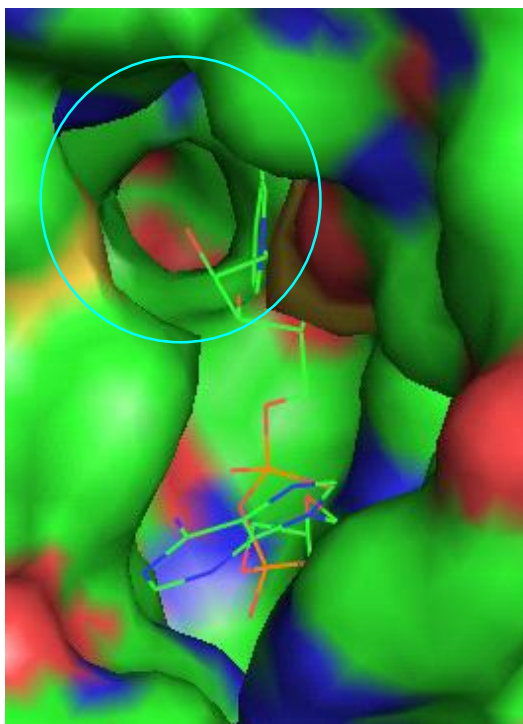
Figure 42: Pocket of the active site of the ER domain.

Only the nicotinamide 4'-*pro-R* hydrogen is freely available in the pocket during the reduction process while the 4'-*pro-S* hydrogen points towards the wall of the pocket. Specific contacts of the NADPH are observed with residues S2072, K2055, G2029, I2119 and V2144.[129] This is in agreement with vFAS. It is known that the 4'-*pro-R* hydrogen of NADPH is added at C-3 to the substrate similar to the stereochemical investigation of SQTKS-ER.[129]

Docking pantheine substrates into this model showed a parallel orientation of the substrate to the cofactor for 4*S*-2-dimethylhex-2-enoyl pantetheine **93**. For the α,β unsaturated moiety a s-*cis* conformation is observed. The distance between the substrate β-carbon and the active hydride of NADPH is 3.6 Å. The model also offers an explanation for the faster reaction of pantetheine substrates as compared to the SNAC substrates. The two methyl groups at the end of the pantetheine residue interact with the hydrophobic area of the pocket at the entry of the tunnel.

This area is constructed by the residues C2097 and L2098. In the full PKS it is assumed that the ACP would be located at the entrance to the tunnel, which is in agreement with the model. Another contact outside the tunnel between ACP and ER domain is suggested. Analysing the position of the α- and β-positions of the substrate shows that the model and experimental data are consistent with respect to to the hydride transfer. Stereochemical *in vitro* assays with **85** showed the selective hydride transfer to the *Re-face* of C-3. Additionally the resulting enol(ate) must be reprotonated. In the case of SQTKS-ER this is expected from the *Re-face* of C-2 to create the known stereochemical outcome. As shown in section 2.1 there are some catalytic residues known that could be involved in this process. Leadlay highlighted tyrosine and valine residues. For vFAS and SQTKS a leucine residue is found at this position. But the reprotonation is different between vFAS and SQTKS-ER. For vFAS the enolate reprotonated *Si* and not *Re* like the investigated ER domain. However, analysing the area at the α-carbon in the model shows that no residue or proton source is available that can predict the stereochemistry at this position.[129]

Docking experiments of the tetraketide substrate **99** were in agreement to the triketides. Orientation and location of the acyl group of **99** to cofactor NADPH **13** was still the same. Only the carbon chain is now located deeper in the active side of the tunnel. In contrast to the previous s-*cis* confirmation now a s-*trans* confirmation is observed. For the docking process of **102** this confirmation is twisted. This time also the location of the substrate is different to **99**. Reasoned to the additional methyl groups **102** is located on top of the active site.[129]

This also explains why the natural tetraketide **102** works as an inhibitor. It is possible for **102** to enter the active site, as shown in the inhibition assays, but it cannot reach a suitable conformation for reduction. Significantly, the racemic mixture of stereoisomers of **104** was slowly reduced showing that at least one of the four isomers can reach a productive conformation for reaction. This suggests that interactions

between the tail of the polyketide, and in particular its methyl groups, with the walls of the active site can control the positioning of the reacting olefin.[129]

2.6   Future Work

For the future the analysis of the active residues that are involved in the reducing step would be helpful. From previous studies with other ER enzymes and domains no residues have so far been found which have been conclusively shown to be involved in the reprotonation step. Two ways are possible for the analysis. First the creation of a crystal of the ER domain could show the correct distances and also the real active site. From this crystal also active residues could be hypothesised and this could lead to investigation of the active site by point mutations. Also on that way possible active residues could be identified. Changing amino acids which form the walls of the substrate-binding pocket could open or extend the active site. In that way the reduction of longer chained pantetheine substrates should be possible. Possible amino acids for these investigations are phenylalanine (F280), leucine (L269) and isoleucine (I270). Also mutation of the amino acids that hinders **102** to get in the correct distance to the catalytic residues could be performed. The assumption of the theory based on the model of SQTKS could be tested.
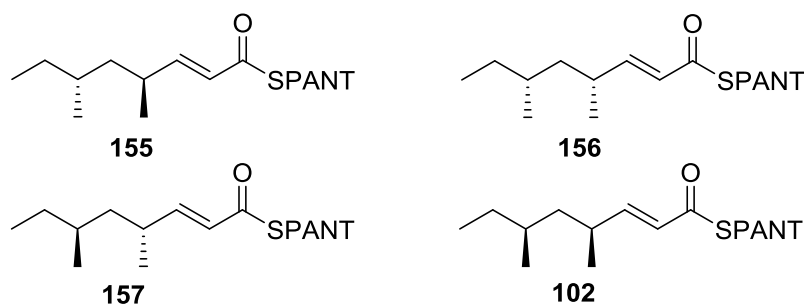
Figure 43: Different stereoisomers of **102**.

For the natural SQTK **102** the synthesis and enzyme assays were performed and analysed. The enantioselective synthesis for the other three isomers has to be developed also corresponding enzyme assays have to be performed. The different isomers are known by literature (Scheme 36).[132-141]
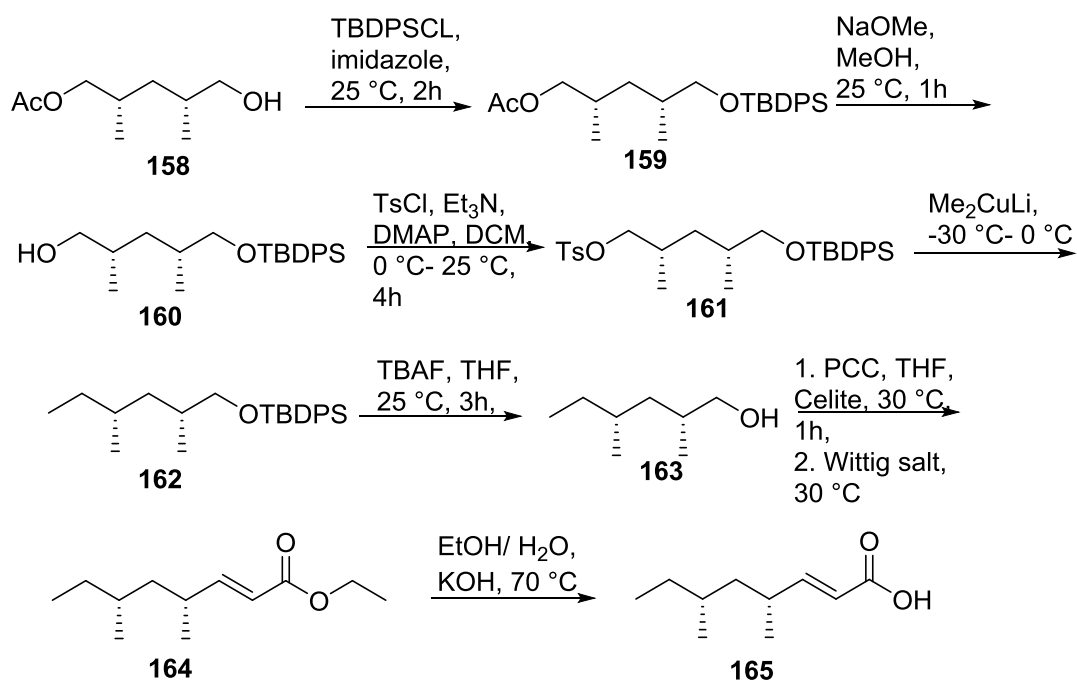
Scheme 36: Synthesis to form the precursor **165** of 4*R*,6*R*-isomer **156**.

Starting with commercial available (2*S*,4*R*)-5-hydroxy-2,4-dimethylpentyl acetate **160** and additional protection of terminal hydroxyl group results in the protected compound **161**. Additionally the acetate group can be hydrolysed to an alcohol by sodium methanolate. In the next step a good leaving group is created by a tosylation with tosyl chloride of the terminal alcohol in the presence of triethylamine and DMAP. The following reactions are a nucleophilic substitution of the tosyl residue by a Gilman Cuprate to form the protected alcohol **162**, which gets deprotected in the next step by tetra-butyl-ammonium fluoride (TBAF). Finally, the known methods of previous reactions can be used to form the carboxylic acid **165** that is used in the final coupling reactions. For all steps yields of 80% and more are reported.[132-141] Synthesis of precursors of the carboxylic acids or esters for isomers **155** and **157** are also known.[141,142,143]

Synthesis of **171** starts with the Evans auxiliary (*S*)-hydroxymethyl pyrrolidinone **166**. Reaction with (S)-(+)-1-iodo-2-methylbutane **167** with additional removal of the auxiliary with 10% HCl and reduction of the carboxylic acid results in the alcohol **168**. Oxidation by TPAP and *N*-methylmorpholine *N*-oxide results in the aldehyde **169**. By additional Horner-Emmons reaction **169** is transferred in the ester **170**. This could be cleaved with potassium hydroxide to the desired product **171** (Scheme 37). The fourth isomer could be synthesized by the alkylation of the oxazilidone amide **171** with the (*R*)-2-methylbutyl trifluoromethanesulfonate **172**. The

resulting product **173** is reduced to the alcohol **174** by LiBH$_4$. Further steps of the synthesis of **177** are described by the production of **171** (Scheme 37).[116,142-145]
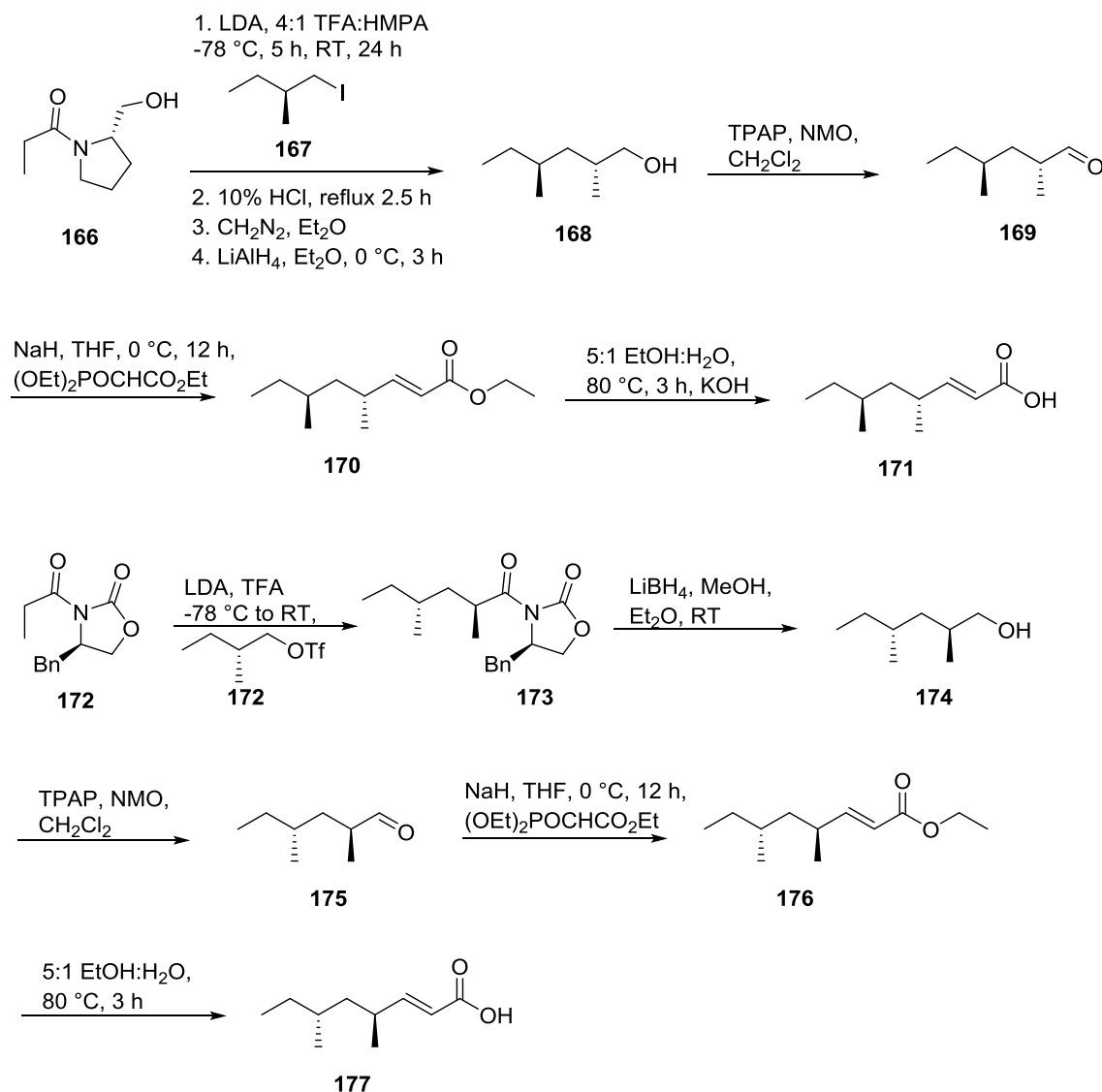
Scheme 37: Synthesis of precursors **171** and **177** of the 4*R*,6*S*-isomer **155** and 4*S*,6*R*-isomer **157**.

Another investigation can focus on the interactions between the pantetheine arm and the amino acid residues of the ER domain. The comparison between SNAC and pantetheine substrates showed a high difference in the reduction process. For the reduction of the tigloyl moiety a factor of 12.5 was measured. The further analysis of the interactions between the pantetheine arm could be performed by an exchange of several heteroatoms. Since the addition of the second amide group has a significant effect several atoms could be replaced to get a better understanding about which parts of the pantetheine arm interacts with the active site. For example a possible candidate is the

nitrogen atom of the amide group that could be replaced by an oxygen to form the ester **178**. Possible compounds are shown (Figure 44).
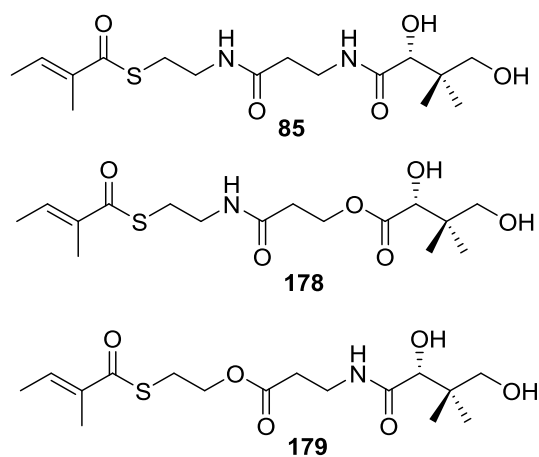
Figure 44: Synthesis of modified tigloylpantetheine structures.

3.0   Project 2: Investigation of the SQTKS-DH Domain

A second domain that is found in the β-modification part of PKS is the DH domain. It is well understood and investigated in mPKS. Several crystal structures from mPKS and FAS are available and these highlight residues which are involved in the dehydration process. However, DH domains from iPKS have not been previously investigated.

The DH domain acts after the KR and directly before the ER domain in the β-processing cycle. The DH catalyses the loss of water from the alcohol **180** formed in the previous step by the KR domain to give an αβ−unsaturated thiolester **181** (Scheme 38). The olefins formed by DH domains are in most cases *trans* configured, but the *cis* configuration is known in some cases.[17]
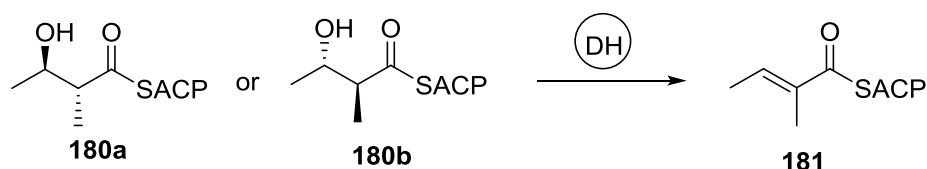
Scheme 38: Basic reaction of the DH domain.

3.1   Previous Structural and Stereochemical Investigations

Recent structural studies have shown that DH domains, in most cases, form dimers in solution. Each monomer consist of a double hot dog fold. An α-helix shows the structure of the "sausage" that is surrounded by a curved β-sheet, which forms the "bun" of the hotdog (Figure 45).[71]
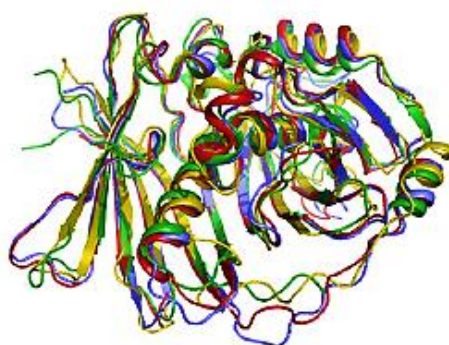
Figure 45: Structure of the double *hot dog* fold of the CurF DH domain.[71]

The active site of the DH is formed by a His-Asp "catalytic diad" system. The histidine is located at the *N*-terminus of the hotdog, while the aspartate is at the *C*-terminus. The

active site is located at the bottom of a V structure formed by both hot dogs. The substrate tunnel is located at the bottom of the V. This structural relation was found for several DH domains including those from CurF and CurK and also Ery DH4 and mFAS.[17,21,61,71]

Figure 46: Structure of the dimer of double *hot dog* folds of EryDH 4.[21]

Formation of the homodimeric structure is necessary for the catalysis process (Figure 46). Every active site is formed by two identical monomers. For the DH domain itself hydrophobic residues are found that have potential in interfaces with other PKS domains (Section 1.3.2).[21,71] X-ray crystal structures for several DH domains of modular PKS enzymes have been reported.[16] These DH crystal structures show a high similarity to the ones of the animal fatty acid synthases.[17, 61]

Figure 47: Sequence alignment of SQTKS-DH to EryDH4, CurK and CurF DH domains.[71]

One example is the crystal structure of EryDH4. For this enzyme a double-hotdog fold for the structure was found. A loop connects two pseudosymmetric halves of the DH monomer. One of these halves posses the catalytic active histidine (residue 45) as part of a conserved HXXXXXXX(Y/F)PG motif.[21,71] Comparing this sequence with the

one of the DH of SQTKS, CurK and CurF showed that this motif is clearly conserved (residues 45 to 55). Comparing all four sequences an identity of 15 to 20% was observed (Figure 47).[21,71] In Type I PKS an aspartic acid residue is also involved in the mechanism of the DH. This residue is found at position 236 of the sequence alignment that contributes in all four PKS enzymes. Analysing the sequences showed that at this region again a high similarity is observed (Figure 47).[21,71]

The glutamine at position 240 of EryDH4 is highlighted as it is also conserved in many PKS DH enzymes, but can be substituted by histidine in some DH proteins. The crystal structure of EryDH4 shows that this residue is connected *via* hydrogen bonds to an invariant tyrosine residue at position 180 (present in SQTKS-DH, EryDH4, CurK and CurF).[21] Another tyrosine residue, ten amino acids away, is found in the GYXYGPXF motif. This tyrosine is located close to the active site histidine and aspartic acid. In the crystal structure of EryDH4 water is bound by this residue and directly coordinated to the catalytic aspartic acid. This motif is also found in the DH sequence of SQTKS but the tyrosine is replaced by histidine (Figure 47). For the other PKS this tyrosine is conserved.[21, 71]

How much information of the crystal structures can be transferred to the aligned sequences of SQTKS-DH is unclear. It shows only that the residues that are involved in the catalytic process are found in modular and iterative PKS. It is not known if these residues have the same task in iterative PKS. Also several motifs were found in all four PKS.
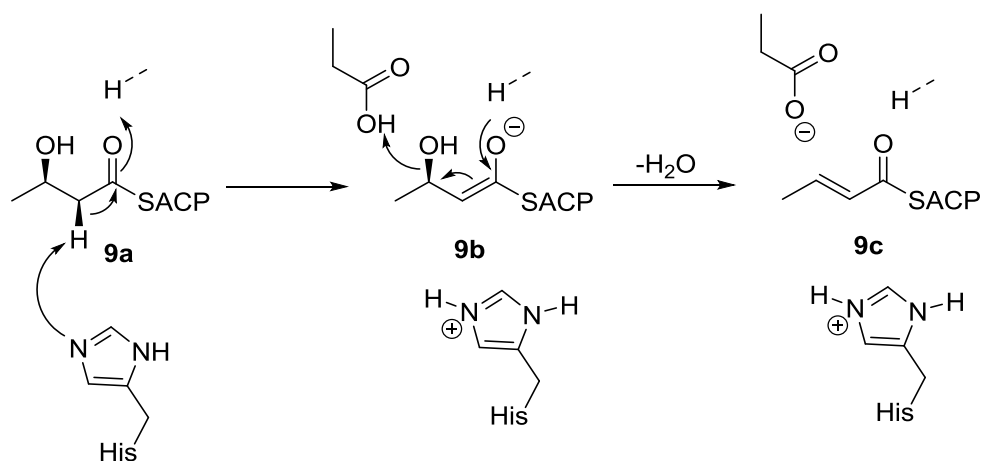
Scheme 39: His-Asp catalytic dyad mechanism of the DH domain.

The proposed catalytic mechanism involves removal of the proton in the α-position of the substrate **9a** by the active site histidine. An enol(ate) intermediate **9b** is formed which is stabilised by hydrogen bonding and alignment of the polar C-O bond with the

hotdog helix dipole. Then, aspartic acid protonates the β-hydroxyl group and water is the leaving group (Scheme 39). The overall mechanism corresponds to an E1cb process. Almost all known DH catalyse an overall *syn* removal of H_2O to form a *trans* olefin **9c**.[17]

3.2 Aims of the project

To get more information about the programming of SQTKS a second domain should be investigated. The DH domain was chosen. There was some information from previous investigations by the Cox group available about this domain. For example the stereochemistry of the substrate for this domain is known.[146] A synthetic route for an acyl pantetheine substrate of the DH is planned as the first aim of this project. It is expected that the pantetheines should be faster substrates than the corresponding SNAC. For final enzymatic investigations it is planned to express the isolated DH domain of SQTKS. This includes the transformation of a plasmid in a bacterial producer strain, the development of the fermentation system of the bacterial strain and the development of a purification protocol for this protein. Following the expression enzymatic investigations of the DH and the synthesized compound is planned. Also is it necessary to develop a suitable method for the enzymatic investigation. The final aim of this project is the investigation of the pantetheine substrate in the presence of **61**. Is there any influence of **61** to the isolated DH domain and an effect of **61** in enzyme assays detectable. It is possible that **61** has an inhibitory effect on the DH enzyme.

3.3 Results and Discussion

3.3.1 Isolation of the Single DH Domain of SQTKS

To investigate the kinetic reaction, activity and the stereochemistry the dehydratase domain of SQTKS was expressed as a soluble protein. The domain boundaries were chosen by sequence alignment with known DH domains from mFAS. In the mFAS structure the DH- and ER domains are bound covalently by a linker and by interfaces of amino acids to each other. Further investigations of this thesis were orientated on interaction between the two isolated domains of SQTKS (Chapter 4). It was suggested that maybe the DH domain could be involved in influencing the stereochemistry at the

α-position during the ER reaction. Previous work (Chapter 2) had shown that in the isolated ER the stereochemistry at this position cannot be controlled as it is in the full SQTKS.

To express the single DH domain, the plasmid construct pOPINF-DH (produced by David Ivison) was transformed into the producer strain *E. coli* BL21 and also in *E. coli* Top 10 cells (Figure 48).[101]
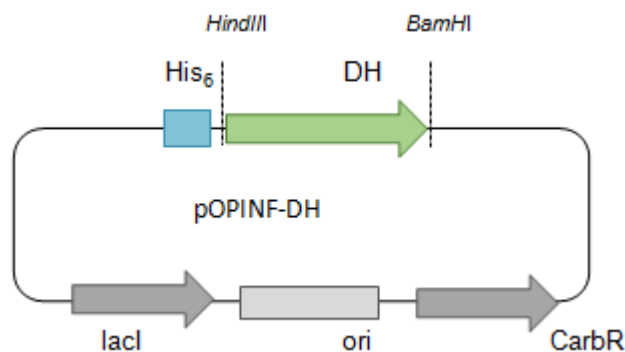
Figure 48: Plasmid in pOPINF_DH vector.

A single colony of the producer strain *E. coli* BL 21 was transferred in 2TY-media to produce a starter culture and incubated over night. The starter culture was diluted 1:100 in 2 litres of 2TY media separated into 20 flasks. After an optical density of OD_{600} 0.6 was reached, the cells were induced at 16 °C with IPTG (injection of 50 μL of a 1 M stock solution). Cultures were cultivated for a further 16 hours and then cells were harvested by centrifugation and lysed by sonification.
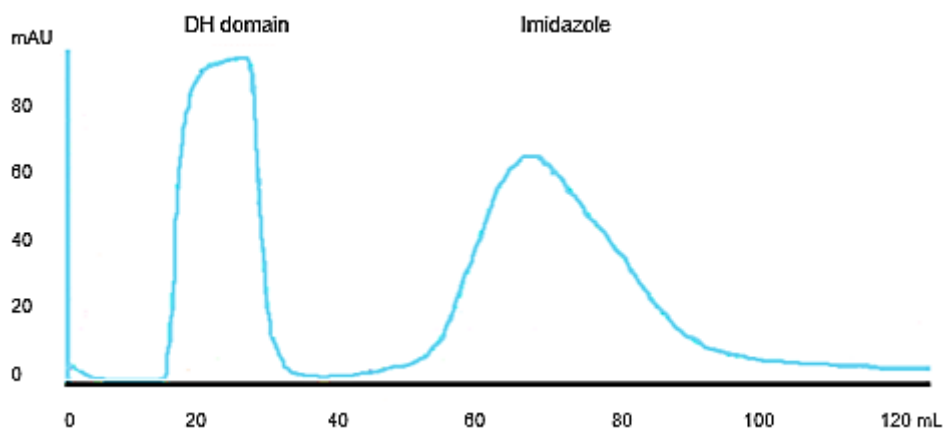
Figure 49: Chromatogram of the re-buffering of the DH domain to remove imidazole.

The resulting lysate was purified by NiNTA chromatography and the final protein was purified similar to the ER domain with a fused His_6-tag. Purified expressed protein was

re-buffered with imidazole-free buffer, since it was confirmed that the protein has a low tolerance to imidazole (Figure 49, Lines D1 and D2).

Finally, the resulting protein was analysed by SDS-page which showed the unexpected mass of a 27.8 kDa protein. The expected size was 38.1 kDa. Since there was no visible fragmentation on the gel, further analysis was necessary to confirm the protein (Figure 50).
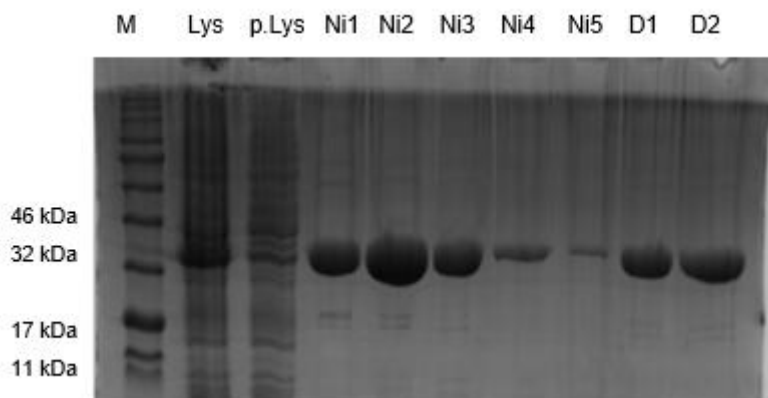
Figure 50: SDS-page analysis of DH expression.

A problem in the SDS-page analysis could be the amount of glycerol (10%) in the purification buffer. It is possible that the protein was not completely unfolded. To confirm this, the protein sequence was analysed by MALDI.

Figure 51: MALDI-analysis of the DH domain. Green bars show the high identity of the observed fragments in comparison to the known amino acid sequence of SQTKS-DH.

The results of the MALDI experiment showed that the expected protein was expressed and that the SDS page did not show the correct size. An identity of 100% was observed

for the obtained fragments. The previous assumption that the protein was not completely unfolded is correct. The His$_6$-tag as starting point and the final amino acid sequence were found. The gaps that in the sequence from the MALDI analysis most likely correspond to peptide fragments which did not ionise in the experiment (Figure 51).

It was possible to express the isolated DH domain in a scale of 30 mg. A similar expression and purification system was used that was successful in previous work for the expression of the ER domain. The change of the expression medium from LB to 2TY resulted in an upscale of isolated protein. Changes of the induction point had also a positive effect.
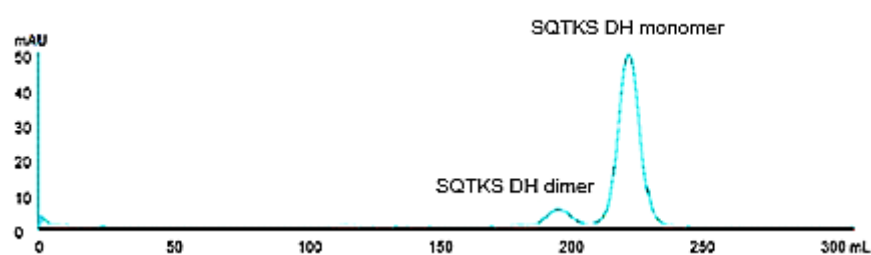
Figure 52: Size-exclusion chromatogram of isolated DH domain in solution.

Analysis of the purified DH domain by size-exclusion chromatography showed two peaks in the chromatogram. Only a small amount of the enzyme forms a dimer in solution, peak at 190 mL. The peak at 210 mL shows that most of the DH domain was eluted as a monomer (Figure 52). The investigation was performed in the same buffer like the ER domain since for this enzyme a calibration of three different enzymes was available.

A reason for the monomeric DH domain could be the amount of glycerol (20%) that was used in the buffer. It is possible that the glycerol forms a surface around the enzyme, which makes it impossible that an interaction between the monomers take place. In general the interface between DH monomers is quite small and formed by highly complementary and hydrophobic surfaces. The result is in contrast to several other DH domains of mPKS and mFAS where it is known that they form dimers in solution.[71]

3.3.2 Synthesis of Pantetheine Substrates for the DH Domain

To test the DH domain for its activity a pantetheine substrate was synthesized. The same synthetic route was used as described previously; EDCI coupling of corresponding acids with the pantetheine acetone acetal. Further tests showed that the DH domain recognises only one stereochemical orientation of the hydroxy group. These investigations were performed by another PhD student of the Cox group with SNAC compounds, which were also in this topic poor substrates.[146] To test the enzymatic activity, a enantiopure pantetheine compound with the known accepted stereochemistry was synthesized.

The synthesis started with the commercially available 3R-hydroxybutanoate methyl ester **182** (Scheme 40). This ester was deprotonated by two equivalents LDA in the first step. In the second step **182** was methylated with iodomethane. This type of stereospecific methylation is called the Frater-Seebach alkylation and is known to give the 2R,3R stereoisomer in this case. Next, the product of this methylation **183** was protected by reaction with *tert*-butyldimethyl-silyl triflate in dichloromethane. The ester **184** was cleaved in the presence of lithium hydroxide in aqueous medium to generate the carboxylic acid **185** which was coupled to pantetheine dimethyl ketal using standard EDCI conditions. This was performed in a similar way to the previously described ER substrates (section 2.3.2).
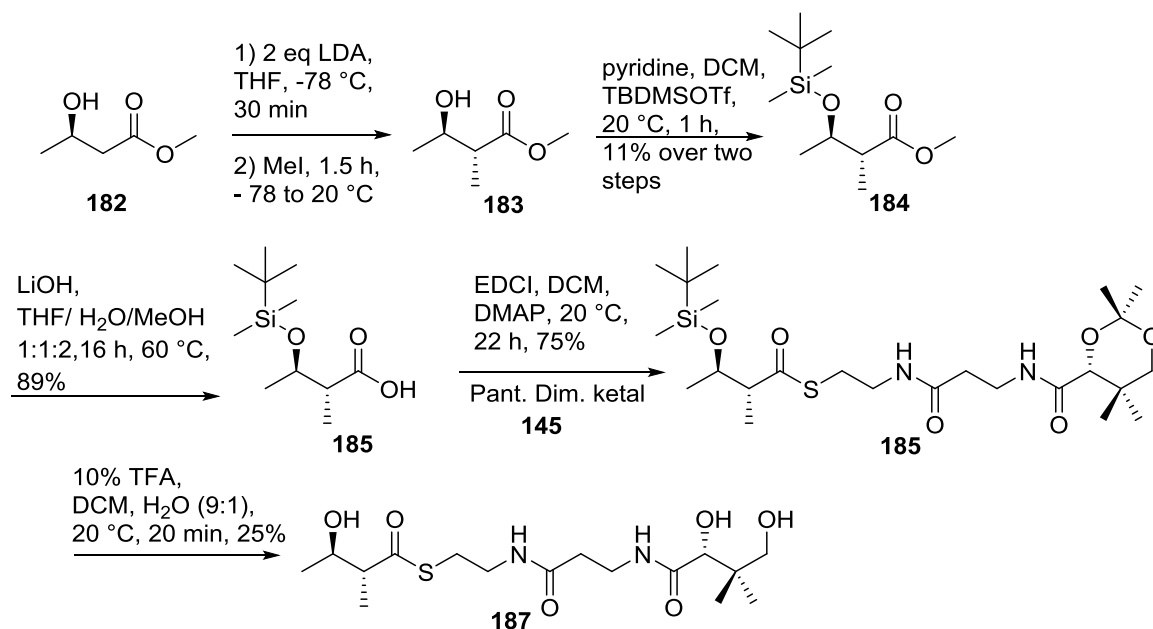
Scheme 40: Synthesis route of (2R, 3R)-3-hydroxy-2-methylbutyl pantetheine **187**.

Finally the deprotection of the pantetheine residue and also of the hydroxyl group was achieved using TFA. The final product had an ee of 97%.[147-149] The substrate was generated during the supervision of the Bachelor Thesis of Sandra Johannsen with the topic "Synthesis of substrates for the SQTKS Dehydratase" (Scheme 40).[150]

3.3.3 Enzymatic Investigation of DH Domain

Analytical scale assays were performed in a total volume of 120 µL at 30 °C in TRIS buffer pH 8.5 containing 0.5 mmol substrate and a final concentration of 0.5 mg/ mL enzyme. The assays were analysed by LCMS (Figure 53). The substrate **187** was converted cleanly to the expected product **85**.
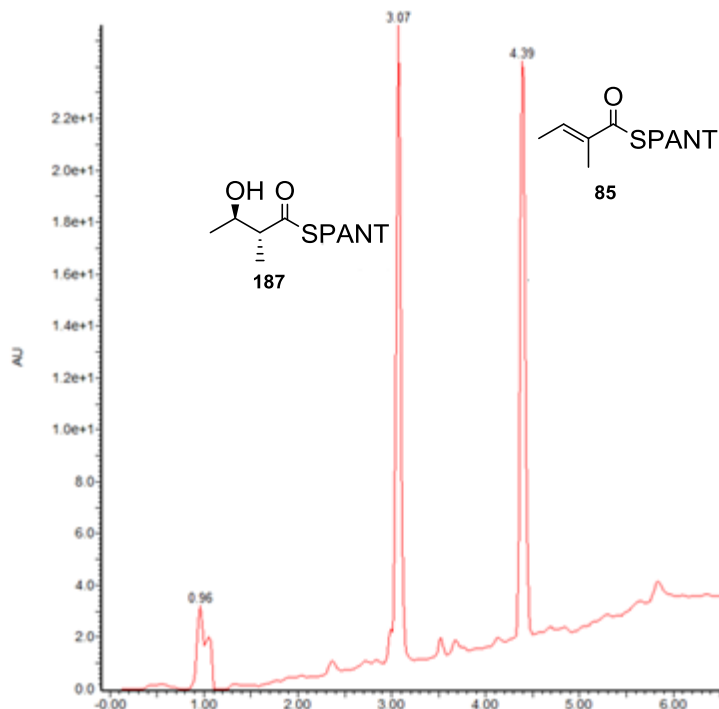
Figure 53: Chromatogram of an enzyme assay of the DH domain. Dehydration of **187** to **85**.

Problems in this case were to measure the initial rate and to get the final K_M and V_{Max} values. Again the LCMS assays were *discontinuous* and difficult to make reproducible. It was not possible to establish a calibration curve for one of the substrates. The measured initial rates also showed a high variance.

Since the LCMS data could not give an accurate kinetic rate, the UV profile of starting material and product was analysed. As the product of the reaction, tigloylpantetheine **85** has an absorption maximum at 260 nm, which the starting material does not have. Again investigations by UV were performed (Scheme 41).
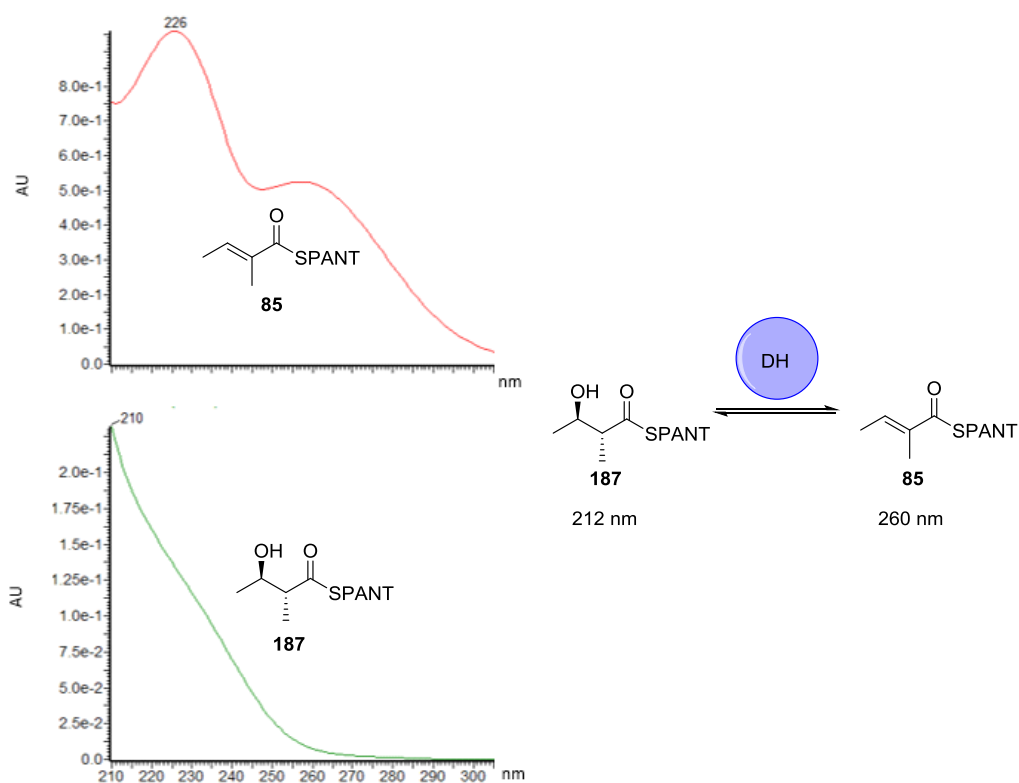
Scheme 41: Dehydration process of 3*R*-Hydroxy-2*R*-methyl butanoyl pantetheine **187** with UV profiles of **85** and **187**.

With this information the assay condition were changed. Similar to the assays of the ER domain the reaction was analysed continuously by UV to create a new method for DH domain analysis using in cuvettes since it was not possible to get good quality data by 96 well plates.
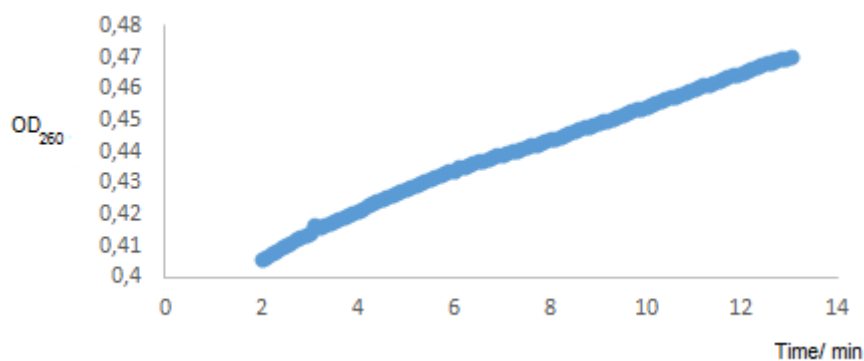
Figure 54: Absorption curve of **85** in the performed enzyme assays.

In this method the total volume of the assay was 400 μL and performed with 330-365 μL of 50 mmol TRIS buffer (pH 8.5), 150 mmol NaCl and 10% glycerol buffer. The substrate was measured in three technical replicates in substrate concentrations from 0.0625 to 0.625 μM. In contrast to following the cofactor concentration in the ER

assays, this time the formation of product **85** was followed directly (Figure 54). This assay gave reliable initial rate data with low variability. Initial rate data was collected in triplicate and plotted *vs* substrate concentration to obtain the Michaelis parameters (Figure 55).
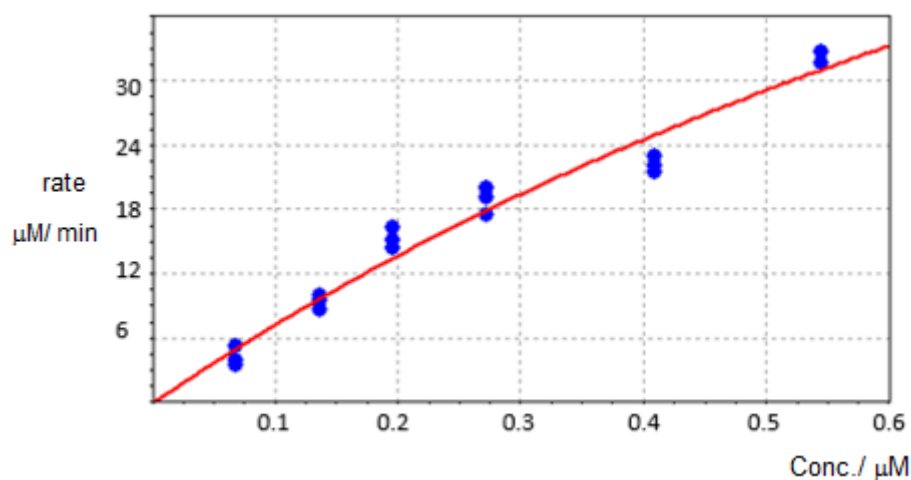
Figure 55: Michaelis Menten Curve of the DH enzyme assay.

The Michaelis Menten Curve was plotted and the corresponding values were calculated by the calculation program *Curve Expert*. For K_M a constant of 1.34 μM was calculated. The resulting V_{Max}/K_M value of 87.3 min^{-1} is again in the same area like the analysis of the ER domain (Figure 55). The calculated k_{cat} value was 117 min^{-1}. A value of 87.3 μM^{-1}min^{-1} was reached for k_{cat}/K_M.

In literature several investigations are shown to determine the stereoselectivity of DH domains. ACP bound species are the natural substrates of iPKS and FAS DH domains, but it is normal to assay these enzymes *in vitro* using acyl-SNACs.[146,151] During the investigation of the SQTKS-DH domain by Emma Liddle in the Cox group, SNAC substrates were used.[146] For the SNAC analoque of **187** a k_{cat} value of 0.063 min^{-1} and a K_M of 4.5 mM was calculated.[146] The resulting conversion to the dehydrated compound was very slow in this case. But these results show that the acetyl pantetheines are effective substrates, similarly to the previous work with the ER domain (Chapter 2).

The kinetic assays confirmed the previous investigations which used SNAC substrates that the 2*R*,3*R* stereoisomer **187** is the substrate of the DH domain. This stereochemical arrangement at C-3 is the same as that known for mPKS domains.[151] Also the performed *syn* elimination similar to the catalytic reaction of SQTKS-DH is observed.[151] In contrast to the SNAC results measured in Bristol the kinetic assays

were not analysed by LCMS because reliable calibration curves for the starting material **187** or product compound **85** could not be made. The LCMS assay was only used in the acyl pantetheine assay as qualitative tool to validate the enzymatic reaction.[146]

It was possible to measure the kinetic data and to calculate the Michaelis Menten curve. Similar to the previous ER domain assays, also for the DH domain faster rates in contrast to the SNAC assays were observed. For the SNAC compound a value of 0.014 mM^{-1}min^{-1} was reached for k_{cat}/K_M. In contrast to this the pantetheine result was 0.087 mM^{-1}min^{-1}. The pantetheine substrate of the DH domain was dehydrated faster by the factor 6.2.[146]

In these *in vitro* studies the additional part of the pantetheine residue has again a positive influence concerning the rate. Similar to the ER domain substrates, interacts the elongated residue with amino acid residues of the active site. A second advantage of the pantetheine residues is the lower flexibility in the active site. Several interactions between the substrate and the enzyme are expected. It is suggested that these interactions are important to locate the acyl group of the pantetheine faster in the correct distance of the catalytic residues.

3.3.4 Inhibition Assays of the DH Domain with SQTK

Interactions between the DH domain and tetraketide **102** were investigated. The tetraketide **102** was tested as an inhibitor of the DH domain. Assays were set up in which **102** was added to standard reaction assays containing the DH and its substrate **187**. These reactions clearly showed that addition of **102** causes measureable inhibition.

Comparing the data of the pure- and inhibited assay shows a measureable inhibition by **102**. This is very surprising for the enzyme. It would be expected that **102** is not a substrate that can visit the active site: **102** is actually the product of the DH domain. A fast release with low interaction would be expected. On the other hand, it is known from different investigations that the dehydration process is an equilibrium in which the reverse (hydration) reaction can be catalysed by the DH domain. This would explain why SQTK **102** can interact with the active site strongly.[151,152] Interestingly in this experiment, the inhibition occurs at a low concentration of **102** (0.13 μM). The rates were slow down in comparison to the assays without SQTK by the factor 3. In contrast to this an amount of 0.13 μM of SQTK lowers the rates of the ER domain by a

factor of only 0.5. Substrate and inhibitor concentrations were in both enzyme assays the same (Figure 56).
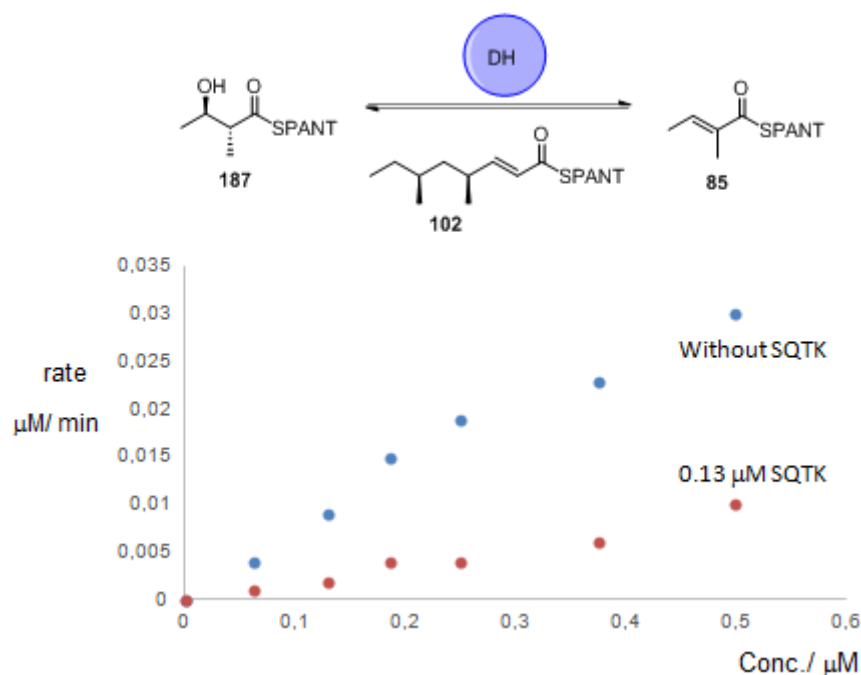
Figure 56: Inhibition enzyme assay for the DH domain with **102**.

Further analysis about the inhibitory effect could be performed. It was shown that the natural tetraketide **102** inhibits the DH domain. Is the stereochemical arrangement of the methyl groups the reason? In additional tests the racemic compound **104** could be used. If the orientation of the methyl groups is important, the inhibition of this compound should be lower.

3.4   Conclusion

To confirm the stereoselectivity of the SQTKS-DH domain a pantetheine substrate with the expected stereochemical information was created. A successfull synthetic route was planned and implemented in the lab. Similar to the developed route in section 2.3.2, first a carboxylic acid was created and coupled with the pantetheine dimetyl ketal residue. The resulting product was transferred into the pantetheine substrate **187**. A new and improved method was developed to analyse the different kinetic assays. First *in vitro* assays were analysed by LCMS but it was not possible to transfer this method to the pantetheine substrate. Only the general reaction of the enzyme with the starting material and product could be analysed on that way.

Analysis of the UV profiles of both compounds showed that **85** has an absorption maximum at 260 nm which is missing in the starting material. Final enzyme assays could be analysed by UV. For this the known method of the ER domain was used and modified. Again cuvettes were used instead of 96 well plates.

The k_{cat}/K_M value could be calculated for the reaction. The results of the ER domain could be confirmed. The pantetheine residue interacts stronger to the active site of the enzymes than the SNAC residue. Also the dehydration process of the acyl pantetheine substrate works faster.

It was shown that **102** acts as an inhibitor for the DH domain, and it can thus enter the active site. The stereochemistry of the methyl groups could be important for the DH domain. This was also shown for the ER domain. Further work will be required to test if this factor is important for the DH.

In the biological part of the project a successfull expression of the DH domain was performed and the expression and purification was improved. A change in the fermentation medium was performed from LB to 2TY. High amounts (25 to 30 mg) of pure protein were expressed and purified. Size exclusion experiments showed that the DH domain does not form dimers in solution.

3.5   Future Work

It was possible to verify the correct stereochemistry of **187** of the DH substrates. Similar behaviour and results were obtained in kinetic studies in comparison to the ER domain.

Interestingly also for this enzyme the inhibition assays with **102** were positive. This was very unexpected because **102** is a product of the reaction. Similar to the ER domain, investigations with different substrates could be possible. These substrates could have variations in chain length, methylation pattern and methylation position. Also in this case the investigations of the kinetics could show some stereochemical functions that are prefered by the DH domain (Figure 57).

It is known for the ER domain that the stereochemistry is important for the catalytic reaction; also for the DH domain several different stereoisomers could be tested. In addition to the natural substrate a series of different isomers of tri- and tetraketides could be synthesized and tested (Figure 57).
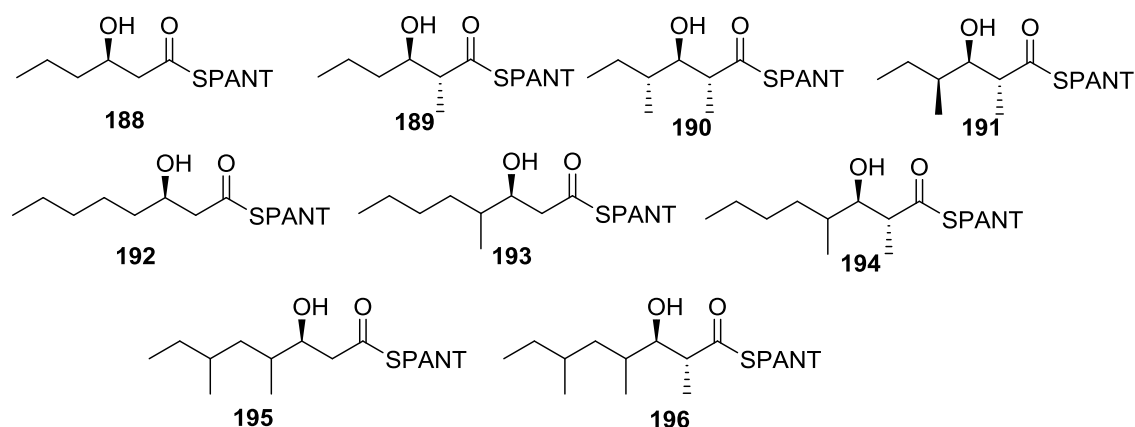
Figure 57: Possible substrate library for DH domain investigations.

A possible variant for the synthesis of substrates **188** and **192** are the Evans aldol reaction (Scheme 42). Starting with Evans auxiliary **197** and coupling with acetyl chloride results in compound **198**. This is converted to amide **199** by an aldol reaction with butyraldehyde or hexanal. After that the amide can be cleaved and the final acids **200** are formed. These acids could be used in EDCI coupling reactions to generate the corresponding pantetheine substrates **188** and **192**.[153]
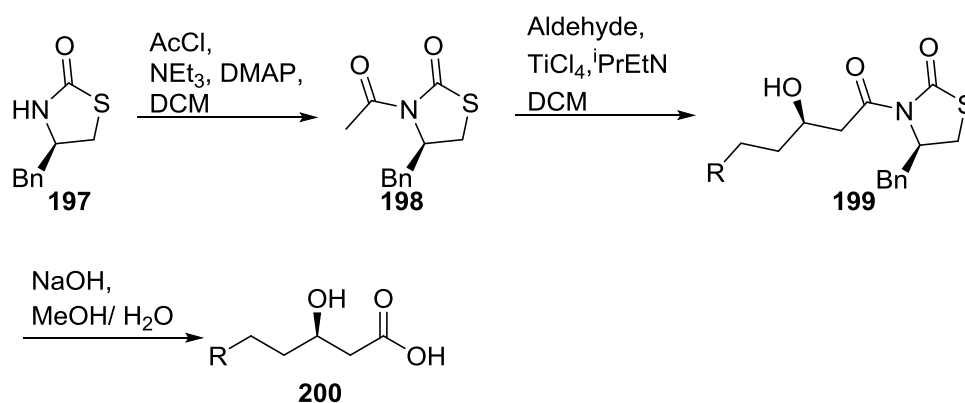
Scheme 42: Synthesis of precursors for substrates **188** and **192**.

Another option to synthesize several substrates to investigate the active side of the DH domain is shown in scheme 43. This preparation starts with (1*S*,2*R*)-*N*-methyl-ephedrine **201** that predicts in the later steps the stereochemistry of the carboxylic acid.

In this proposed route **201** is used as starting material that is coupled with propionyl chloride in THF to give the ester **202**. This gets converted with TMSCl and LDA to the stabilized silyl ketene acetal **203** which has a ratio of 95:5 *E/Z* selectivity.[154,155] After that another aldol reaction, similar to the previous reported one, is required. In this step titanium tetrachloride and triphenylphoshine are used in the presence of an aldehyde to form compound **204**. The tertiary amide blocks the attack to

the aldehyde from one side so that only the *R-R*-configuration can be prepared this time. This is the correct stereochemistry which was found out to be active for the DH domain (Scheme 43).[154,155]
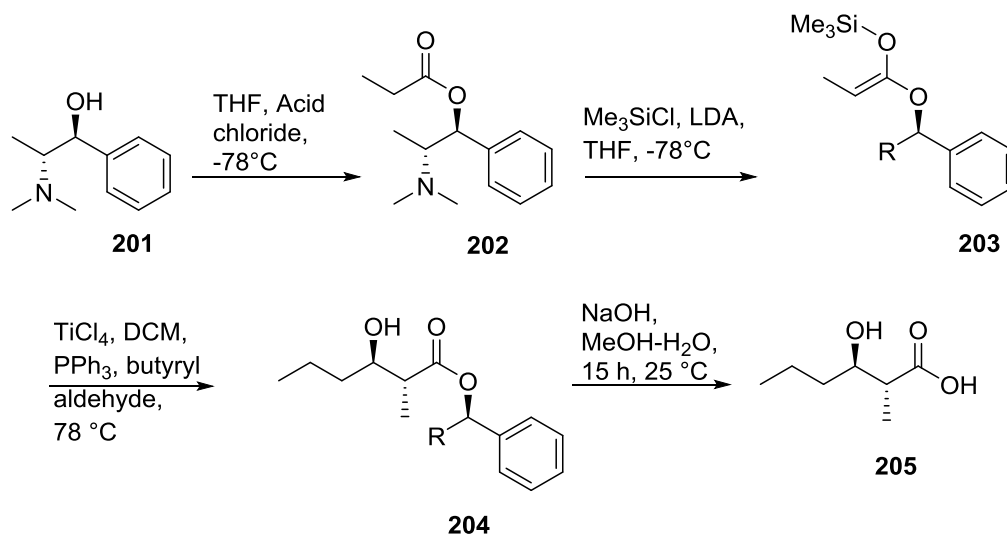
Scheme 43: Synthesis of precursors for substrates **188** and **189**.

Finally the ester **204** is cleaved with sodium hydroxide in a methanol/ water mixture and the desired carboxylic acid **205** is obtained for the next coupling reactions with EDCI. During the PhD it was possible to create compound **203**. Limited to the time and progress at this stage this method was not completed.[154,155]

Several investigations showed the influence of different residues that were highlighted in the previous chapter. To confirm this structural motifs and orientations of the different amino acids in the active site a crystal structure of the DH domain has to be established. Analysing these crystals could represent the correct distances of the catalytic residues histidine and aspartic acid that are involved in the dehydration process. The predictions between the other motifs and their function could be analysed on that way.

Another possibility could be the modification of the active site by mutagenesis experiments. Changing the proposed active residues should lead in an inactivation of the enzyme and show negative results in the dehydration process. For further investigations, which are shown in chapter 4 the mutagenesis of the active site is essential to create an experiment with reproducible results.

4.0   Project 3: Biophysical Investigations of DH and ER Domains

Type I PKS, such as SQTKS, consist of several catalytic domains which are covalently linked together. In the previous chapters the individual selectivities of the isolated ER and DH domains of SQTKS have been examined. It is also possible that protein-protein interactions between the individual catalytic domains could modulate their activities and selectivities.

One example of PKS domain-domain interaction was found in the crystal structure of the ER-KR didomain of the second module of the spinosyn mPKS. In contrast to other ER domains, this domain exists as a monomer rather than a dimer. The interface between the ER and KR domains is around 600 Å^2. This domain interface is more than 50% larger than the equivalent interface in mFAS. Most of the interaction results from contacts between nonconserved hydrophilic residues of the KR with the substrate binding subdomain of the ER.[61,72] It is thus possible that contacts between the KR and ER could affect the ER active site, affecting its activity and selectivity.

Analysis of the complete protein structure of mFAS shows that its DH and ER domains are in contact (section 1.3.1).[28,61] The overall sequence similarity between mFAS and SQTKS suggests that the SQTKS-ER and DH may also be in contact (Figure 58). The investigations of the stereoselectivity of the isolated SQTKS-ER domain performed by Doug Roberts showed that it cannot properly control the reprotonation step at the α-carbon, resulting in racemic product. It is possible that this is caused by the lack of protein-protein interactions with the DH domain.
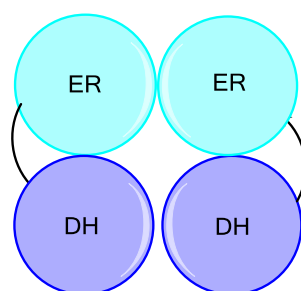

Figure 58: Linker region between ER and DH.

In order to investigate whether domain-domain interactions could be important in SQTKS, three different types of experiments were planned. First, kinetic experiments were planned in the presence or absence of different protein components. Second, interactions between the proteins themselves could be measured directly by isothermal

calorimetry (ITC). Finally, if protein protein interactions could be observed, then the rates of these interactions could be measured using surface plasmon resonance (SPR).

It is possible to measure kinetic constants for *substrates* of enzymes, and in this way map out the selectivities for isolated domains for compounds for which they catalyse reactions. However it is much harder to do this for *non-substrates - i.e.* compounds which for chemical reasons cannot be reacted. For example β-ketones cannot be substrates for ER enzymes. In iterative PKS systems it is important to know if non-substrates can spend any time in non-reacting active sites - for example can β-ketones spend time in ER active sites? If such interactions are significant they could contribute to the programming selectivity of the PKS. One way of investigating these non-reacting interactions is to study inhibition - for example we showed that **102** is an inhibitor of the ER and DH domains indicating that it can enter and bind, but such assays are tedious and do not show how much time non-reacting molecules spend in active sites (section 2.3.5 and section 3.3.4). These types of interactions have not been investigated before in any PKS or FAS systems and we reasoned that SPR could be very useful for these types of studies.

4.1. Aims of the project

To get more information about the protein structure of SQTKS and the recognition of substrates further investigations were planned. The focus of the project is on the interaction of the isolated domains with each other. Since it is assumed that both enzymes are connected[61] an interaction may be observed. Also interactions between subtrates that are involved in SQTKS should be investigated. We also planned to investgate whether compounds which are not substrates may interact with the isolated catalytic domains of SQTKS. The first aim of this project is to find a method to measure interactions between the isolated DH and ER domains. Possible analytical systems are ITC and SPR. Kinetic assays will also be used to determine if the presence of both domains can change the observed rates of substrate processing.[49] The second aim is the synthesis of acyl pantetheine substrates for the KR and *C*-MeT domains. These substrates should mimic possible intermediates of SQTKS. Further information about interactions between the isolated domains and different unusual substrates are expected. Key questions include whether it is possible for all substrates to visit every active site?

How long do they fill the active site? Do some structural motifs work as inhibitors? The third aim is to find an analytical system that can measure interactions between small molecules and isolated proteins. Possible candidates are ITC and SPR. It may also be possible to measure with both systems kinetic data that can give the expected information about interactions between substrates and protein.

4.2. Biophysical Investigation of DH and ER Domains in Solution

Assays of the ER domain in the presence of the DH domain.

First, a concept for an enzyme assay was developed where both enzymes were investigated together. The assays were performed in the same way that was used in the previous tests (section 2.3.4) in cuvettes in a volume of $400\,\mu L$ using $0.25\,\mu M$ tigloylpantetheine **85** as the substrate, with NADPH **13** as the cofactor. The concentration of the ER domain was held constant at 0.1 mg / mL. A range of different DH domain concentrations were used in the assays (0.0-0.1 mg/ mL). The rate of consumption of **13** was observed at 340 nm in triplicate. Initial rates were measured and compared to the isolated stand-alone ER domain.
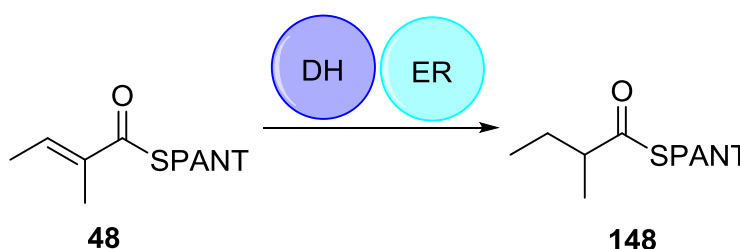
Scheme 44: Enzyme assay of **85** in the presence of ER and DH domain.

Low amounts of the DH domain (0.0125-0.025 mg/ mL) showed no significant changes in the initial rates catalysed by the ER. For higher amounts, the rates decreased (Figure 59). An effect to the ER domain is measurable. If a direct protein-protein interaction or if the reversed reaction of the DH domain is responsible for the decrease is unclear.
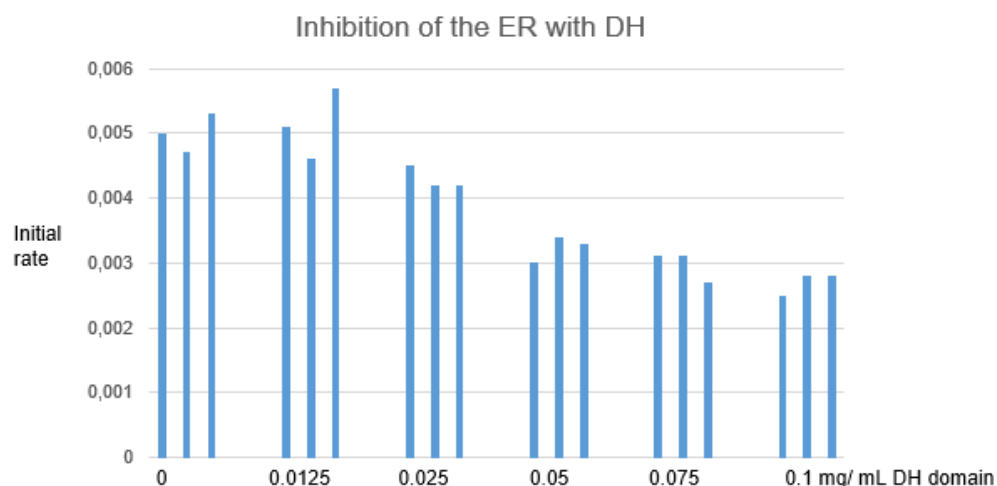
Figure 59: Triplices of initial rates of enzyme assays including DH and non DH domain for **85**.

Size exclusion Chromatography

If the ER and DH domains can interact it is possible that they could form stable heterodimeric, or higher order, species. These would be larger than the isolated proteins and may be detectable by gel-filtration chromatography where the elution volume is sensitive to molecular size.
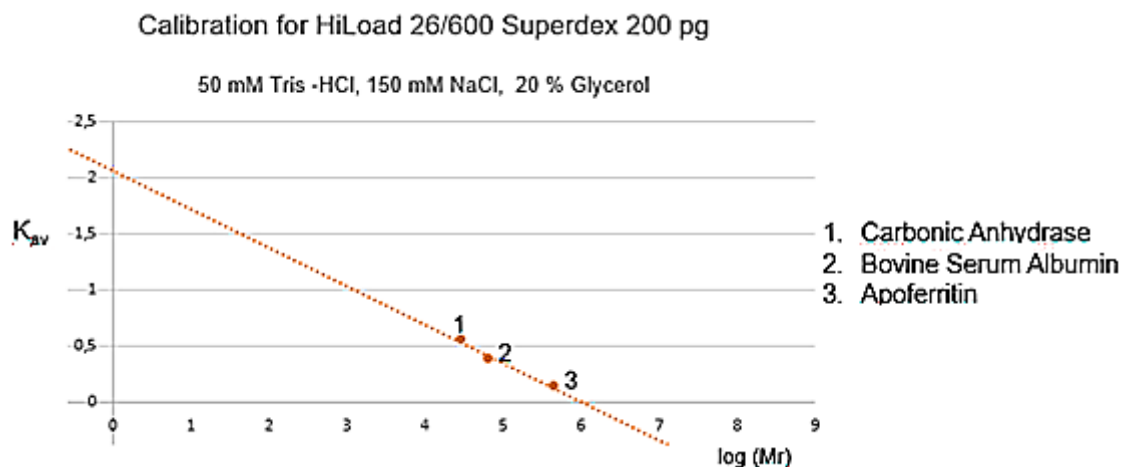
Figure 60: Calibration of HiLoad 26/600 Superdex 200 column using 50 mmol TRIS, 150 mmol NaCl and 20% glycerol buffer.

A gel filtration column (Size exclusion column- HiLoad 26/600 Superdex 200pg, GE Healthcare, 320 ml) was calibrated using commercial standards (carbonic anhydrase, 28 kDa; bovine serum albumin [BSA], 66 kDa; and apoferritin, 443 kDa; (Figure 60 and Figure 61). All enzymes were diluted as a mixture in 50 mmol TRIS, 150 mmol NaCl and 20% glycerol buffer to make a standard curve.
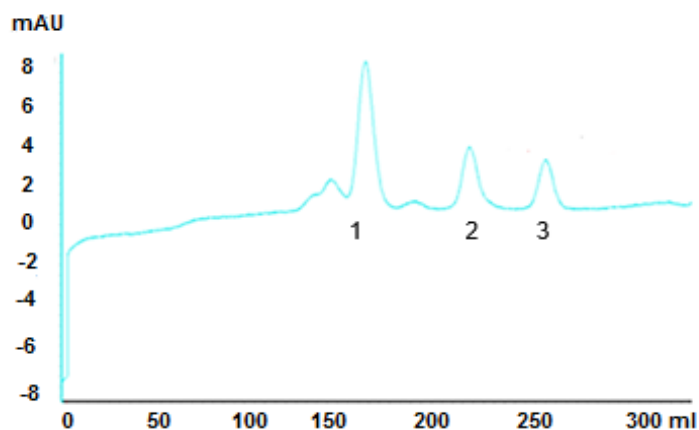
Figure 61: Size-exclusion chromatogram of calibration enzymes.

The size-exclusion of the DH domain analysis showed two peaks in the chromatogram. Only a small amount of the enzyme forms a dimer (Figure 62) in solution, peak at 190 mL. Most of the DH domain was eluted as monomer (210 mL).
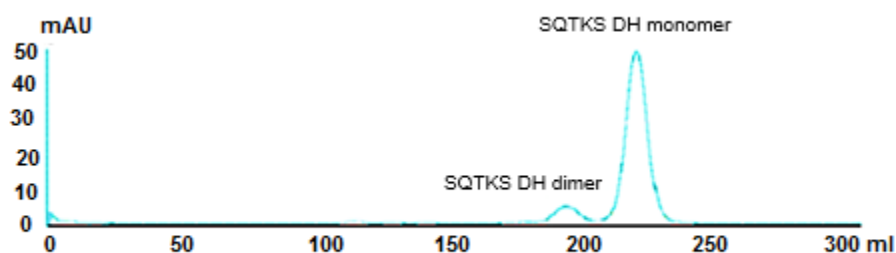
Figure 62: Size-exclusion chromatogram of isolated DH domain in solution.

The same test was performed with the stand alone ER domain. Also for this domain dimerization is known from mFAS and other PKS.[61,156] In the FPLC chromatogram only one major peak was observed. Comparison of the elution volume with the standard curve shows a dimeric ER domain (Figure 63). This fragment is around ~76 kDa
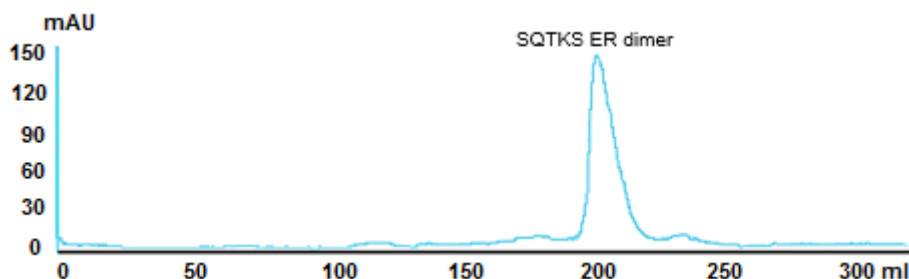
Figure 63: Size-exclusion chromatogram of isolated ER domain in solution.

Finally a mixture of both enzymes was loaded on the FPLC. An interaction of the domains in solution should result in larger protein complexes (calculated as 160 kDa for

ER$_2$DH$_2$). Two peaks were detected, one for the ER- at 190 mL and one for the DH domain at 220 mL (Figure 64). No other peaks were observed in the chromatogram, which could show any other complexes of the DH and ER domain together. Interactions of both enzymes would be expected in signals around 150 to 160 mL. At this time fragments complexes with the expected mass of ~160 kDa of both enzymes would be eluted.
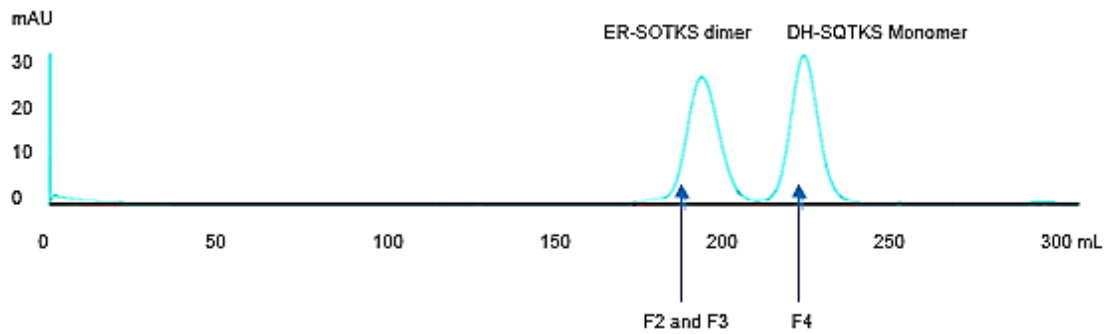
Figure 64: Chromatogram of DH and ER in solution.

For further analysis of the different FPLC runs fractions were collected over the whole elution time. After that the fractions were analysed by SDS page. On the SDS page the experiment showed the same results that were expected by the chromatograms of the single domains (Figure 65). The fractions F2 and F3 shows the ER in dimeric form and also the amount of DH dimer which was found in the analysis of the DH domain. These protein complexes have a size of ~76 kDa and are in agreement with the previous investigation. If a protein complex would be formed it should elute earlier than these peaks. Fraction F4 shows only the DH monomer.
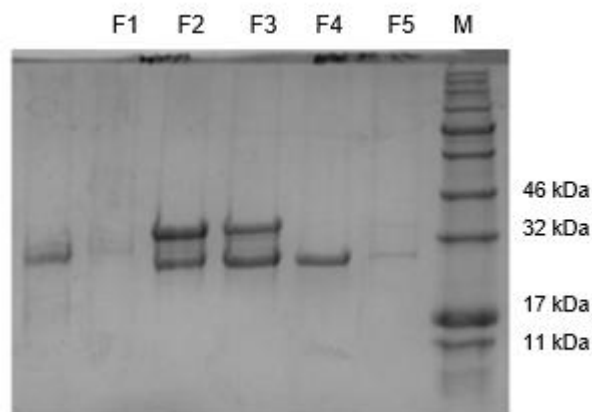
Figure 65: SDS page of the size exclusion experiment of ER and DH analysis by FPLC.

4.3 ITC investigation of isolated ER domain

Isothermal titration calorimetry (ITC) can measure the direct interaction between two proteins, or between a protein and a small molecule. ITC relies on the use of two identical cells which are heated in an insulated jacket.[157] Sensitive thermo elements detect differences in temperature between the cells. One of the cells (200 to 300 μl) is used as a reference cell, the other one is the sample cell. Both cells have the same contents (protein, ligand and buffer) before the experiment starts. A typical concentration for the protein is 0.1 mM. A ligand is then titrated into the sample cell during the experiment. If the ligand and protein interact, there will be a change in temperature in the sample cell (Figure 66).[157]
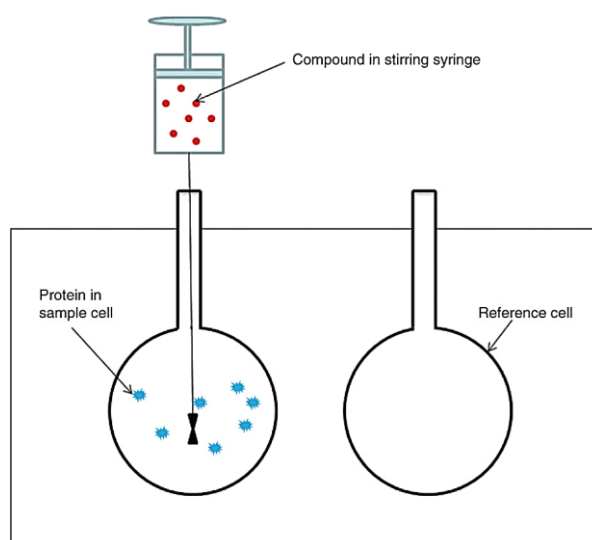
Figure 66: Setup of isothermal titration calorimetry experiment.[157]

A test run of ITC experiments was performed (Figure 67). In this experiment, the ER domain was used as protein in the sample cell (protein concentration 0.1 mM). Tigloylpantetheine **85** was chosen as the test ligand (1.4 mM). This was injected in several aliquots over 7000 seconds to the sample. The temperature was held constant at 20 °C.

The experimental results plot the observed energy change *vs* time (Figure 67). Every peak of graph a) corresponds to the introduction of 2.69 μL of **85** to the sample cell. The reference cell is demonstrated by b). Compared with the results known from the kinetic studies, similar results in the μM area were obtained. For K_d a value of 1.33×10^{-6} M was reached. The value for the enthalpy was 4.865 kJ / mol and for the entropy 0.130 kJ / mol. In the experiment n = 1.029 for the stoichiometry was calculated.
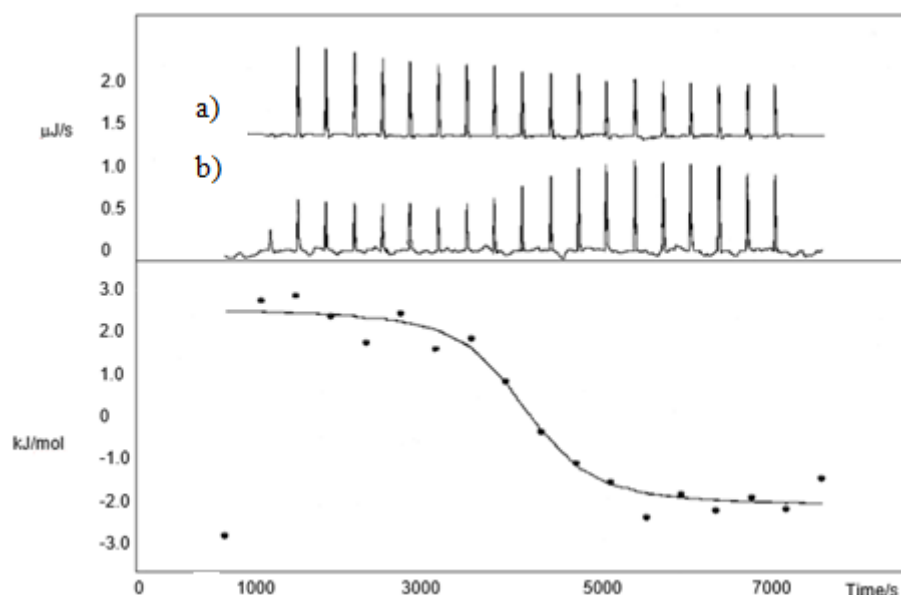
Figure 67: ITC run of **85** with the ER domain.

Interestingly no NADPH **13** was needed in the measuring. This shows that for a complete folding and for the stabilization no cofactor is necessary. Also interactions and binding events between substrate and enzyme can be observed without **13**.

A problem that was observed during the experiment was the partial precipitation of the ER domain in the sample cell. Effects on the following experiments are possible. The precipitation could be the result of the used buffer, or of the stirrer in the chamber, or a problem of the heating. The biggest problem of this ITC experiment is the large amount of protein (0.1 mM) that is needed. Also is it limited to the lack of sensitivity. Only a small value for the enthalpy was detectable which shows also significant errors in the resulting curve. For further investigations higher amounts of enzyme seems to be necessary. Because of the requirement for a high amount of protein and the observed precipitation, the interaction between DH and ER domain was not performed. It was expected that the same problems would be observed like the ones of the substrate-protein performance.

4.4   Surface Plasmon Resonance Studies

Surface plasmon resonance (SPR) analysis is one of the newest analysis methods for protein-protein and protein-ligand interactions. The system allows measurements of both kinetic and thermodynamic properties of two possible binding partners. A major advantage is the small amount of protein required: typical protein concentration is in the µM range.[158]

In SPR a protein or ligand is immobilized on the surface of a metal - usually gold or silver - in a flow cell. A second ligand (small molecule or protein) is then passed through the flow cell. If an interaction between the two components takes place, a change in refractive index on the surface of the metal is measurable. The result is shown as a graph of resonance units *vs* time. From the generated interaction curve the association (k_{on}) and dissociation (k_{off}) rates can be measured. The ratio of k_{on}/k_{off} gives the binding constant.

To create a higher density of immobilized ligand, special modified surfaces with carboxy dextran matrix have been developed. On these surfaces it is also possible to link smaller substrates. For example drugs can be immobilized and tested by the overflow of proteins on their efficiency.[159]

The general procedure is shown in Figure 68. The injection of the ligand results in an *association curve* that describes the interaction between both partners. In the following stage an equilibrium is reached. Finally, the injection of the ligand is stopped and a *dissociation curve* is observed.[160,161]
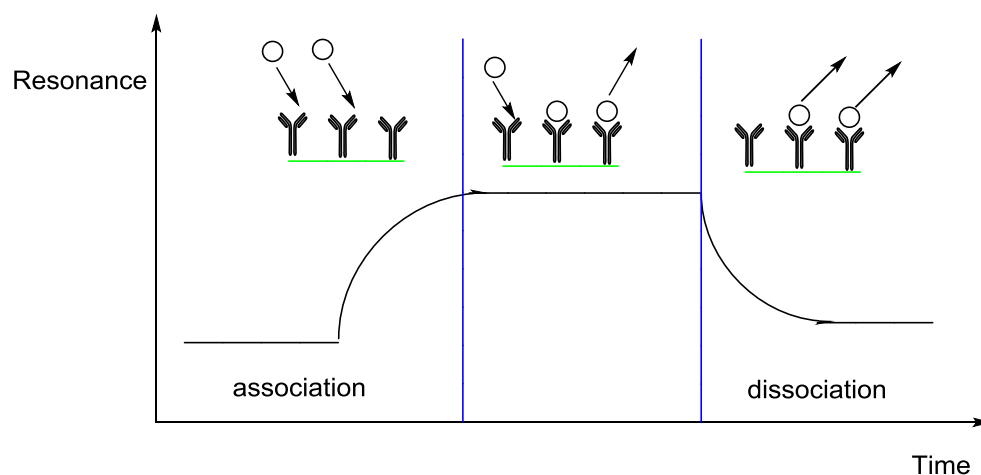
Figure 68: Binding and unbinding states during SPR experiments.

4.4.1 SPR of Small Molecules

The modification of the gold surface is one of the most important tasks which must be completed before SPR analysis. For the analysis of protein-small molecule interaction two approaches are possible. First, the protein itself can be attached to the surface, and the ligand flowed over it. Second the reverse protocol could be devised in which the small molecule is linked to the surface. In the first method it is usually simple to attach the protein to the surface, but the sensitivity of the subsequent measurement is low because addition of the small molecule causes only a small change in the refractive index. For this reason it is preferable to attach the small molecule to the surface, but this too can have problems, particularly if the binding moiety of the small molecule to the protein is masked by the surface. For this reason small molecules are often attached to the surfaces using linker molecules of varying lengths.[162-163]

Kanoh *et al.* showed one possible strategy for a surface modification. A chemical modification strategy which could be used in a photo-cross linked reaction was developed. A tri(ethylene glycol) derivative **206** was first oxidized to an aldehyde **207** which was then reductively aminated with a primary amine. The resulting diazarine **208** has an active nitrogen bond that can be used in photo-cross-linking reactions (Scheme 45).[164]
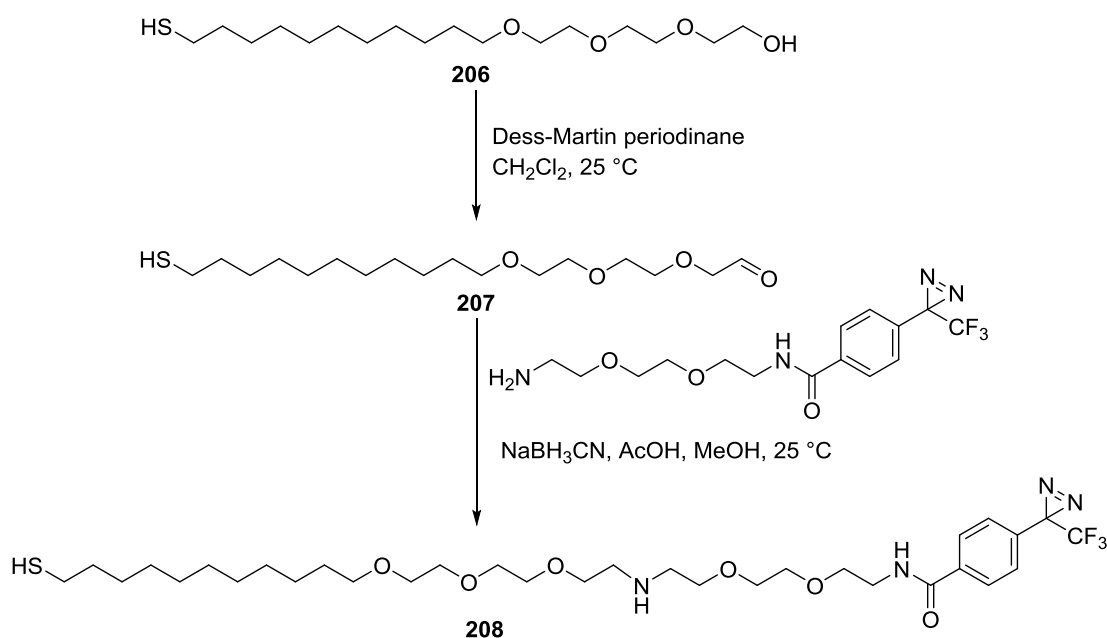
Scheme 45: Possible synthesis of photo-cross-linker.

This photoactive compound was cross-linked to the gold surface *via* the thiol. Small molecules with different functional groups could then be immobilised by a photochemical reaction with the diazarine group (Scheme 46).[164]
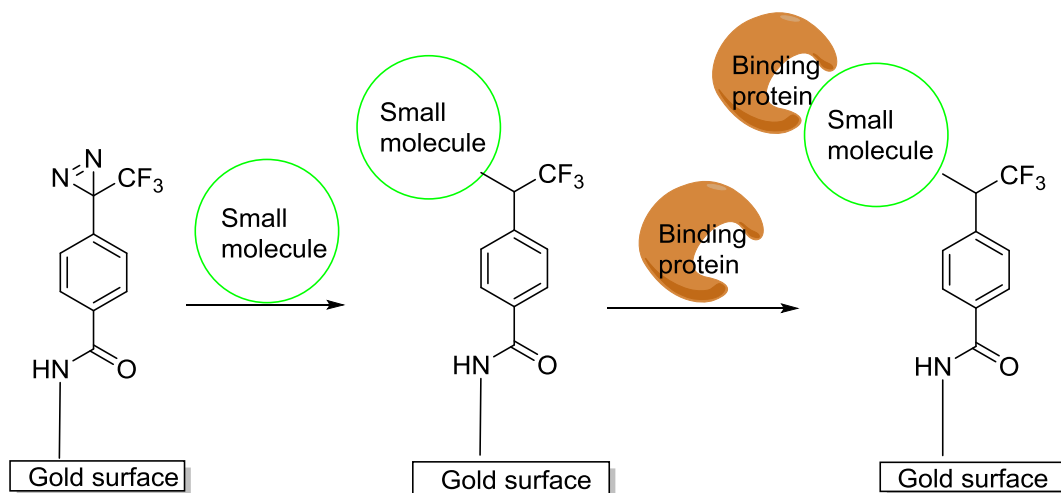
Scheme 46: Photo-cross-linked small molecule on gold surface.

Further experiments with the modified gold surface were performed. To prove the linking system a library of commercial available small molecules and corresponding antibodies and proteins was established. This library included cyclosporine A, digoxin, digitoxin, digoxigenin, estradiol and corticosterone. In that way, specific bindings could be observed between the immobilized steroidal molecules and the corresponding antibodies. A regeneration cycle was also developed. A wash of the gold surface with 10 mM aequeous HCL solution resulted in protein free surface and had no effect to the modified linker. The linker could then be used for another SPR test that showed the same results.[164]

4.4.2 SPR Investigation of Coupled ER domain on the Surface

In our first performed experiments, the isolated ER domain was cross-linked on a carboxy-methyl dextran (CMD) chip by EDCI coupling. Free carboxyl groups are located on the surface which can be used for cross linking surface amines on the protein to form amides. The DH was then flowed over the ER-modified surface and the interaction monitored in the form of the change of the refractive index (Figure 69).[165]

However no response could be observed (Figure 70). It was not possible to measure the k_{on} or k_{off} rates. This seems to agree with the previous results, where no

interaction was observed between the ER and DH. The same negative results were observed in a complementary experiment where the DH was attached to the surface and the ER flowed over it.
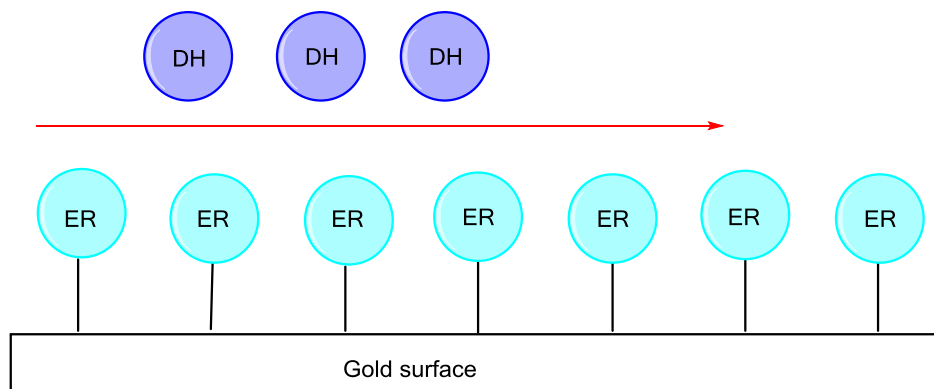
Figure 69: SPR overflow of ER- with DH domain.

The sample channel and the reference channel are shown to run similar. The injection of the protein started at 60 seconds and stopped at 230 seconds (Figure 70 a). A protein concentration of 2 mg/ mL of the DH domain was injected. The flow rate of the experiment was 10 µL/ min.
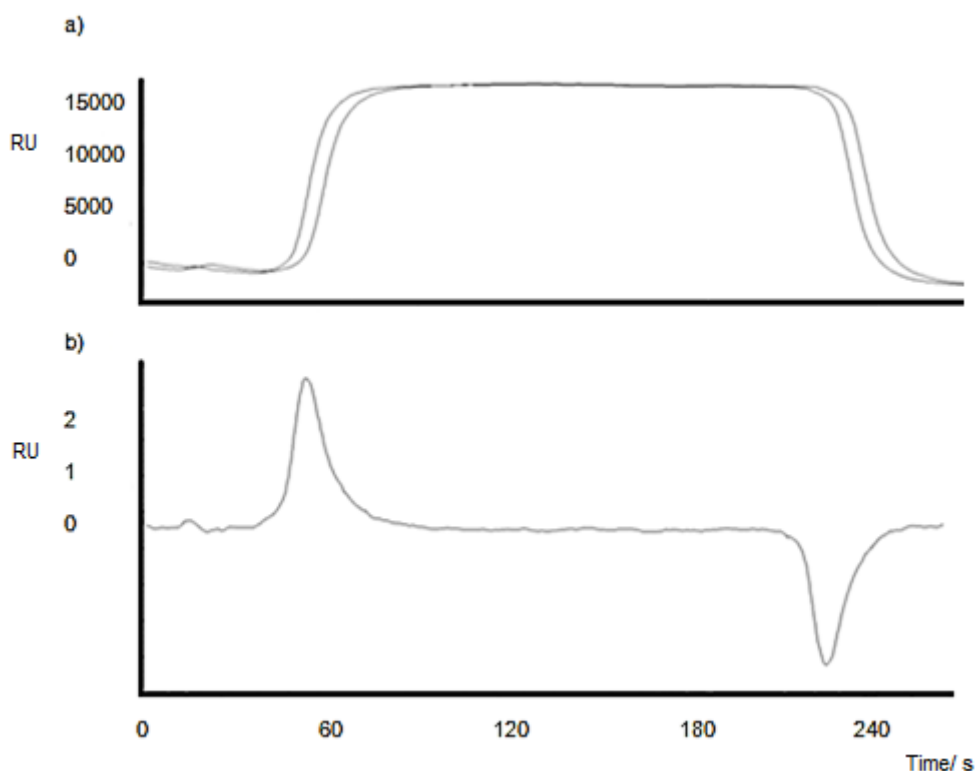
Figure 70: ER overflow with DH domain (a) and resulting interaction curve by the subtraction of reference and sample channel (b).

The subtraction of both channels showed the previous base line (Figure 70b). At 60 seconds and 230 seconds artefacts are visible that could result from small differences in buffer composition. Probably the reason for the artefacts are valve changings.

A second experiment was performed. In this experiment the DH domain was cross linked on the surface and used as possible binding ligand. The used protein concentration was similar to the previous performed experiment 2 mg/mL and also the same flow rate was used. Also the resulting subtracting curve of the experiment showed no interaction (Figure 71).

Figure 71: Interaction curve of the DH domain with overflowed with DH.

Both experiments are in agreement with the results that were obtained by the size exclusion experiments. For the DH-ER interaction no complexes around 160 kDa were found. Also for the DH domain was shown in the size exclusion experiments to be monomeric. Results from all analyses suggest that both separately expressed enzymes work individually and do not interact with each other. An interaction would be expected from the assumed model of FAS. In contrast to crystal structures of fatty acids the expected interaction between ER and DH domain is missing.

4.4.3 Protein-Substrate Interaction Analysed by SPR

The previous experiments showed no indication of an interaction between the DH and ER domains. In the following experiments SPR was used to investigate the selectivities of the individual DH and ER domains - and in particular whether small molecules which are not *substrates* can still be bound by, and spend time in, the active sites of the enzymes.

In the first experiments the ER domain was cross linked on the carboxy methyl dextran surface. The His$_6$-tag of the purified protein was used as a linker for the binding process to the surface similar to the previous coupling process (section 4.3.2). A change in the refraction index was measured that showed the clear binding between the protein and surface. Then different concentrations of tigloylpantetheine **85** (0.1 mM to 10 mM) were flowed over the cross linked protein surface. Changes in the refraction index were measured between the reference channel and test-channel. The flow rate of the experiment was settled to 25 μL/min and the dissociation time held constantly at 3 min. Subtracting the reference channel from the cross linked channel showed that no interaction was obtained. The calculation of an association and dissociation was not possible (Figure 72).
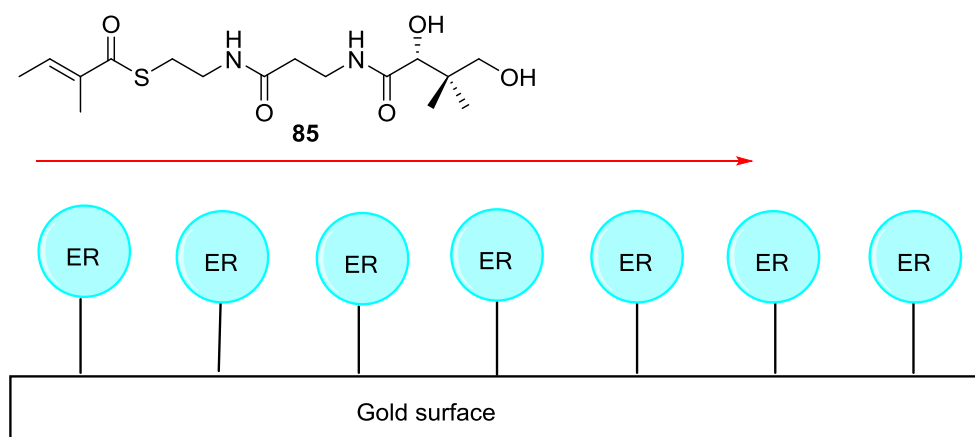
Figure 72: SPR experiment of cross-linked ER domain with **85**.

The described SPR investigation was used without the known cofactor for the ER domain (section 2.3.4). It could be possible that NADPH is necessary for the binding between the substrate and the enzyme. A use of NADPH would result in the reduction of the substrate during the binding process. Another possibility would be the use of NADP$^+$ to imitate the cofactor.

The negative result of the experiment could have several reasons. For example, a small molecule is used as the ligand, which means that only a small interaction and a small change in the refraction index could be detected. Previous investigations showed that the use of small molecules as immobilized ligands were more successful.[164]

4.4.4. Synthesis of Substrates for attachment to SPR Surfaces

The previous results lead us to modify the experiment. Instead of binding the protein to the surface, we decided to bind the substrate component. We have already shown that acyl pantetheines are very good substrates of the ER and DH enzymes (section 2.3.4 and section 3.4), and modelling has shown that specific interactions with the pantetheine itself are important. In order to move the pantetheine and acyl group slightly away from the surface, and to provide an attachment mechanism we decided to modify/extend the pantetheine with a short glycine linker which would allow the pantetheine to be tethered as an amide to the surface. (Figure 73).
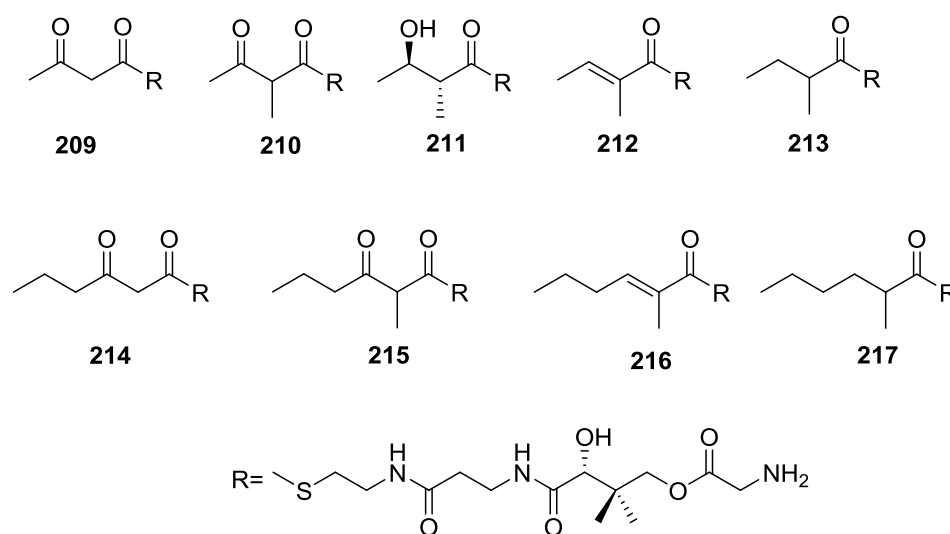
Figure 73: Library of substrates for SPR investigations.

The library of compounds was designed to include diketides (**209** - **213**) and triketides (**214** - **217**). The library also contains all possible β-processing intermediates such as ketones (**209**, **210**, **214** and **215**), alcohols (**211**), alkenes (**212** and **217**) and alkanes (**213** and **217**). The library also includes α-methylated (**210** - **213** and **215** - **217**) and non-methylated (**209** and **214**) compounds.

Precursors of compounds **209**, **210**, **214**, and **215** were synthesized separately. The synthesis of all four compounds started with Meldrum's acid **218** reacted with appropriate acid chlorides in the presence of pyridine as described in the literature.[166,167]
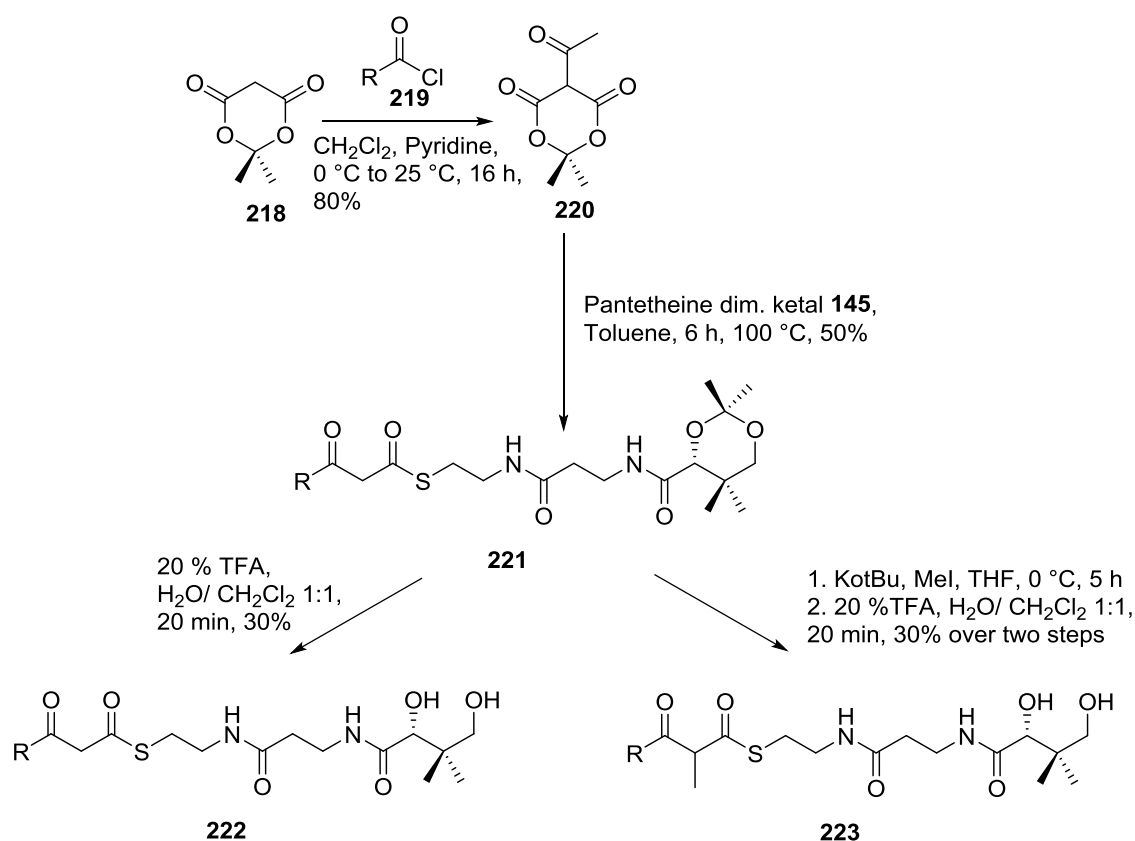
Scheme 47: Synthesis of β-carbonyl pantetheine substrates.

The acylated product **220** was heated in toluene with pantetheine dimethyl ketal to give the desired product **221**. This reaction is known to create SNAC substrates,[100] but has not been previously described for pantetheines. Protected pantetheine **221** could either be deprotected directly to give **222** by standard methods or α-methylated (*e.g.* **223**) with potassium *tert*-butoxide and methyl iodide and then deprotected (Scheme 47).[168]

The known method for pantetheine substrate synthesis was used to create the pantetheine substrates **85**, **91**, and **187** (Chapter 2 and 3). These compounds were then reacted with BOC-glycine under standard EDCI coupling conditions to give the BOC-gly-pant-acyl species, and these were simply deprotected to give the desired **211**, **212**, and **216** (Scheme 48).

The pantetheine substrates were purified by HPLC and then extended with BOC-glycine to create the pantetheine modified compounds (Figure 75). In general the BOC-protected intermediate **224** was not isolated, but deprotection with TFA in dichloromethane took place. The final products were purified by HPLC (Scheme 48).
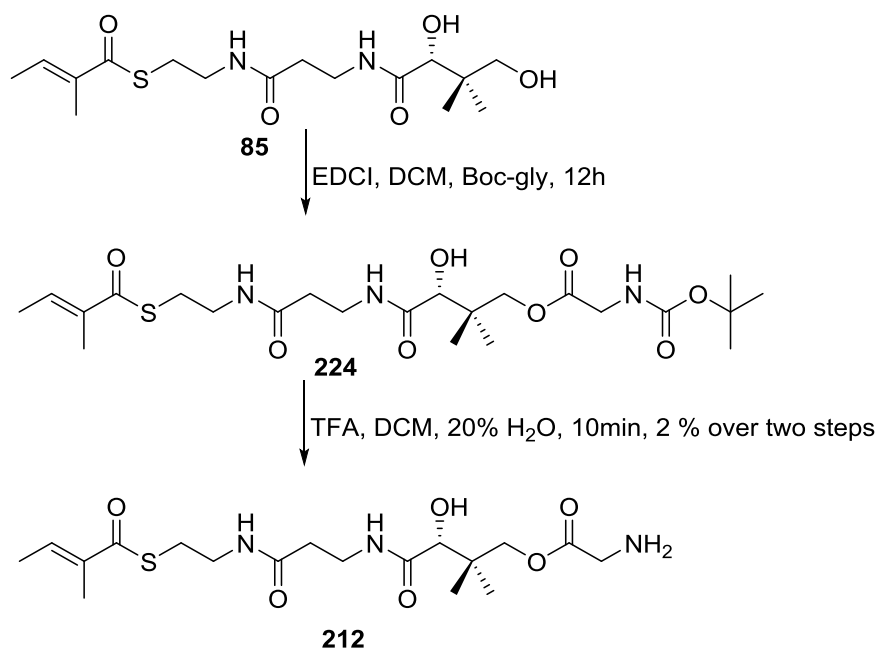
Scheme 48: Synthesis of tigloyl pantetheine glycine **212**.

Three intermediates were obtained during the final extension procedure (Figure 74). The main product of the reaction was the desired terminal coupled product **224**. The esterification of the secondary alcohol to form **225** was also observed: this compound was characterized by NMR. Doubly reacted material **226** was found in traces by LCMS.
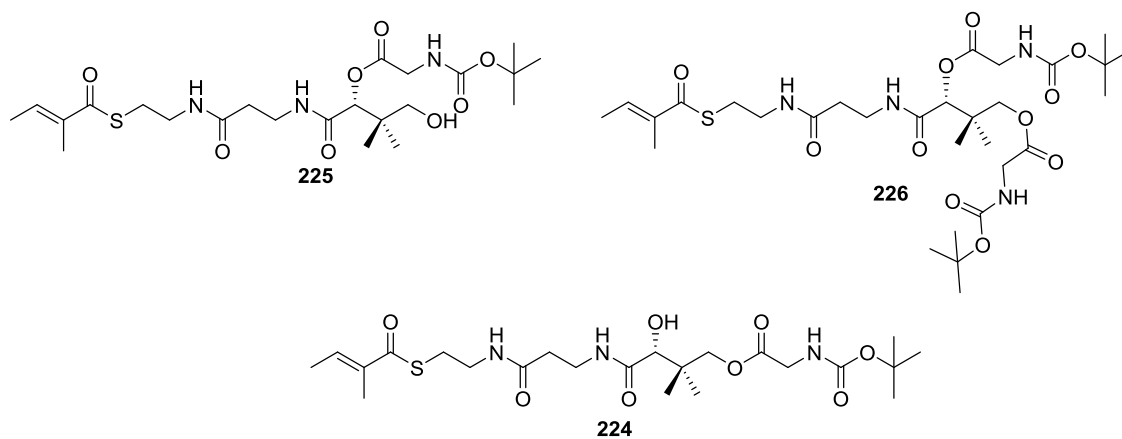
Figure 74: Intermediates of coupling reaction between **85** and boc-glycine.

4.4.5 SPR analysis of surface-linked ligands.

Assays were set up to test whether the attachment of the terminal glycine might inhibit the enzymatic reaction. 0.13 μM of compound **212** was incubated with the ER protein and NADPH **13**. The consumption of **13** was observed, indicating that this change in the substrate was tolerated (Figure 75).
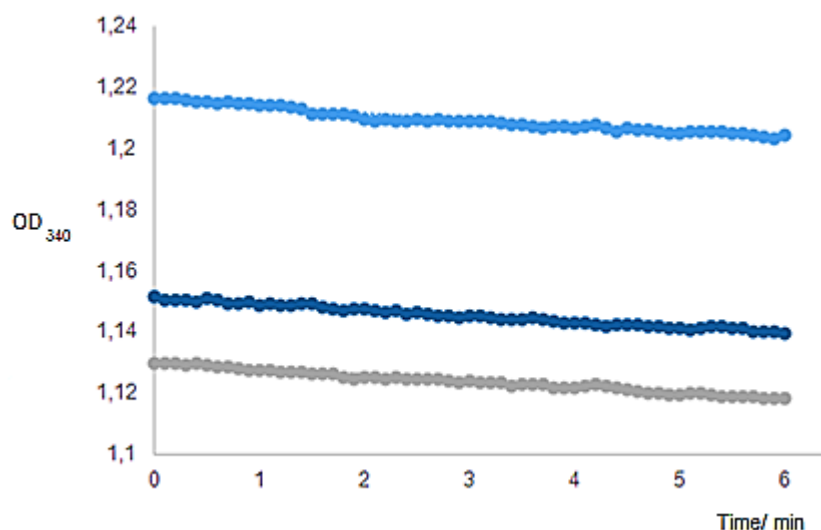
Figure 75: Absorption curves of the three replicates of tigloyl pantetheine glycine **212** at 0.13 μM.

The following SPR measurements were performed with sensor chip HC1000m. This chip is optimized for small molecules/ and peptide/ protein interaction. The surface of the chip is modified by a polycarboxylate hydrogel with a medium charge density which has a thickness of 500 nm.[169]

Under a continuous flow of 10 μL/min the sensorchip was installed in the SPR. Several buffers were tested for the coupling process of **212** with the chip surface. As coupling buffer a 10 mM maleate solution with a pH 7 was selected. A premixed activation mix was loaded to the gold chip. This buffer contains 100 mM EDCI. The buffer was incubated with the chip surface for 15 minutes. After that the substrate was loaded on the surface and incubated with the activated surface. Concentrations of the substrate were tested for 5-10 mM solutions. For the highest concentration, the best binding in the following experiments was observed (Figure 76).
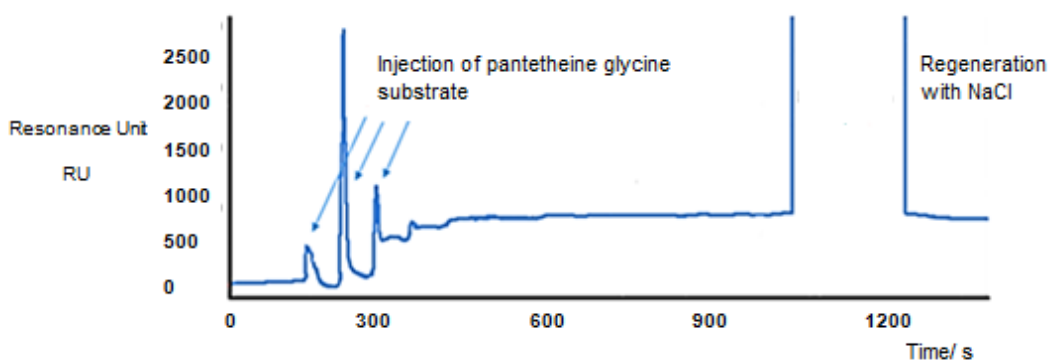
Figure 76: Modification of the gold surface by injection of pantetheine-glycine substrates.

Then the whole surface was washed with ethanolamine to block possible active residues of the surface that did not interact with the substrate. Finally, several wash runs were performed before the cross linked substrate was overflowed with the ER domain at a flow rate of 10 µL/ min. Concentrations of 0.25 mg/ mL to 10 mg/ mL of the ER domain were used (Figure 77).
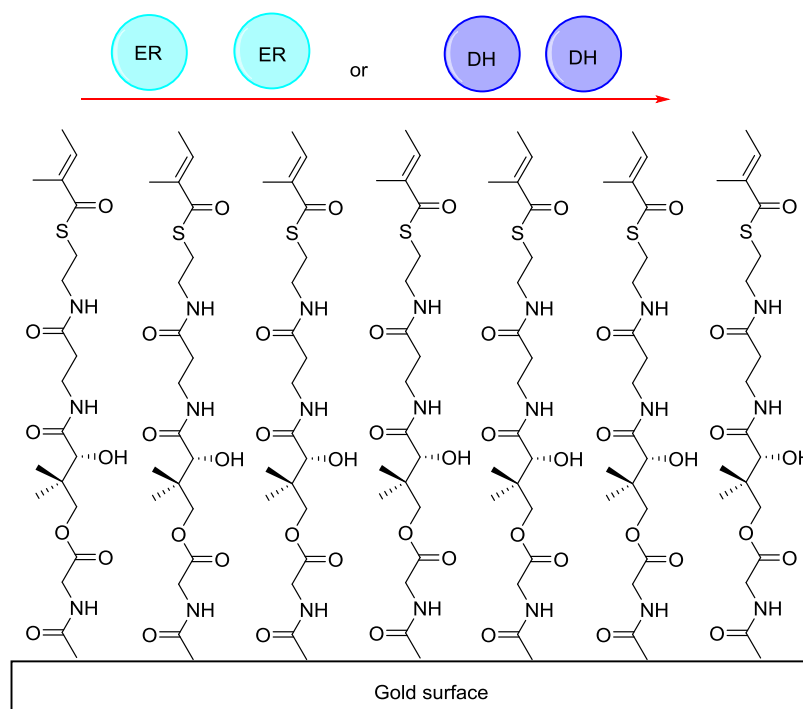
Figure 77: Coupled **212** on gold surface with ER- or DH domain overflow.

In contrast to the previous experiments, a positive resonance for the interaction was observed. This time the change of the refractive index was more significant than the change of the previous tests: a k_D 4.03 x 10^{-6} M was measured. Similar to the test of the ITC (section 4.2) no NADPH cofactor was used showing that the cofactor is not required to bind before the substrate.
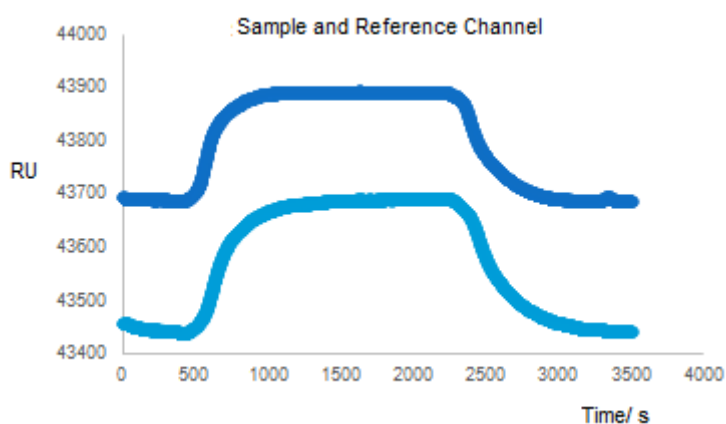
Figure 78: Reference and sample channel cross-linked **212** with ER domain (4 mg/mL).

The sample and reference channel shows the injection of the protein at 500 seconds (Figure 78). For both channels a change in the refractive index is visible. Change of the injection buffer is observed at 2500 seconds. At this point the protein overflow is stopped. The same baseline is reached which was observed before the injection started. The interaction of protein and substrate was calculated by the subtraction of sample and reference channel (Figure 79). The results show a clear association period (0-200 seconds) followed by equilibrium between bound and unbound protein (200-2000 seconds). After that the dissociation follows.
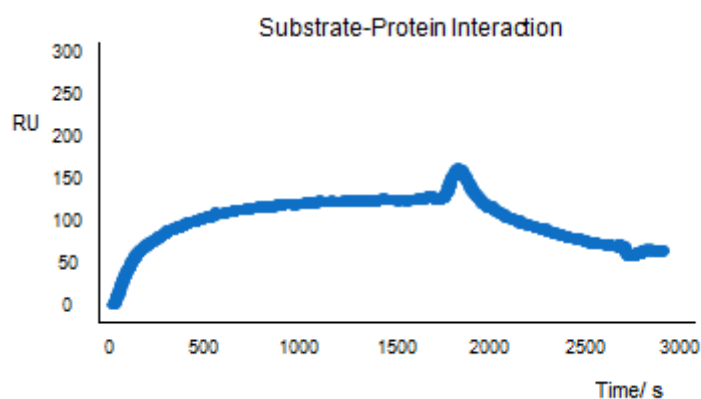
Figure 79: Interaction of **212** with ER domain (4 mg/ mL).

Another SPR experiment was set up with the same modified gold surface. This time **212** was overflowed by a solution that contains the same concentrations of the DH domain. This experiment also indicates an interaction (Figure 80). For the DH domain it runs faster and reaches the equilibrium between 400 and 1500 seconds. At 2000 seconds the dissociation starts. However, first the signal rises at this position but shows the expected curve.
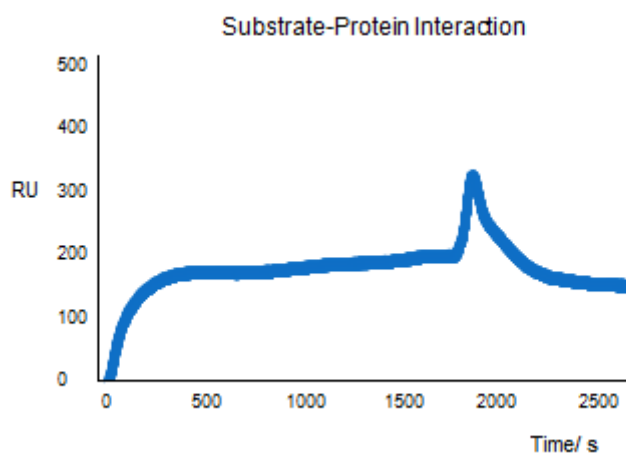
Figure 80: SPR interaction between **212** and DH domain overflow.

This behaviour was unexpected because the tigloyl pantetheine glycine **212** unit is the *product* rather than the substrate of the DH domain and not expected to bind significantly. The result is, however, supported by the previous observation that SQTK can inhibit the DH domain (section 3.3.4).

Based on these experiments the other substrates of the library were also cross-linked to the surface and overflowed with solutions of the ER and DH proteins. Generally the protein concentrations were varied between 0.25 mg/mL to 10 mg/mL. The flow rate of the instrument was set up to 10 μL/min.

SPR interactions of the DH domain

In the following experiments, three different results were observed when a solution containing the isolated DH domain was flowed over the surface-linked substrates. The first SPR investigation was performed with the triketide 3-oxohexanoyl substrate **214** (Figure 81). The experiment begins by flowing buffer over the surface and no signal is observed. After 50 seconds the flow is changed to buffer plus DH. A clear association is visible between 50 and 210 seconds. **214** interacts with the DH domain at this point until the maximum at 210 seconds is reached. For lower protein concentrations a linear graph is rising. For higher concentrations the expected curve was obtained. For all concentrations tested no equilibrium is reached during the experiment.

Figure 81: DH overflow of 3-oxohexanoyl pantetheine glycine **214**. Protein concentrations are shown by the different colours: 0.25 mg / mL, black; 0.5 mg / mL, red; 1 mg / mL, blue, 2 mg / mL, green, 4 mg / mL, yellow; 6 mg / mL, light blue; 10 mg / mL, purple.

After 220 seconds the flow is changed back to buffer and a dissociation curve is observed. This experiment shows a clear interaction between enzyme and bound intermediate. Interestingly an unnatural substrate is recognized by the DH domain. Overall for the highest protein concentration an interaction of 120 resonance units was observed. Similar results were obtained for the diketide version **209** (see Appendix A1)

of this structural motif. Optimization of the SPR data could be performed by increasing the flow rate from 10 μL/min to 25 μL/min.

The 3-oxo-2-methylhexanoyl triketide **215** was analysed next (Figure 82). This compound is the true substrate of the KR domain. In comparison to **214** a hydrogen at C-2 is substituted with a methyl group. In the first 50 seconds, only buffer flows over the surface. Artefacts are visible at 50 seconds. At this point the buffer is changed to the protein solution for the next 160 seconds.
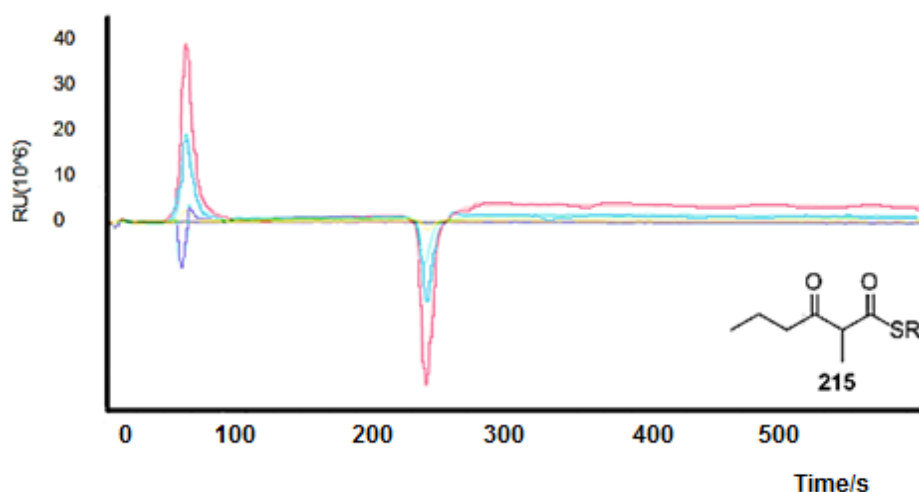
Figure 82: DH overflow of 3-oxo-2-methylhexanoyl pantetheine glycine **215**.

In contrast to the first experiment, no association and dissociation could be measured. At 220 seconds a second artefact is visible which corresponds to the time at which the protein solution is changed to buffer. The same result was observed for the diketide version **210** (see Appendix A2). It seems that the methyl group in the α-position has a significant influence to the experiment.

It was not tried to measure interactions with compound **211** because this is a substrate of the DH and reactions would be expected to dehydrate the substrate on the surface. Also from the previous investigation it was already verified that **211** is a compound of the DH domain and can visit the active site. The next assay simulates used the 2-methyl-hexenoyl triketide **216**. Weak interactions of 20 resonance units were detectable between the substrate and DH which appeared to vary with protein concentration. However, the weakness of the data, and large artefacts caused by the switching valve made it impossible to calculate association and dissociation constants. Very similar results were obtained for **212** with only weak interactions observed (see Appendix A3). This is in contrast the previous performed studies where high interactions were measured (section 4.3.5).
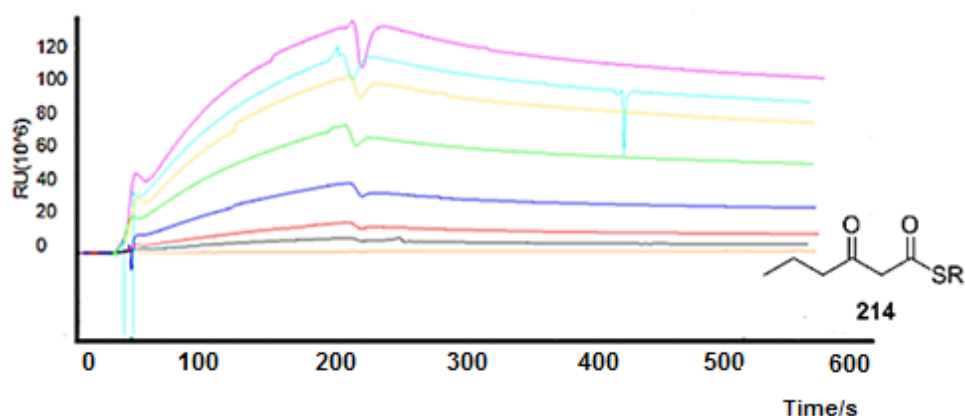
Figure 83: DH overflow of 2-methylhexenoyl pantetheine glycine **216**. Protein concentrations are shown by the different colours: 0.25 mg/ mL, underlined red; 0.5 mg/ mL, underlined red; 1 mg/ mL, red, 2 mg/ mL, light blue, 4 mg/ mL, green; 6 mg/ mL, purple; 10 mg/ mL, black.

Finally the triketide alkane **217** was tested. For the first 50 seconds only buffer overflows the surface. After that the protein is injected from 50 to 220 seconds. Similar to the previous investigation of **216**, the measurement of association and dissociation constants was not possible because of weak data and artefacts. The equilibrium between association and dissociation is not reached which is shown by the rising graph (Figure 84). Also **213** (see Appendix A4) agrees with this investigation and runs similar.
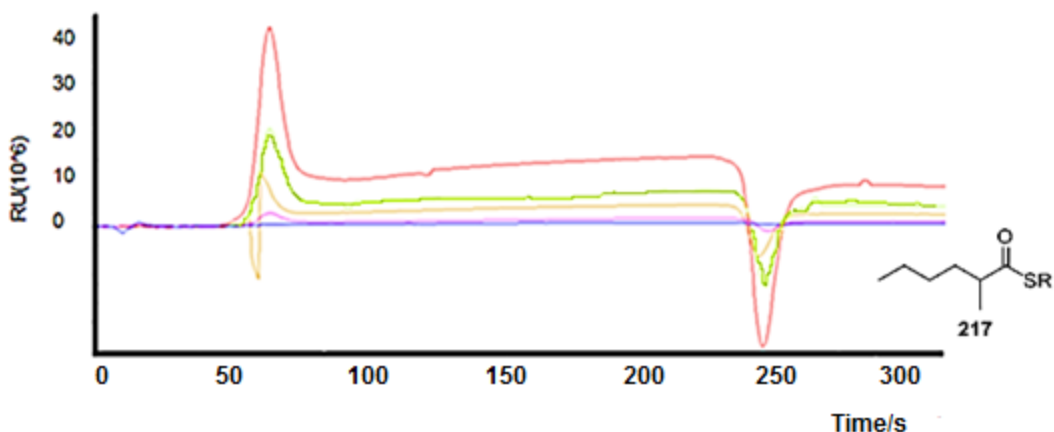
Figure 84: Reduction of 2-methylhexanoyl pantetheine glycine **217**. Protein concentrations are shown by the different colours: 0.25 mg/ mL, underlined blue; 0.5 mg/ mL, underlined blue; 1 mg/ mL, blue, 2 mg/ mL, purple, 4 mg/ mL, brown; 6 mg/ mL, green; 10 mg/ mL, red.

A problem observed for all measurements are artefacts at 50 seconds and 240 seconds. For washing processes (dissociation and regeneration) the system is switched to the by-pass mode. Before the association starts the valve is switched to the sample loop (Figure 85). The artefacts at 50 second and 240 seconds result from the switch of the

valve from position 1 to position 2 and back. In cases of weak association this makes it nearly impossible to measure the dissociation and association constants.
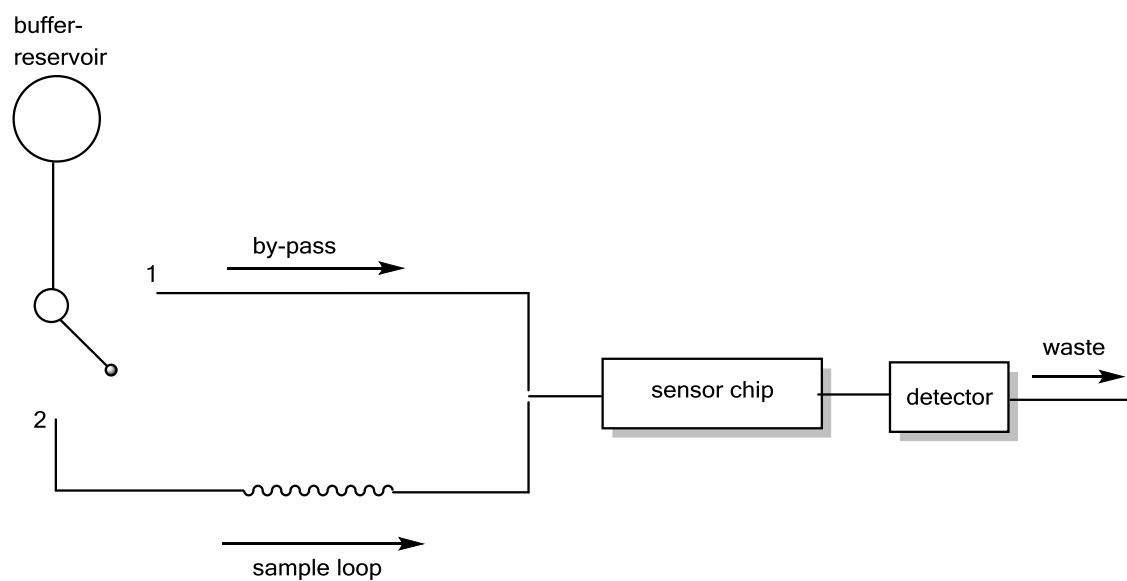
Figure 85: Flow path during SPR investigation.

Table 1 gives an overview of the nine different linked substrates that were overflowed and analysed by the DH domain.

Structural motif	Interaction	Appendix	Structural motif	Interaction	Appendix
209	x	A1	**214**	x	
210	-	A2	**215**	-	
211	not measured	-	**216**	x	
212	x	A3	**217**	x	
213	x	A4			

Table 1: Interaction partners of the DH domain.

SPR Analysis of the ER Domain

The substrates for the different modification steps were also tested with the ER domain. Similar to the measurements of the DH domain it was possible to observe interactions between the ER domain and the β-oxo triketide **214** (Figure 86).

In contrast to the analysis of the DH experiment, the association does not follow the expexted curve, and this may be an indication of a flow rate which is too low. The equilibrium between bound ER domain and the substrate was not reached during the analysis time and association and dissociation constants are impossible to determine. However the data does show that the ER domain exhibits strong binding to the modified surface. This is visible in low dissociation curve. An interaction of 125 resonance units was observed for this experiment (Figure 86). Also for the diketide substrate **209** of these modification step shows the same result that was obtained for **214** (see Appendix, A8).

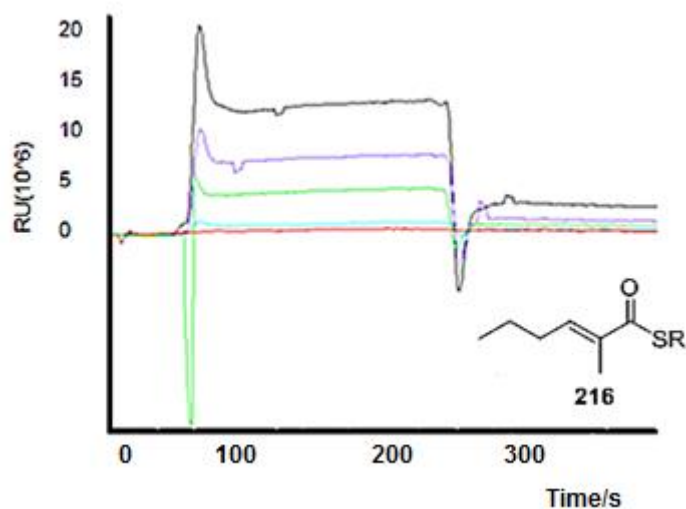**Figure 86:** ER overflow of 3-oxohexanoyl pantetheine glycine **214**. Protein concentrations are shown by the different colours: 0.25 mg/ mL, not mentioned; 0.5 mg/ mL, black; 1 mg/ mL, red, 2 mg/ mL, blue, 4 mg/ mL, green; 6 mg/ mL, light blue; 10 mg/ mL, yellow.

The α-methylated ketones **210** and **215** interact very weakly with the ER (Figure 87). The data is similarly poor in each case since the expected curve is not observed. A negative interaction is observed also for **215** (see Appendix A5). Why the interactions show up negative is unclear, since for all investigations and the protein stock solution the same buffer was used.

Figure 87: ER overflow of 3-oxo-2-methyl-butyryl pantetheine glycine **210**. Protein concentrations are shown by the different colours: 0.25 mg/ mL, not mentioned; 0.5 mg/ mL, yellow; 1 mg/ mL, black, 2 mg/ mL, light blue, 4 mg/ mL, blue; 6 mg/ mL, purple; 10 mg/ mL, green.

The experiment of **212** shows an interaction with the ER domain (Figure 88). It is a natural substrate of the ER domain and is reduced in the first elongation step. In contrast to the triketide **216** (see Appendix A6) the mimicked diketide showed a clear interaction. This agrees with the expected behaviour of this substrate. For the different concentrations of the enzyme the increase was observed.

For higher concentrations the equilibrium of bound enzyme was reached. The association shows for low concentrations a linear course. This indicates that the flow rate was too low. For higher concentrations the expected curve is visible. Also the dissociation curve is for all concentrations very slow. This is a second indication that the flow rate is too low.
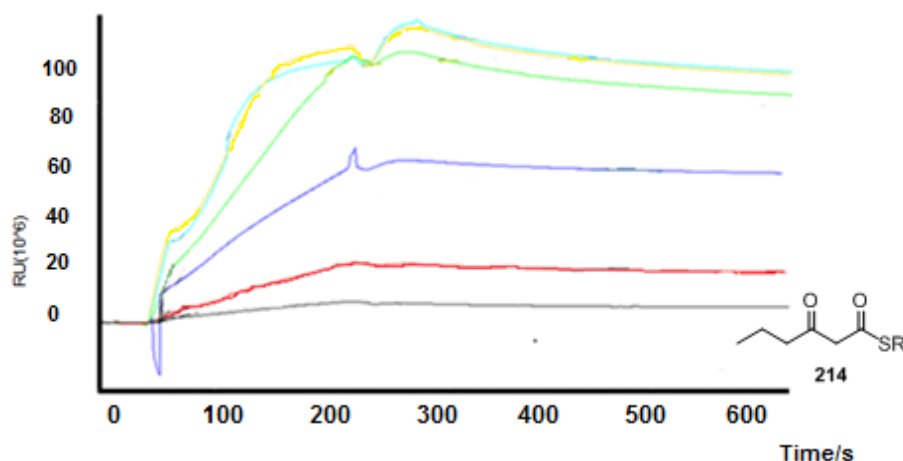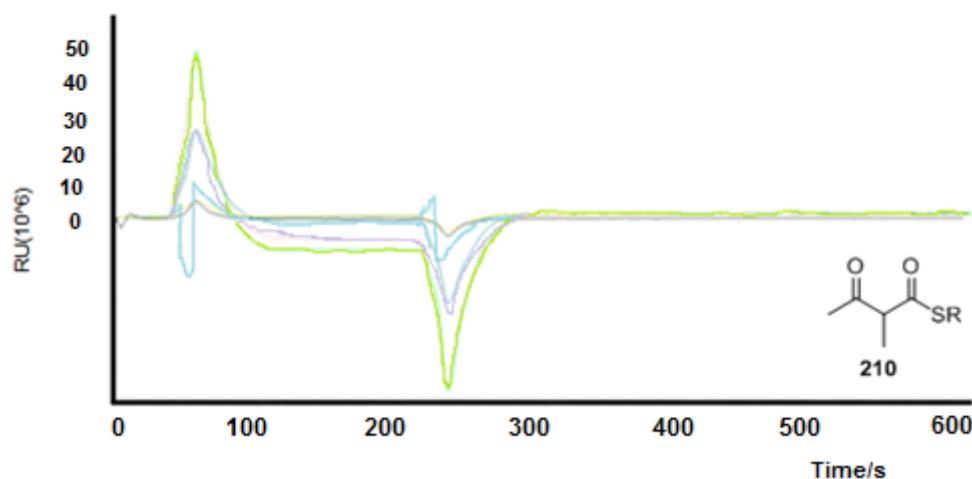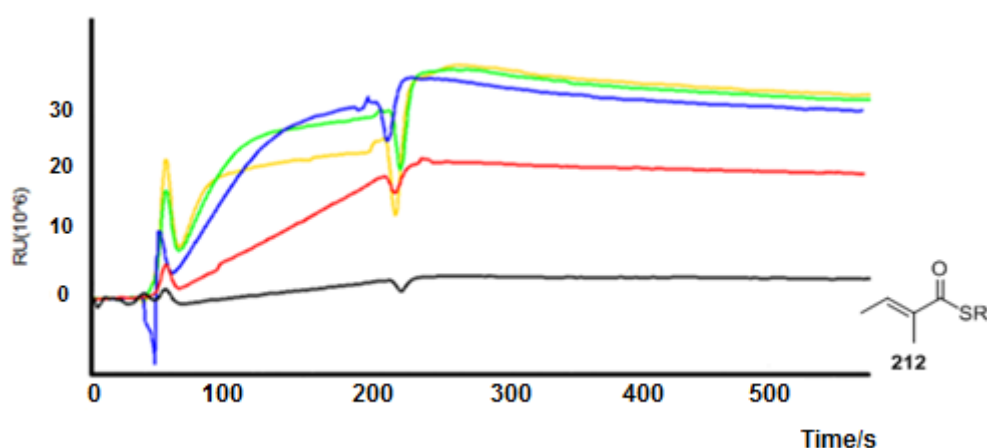

Figure 88: ER overflow of tigloyl pantetheine glycine **212**. Protein concentrations are shown by the different colours: 1 mg/ mL, black, 2 mg/ mL, red, 4 mg/ mL, yellow; 6 mg/ mL, green; 10 mg/ mL, blue.

The bound material can not be washed away quickly by this flow rate. For the triketide version of this structural motif a similar graph to the analysis of **212** (Figure 88) was obtained. During the experiment no NADPH or NADP$^+$ was used, ensuring that no reaction took place.

In the next experiments, the alkanes 2-methylbutyryl diketide **213** and 2-methylhexanoyl triketide **217** were investigated. For both substrates a negative interaction curve was again observed. This was an unexpected result for these compounds. Both compounds are the release products of the ER domain. They should leave the active site fast; otherwise the PKS would be blocked. The shown interaction is unexpected (see Appendix A7 and A10).

The final experiment shows the result of cross-linked tigloyl pantetheine glycine **212** that is overflowed with the ER domain at a faster flow rate (25 µL/ min). It shows clearer dissociation and association curves (Figure 89). The equilibrium is more pronounced in comparison to the previous investigations. That the equilibrium is reached between 150- and 220 seconds shows the sensitivity of the analysing system. A better dissociation curve could be generated in contrast to the previous runs. Increasing the flow rate has also reduced the influence of the artefacts at 50 and 250 seconds.
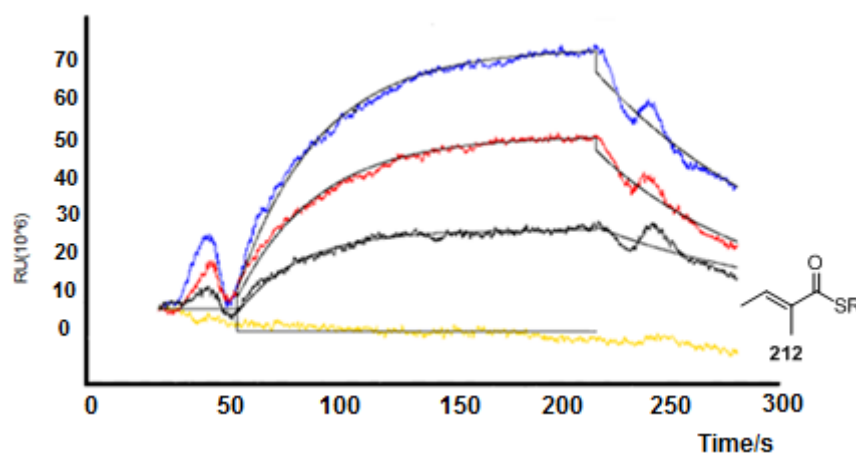
Figure 89: ER overflow of **212** with a higher flow rate. Protein concentrations are shown by the different colours: 2 mg/ mL, red, 4 mg/ mL, yellow; 6 mg/ mL, green.
.

The results for interaction between ER domain and the synthesized substrates are summarized in table 2. The overview of the overflowed substrates were analysed by the ER domain. It seems that all substrates have interactions with the enzyme.
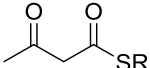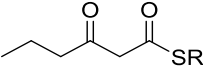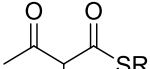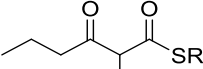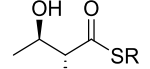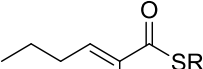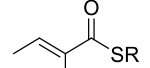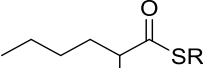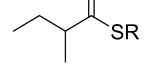
Structural motif	Interaction	Appendix	Structural motif	Interaction	Appendix
209	x	A8	**214**	x	
210	x		**215**	x	A5
211	x	A9	**216**	x	A6
212	x		**217**	x	A7
213	x	A10			

Table 2: Interaction partners of the ER domain.

4.5 Discussion

To investigate potential interactions between the isolated DH and ER domains of SQTKS both individual domains were investigated in the presence of the other. Enzyme assays were performed that included both enzymes. In a kinetic analysis of the ER enzyme, it was found that the rate of reduction of substrate **85** was reduced by the presence of the DH enzyme in increasing concentrations. Two explanations are possible. The first one suggests interactions between the ER and DH. The presence of the second enzyme may have effects on the active site of the ER. The second one highlights the reversed reaction of the DH domain which has been observed in previous investigations (Figure 90).[151,152]
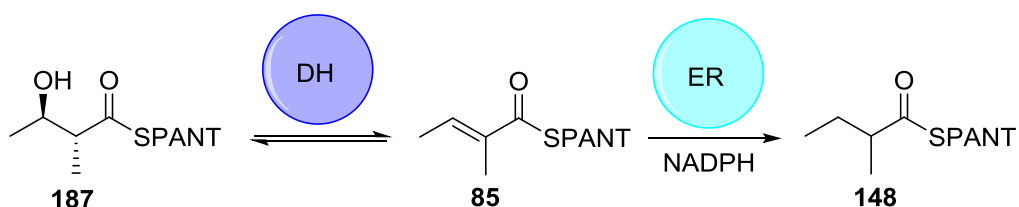
Figure 90: Possible equilibrium between substrates **85**, **187**, **148**.

Formation of β-alcohol **187** would reduce the concentration of enoyl substrate **85** and thus slow the reaction. Since no other experiment suggested that the ER and DH associate this is the most likely reason for the observation.

In further experiments no interactions between both isolated domains were observed. In our experiments size exclusion chromatography was used to detect possible protein-protein association. These experiments did not show any evidence for formation of ER-DH multimers. Further investigations by SPR also suggested minimal interactions between these domains. This was an unexpected result because, based on the crystal structure of mFAS, an enzyme to which SQTKS shows end-to-end sequence homology and the same domain organisation, we expected some measureable interactions.[28,61]

There are several reasons for the inability to observe protein-protein interactions between these domains. First, it is possible that their interactions are actually minimal. The crysal structure of mFAS shows that only a small part of the DH and ER domains interact.[28] Second, it may be possible that an additional linker sequence, not included as part of the current ER and DH sequences, is necessary to bring both domains together.[28] An expression of the complete DH-ER fragment with additional crystallization could solve this question. A similar experiment was performed by Zheng and coworkers and discussed earlier (section 4.0).[72] Currently for all isolated DH domains of PKS a dimeric structure for the DH has been observed.[17,71] But the SQTKS-DH exists primarily as a monomer. This also suggests that an important part that is necessary for protein-protein interaction was not expressed. For the ER domain the expected dimeric organisation was observed, in agreement with the ER domain of mFAS.[28]

A third possibility for the lack of observed DH-ER interactions could be the requirement to include glycerol in all the purification and assay buffers. Glycerol is required to stabilise the isolated ER in particular, and without it rapid protein precipitation is observed. The glycerol could prevent protein-protein interactions by forming an amphiphilic surface around the isolated domains - indeed this was the rationalisation for using it in the first place. This could be the starting point for new investigations. For example it would be interesting to mix ER and DH in glycerol containing buffers, and then slowly dialyse away the glycerol to see if stable and soluble DH-ER multimers could be formed (Figure 91).
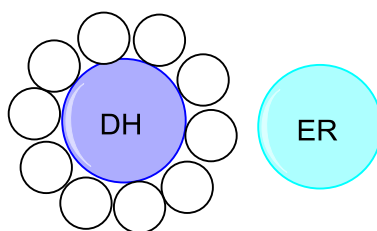
Figure 91: Glycerol surface of the DH domain.

Investigation of protein-intermediate interactions formed the second part of this project. These experiments were performed by two different ways, ITC and SPR. The ITC experiment of tigloylpantetheine **85** and the ER showed the similar results to the performed enzyme assays (Chapter 2.3.4). During the experiment precipitation of the ER domain was observed. This could be reasoned to the heating process of ITC or the stirrer in the solution. The precipitation and the high amount of enzyme required meant that ITC was not a generally useful method for analysis of the isolated protein domains. In further experiments an SPR system was used. The modification of the surface is known by several experiments of this technique.[170-172]

Information gained from enzyme assays and protein modelling (chapter 2) showed that the pantetheine arm interacts with both the ER and DH proteins because acyl pantetheines are significantly better substrates than the much shorter acyl SNACs. The pantetheine is already used by nature as a *linker* to connect the substrate to the ACP and allow it to penetrate deep into the active sites of the β-processing enzymes. We reasoned that we could use the pantetheine as a similar linker to link the acyl groups to a metal surface. In order to move the pantetheine slightly further away from the surface, and also to provide an amine for chemical connection, we added BOC-glycine to the primary alcohol of the pantetheines which had already been synthesised (section 2.3.3). BOC-deprotection and then EDCI catalysed amide formation with free carboxylates on the metal surface effectively linked the acyl pantetheines to the surface. Also the synthesis of the different structural motifs of other PKS domains was possible.

Modelling of substrate **216** into the ER domain in the presence of the cofactor NADPH **13** was performed by other members of the Cox group (Figure 92 b). The model shows that the terminal amine group of the acyl pantetheine glycine is positioned outside the ER domain (Figure 92 a). Similar to the previous modelled pantetheine substrates the interaction between the pantetheine arm and the protein is visible. The orientation of the hydride transfer of **13** to the substrate is also possible (Figure 92 c). The reduction process is not affected.
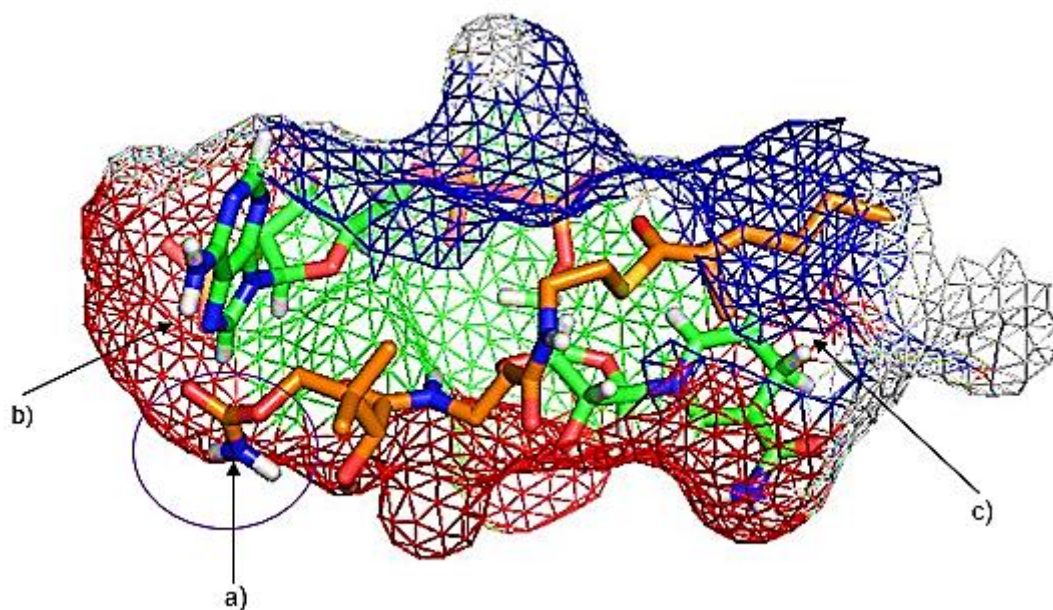
Figure 92: Modelling of substrate **216** into the ER domain (a).

Interaction between surface and substrates

Currently there are no studies known in literature that work with isolated PKS domains and SPR systems. Some other experiments of enzymes and cross-linkers are described in previous sections.

The DH enzyme has a high acceptance for the different functional groups that are involved in the β-modification cycle of SQTKS. In general, the interactions were detected, but technical problems were encountered in the execution of the experiments by the system. The dissociation and association curves were influenced by valve changing. Also the buffers with 10% and 20% glycerol seems to be a problem. Repeating these experiments, maybe with a faster flow rate, would bring the enzyme-substrate interaction faster in equilibrium. This would also effect the association and dissociation, which would lead in stronger curves. A faster flow rate would also result in less diffusion between the four channels. Possibly the artefacts that are produced by the valve changing would be limited or reduced.

For the DH domain nearly all intermediates showed interaction. Compounds **211** and **215** are the only intermediates that show no interaction. Possibly the three dimensional orientation of **215** does not fit in the active site. The DH domain normally accepts methyl groups, which is known from the programming of SQTKS. Compound **214** also showed interaction with the DH domain. The KR domain reduces the structural motif of **215** that is used in the next modification by the DH domain. During this

reduction the three-dimensional structure changes from planar into tetrahedral. Possible that the planar structure with additional methyl group cannot enter the tunnel of the active site.

For some substrates in combination with the ER domain unclear results were detected. The β-keto motif which is the substrate for the *C*-MeT small interactions could be measured. Also the experiment with **212** showed the expected results. For the other substrates the ER domain showed poor results. It seems that the measurings are influenced by something. However before the protein flows over the surface the signal decreases. The base line is similar before and after the injection of the protein solution. The same statement can be made for the used buffer. The running buffer of the SPR experiment was the same that was used for the stock solution of the ER enzyme. However, the ER domain seems to have a broad substrate specifity and accepts also other structural motifs of PKS intermediates. This was also shown in the previous enzymes assays were nearly all substrates up to the tetraketides could be reduced (section 2.3.4). Also reductions of pentaketides were possible.

For both domains, ER and DH, it was shown that the SPR method is usable to prove interactions between the different substrates of a PKS and isolated enzymes. For better understanding of possible programming, it would be interesting to repeat the experiment series with different conditions. To increase the flow rate for example would load the protein faster on the cross linked surface. One test run was performed for the ER domain with a flow rate of 25 µL/ min and this did give better quality data. However the flow rate is limited by the amount of glycerol required in the buffers, and in the longer term it would be a good idea to find other buffers in which the proteins are stable which do not requirev the addition of glycerol. The ER experiment could also be influenced by the use of a cofactor. A change could maybe observe with the use of $NADP^+$ in the buffer. Maybe the interaction is stronger or lower for the different intermediates.

4.6   Conclusion

Different experiments of the isolated domains in solution were performed. Modified enzyme assays with isolated DH and ER domains showed a significant influence to the initial rates. The initial rates of **85** slow down in the presence of the DH domain. Size exclusion investigations of the isolated domains were performed. There was no

evidence that a protein complexe between the isolated domains was formed in solution. In further experiments by SPR investigations this result was confirmed: there was no interaction of the two isolated domains. Further protein-intermediate investigations were performed by SPR. For this an improved synthesis method for different pantetheine glycine substrates was developed and the synthesis of different structural motifs was possible. For the cross-linking process to the SPR surface different conditions were tried. It was possible to establish a method for the pantetheine glycine substrates for the cross-linking. The modification of the surface was possible and the modified surfaces could be used as analytical tools to investigate the interaction between the protein and intermediates.

The initial experiments reported here show that in general it is possible to observe interactions. The DH and ER show a broad of selectivity and seem to be able to interact with many of the intermediates. This means that the isolated domains of SQTKS are not programmed by strict structural motifs. Otherwise only two substrates should be recognised; the starting and end product of the catalysed reaction.

A problem with the SPR analysis seems to be the low flow rate of 10 μl/ min and the used buffer that contains 10 or 20 % glycerol. The equilibrium of bound and unbound protein was only reached for a few substrates. Another problem was the poor data that was calculated for partners of the ER domain. The final performed measurements using a flow rate of 25 μl/ min resulted in optimized SPR curves in which equilibrium is reached, and the artefacts of the buffer are decreased. However the faster flow rate means that more enzyme will be required for the future assays.

4.7   Future Work

To get more significant data it is possible to combine SPR and MS.[173] Two analytical independent analysis methods are described in literature. One is the direct coupling of MALDI-TOF to the sensor chip.[174] The second method is analysis of captured ligands. The ligand gets bound in previous steps to an immobilized ligand on the surface. Unbound and weak bound material gets washed out from the ligand. Finally the buffer change can be performed that disrupts the interaction between analyte and surface. Collected ligands can be load directly into MALDI or post-processed.[175,176] Combination of MS and SPR could be a useful tool for the investigation of the isolated

domains of SQTKS. Currently the modified surface is proven by the change of the refractive index. Removal of the sensor chip out of the SPR and chemical treatment of the surface could separate the cross linked material from the surface.

It could also be used to create an inhibitor for the DH domain. It is known by *E. coli* FAS that the structural motif of **227** binds covalently to the active site (Figure 93). The investigation in the FAS project was based on ACP derived substrates. Compound **227** shows the pantetheine motif with additional glycine residue that could act as an inhibitor. If the inhibitor works the DH domain should be covalently bound to the surface.[177]
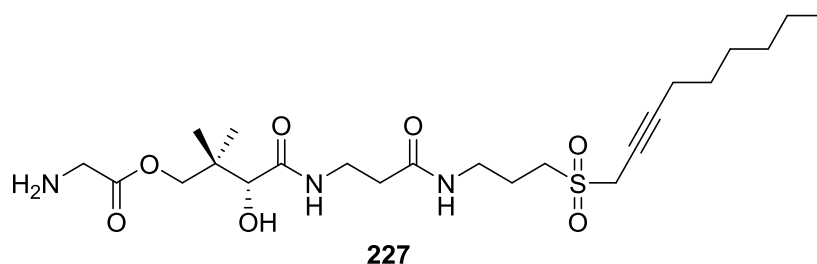
Figure 93: Possible inhibitor of DH domain.

It seems, that in the previous investigations the high amount of glycerol was the crucial effect that the interactions were not visible. Similar performance could be tried again with the isolated DH and ER domains with other buffers. For this several tests could be performed to test the stability of the isolated proteins. The lower amount of glycerol could result in a more sensitive system. A reduce of spikes in the measuring could be a possible consequence. Also the mechanical part could be influenced. In most of the measuring's the switching of the valves is seen. The viscosity of the used buffer could increase this effect.
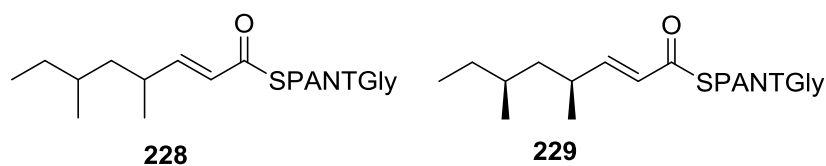
Figure 94: Further pantetheineglycine compounds could give conclusions for the programming of SQTKS.

Since the previous investigations showed that it is possible to perform this type of experiment, also the extension of a substrate library could be possible. From the kinetic analysis, it is clear that **102** is an inhibitor of the isolated enzymes. The comparison of the racemic- with the enantiopure substrate could highlight selectivity of the active site (Figure 94).

5.0 Project 4: Tailoring Enzymes Involved in the Biosynthesis of Squalestatin S1

Tailoring enzymes catalyse many different reactions during the later stages of natural product biosynthesis, and are thus responsible for the diversification of natural product structures. A good example of this is the conversion of proansamycin X **231** to the bioactive compound rifamycin B **234**.[178-183]
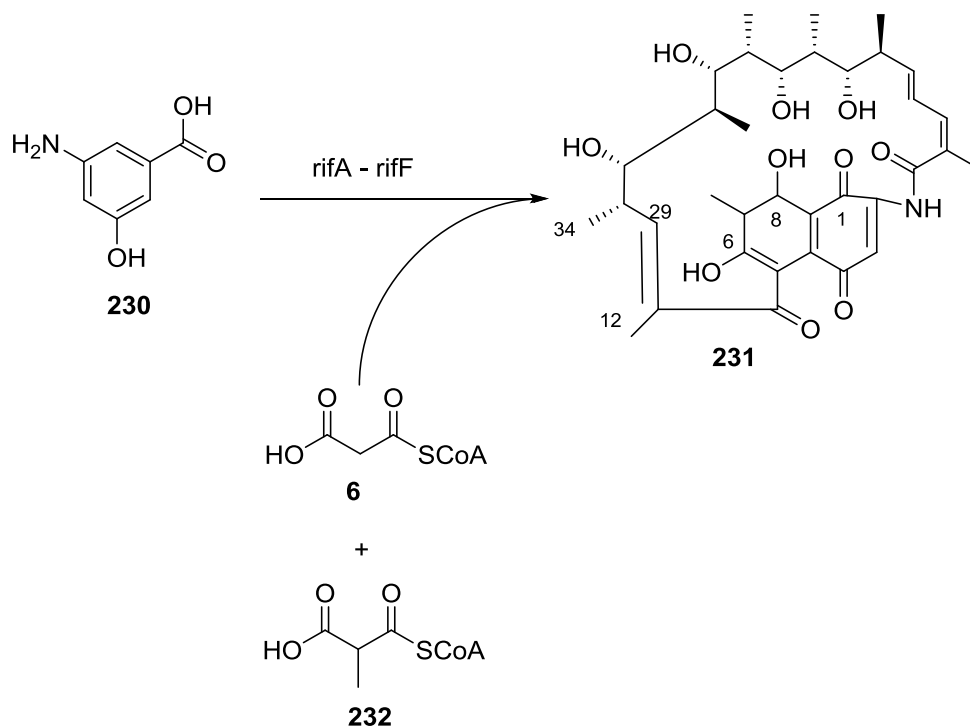
Scheme 49: Formation of proansamycin X **231**.

Proansamycin X **231** is the product of a modular PKS (RifA − RifE) which uses 3-amino-5-hydroxybenzoic acid **230** as a starter unit. Extensions are performed with malonyl-CoA **6** and methylmalonyl-CoA **232** (Scheme 49).[179-183] RifF then releases the cyclic amide **231** as the first enzyme-free intermediate. The rifamycin tailoring enzymes perform a hydroxylation at C-34 and an oxidation at C-8 to create rifamycin W **233** (Scheme 50) which is a central intermediate of several rifamycin derivatives and a known precursor of rifamycin B **234**.[179-183]

During the formation of **234** a backbone rearrangement is observed. The C-12 to C-29 olefin is cleaved, and an oxidative removal of formic acid at C-34 and reduction of the quinone is also observed. Final modifications include *O*-acetylation at C-25 and *O*-methylation at HO-27. The introduction of these side chains during rifamycin B

biosynthesis is the final modification. Similar late-stage acylations are also observed for compounds like lovastatin **26**.[184,185]
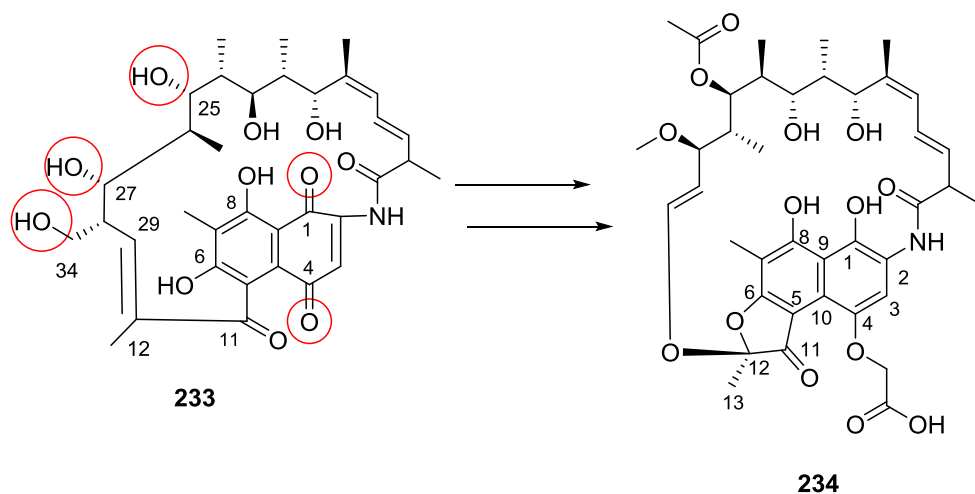
Scheme 50: Post-PKS modification of rifamycin W **233** to rifamycin B **234**.

5.1 Acyltransferases

Lovastatin **26** is formed from a nonaketide **29** linked as an ester to a diketide **235** (Scheme 51). The transfer of the diketide acyl residue is the final step of the biosynthesis, however, no free diketide intermediate was found by LCMS analysis. This is because the α-methylbutyryl acyl group **235** is captured directly by the 46 kDa acyl transferase (AT) protein LovD from the diketide synthase LovF.
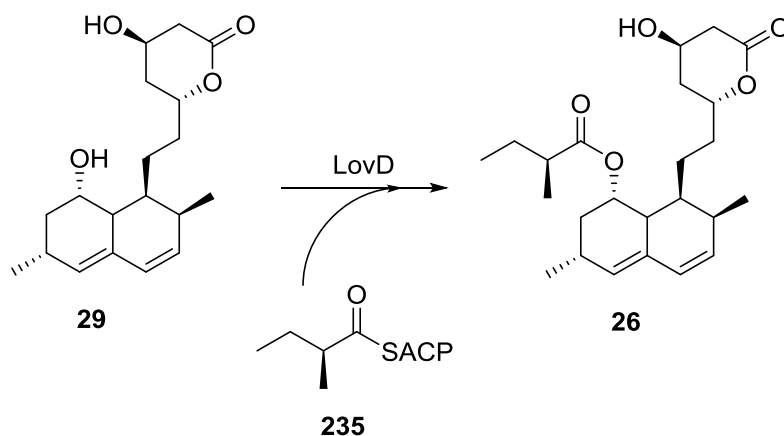
Scheme 51: Diketide transfer during lovastatin biosynthesis.

In the second step the hydroxyl group of **29** reacts in a transacylation with the LovD-bound diketide. Ser-76 was proposed as the active site nucleophile of LovD. Other

possible catalytic amino acids of LovD are Lys-79, Tyr-188, and Lys-315 (Scheme 52).[186,187]
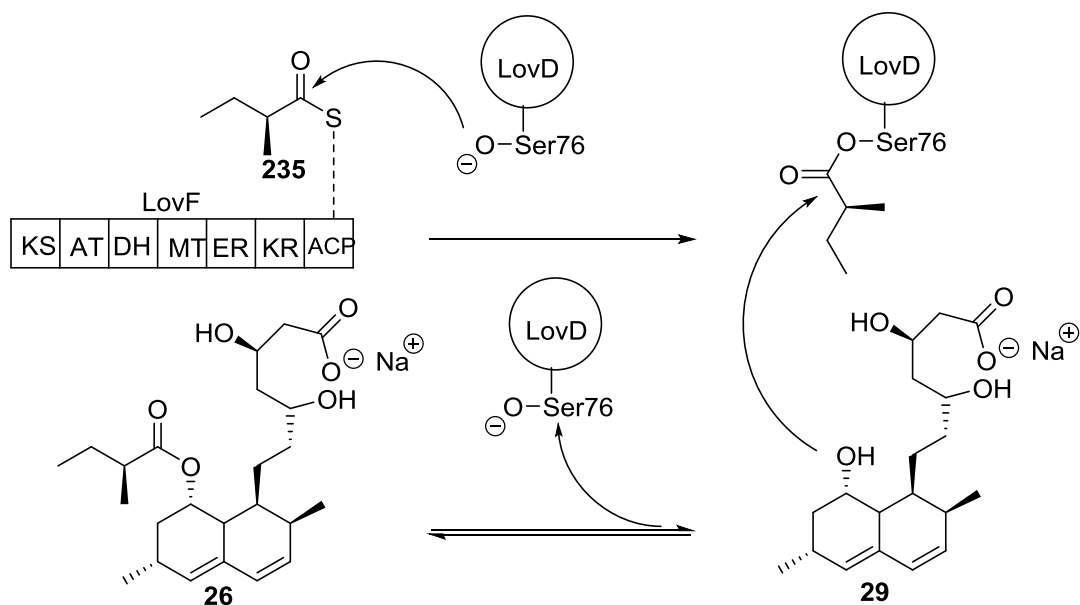
Scheme 52: Proposed mechanism of the transacylase LovD.

Tang and coworkers showed that LovD could be used *in vitro* for chemoenzymatic modifications. LovD was expressed in *E. coli* BL21 and purified by Nickel-NTA chromatography and then used in enzyme assays. Butyryl-CoA **236** was incubated with the precursor **29** and LovD and the expected product **237** was obtained (Scheme 53).[186, 187]
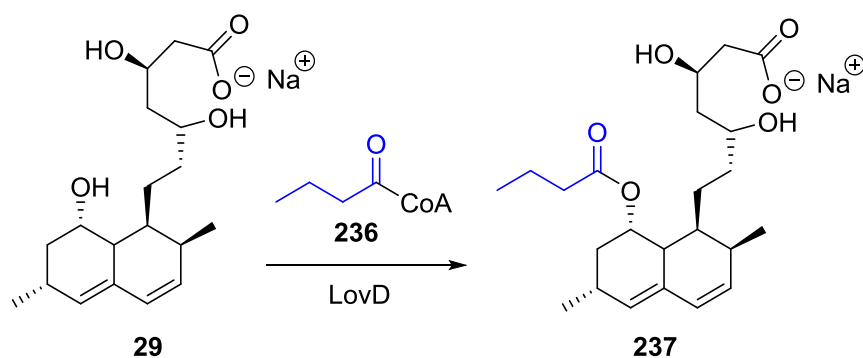
Scheme 53: Enzyme assay of **29** and butyryl CoA **236**.

It was also possible to create the more biologically active compound simvastatin **239** using this methodology. For the chemoenzymatic reaction α-dimethylbutyryl-SNAC **238** was used (Scheme 54).
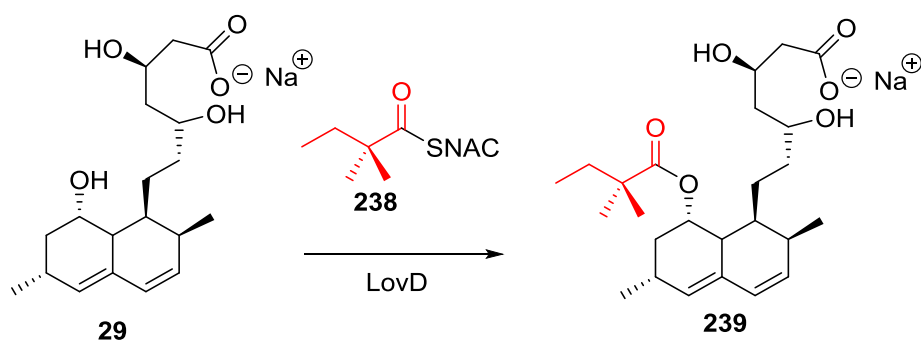
Scheme 54: Enzyme assay of **29** and α-dimethylbutyryl-SNAC **238** to form simvastatin **239**.

Other lovastatin analogues were also produced by chemoenzymatic reactions. Analysis of the different enzyme assays showed a preference of LovD for C_3-C_6 chain-length acyl groups. Different decalin cores were tested. One variation investigated the replacement of the methyl group at C-6 by a hydroxy group. Two possible positions for an acyl transfer were now available. The resulting product of the enzyme assays showed high selectivity for HO-4 acylation. Diacetylation was not observed. This showed the broad substrate specifity of LovD to the side chain that is transferred to the final core compound. In contrast to that, the position of the acyl transfer is very specific (Scheme 55).[186, 187]
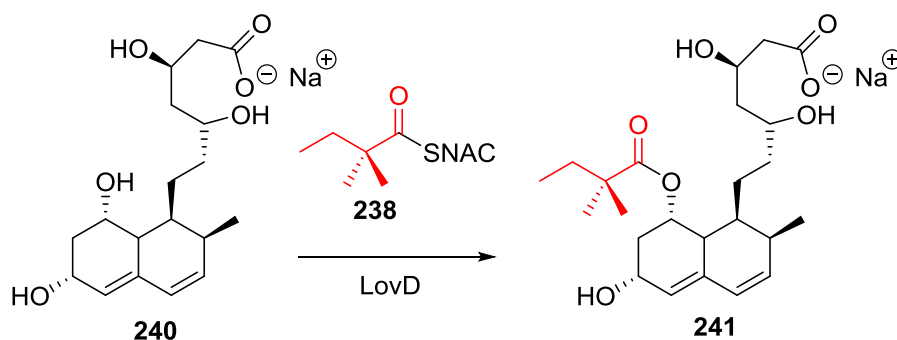
Scheme 55: Chemoenzymatic synthesis of huvastatin **241**.

The AT enzyme tricothocene-3-*O*-acetyltransferase (Tri101) is known from the biosynthetic pathway for T-2 toxin **243** which is produced by various species of the fungus *Fusarium* and is responsible for grain contamination (Scheme 56). Similar to the biosynthesis of lovastatin **26** the AT works almost at the end of the biosynthetic pathway. The AT is responsible for the acetylation of the HO-3 hydroxyl group of the precursor of T-2 toxin (Scheme 56).[188]
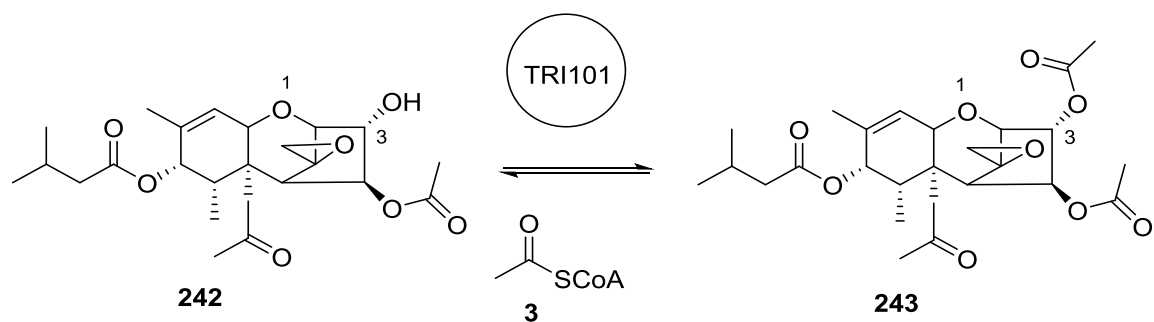
Scheme 56: Acetylation of T-2 toxin by Tri101.

Acetylation at HO-3 lowers the toxicity of the tricothecene core drasticly. Without an acyl group at this position a much higher biological effect was observed. It is proposed that acetylation is used as a self protection mechanism by the *Fusarium* fungus. HO-3 could also be a possible position for a resistance mechanism for plants. Lowering or removal of the toxicity could protect plants from fungal disease. Modifications with glycosyl residues at C-3 showed successful reduction of the toxic effect. Also oxidation of the C-3 hydroxy motif into a keto group showed significant effects.[188]

Isolation and purification of Tri101 was performed in a similar way to LovD. Crystallisation experiments in the presence of CoA substrates showed important motifs that were found in other AT domains including HXXXD and DFGWG. The HXXXD motif is located near to the acetyl-CoA and substrate binding sites and is an essential catalytic motif. The DFGWG motif is a component of a structurally important loop.[188]

5.2   Aims of the project

Squalestatin S1 **56** is synthesized by two independent iPKS. Further investigations showed that two possible ATs are present in the squalestatin gene cluster. Both were expressed by group members of the Cox group. It is assumed that both ATs work late during the biosynthesis of squalestatin S1. One aim of this project is the synthesis of possible precursors that are involved in the acyl transfer. These precursors are the squalestatin tetraketide **61** and different squalestatin cores. The development of a suitable enzyme assay is the second aim of this project. Several assay conditions and substrate structures will be tested. Also the synthesis of new squalestatins will be attempted using the AT as a catalyst *in vitro*.

5.3   Investigation of AT1 and AT2 from the Squalestatin Gene Cluster

Squalestatin S1 **56** consists of a highly modified hexaketide esterified to a tetraketide. The hexaketide makes up the core structure of the compound, and, as in lovaststin **26**, the tetraketide forms an ester side-chain, in this case to O-6. The tetraketide and the hexaketide are produced by two separate highly reducing PKS. In addition an acetyl unit is esterified at O-12. Two squalestatin biosynthetic gene clusters were found by genome analysis of the two different fungi (*Phoma sp*. C2932 and MF5453) which produce **56**. Both clusters contain PKS genes which encode SQTKS (squalestatin tetraketide synthase) and SQHKS (squalestatin hexaketide synthase), and this has been verified by gene knockout experiments. The clusters also include two acyl transferase encoding genes (*mfM4* encoding AT1 and *mfR4* encoding AT2) which could be responsible for the two esterifications required during biosynthesis (Scheme 57).[97]
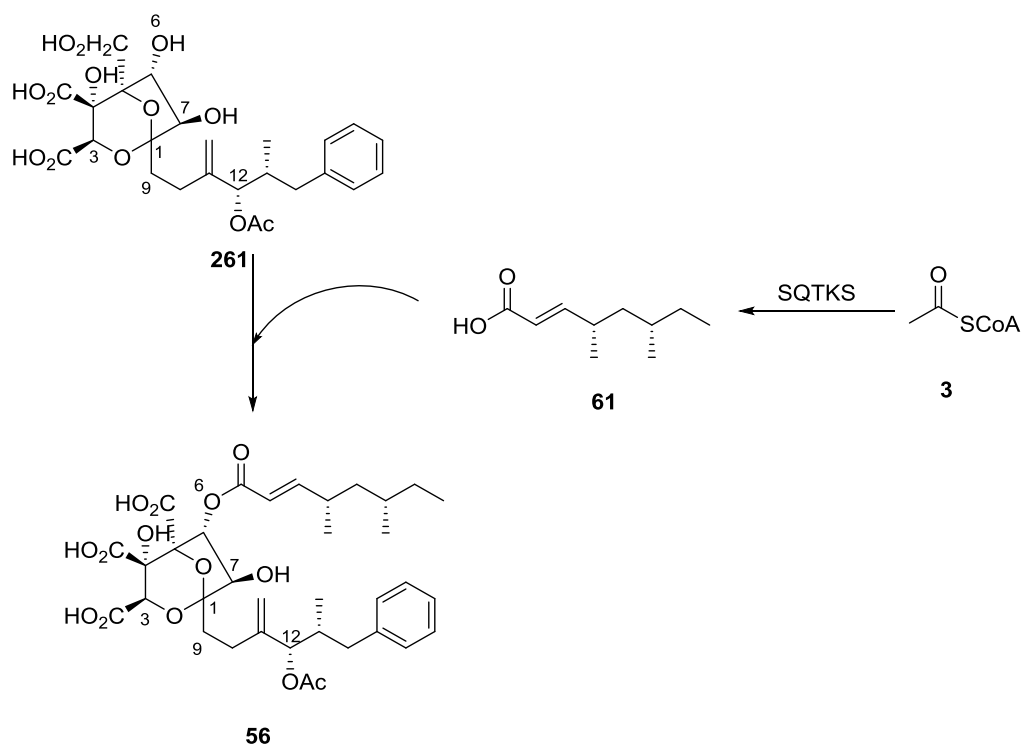
Scheme 57: Crucial steps during biosynthesis of **56**.

At the start of this project it was not clear which of the two ATs was responsible for each step. Also the substrates that are used by the AT domains are unclear: it was not known in which order the acetyl and tetraketide groups were added, and it was not known whether the tetraketide should be linked to CoA as in T-toxin biosynthesis, or to acyl carrier protein (ACP) as in lovastatin biosynthesis.[97] It was therefore planned to

investigate the activity of the two ATs *in vitro*. This would require cloning and expression of each AT-gene, production of suitable substrates, and development of sensitive analytical methods for the detection of substrates and products.

5.4   Heterologous Expression of the Acyltransferases AT1 and AT2

AT1 belongs to family of acyltransferases with an HXXDG motif. This motif is important for the function of the active site. AT1 is similar to Tri101 (20% identity, 37% similarity). In particular, important residues for CoA binding in Tri101 such as L282, T298, D300, and L425 are conserved in AT1 suggesting that AT1 itself might accept CoA substrates.[97] For AT2, homology to the acyltransferase 3 superfamily was observed. Good alignments were found with an uninvestigated acyltransferase from *Dothistroma septosporum* (39% identity, 54% similarity), but no further useful information could be found. Which motif or which residues are important for the transfer reaction are currently unknown.[97]

For *in vitro* analysis the enzymes had to be isolated. The heterologous expression of AT1 started with ligation of DNA from MF5453 into pET28a(+). After that the resulting plasmid was transformed into *E.coli* BL21 DE3. Cells were grown in liquid culture and the protein production was induced with 0.1 mM IPTG. Finally the cells were lysed by sonication and the lysate purified by FPLC. The target protein was tagged with His$_6$-tag and purified using a Nickel-NTA column.[97] This work was performed by Dr Nina Duensing and Verena Belt in the Cox group. Despite significant effort the AT2 protein could not be expressed in soluble form.

5.5   Chemical Cleavage of SQS1 and Substrate Synthesis

In order to set up *in vitro* assays for AT1 suitable substrates were required. Most AT enzymes seem to act near the end of their biosynthetic pathways and we guessed that this might also be true for AT1. However it was not known if AT1 acted before or after AT2, and we did not know if AT1 acylated at O-6 or O-12. We therefore needed to produce substrates containing the squalestatin core attached to either no acyl group **246**, just the O-6 tetraketide **245** or just the O-12 acetyl group **244**.

Squalestatin S1 **56** was hydrolysed under basic conditions using less than 2.0 equivalents of hydroxide. Analytical LCMS showed that this produced a mixture of unreacted **56**, the two mono-acylated compounds **244** and **246** and the doubly hydrolysed core compound **245**. All squalestatin derivatives were purified by HPLC. Compounds **244**-**246** were obtained as pure single compounds in this way and enzymatic assays could not be influenced by chemical inpurities.[97] The tetraketide **61** itself was also observed. Organic extraction of the reaction mixture at pH 11 removed compounds **244**-**246** which were then purified by high pressure liquid reversed phase chromatography. The aqueous phase was then acidified to pH 1 and extracted a second time with ethyl acetate to give the tetraketide **61** in pure form. NMR analysis of all compounds showed them to be pure and of the expected structures (Scheme 58).[97]
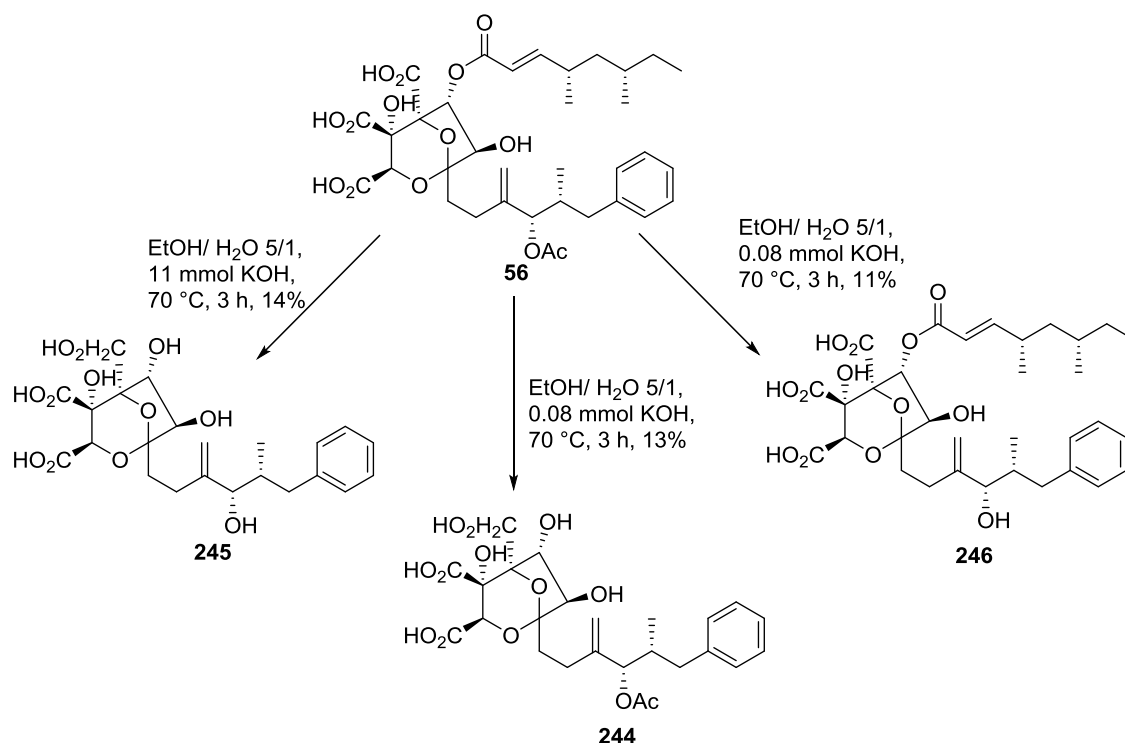
Scheme 58: Synthesis of potential precursors in the biosynthesis of **56**.

To investigate the AT domains an LCMS method was developed. First a standard solution of SQS1 was measured (Figure 95a). In a second experiment the metabolites of the fungus MF 5453 were extracted (Figure 95c). Comparison of retention times and masses of the extract from the wild-type fungus showed that **56** was produced.
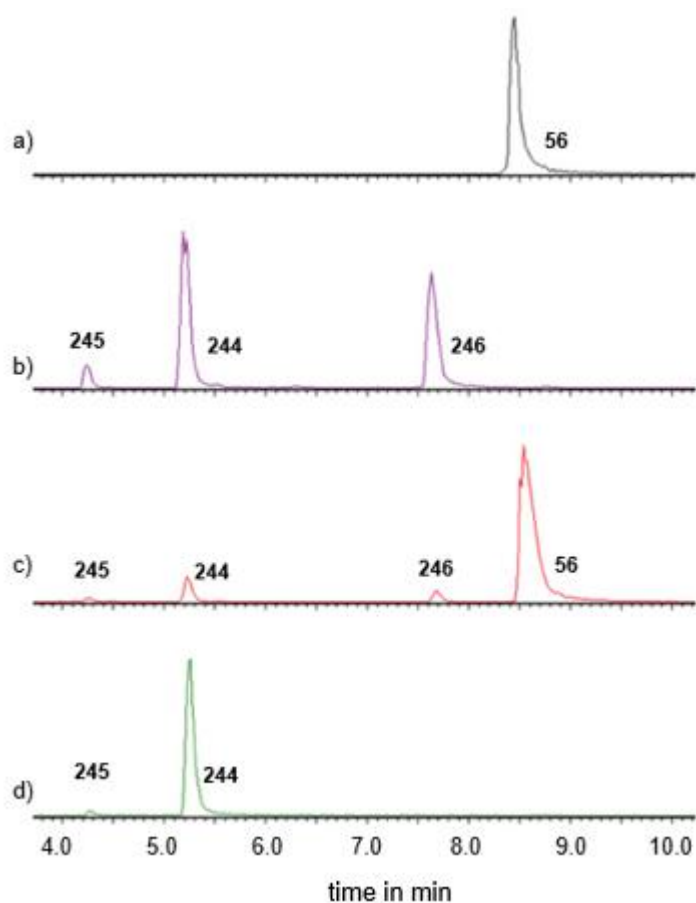
Figur 95: ES⁻ TIC LCMS traces of of **56**: a) Standard of **56**; b) standards of squalestatin derivatives; c) wild type extract of **56** with **244** as by product; d) gene knock out of AT1 results in **244** as main product.[97]

As by-product the squalestatin derivative **244** was extracted. Additional knock out experiments showed that compound **244** as main product was produced (Figure 95d). This is more evidence that the transfer of the tetraketide to the core product is the last step in the biosynthesis.[97]
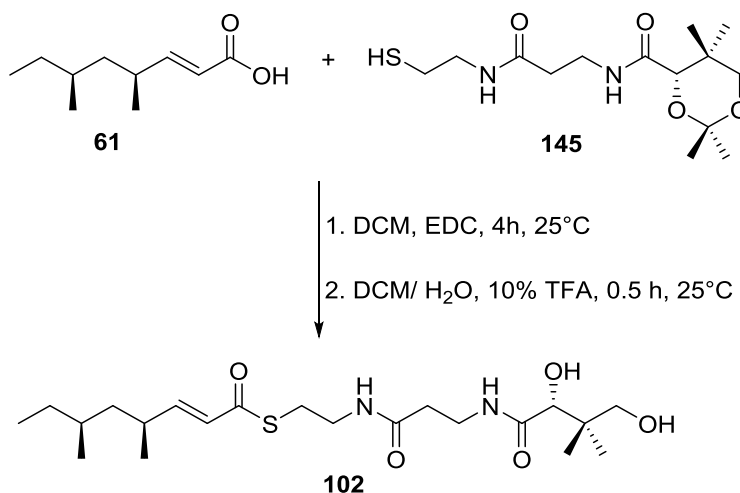
Scheme 59: Synthesis of 4*S*-6*S*-dimethyloct-2-enoylpantetheine **102**.

The coupling substrates were synthesized in the following way. Tetraketide **61** was converted to the corresponding pantetheine thiolester **102** by the usual coupling method, followed by TFA deprotection. The synthesis of the CoA substrate was performed in the presence of CDI followed by the addition of coenzyme A (Scheme 60). Purification of **248** was difficult, but reaction mixtures containing a significant proportion of **248** (LCMS analysis) could be used successfully in assays (section 5.6).
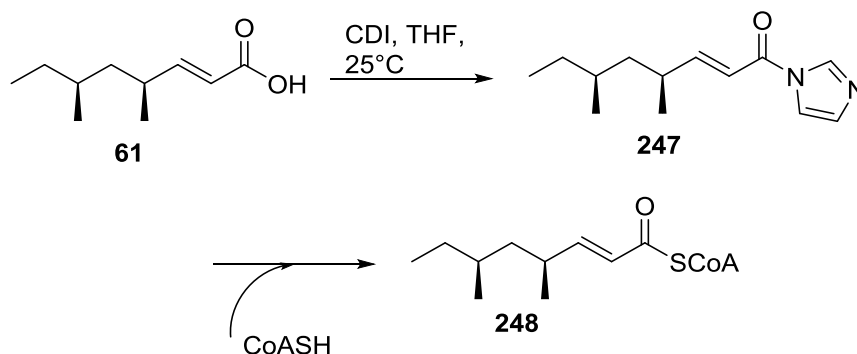
Scheme 60: Synthesis of 4-6-dimethyloct-2-enoyl CoA **248**.

5.6   *In vitro* Investigation of the Acyl Transferase AT1

In vitro assays in a volume of 100 μL were set up to test the activity of AT1. Each of the three core substrates **244**-**246** were incubated in potassium phosphate buffer at pH 8, 30 °C for 24 h with purified AT1 and tetraketide pantetheine **102**.

At the end of the reaction time the protein was precipitated by addition of acetonitrile and the supernatant was analysed by HPLC-MS. No assay solution showed any conversion to the predicted target. Different assay conditions, for example changes in the pH or temperature were tried, but no product could be observed. Additionally the same investigations were made for incubation of core **245** and AT1 enzyme in the presents of acetyl pantetheine but no transfer was observed.

These results showed that pantetheines cannot act as substrates for AT1. We then repeated the assays using CoA substrates under identical conditions. Initial reactions used commercially available acetyl-CoA **249** (Scheme 61).
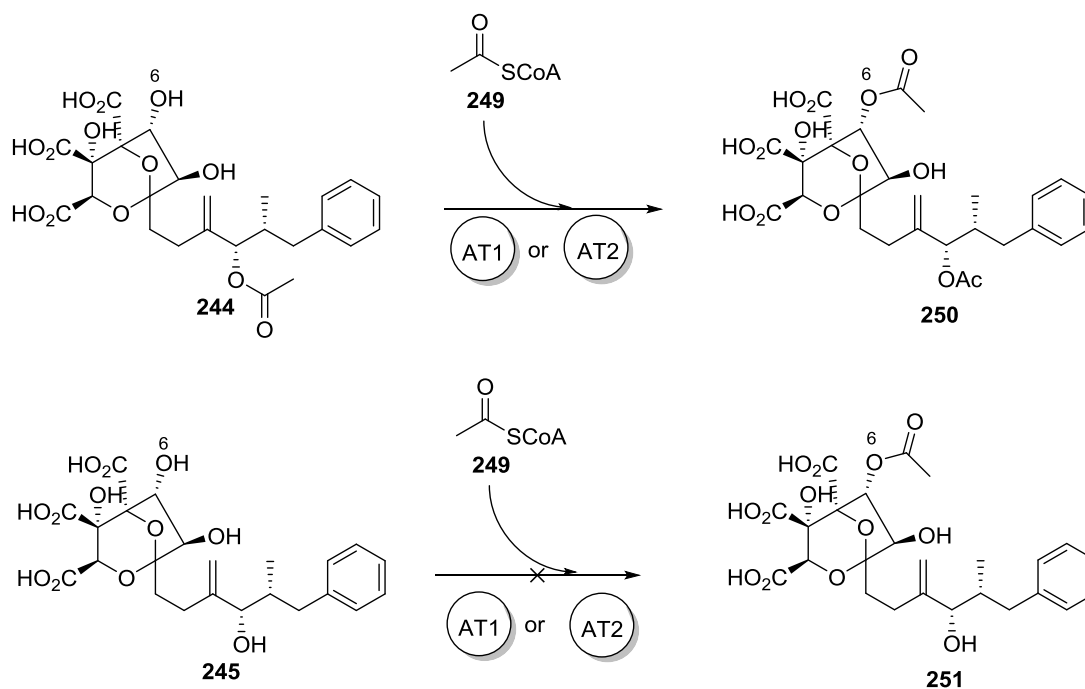
Scheme 61: Acyl transfer to the different cores of **56**.

Analysis of reaction with the fully hydrolysed core **245** did not show new compounds. In contrast to that, the new squalestatin analogue **250** was found in the LCMS-traces using the acetylated core **244** in combination with acetyl CoA **249** (Figure 96). In contrast, no reaction was observed for the reaction of the O-6 tetraketide substrate **246** with acetyl CoA **249** in the presence of AT1.
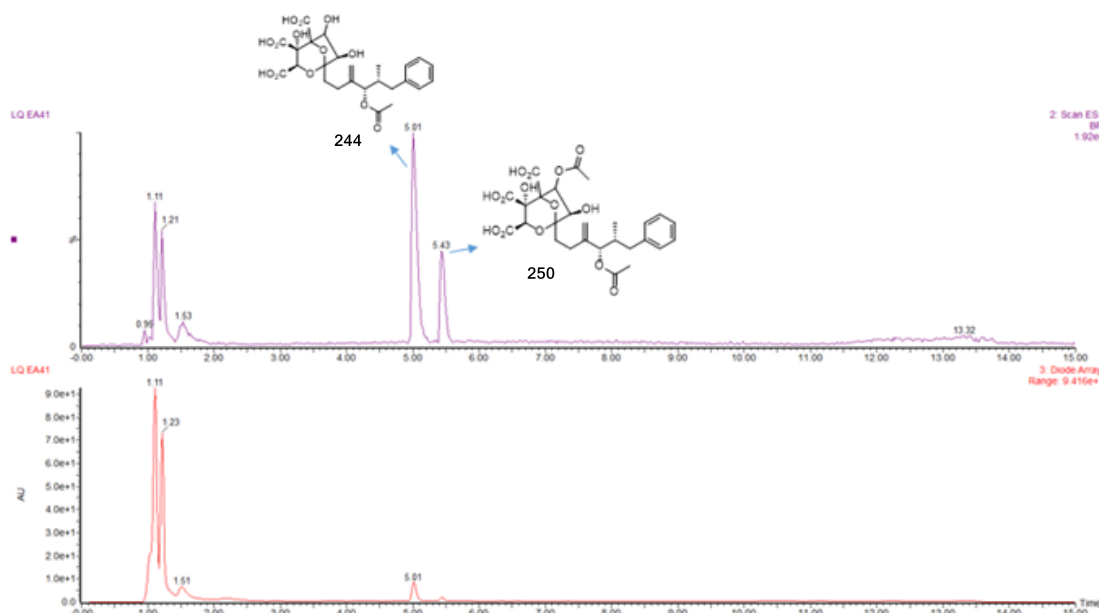
Figure 96: LCMS-trace of successful transfer of **249** to core **244**.

It was not clear at which position the acetylation occurred, as hydroxyls are also available at C-4 and C-7. However, the successful transfer indicated three important points: first, AT1 requires a CoA-residue; secondly this step in the biosynthesis requires the prior acetylation at O-12; and third that only a single acyl transfer occurs. Acetylation at O-12 is most-likely catalysed by AT2 in an earlier step.

To extend the previous experiments, other CoA substrates were fed to AT1 in the presence of the 12-*O*-acetylated core **244**. Investigations with commercial available hexanoyl-CoA and octanoyl-CoA showed transfer of the acyl-group to the core **244**. Similar to the tests before, only enzyme assays with AT1 and the acetylated core **244** showed the new compounds **252** and **253** (Figure 97).
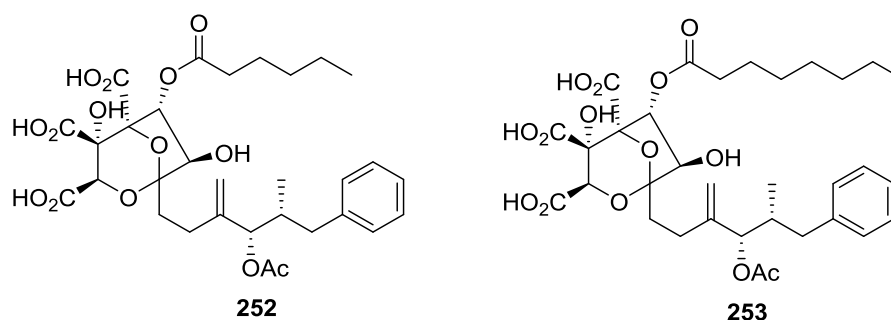
Figure 97: New squalestatin compounds **252** and **253** generated by enzymatic reaction with AT1.

Finally the position of where the acyl group is transferred needed to be confirmed. To test that the transfer goes to the expected position of the core, the tetraketide CoA **248** was incubated with core **244** and AT1 and transfer was successfully observed. The retention time of the product of this reaction was compared with the retention time of squalestatin S1 **56** itself. The comparison to **56** showed that the product of the enzyme assay has the same retention time and MS fragmentation pattern. This shows that the reaction produced squalestatin S1 **56** and thus transfer must be to the O-6 position.
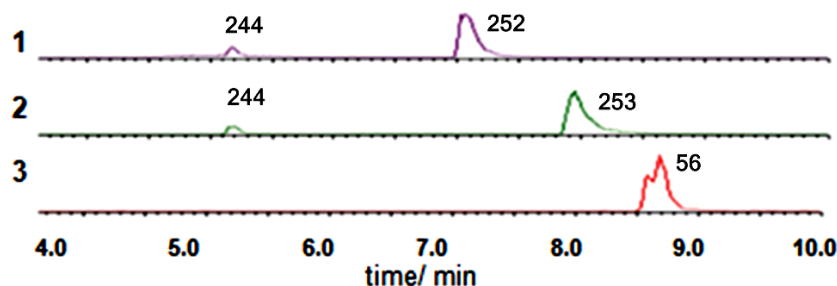
Figure 98: ES⁻ LCMS traces of acyl transfer from CoA to **244**. *In vitro* assay of AT1 and **244** with hexanoyl CoA (**1**), *in vitro* assay of AT1 and **244** with octanoyl CoA (**2**) and incubation of **244** and AT1 with SQTK-CoA

5.7 Discussion

Comparing the structures of the known squalestatins (section 1.5) it seems that different polyketides and fatty acids form the O-6 sidechains with the 4,8-dioxabicyclo[3.2.1]octane core which is identical in all known compounds. In most cases at position C-12 an acyl ester is found. This position was very important in the previous enzyme assays. Interesting could be the investigation of this acetyl ester moiety in other statins, if the same importance can be observed. The final step of the biosynthesis must be the acyl transfer at O-6.

The O-6 side chain of the squalestatin compounds has a much higher diversity in chain length, methylation pattern and methylation position. Comparing **56** with zaragozic acid C **57** the hexaketide is still the same, also with similar post PKS modifications without the ethylene group at C-12, where a methyl group of SAM was not transferred. The diversity between the two compounds is found for the side chains. A tetraketide is transferred for **56** in contrast to a pentaketide chain, for **57** (section 1.5).

Only squalestatin core **244** could show activity for enzyme reactions with AT1. The other two different cores **245** and **246** were not recognized by the enzyme. Also a broad substrate specifity of AT1 was shown by the different CoA substrates that were used in the different assays. The current investigations showed that substrates from two to eight carbon atoms could be transferred. In that way it was possible to develop new squalestatin derivatives. Also other substrates were tested in combination with AT1. But new compounds could not be observed by the use of acyl pantetheine substrates. This highlights the importance of the adenine residue of the CoA substrates. It is assumed by the structure of **244** that the acyl transfer of the tetraketide is the last step in the biosynthesis of SQS1 **56**.

Another investigation for AT domains in fungal PKS was performed by Tang *et al*. The lovastatin precursor monacolin J **29** was incubated with the AT enzyme LovD. Also this transferase acts in the last step of the biosynthesis of **26**. In this work CoA and SNAC substrates were used to show the successful acyl transfer to the core compound. In contrast to the performed enzyme assays with AT1 required in this project the CoA structure of the acyl substrates was not important.

In contrast to **26** a different mechanism is proposed for the formation of **56**. It is proposed, that the tetraketide gets released by phpks1. After that the tetraketide is transferred to CoA to generate the corresponding coenzyme A intermediate. How this CoA transfer works and which other enzymes are involved is currently unknown.

Finally the squalestatin core **244** attacks the CoA substrate with the hydroxyl group at C-6 (Scheme 62).
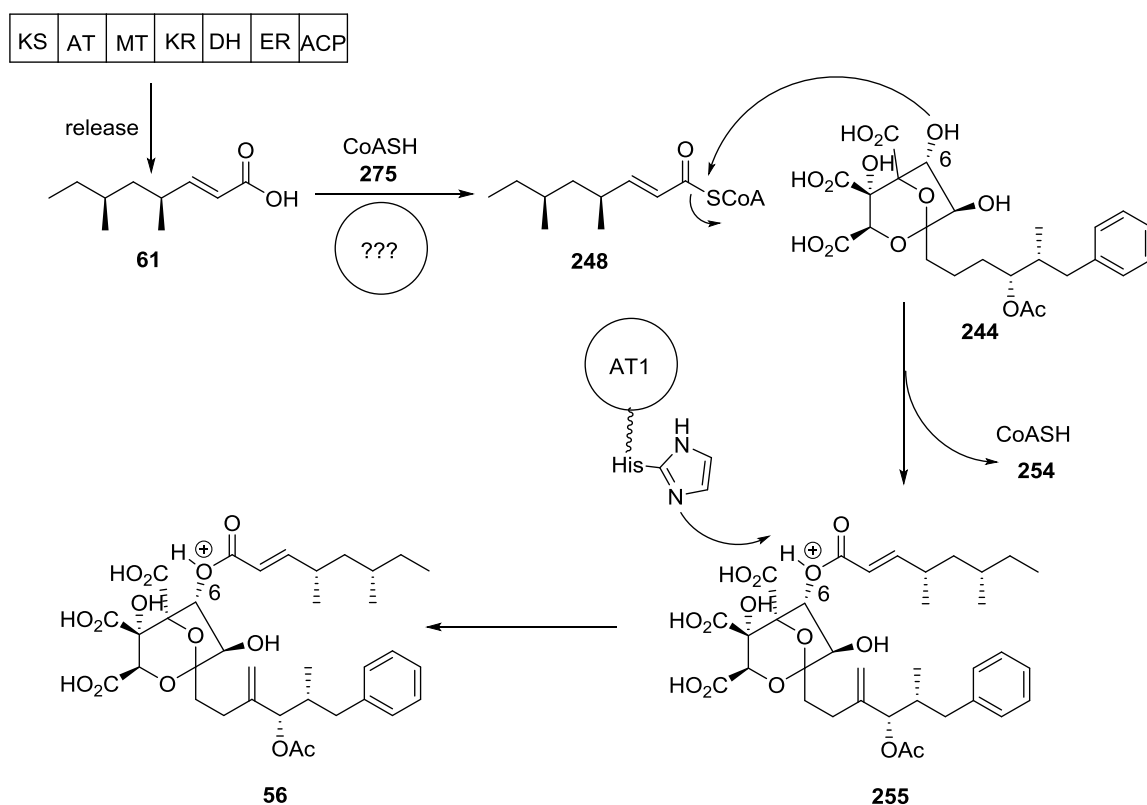
Scheme 62: Proposed mechanism of acyl transfer to form **56**.

The adenine residue of CoA is important for recognition. Without it the transfer cannot take place, which was shown in different pantetheine assays. This proposal is similar to the mechanism of Tri101, which has similar active residues in the active site. Other amino acid residues that are important for the binding of the tetraketide are currently unknown. Possible candidates involved in CoA binding conserved between AT1 and Tri101 are L282, T298, D300, and L425. These residues were found in crystal analysis of Tri101 (Scheme 62).[188]

5.8   Conclusion

To investigate the functions of two AT enzymes that are involved in the biosynthesis of squalestatin S1 **56** different substrates were prepared. Three different cores were created by hydrolysis of squalestatin S1 **56** itself. For the enzymatic investigation an assay was developed that showed the successful transfer of the different CoA esters to the core **244**. The core **244** was identified as the natural substrate for AT1. It is also the natural substrate of the last step in the biosynthesis of **56**. Both other isolated cores, **245** and

246 showed no activity to AT1, which shows for the core substrate the high selectivity of the enzyme. Acytylation at position C-12 is important for the observed selectivity.

In contrast to this was it possible to create several new substrates by reaction with a variety of acyl CoAs. Two new squalestatins (**252** and **253**) could by synthesized *in vitro*. To validate the specific transfer to position O-6 the natural tetraketide was synthesized as its CoA thiolester. This produced a compound identical to squalestatin S1 **56** by LCMS analysis.

5.9   Future Work

The contrast of substrate selectivity of AT1 is interesting. AT1 can clearly catalyse the transfer of various acyl groups to O-6, but it seems quite selective for the structure of the core and very regioselective for the nucleophilic oxygen. How the interaction of the core works with the AT domain enzyme and which residues are important is currently unknown and could be useful to investigate in future. Protein alignment could highlight several motifs of amino acid residues that could be important. Predictions of the active site could also be made, also about possible catalytic residues of the active site that could be involved in the side chain transfer. Confirmation of these active residues by mutation experiments and / or production of protein crystals could be another target. Results of these investigations could give another perspective to other formed squalestatin compounds.

Another open question is the function of AT2. Is AT2 the missing acyl transferase which is responsible for the second transfer of the acyl group at position C-12? The structure that is the possible acceptor molecule in this transfer is currently unknown. A possible structure for the acceptor molecule could be an open chain in the previous biosynthesis of the hexaketide. This acceptor molecule could be generated in a chemical way or by gene knock outs. However the insolubility of the AT2 protein remains a problem which must also be solved for future *in vitro* experiments. It may be possible to isolate several compounds by knock out experiments that are involved in the biosynthesis of SQS1. These compounds could be tested with the isolated AT2 protein. Interesting in this case could be the substrate selectivity of AT2. Is the domain similarly programmed to AT1? If so, it should have a high selectivity for the acceptor molecule. In contrast a variation in the side chain should be possible.
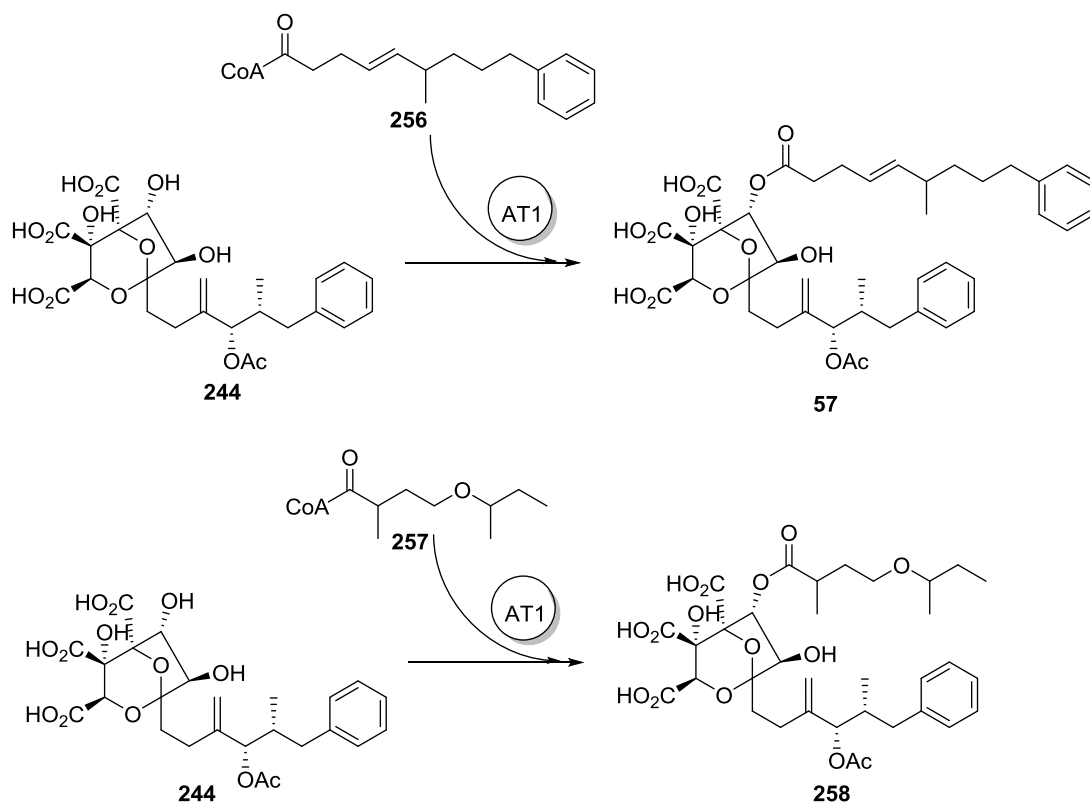
Scheme 63: Possible *in vitro* assays for new squalestatins.

Another possible target for the future work could be an investigation of AT1 in more detail. For the moment only the broad substrate selectivity is known. The position on which the side chain is transferred seems to be selective. Further investigations concerning the length of the side chain could be interesting (Scheme 63). How tolerant is the enzyme against different other structures of side chains. Replacement of a carbon atom in the side chain by an oxygen to form an ether could be tested. Is it possible to create a statin that is similar to zaragosic C **57** for example with this AT domain? If this behavior could be observed it could be a possible explanation of shunt products that was reported by Glaxo and Merck. In that way, new motifs and structures could be observed with different functional groups. This could have a positive change to the general use of squalestatin analogues as a drug. Side effects could be potentially limited by changes of the structure.

6.0   Experimental details

All Solvents were used without any purification or drying process unless otherwise described. Anhydrous tetrahydrofuran, diethyl ether and dichloromethane and NADPH were bought from Carl Roth. Other chemicals were obtained from Sigma Aldrich and Acros Organics.

6.1   Equipment

NMR analysis: ^{1}**H-NMR** analysis was performed using BRUKER DPX 200, Avance 400, DPX 400 and DRX 500 instruments. Signals are determined in some cases with two dimensional NMR ^{1}H, ^{1}H-COSY, 1H, ^{13}C-HSQC and ^{1}H, ^{13}C-J_3-HMBC. ^{13}C-NMR analysis was performed using BRUKER Avance 400, DPX 400 and DRX 500 instruments. Deuterated chloroform (ref. 7.26 ppm / 77.2 ppm)[189] and deuterated acetonitrile (ref. 1.94 ppm / 118.4 ppm) were used as solvents and served as internal reference. All δ values are in ppm. All J values are in Hz.

Column Chromatography: For column chromatography silica 60 Å (particle size 35-70 micron, Sigma-Aldrich or 40-63 micron, Macherey-Nagel) was used. Columns were packed under N_2 pressure. Products were eluted with the indicated solvent mixtures. Purified fractions were analysed by TLC and combined if same R_f was observed. Final products were evaporated in *vacuo*.

TLC: TLC analysis was preformed on TLC plates with a poly Ester backed 0.2 mm silica gel phase from Macherey and Nagel using the indicated solvent systems. Analysis of the plates were performed by ultraviolet light (254 nm) or with potassium permanganate (5 mmol) or *o*-anisaldehyde anisaldehyde (15 g), EtOH (250 ml) and concentrated H_2SO_4 (2.5 ml) solution.

Analytical LCMS: Analytical LC-MS data were obtained with using a Waters LCMS system comprising of a Waters 2767 autosampler, Waters 2545 pump system, a Phenomenex Kinetex column (2.6 μ, C_{18}, 100 Å, 4.6 × 100 mm) equipped with a Phenomenex Security Guard precolumn (Luna C_5 300 Å) eluted at 1 mL/min. Detection was by Waters 2998 Diode Array detector between 200 and 600 nm; Waters 2424 ELSD and Waters SQD-2 mass detector operating simultaneously ines + and **ES-** modes between 100 *m/z* and 650 *m/z*. Solvents were: **A**, HPLC grade H_2O containing 0.05% formic acid; **B**, HPLC grade MeOH containing 0.045% formic acid; and **C**, HPLC grade CH_3CN containing 0.045% formic acid. Gradients were as follows. *Method 1*. Kinetex/CH_3CN: 0 min, 10% **C**; 10 min, 90% **C**; 12 min, 90% **C**; 13 min, 10% **C**; 15 min, 10% **C**.

Preparative LCMS: Purification of compounds was generally achieved using a Waters mass-directed autopurification system comprising of a Waters 2767 autosampler, Waters 2545 pump system, a Phenomenex Kinetex Axia column (5 μ, C_{18}, 100 Å, 21.2 × 250 mm) equipped with a Phenomenex Security Guard precolumn (Luna C_5 300 Å) eluted at 20 mL/min at ambient temperature. Solvent **A**, HPLC grade H_2O + 0.05% formic acid; Solvent **B**, HPLC grade CH_3CN + 0.045% formic acid. The post-

column flow was split (100:1) and the minority flow was made up with HPLC grade CH_3CN + 0.045% formic acid to 1 mL·min^{-1} for simultaneous analysis by diode array (Waters 2998), evaporative light scattering (Waters 2424) and ESI mass spectrometry in positive and negative modes (Waters SQD-2). Detected peaks were collected into glass test tubes. Combined tubes were evaporated (vacuum centrifuge), weighed, and residues dissolved directly in solvent for use or analysis.

IR analysis: IR analysis was performed with the Fourier transform spectrophotometer IRAffinity-1S from the company Shimadzu.

Protein purification: The protein purification was performed with an FPLC ÄKTA pure system from the company GE Healthcare. For FPLC analysis a combination with the software UNICORN 6.3 and different columns (Nickel column Protino Ni-NTA Columns 5 mL, Size exclusion column- HiLoad 26/600 Superdex 200pg (GE Healthcare), 320 mL) was used.

UV-Analysis: UV assays were measured with a JASCO-V630-spectrophotometer in quartz glass cuvettes with a diameter of 10 mm. The temperature was controlled by the JASCO-V630-Spectrophotometer at 25 °C. The processed data (by JASCO/Spectramanager) was after that recalculated with Microsoft EXCEL.

Curve Fitting: The recalculated initial rates from EXCEL were plotted in the free available software Curve Expert. From this plotted curvesthe K_M and v_{Max} values were determined with this plotting program. Corresponding v_{Max} over K_M values were then drawn by Microsoft EXCEL.

Surface Plasmon Resonance: The SPR analysis was performed with a four channel instrument from the company Reichert (Reichert 4*SPR*). The instrument includes an internal autosampler up to 768 samples. Other internal features are a degasser, sample loop and optical analysis system. As basic solvents maleate buffer (pH 7) and double destilled water were used. As software an internal programmed system of the company Reichert was used. This system allowed the measurings of interactions between two partners. TRACE DRAWER, a second developed software of Reichert, performed addtitional the analysis of the measurements.

Isothermal Titration Calorimetry (ITC): For ITC measurements an instrument of the company Taininstruments was used. Cells are made of gold. The volume of the reaction and reference chamber is limited to 190 μL. Optimal temperature for investigations in the cells is between 2 °C and 80 °C. As basic solvents double destilled water and TRIS buffer were used.

6.2   Synthesis of Intermediates and Substrates

6.2.1 Preparation of SNAC Compounds

N-S-diacetyl cysteamine (259).[190]
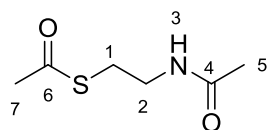
To a solution of cysteamine (2.4 g, 30.8 mmol) in water (20 mL) potassium hydroxide (6 M) was added at 0 °C until pH 8 was reached. Acetic anhydride (9.5 mL, 92.40 mmol) was added dropwise to the mixture keeping the pH at 8. After that the pH was adjust to 7 with 2 M HCl and stirred for 1.5 hours. Then NaCl was added until saturation and the solution was extracted with dichloromethane (3 × 15 ml), dried over MgSO$_4$ and concentrated *in vacuo*. No further purification was necessary. The obtained product was a colourless oil (4.7 g, 30.00 mmol, 98%) R_f: 0.18 (ethyl acetate / hexane 1:1). **^{1}H-NMR** (CDCl$_3$, 400 MHz): δ 1.90 (s, 3H, 5-CH$_3$); 2.28 (s, 3H, 7-CH$_3$); 2.95 (t, *J* = 6.4, 2H, 1-CH$_2$); 3.42 (dt, *J* = 6.3, *J* = 6.3, 2H, 2-CH$_2$); 5.95 (brs, 3-NH). **^{13}C-NMR** (CDCl$_3$, 100 MHz): δ 23.2 (5-CH$_3$); 28.8 (7-CH$_3$); 30.6 (1-CH$_2$); 39.6 (2-CH$_2$), 170.5 (4-CO); 196.4 (6-CO). **ES-MS:** *m/z* (%): 323.5 [M$_2$]H$^+$ (22%), 203.5 [M+CH$_3$CN]H$^+$ (12%), 162.2 [M]H$^+$ (100%), 161.0 [M-CH$_3$CO + CH$_3$CN]H$^+$ (15%), 120.2 [M-CH$_3$CO]H$^+$ (82%).[125]

N-acetyl cysteamine (260).[191]
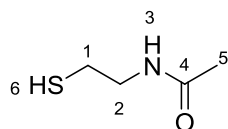
To a solution of *N-S*-diacetyl cysteamine (2.48 g, 15.4 mmol) in water (10 mL) potassium hydroxide (2.79 g, 49.4 mmol) was added at 0 °C. After that the solution was warmed to room temperature and stirred for one hour. Then the reaction was cooled down to 0 °C and acidified to pH 5 with 2 M HCl. Then NaCl was added until saturation and the solution was extracted with dichloromethane (3 × 15 mL), dried over MgSO$_4$ and concentrated *in vacuo*. No further purification was necessary. The obtained product was a colourless oil (1.77 g, 14.80 mmol, 98%). R$_f$: 0.07 (ethyl acetate/ hexane 1:1). **^{1}H-NMR** (CDCl$_3$, 400 MHz): δ 1.35 (t, *J* = 7.9, 1H, 6-SH); 1.95 (s, 3H, 5-CH$_3$); 2.65 (dt, *J* = 6.5, *J* = 6.2, 2H, 1-CH$_2$); 3.41 (dt, *J* = 6.2, *J* = 6.2, 2H, 2-CH$_2$); 6.06 (brs, 3-NH). **^{13}C-NMR** (CDCl$_3$, 75 MHz): δ 23.2 (5-CH$_3$); 24.2 (2-CH$_2$); 42.5 (1-CH$_2$), 170.5 (4-CO). **ES-MS:** *m/z* (%): 239.3 [M$_2$]H$^+$ (14 %), 161.3 [M+CH$_3$CN]H$^+$ (32 %), 120.2 [M]H$^+$ (100 %). **IR (ν = cm^{-1}):** 3294 (N-H), 3080 (C-H), 2936 (C-H), 1649 (C=O), 1545 (N-H).[125]

General Procedure SNAC-Compounds.

Acid (4.00 mmol) and *N*-acetylcysteamine (0.48 g, 4.00 mmol) were dissolved in dichloromethane (9 mL) and the mixture was cooled to 0 °C. Then *N, N*-dimethylaminopyridine (0.1 g, 0.8 mmol) and *N*-(3-Diethylamino-propyl)-*N*-ethyl-carbodiimide (0.83 g, 4.00 mmol) were added to the reaction. The mixture was warmed to 25 °C and then stirred for three hours. The mixture was quenched with 2 M HCl (10 mL) and extracted with dichloromethane (3 × 15 mL). The organic layer was washed with saturated

NaHCO$_3$ and brine. The product was dried over MgSO$_4$ and concentrated *in vacuo*. The crude product was purified by column chromatography (ethyl acetate).[125]

Tigloyl-*N*-acetylcysteamine (107).[129]
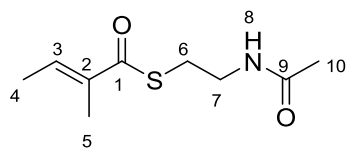
The obtained product was an oil (0.78 g, 3.90 mmol, 98%). R$_f$: 0.56 (ethyl acetate). **^{1}H-NMR** (CDCl$_3$, 200 MHz): δ 1.86 (s, 3H, 4-CH$_3$); 1.90 (s, 3H, 5-CH$_3$); 2.00 (s, 3H, 10-CH$_3$); 3.10 (t, *J* = 6.5, 2H, 6-CH$_2$); 3.48 (dt, *J* = 6.2, *J* = 6.2, 2H, 7-CH$_2$); 5.97 (brs, 1H, 8-NH); 6.89 (qq, *J* = 1.3, *J* = 7.0, 1H, 3-CH). **ES-MS:** *m/z* (%): 403.4 [M$_2$]H$^+$ (100%), 202.4 [M]H$^+$ (61%). **IR (ν = cm^{-1}):** 3280 (N-H), 3080 (CH=C), 2931 (C-H), 1649 (C=O), 1545 (N-H).[192]

Angelic-*N*-acetylcysteamine (261).[129]
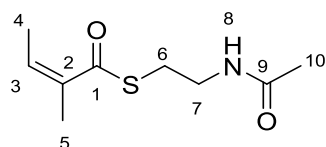
The obtained product was an oil (0.76 g, 3.70 mmol, 94%). R$_f$: 0.58 (ethyl acetate). **^{1}H-NMR** (CDCl$_3$, 200 MHz): δ 1.86 (s, 3H, 4-CH$_3$); 1.90 (s, 3H, 5-CH$_3$); 2.00 (s, 3H, 10-CH$_3$); 3.10 (q, *J* = 6.5, 2H, 6-CH$_2$); 3.48 (dt, *J* = 6.2, *J* = 6.2, 2H, 7-CH$_2$); 5.97 (brs, 1H, 8-NH); 6.1 (qq, *J* = 1.3, *J* = 7.0, 1H, 3-CH). **ES-MS:** *m/z* (%): 403.4 [M$_2$]H$^+$ (100%), 243.4 [M+CH$_3$CN]H$^+$ (8%), 202.2 [M]H$^+$ (56%). **IR (ν = cm^{-1}):** 3274 (N-H), 3079 (CH=C), 2933 (C-H), 1684 (C=O), 1650 (C=O), 1546 (N-H).[192]

Crotonyl-*N*-acetyl-cysteamine (262).[129]
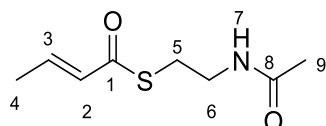
The obtained product was a yellow oil (0.10 g, 0.50 mmol, 14%). R$_f$: 0.49 (ethyl acetate). **^{1}H-NMR** (CDCl$_3$, 400 MHz): δ 1.90 (dd, *J* = 1.7, *J* = 7.1, 3H, 4-CH$_3$); 1.96 (s, 3H, 9-CH$_3$); 3.08 (t, *J* = 6.6, 2H, 5-CH$_2$); 3.45 (q, *J* = 6.1, 2H, 6-CH$_2$); 5.89 (brs, 1H, 7-NH); 6.15 (dq, *J* = 1.7, *J* = 15.4, 1H, 2-CH); 6.94 (dq, *J* = 6.8, *J* = 15.4, 1H, 3-CH). **^{13}C-NMR** (CDCl$_3$, 100 MHz): δ 18.0 (4-CH$_3$); 23.2 (9-CH$_3$); 28.2 (5-CH$_2$); 39.9 (6-CH$_2$); 129.9 (2-CH); 141.9 (3-CH); 170.3 (8-CO); 190.2 (1-CO). **ES-MS:** *m/z* (%): 376.4 [M$_2$]H$^+$ (25%), 188.2 [M]H$^+$ (100%). **IR (ν = cm^{-1}):** 3258 (N-H), 3068 (CH=CH), 2942 (C-H), 1684 (C=O), 1659 (C=O), 1634 (C=O).[192]

(±)-2-Methyl-butyryl-*N*-acetylcysteamine (263).[129]
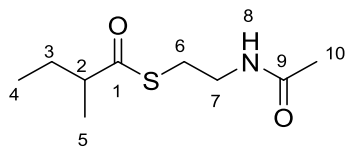
The obtained product was an oil (0.45 g, 2.20 mmol, 55%). R_f: 0.53 (ethyl acetate). **^{1}H-NMR** (CDCl$_3$, 400 MHz): δ 0.90 (t, J = 7.6, 3H, 4-CH$_3$); 1.15 (d, J = 7.2, 3H, 5-CH$_3$); 1.50 (m, 2H, 3-CH$_2$); 1.95 (s, 3H, 10-CH$_3$); 2.57 (m, 1H, 2-CH); 3.01 (t, J = 6.6, 2H, 6-CH$_2$); 3.42 (dt, J = 6.1, J = 6.1, 2H, 7-CH$_2$); 5.88 (brs, 1H, 8-NH). **^{13}C-NMR** (CDCl$_3$, 100 MHz): δ 11.5 (4-CH$_3$), 17.2 (5-CH$_3$); 23.2 (10-CH$_3$); 27.1 (3-CH$_2$); 28.1 (6-CH$_2$); 39.8 (7-CH$_2$); 50.2 (2-CH); 170.3 (9-CO); 204.6 (1-CO). **ES-MS:** *m/z* (%): 204.2 [M]H$^+$ (58%), 162.2 [M-CH$_3$CO + H]H$^+$ (100%). **IR (ν = cm^{-1}):** 3276 (N-H), 3079 (C-H), 2968 (C-H), 2933 (C-H), 2876 (C-H), 1684 (C=O), 1651 (C=O), 1546 (N-H).[192]

Benzoic-*N*-acetylcysteamine (264).[193]
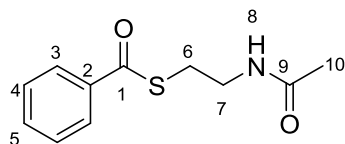
The obtained product was an oil (0.76 g, 3.40 mmol, 85 %). R_f: 0.58 (ethyl acetate). **^{1}H-NMR** (CDCl$_3$, 200 MHz): δ 2.00 (s, 3H, 10-CH$_3$); 3.26 (t, J = 6.7, 2H, 6-CH$_2$); 3.56 (q, J = 6.5, 2H, 7-CH$_2$); 5.93 (brs, 1H, 8-NH); 7.49 (m, 2H, 4-CH), 7.6 (m, 5H, 5-CH); 7.99 (m, 2H, 3-CH). **ES-MS:** *m/z* (%): 447.4 [M$_2$]H$^+$ (1%), 224.2 [M]H$^+$ (13%), 118 [M-C$_7$H$_5$O]H$^+$ (8%), 105.2 [M-C$_4$H$_8$NOS]H$^+$ (100%). **IR (ν = cm^{-1}):** 3300 (N-H), 3084 (C-H), 2930 (C-H), 1649 (C=O), 1596 (C=O), 1550 (N-H).[192]

6.2.2 Preparation of Carboxylic Acids.

General method 1: Malonic acid (2.5 g, 24.00 mmol) and aldehyde (38.00 mmol) were dissolved in pyridine (8 mL) and morpholine (35 μL). The solution was stirred for 17 hours at 25 °C and was heated to 115 °C and stirred for further 6 hours. The mixture was quenched with 1 M NaOH (20 mL) and extracted with diethyl ether (3 × 15 mL). Then the aqueous phase was acidified with 2 M HCl and extracted with diethyl ether (3 × 15 mL). The organic layer was dried over MgSO$_4$ and concentrated *in vacuo*.[115]

Hex-2-enoic acid (116).[129]
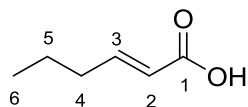
The obtained product was a colourless oil (1.43 g, 9.00 mmol, 50%) **^{1}H-NMR** (CDCl$_3$, 400 MHz): δ 0.94 (t, J = 7.4, 3H, 6-CH$_3$); 1.50 (m, 2H, 5-CH$_2$); 2.25 (dq, J = 1.4, J = 7.2, 2H, 4-CH$_2$); 5.84 (dt, J = 1.5, J = 15.4, 1H, 2-CH); 7.10 (dt, J = 7.1, J = 15.4, 1H, 3-CH); 9.78 (brs, 1H, OH). **^{13}C-NMR** (CDCl$_3$, 100 MHz): δ 13.6 (6-CH$_3$), 21.1 (5-CH$_2$); 34.3 (4-CH$_2$); 120.7 (2-CH); 152.3 (3-CH); 172.0 (1-COOH). **ES-MS:** *m/z* (%): 227 [M$_2$]H $^-$ (100%), 158 [M+CH$_3$CN]H$^+$ (12%) **IR (ν = cm^{-1}):** 2962 (C-H), 2933 (O-H), 2875 (C-H), 2671 (C-H), 1694 (C=O), 1650 (C=C).[115, 116]

(±)-4-Methylhex-2-enoic acid (115a).[129]
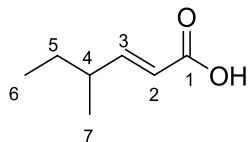
The obtained product was a yellow oil (1.43 g, 11.00 mmol, 47%). **^{1}H-NMR** (CDCl$_3$, 400 MHz): δ 0.89 (t, J = 7.1, 3H, 6-CH$_3$); 1.06 (d, J = 6.6, 1H, 7-CH$_3$); 1.39-1.46 (m, 2H, 5-CH$_2$); 2.21-2.31 (m, 1H, 4-CH); 5.79 (dd, J = 1.3, J = 15.7, 1H, 2-CH); 6.99 (dd, J = 7.7, J = 15.7, 1H, 3-CH). **^{13}C-NMR** (CDCl$_3$, 100 MHz): δ 11.6 (6-CH$_3$), 18.8 (7-CH$_3$); 28.7 (5-CH$_2$); 38.3 (4-CH); 119.0 (2-CH); 157.5 (3-CH); 172.1 (1-CO). **ES-MS:** m/z (%): 170 [M+CH$_3$CN]H$^+$ (100%), 129 [M]H$^+$ (28%);. **IR (ν = cm^{-1}):** 2964 (C-H), 2929 (O-H), 2877 (C-H), 1692 (C=O), 1650 (C=C).[115, 116]

Hept-2-enoic acid (117).[129]
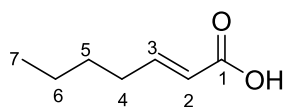
The obtained product was a yellow oil (1.71 g, 13.00 mmol, 57 %). **^{1}H-NMR** (CDCl$_3$, 400 MHz): δ 0.94 (t, J = 6.9, 3H, 7-CH$_3$); 1.40 (m, 4H, 6-5-CH$_2$); 2.23 (qd, J = 1.6, J = 7.0, 2H, 4-CH$_2$); 5.82 (dt, J = 1.6, J = 15.7, 1H, 2-CH); 7.10 (dt, J = 6.5, J = 15.2, 1H, 3-CH). **^{13}C-NMR** (CDCl$_3$, 100 MHz): δ 13.8 (7-CH$_3$), 22.2 (6-CH$_2$); 29.9 (5-CH$_2$); 32.0 (4-CH$_2$); 120.4 (2-CH); 152.5 (6-CH); 171.9 (1-CO). **ES-MS:** m/z (%): 257 [M$_2$]H $^+$ (3%), 170 [M+CH$_3$CN]H$^+$ (100%), 129 [M]H$^+$ (8%), 111 [M-H$_2$O]H$^+$ (9%), **IR (ν = cm^{-1}):** 2959 (C-H), 2930 (O-H), 2873 (C-H), 1693 (C=O), 1649 (C=C).[115, 116]

Oct-2-enoic acid (118).[129]
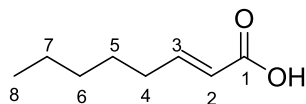
The obtained product was a yellow oil (1.81 g, 13.00 mmol, 53%). **^{1}H-NMR** (CDCl$_3$, 400 MHz): δ 0.91 (t, J = 6.9, 3H, 8-CH$_3$); 1.25-1.50 (m, 6H, 7-6-5-CH$_2$); 2.23 (qd, J = 1.6, J = 7.0, 2H, 4-CH$_2$); 5.82 (dt, J = 1.6, J = 15.7, 1H, 2-CH); 7.06 (dt, J = 6.5, J = 15.2, 1H, 3-CH). **^{13}C-NMR** (CDCl$_3$, 100 MHz): δ 14.0 (8-CH$_3$), 22.4 (7-CH$_2$); 27.5 (6-CH$_2$); 31.7 (5-CH$_2$); 32.3 (4-CH$_2$); 120.5 (2-CH); 152.6 (3-CH); 171.8 (1-COOH). **ES-MS:** m/z (%): 283 [M$_2$]H$^-$ (21%), 141 [M]H$^-$ (100%). **IR (ν = cm^{-1}):** 2958 (C-H), 2929 (O-H), 2859 (C-H), 1693 (C=O), 1650 (C=C).[115, 116]

Dec-2-enoic acid (119).[129]
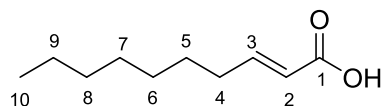
The obtained product was a yellow oil (1.8 g, 11.00 mmol, 28%) **^{1}H-NMR** (CDCl$_3$, 400 MHz): δ 0.90 (t, J = 5.2, 3H, 10-CH$_3$); 1.29-1.50 (m, 10H, 9-8-7-6-5-CH$_2$); 2.25 (dq, J = 1.3, J = 7.0, 2H, 4-CH$_2$); 5.84 (dt, J = 1.6, J = 15.4, 1H, 2-CH); 7.10 (dt, J = 7.0, J = 15.4, 1H, 3-CH). **^{13}C-NMR** (CDCl$_3$, 100 MHz): δ 14.1

(10-CH$_3$), 22.6 (9-CH$_2$); 27.8 (8-CH$_2$); 29.0 (7-CH$_2$); 29.1 (6-CH$_2$); 31.7 (5-CH$_2$); 32.3 (4-CH$_2$); 120.5 (2-CH); 152.5 (3-CH); 171.9 (1-CO). **ES-MS:** *m/z* (%): 511.5 [M$_3$]H$^+$ (25%), 341.7 [M$_2$]H$^+$ (100%), 212.4 [M]H$^+$ (97%), 171.2 [M]H$^+$ (10%), 153.5 [M-H$_2$O]H$^+$ (70%). **IR (ν = cm^{-1}):** 2956 (C-H), 2925 (O-H), 2858 (C-H), 2671 (C-H), 1694 (C=O), 1650 (C=C).[115, 116]

General Method 2:

Step 1. A solution of dichloromethane (5 mL) and butanale (0.07 mL, 1.00 mmol) was stirred at 0 °C. (Carbethoxyethylidene)triphenylphosphorane (0.72 g, 2.00 mmol) was added to this solution warmed to 25 °C and stirred for 18 hours. Then the solvent was evaporated under a nitrogen flow. The crude product was purified by column chromatography (ethyl acetate/ hexane 1:10).

Step 2. To a solution of the corresponding Ester in ethanol/water 5:1 (5 mL/ 1 mL) potassium hydroxide was added to the solution. After stirring under reflux for 3 hours diethyl ether was added. The mixture was washed with NaHCO$_3$ (3 × 10 mL). Then the aqueous layer was acidified with 2 M HCl until pH 1 and extracted with ethyl acetate (3x 10 ml). The organic layer was dried over MgSO$_4$ and concentrated *in vacuo*.[116, 117]

Ethyl-2-methylhex-2-enoate (120a).[129]
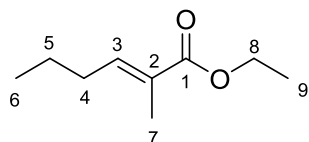
The obtained product was a colourless oil (0.06 g, 0.40 mmol, 37%). R$_f$: 0.95 (ethyl acetate/ hexane 1:10). **^{1}H-NMR** (CDCl$_3$, 400 MHz): δ 0.93 (t, *J* = 7.3, 3H, 6-CH$_3$); 1.29 (t, *J* = 7.1, 3H, 9-CH$_3$); 1.39-1.55 (m, 2H, 5-CH$_2$); 1.82 (m, 3H, 7-CH$_3$); 2.18 (qd, *J* = 1.2, *J* = 7.4, 2H, 4-CH$_2$); 4.18 (q, *J* = 6.9, 2H, 8-CH$_2$); 6.74 (tq, *J* = 1.4, *J* = 7.5, 1H, 3-CH). **^{13}C-NMR** (CDCl$_3$, 100 MHz): δ 12.4 (6-CH$_3$), 13.9 (9-CH$_3$), 14.3 (7-CH$_3$), 21.9 (5-CH$_2$); 30.7 (4-CH$_2$); 60.4 (8-CH$_2$); 127.9 (2-C); 142.2 (3-CH); 168.4 (1-CO). **ES-MS:** *m/z* (%): 313 [M$_2$]H$^+$ (12%), 198 [M+CH$_3$CN]H$^+$ (100%), 157 [M]H$^+$ (95%). **IR (ν = cm^{-1}):** 2961 (C-H), 2934 (O-H), 2873 (C-H), 1710 (C=O), 1650 (C=C).[116]

2-Methylhex-2-enoic acid (121a).[129]
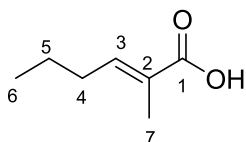
The obtained product was a red oil (0.16 g, 1.30 mmol, 50%). **^{1}H-NMR** (CDCl$_3$, 400 MHz): δ 0.91 (t, *J* = 6.84, 3H, 6-CH$_3$); 1.32-1.50 (m, 2 H, 5-CH$_2$); 1.85 (s, 3H, 7-CH$_3$); 2.22 (q, *J* = 7.2, 2H, 4-CH$_2$); 6.93 (tq, *J* = 1.4, *J* = 7.6, 1H, 3-CH). **^{13}C-NMR** (CDCl$_3$, 100 MHz): δ 12.0 (6-CH$_3$), 13.8 (7-CH$_3$), 21.7 (5-CH$_2$), 30.6 (4-CH$_2$), 127.0 (2-C), 145.2 (3-CH), 173.1 (1-CO). **ES-MS:** *m/z* (%): 257 [M$_2$]H$^+$ (12%), 170 [M+CH$_3$CN]H$^+$ (100%), 129 [M]H$^+$ (60%); 111 [M-H$_2$O]H$^+$ (12%). **IR (ν = cm^{-1}):** 2956 (C-H), 2931 (C-H), 2857 (C-H), 1685 (C=O), 1644 (C=C).[117]

(±)-Ethyl-2, 4-dimethylhex-2-enoate (120b).[129]

The obtained product was a colourless oil (0.28 g, 1.60 mmol, 80%). R_f: 0.78 (ethyl acetate/ hexane 1:10). **^{1}H-NMR** (CDCl$_3$, 400 MHz): δ 0.85 (t, J = 7.1, 3H, 6-CH$_3$); 1.00 (d, J = 7.1, 3H, 7-CH$_3$); 1.28-1.55 (m, 2H, 5-CH$_2$); 1.30 (t, J = 6.4, 3H, 10-CH$_3$); 1.82 (s, 3H, 8-CH$_3$); 2.41 (m, 1H, 4-CH); 4.19 (q, J = 7.1, 2H, 9-CH$_2$); 6.52 (dq, J = 1.3, J = 10.3, 1H, 3-CH). **^{13}C-NMR** (CDCl$_3$, 100 MHz): δ 11.9 (6-CH$_3$), 12.6 (7-CH$_3$), 14.3 (10-CH$_3$), 19.7 (8-CH$_3$), 29.7 (5-CH$_2$), 34.9 (4-CH), 60.4 (9-CH$_2$), 126.6 (2-C), 147.9 (3-CH), 168.4 (1-CO) **ES-MS:** m/z (%): 184 [M-CH$_2$CH$_3$+CH$_3$CN]H$^+$ (100%), 171 [M]H$^+$ (52%), 142 [M-CH$_2$CH$_3$]H$^+$ (12%). **IR (ν = cm^{-1}):** 2961 (C-H), 2930 (C-H), 1709 (C=O), 1650 (C=C).[116]

(±)-2-4-Dimethylhex-2-enoic acid (121b).[129]
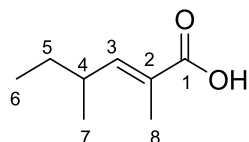
The obtained product was a red oil (0.19 g, 1.30 mmol, 50%). **^{1}H-NMR** (CDCl$_3$, 400 MHz): δ 0.86 (t, J = 6.0, 3H, 6-CH$_3$); 1.01 (d, J = 6.0, 3H, 7-CH$_3$); 1.24-1.49 (m, 2H, 5-CH$_2$); 1.85 (s, 3H, 8-CH$_3$); 2.38-2.49 (m, 1H, 4-CH); 6.68 (qq, J = 1.4, J = 11.6, 1H, 3-CH). **^{13}C-NMR** (CDCl$_3$, 100 MHz): δ 11.8 (6-CH$_3$), 12.2 (7-CH$_3$), 19.5 (8-CH$_3$), 29.5 (5-CH$_2$), 35.1 (4-CH), 125.7 (2-C), 150.8 (3-CH), 173.3 (1-CO). **ES-MS:** m/z (%): 184 [M+CH$_3$CN]H$^+$ (100%), 143 [M]H$^+$ (22%). **IR (ν = cm^{-1}):** 2961 (C-H), 2929 (C-H), 2875 (C-H), 1682 (C=O), 1643 (C=C).[117]

(±)-Methyl-4-methylhex-2-enoate (120c).[129]

The obtained product was a colourless oil (0.51 g, 3.60 mmol, 90%). R_f: 0.78 (ethyl acetate/ hexane 1:10). **^{1}H-NMR** (CDCl$_3$, 400 MHz): δ 0.88 (t, J = 6.4, 3H, 6-CH$_3$); 1.04 (d, J = 6.9, 3H, 7-CH$_3$); 1.36-1.44 (m, 2H, 5-CH$_2$); 2.17-2.27 (m, 1H, 4-CH); 3.73 (s, 3H, 8-CH$_3$); 5.78 (dd, J = 1.1, J = 15.6, 1H, 2-CH); 6.87 (dd, J = 6.9, J = 16.3, 1H, 3-CH). **^{13}C-NMR** (CDCl$_3$, 100 MHz): δ 11.7 (6-CH$_3$), 18.9 (7-CH$_3$), 28.7 (5-CH$_2$), 38.1 (4-CH), 51.4 (8-CH$_3$), 119.3 (2-CH), 154.8 (3-CH), 167.3 (1-CO) **ES-MS:** m/z (%): 143 [M]H$^+$ (100%), 111 [M-OCH$_3$]H$^+$ (72%). **IR (ν = cm^{-1}):** 2963 (C-H), 2876 (C-H), 1722 (C=O), 1656 (C=C).[116]

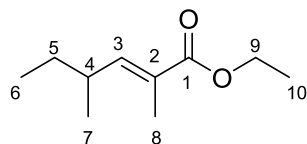**Ethyl-2-methylhept-2-enoate (120d).**[129]
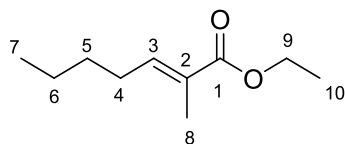
The obtained product was a colourless oil (0.18 g, 0.90 mmol, 94%). R_f: 0.82 (ethyl acetate/ hexane 1:10). **^{1}H-NMR** (CDCl$_3$, 400 MHz): δ 0.91 (t, J = 7.2, 3H, 7-CH$_3$); 1.29 (t, J = 7.2, 3H, 10-CH$_3$); 1.35-1.44 (m, 4H, 5-6-CH$_2$); 1.82 (s, 3H, 8-CH$_3$); 2.16 (q, J = 7.1, 2H, 4-CH$_2$); 4.18 (q, J = 7.2, 2H, 9-CH$_2$); 6.74 (tq, J = 1.4, J = 7.5, 1H, 3-CH). **^{13}C-NMR** (CDCl$_3$, 100 MHz): δ 12.3 (7-CH$_3$), 13.9 (8-CH$_3$), 14.3 (10-CH$_3$), 22.5 (6-CH$_2$), 28.4 (4-CH$_2$), 30.7 (5-CH$_2$); 60.4 (9-CH$_2$); 127.7 (2-C); 142.4 (3-CH); 168.4 (1-CO). **ES-MS:** m/z (%): 341 [M$_2$]H$^+$ (18%), 212 [M+CH$_3$CN]H$^+$ (100%), 171 [M]H$^+$ (78%). **IR (ν = cm^{-1}):** 2926 (O-H), 2857 (C-H), 1685 (C=O), 1644 (C=C).[117]

2-Methylhept-2-enoic acid (121d).[129]
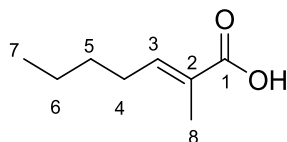
The obtained product was a red oil (0.11 g, 0.80 mmol, 93%). **^{1}H-NMR** (CDCl$_3$, 400 MHz): δ 0.91 (t, J = 6.84, 3H, 7-CH$_3$); 1.32-1.50 (m, 4H, 5-6-CH$_2$); 1.83 (s, 3H, 8-CH$_3$); 2.18 (q, J = 7.2, 2H, 4-CH$_2$); 6.90 (tq, J = 1.4, J = 7.6, 1H, 3-CH). **^{13}C-NMR** (CDCl$_3$, 100 MHz): δ 11.9 (7-CH$_3$), 13.9 (8-CH$_3$), 22.4 (6-CH$_2$), 28.6 (4-CH$_2$), 30.5 (5-CH$_2$), 126.8 (2-C), 145.5 (3-CH), 172.8 (1-CO). **ES-MS:** m/z (%): 285 [M$_2$]H$^+$ (10%), 184 [M+CH$_3$CN]H$^+$ (100%), 143 [M]H$^+$ (10%); 125 [M-H$_2$O]H$^+$ (10%). **IR (ν = cm^{-1}):** 2956 (C-H), 2931 (C-H), 2857 (C-H), 1685 (C=O), 1644 (-C=C).[116]
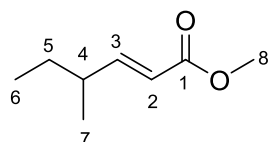
Ethyl-2-methyloct-2-enoate (120e).[129]
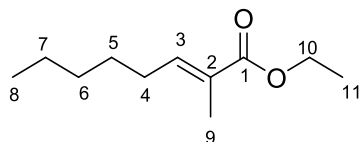
The obtained product was a colourless oil (0.18 g, 0.90 mmol, 94%). R_f: 0.65 (ethyl acetate/ hexane 1:10). **^{1}H-NMR** (CDCl$_3$, 400 MHz): δ 0.88 (t, J = 6.5, 3H, 8-CH$_3$); 1.25-1.55 (m, 9H, 7-6-5-CH$_2$-11-CH$_3$); 1.82 (d, J = 0.93, 3H, 9-CH$_3$); 2.15 (q, J = 7.2, 2H, 4-CH$_2$); 4.18 (q, J = 7.2, 2H, 10-CH$_2$); 6.77 (tq, J = 1.6, J = 7.6, 1H, 3-CH). **^{13}C-NMR** (CDCl$_3$, 100 MHz): δ 12.3 (8-CH$_3$), 14.0 (9-CH$_3$), 14.3 (11-CH$_3$), 22.5 (7-CH$_2$), 28.3 (5-CH$_2$), 28.7 (4-CH$_2$), 31.6 (6-CH$_2$), 60.4 (10-CH$_2$), 127.7 (2-C), 142.5 (3-CH), 168.4 (1-C) **ES-MS:** m/z (%): 369 [M$_2$]H$^+$ (33%), 226 [M+CH$_3$CN]H$^+$ (100%), 185 [M]H$^+$ (65%). **IR (ν = cm^{-1}):** 2926 (C-H), 2859 (C-H), 1709 (C=O), 1650 (C=C).[116]

2-Methyloct-2-enoic acid (121e).[129]
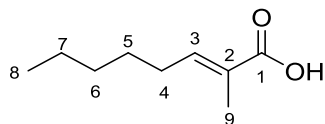
The obtained product was a red oil (0.16 g, 1.30 mmol, 50 %). **¹H-NMR** (CDCl$_3$, 400 MHz): δ 0.92 (t, J = 6.9, 3H, 8-CH$_3$); 1.26-1.52 (m, 6H, 5-6-7-CH$_2$); 1.86 (d, J = 1.33, 3H, 9-CH$_3$); 2.22 (q, J = 7.3, 2H, 4-CH$_2$); 6.94 (tq, J = 1.4, J = 7.5, 1H, 3-CH). **¹³C-NMR** (CDCl$_3$, 100 MHz): δ 12.0 (8-CH$_3$), 14.0 (9-CH$_3$), 22.5 (7-CH$_2$), 28.1 (5-CH$_2$), 28.8 (4-CH$_2$), 31.5 (6-CH$_2$), 126.8 (2-C), 145.5 (3-CH), 173.1 (1-CO). **ES-MS:** m/z (%): 313 [M$_2$] H $^+$ (10%), 198 [M+CH$_3$CN]H$^+$ (100%), 157 [M]H$^+$ (22%). **IR (ν = cm^{-1}):** 2926 (OH), 2859 (C-H), 1682 (C=O), 1642 (C=C).[117]

**Ethyl-2-methyldec-2-enoate (120f).**[129]
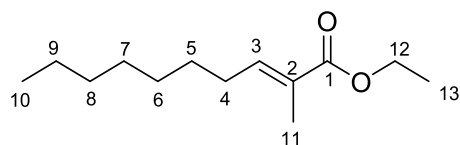
The obtained product was a colourless oil (0.15 g, 0.70 mmol, 66%). R$_f$: 0.85 (ethyl acetate/ hexane 1:7). **¹H-NMR** (CDCl$_3$, 400 MHz): δ 0.88 (t, J = 6.8, 3H, 10-CH$_3$); 1.25-1.58 (m, 13H, 9-8-7-6-5-CH$_2$-13-CH$_3$); 1.82 (d, J = 0.93, 3H, 11-CH$_3$); 2.15 (q, J = 7.4, 2H, 4-CH$_2$); 4.18 (q, J = 7.2, 2H, 12-CH$_2$); 6.75 (tq, J = 1.3, J = 7.4, 1H, 3-CH). **¹³C-NMR** (CDCl$_3$, 100 MHz): δ 12.3 (10-CH$_3$), 14.1 (11-CH$_3$), 14.3 (13-CH$_3$), 22.6 (9-CH$_2$), 28.6 (7-CH$_2$), 28.7 (6-CH$_2$), 29.1 (5-CH$_2$), 29.4 (4-CH$_2$), 31.8 (8-CH$_2$), 60.4 (12-CH$_2$), 127.6 (2-C), 142.5 (3-CH), 168.4 (1-CO) **ES-MS:** m/z (%): 425 [M$_2$]H$^+$ (50%), 254 [M+CH$_3$CN]H$^+$ (100%), 213 [M]H$^+$ (52%). **IR (ν = cm^{-1}):** 2925 (-C-H), 2856 (-C-H), 1710 (C=O), 1650 (-C=C), 1463 (CO), 1366 (C-O), 1266 (C-O).[116]

2-Methyldec-2-enoic acid (121f).[129]
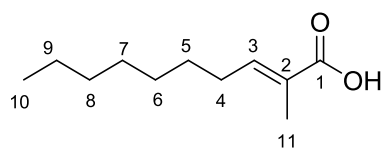
The obtained product was a red oil (0.11 g, 0.60 mmol, 86%). **¹H-NMR** (CDCl$_3$, 400 MHz): δ 0.87-0.90 (m, 3H, 10-CH$_3$); 1.26-1.30 (m, 10H, 9-8-7-6-5-CH$_2$); 1.83 (d, J = 0.93, 3H, 11-CH$_3$); 2.19 (q, J = 7.3, 2H, 4-CH$_2$); 6.90 (td, J = 1.5, J = 7.6, 1H, 3-CH). **¹³C-NMR** (CDCl$_3$, 100 MHz): δ 12.3 (10-CH$_3$), 14.1 (11-CH$_3$), 22.6 (9-CH$_2$), 28.4 (7-CH$_2$), 28.9 (6-CH$_2$), 29.1 (5-CH$_2$), 29.3 (4-CH$_2$), 31.8 (8-CH$_2$), 126.8 (2-C), 145.6 (3-CH), 172.8 (1-CO). **ES-MS:** m/z (%): 369 [M$_2$]H$^+$ (10%), 226 [M+CH$_3$CN]H$^+$ (100%), 167 [M-H$_2$O]H$^+$ (52%). **IR (ν = cm^{-1}):** 2925 (C-H), 2363 (O-H), 1712 (C=O), 1650 (C=C).[117]

General Method 3:

Step 1. Potassium *tert*-butanoxide (1.63 g, 14.5 mmol) was added to dry THF (20 mL) and cooled down to 0 °C. After that triethylphosphonobutyrate (3.5 mL, 14.5 mmol) was added and the solution stirred for 10 min. Aldehyde (14 mmol) was added and the mixture warmed up to roomtemperature. The solution was stirred for 3 hours and then water (20 mL) was added and extracted 3 × with ethyl acetate (20 mL). The combined organic layers were washed with brine and dried over $MgSO_4$. The crude product was purified by column chromatography (ethyl acetate/ hexane 1:10).

Step 2. To a solution of the corresponding Ester in ethanol/water 5:1 (5 mL/ 1 mL) potassium hydroxide was added to the solution. After stirring under reflux for 3 hours diethyl ether was added. The mixture was washed with $NaHCO_3$ (3 × 10 mL). Then the aqueous layer was acidified with 2 M HCl until pH 1 and extracted with ethyl acetate (3x 10 mL). The organic layer was dried over $MgSO_4$ and concentrated *in vacuo*.[118]

Ethyl-2-ethylhex-2-enoate (123a).[129]
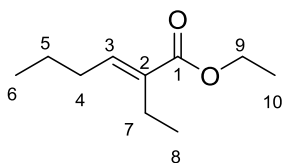
The mixture of the *E*- and *Z*-isomers was a colourless oil (1.50 g, 8.80 mmol, 63%). R_f: 0.69 (ethyl acetate/ hexane 1:10). **^{1}H-NMR** (CDCl$_3$, 400 MHz): δ 0.90-1.05 (m, 6H, 6-8-CH$_3$); 1.28-1.32 (m, 3H, 10-CH$_3$); 1.38-1.52 (m, 2H, 5-CH$_2$); 2.16 (q, *J* = 6.9, 2H, 4-CH$_2$); 2.24-2.40 (m, 2H, 7-CH$_2$); 4.16-4.23 (m, 2H, 9-CH$_2$); 5.83 (t, *J* = 7.9, 0.3 H, 3-CH); 6.71 (t, *J* = 7.4, 0.7 H, 3-CH). **^{13}C-NMR** (CDCl$_3$, 100 MHz): δ 13.6 (6-CH$_3$), 13.9 (8-CH$_3$), 14.3 (10-CH$_3$), 20.0 (7-CH$_{2E}$), 22.1 (4-CH$_{2E}$), 22.7 (9-CH$_{2Z}$), 27.3 (5-CH$_{2Z}$), 30.4 (4-CH$_{2E}$), 31.5 (4-CH$_{2Z}$), 59.8 (9-CH$_{2Z}$), 60.3 (9-CH$_{2E}$), 133.9 (2-C$_Z$), 134.1 (2-C$_e$), 140.0 (3-CH$_Z$), 141.4 (3-CH$_E$), 168.0 (1-C$_Z$), 168.4 (1-C$_E$) **ES-MS:** *m/z* (%): 184 [M-CH$_2$CH$_3$+CH$_3$CN]H$^+$ (18%), 171 [M]H$^+$ (8%), 143 [M.CH$_2$CH$_3$]H$^+$ (100%). **IR (v = cm^{-1}):** 2963 (C-H), 2935 (C-H), 2874 (C-H), 1709 (C=O), 1646 (C=C).[118]

2-Ethylhex-2-enoic acid (125a).[129]
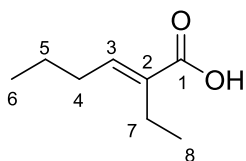
The obtained product was a red oil (1.2 g, 8.40 mmol, 96%). **^{1}H-NMR** (CDCl$_3$, 400 MHz): δ 0.91-1.08 (m, 6H, 6-8-CH$_3$); 1.40-1.54 (m, 2H, 5-CH$_2$); 2.20 (q, *J* = 7.7, 2H, 4-CH$_2$); 2.26-2.34 (m, 2H, 7-CH$_2$); 6.03 (t, *J* = 7.6, 1H, 3-CH$_Z$); 6.88 (t, *J* = 7.6, 1H, 3-CH$_E$). **^{13}C-NMR** (CDCl$_3$, 100 MHz): δ 13.8 (6-CH$_3$), 13.8 (8-CH$_3$), 19.7 (7-CH$_{2Z}$), 22.0 (7-CH$_{2E}$), 27.4 (5-CH$_2$), 30.5 (4-CH$_{2Z}$), 31.7 (4-CH$_{2E}$), 132.6 (2-C$_Z$), 133.3 (2-C$_E$), 144.8 (3-CH$_Z$), 144.9 (3-CH$_E$), 173.3 (1-CO). **ES-MS:** *m/z* (%): 184 [M+CH$_3$CN]H$^+$ (18%), 143 [M]H$^+$ (100%). **IR (v = cm^{-1}):** 2963 (C-H), 2934 (C-H), 2874 (C-H), 1681 (C=O), 1637 (C=C).[118]

Ethyl-2-ethyloct-2-enoate (123b).[129]
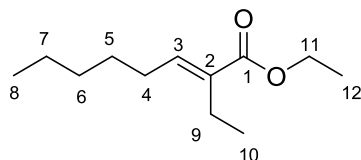
The mixture of the E- and Z-isomers was a colourless oil (2.10 g, 10.60 mmol, 74%). R_f: 0.63 (ethyl acetate/ hexane 1:10). **^{1}H-NMR** (CDCl$_3$, 400 MHz): δ 0.86-1.05 (m, 6H, 8-10-CH$_3$); 1.27-1.33 (m, 7H, 5-7-CH$_2$-12-CH$_3$); 1.36-1.48 (m, 2H, 6-CH$_2$); 2.16 (q, J = 7.2, 2H, 4-CH$_2$); 2.23-2.43 (m, 2H, 9-CH$_2$); 4.16-4.23 (m, 2H, 11-CH$_2$); 5.83 (t, J = 7.9, 0.3 H, 3-CH); 6.71 (t, J = 7.2, 0.7 H, 3-CH). **^{13}C-NMR** (CDCl$_3$, 100 MHz): δ 13.6 (8-CH$_3$), 13.9 (10-CH$_3$), 14.3 (12-CH$_3$), 20.0 (9-CH$_{2E}$), 22.1 (9-CH$_{2Z}$), 22.7 (7-CH$_2$), 28.3 (5-CH$_{2Z}$), 28.5 (5-CH$_{2E}$), 29.3 (6-CH$_{2Z}$), 29.4 (6-CH$_{2E}$), 31.5 (4-CH$_{2E}$), 31.6 (4-CH$_{2Z}$), 59.9 (11-CH$_{2Z}$), 60.3 (11-CH$_{2E}$), 133.7 (2-C$_Z$), 133.9 (2-C$_E$), 140.0 (3-CH$_Z$), 142.4 (3-CH$_E$), 168.0 (1-C$_Z$), 168.4 (1-C$_E$ **ES-MS:** m/z (%): 199 [M]H$^+$ (18%), 171 [M.H$_2$O]H $^+$ (72%). **IR (ν = cm^{-1}):** 2960 (C-H), 2929 (C-H), 2873 (C-H), 1709 (C=O), 1645 (C=C).[118]

2-Ethyl-oct-2-enoic acid (125b).[129]
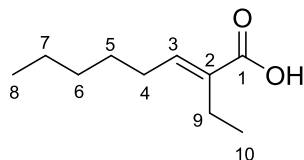
The obtained product was a red oil (1.0 g, 6.00 mmol, 60 %). **^{1}H-NMR** (CDCl$_3$, 400 MHz): δ 0.91-1.08 (m, 6H, 8-10-CH$_3$); 1.28-1.38 (m, 4H, 6-7-CH$_2$); 1.40-1.49 (m, 2H, 5-CH$_2$); 2.20 (q, J = 7.4, 2H, 4-CH$_2$); 2.26-2.34 (m, 2H, 9-CH$_2$); 2.49 (q, J = 7.4, 2H, 5-CH$_2$); 6.02 (t, J = 7.1, 1H, 3-CH$_Z$); 6.88 (t, J = 7.4, 1H, 3-CH$_E$). **^{13}C-NMR** (CDCl$_3$, 100 MHz): δ 13.8 (8-CH$_3$), 13.9 (10-CH$_3$), 19.8 (9-CH$_{2Z}$), 22.5 (9-CH$_{2E}$), 27.4 (7-CH$_2$), 28.4 (6-CH$_2$), 29.2 (5-CH$_2$), 30.5 (4-CH$_{2Z}$), 31.7 (4-CH$_{2E}$), 132.4 (2-C$_Z$), 133.3 (2-C$_E$), 144.7 (3-CH$_Z$), 146.1 (3-CH$_E$), 172.8 (1-CO). **ES-MS:** m/z (%): 212 [M+CH$_3$CN]H$^+$ (11%), 171 [M]H$^+$ (82%). **IR (ν = cm^{-1}):** 2959 (C-H), 2927 (C-H), 2859 (C-H), 1681 (C=O), 1637 (C=C).[118]

6.2.3 Further Preparations of Carboxylic Acids

(2E, 4S)-Dimethylhex-2-enoic acid (121g).[129]
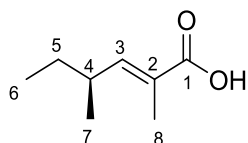
2S-methylbutanol (1.00 mL, 10 mmol) and pyridinium chlorochromate (2.2 g, 10 mmol) and celite (1.31 g) were dissolved in THF (30 mL). The reaction was followed by TLC and after full consumption of the alcohol (Carbethoxyethylidene)triphenylphosphorane (4.20 g, 12.00 mmol) was added and the reaction refluxed for 7 hours. Then diethyl ether was added and the mixture was filtered by Florosil. The filtered solution was concentrated under vacuo and purified by column chromatographie (hexane/ ethyl acetate, 4:1). To a solution of (2E, 4S)-dimethylhex-2-enoate (0.40 g, 3.40 mmol) in ethanol/water 5:1

(5 mL/ 1 mL) potassium hydroxide (1.22 g, 22.00 mmol) was added to the solution. After stirring under reflux for 3 hours diethyl ether was added. The mixture was washed with $NaHCO_3$ (3 × 10 mL). Then the aqueous layer was acidified with 2 M HCl until pH 1 and extracted with ethyl acetate (3 × 10 mL). The organic layer was dried over $MgSO_4$ and concentrated *in vacuo*. The obtained product was a red oil (0.57 g, 3.30 mmol, 98%). **^{1}H-NMR** (CDCl$_3$, 400 MHz): δ 0.88 (t, *J* = 7.4, 3H, 6-CH$_3$); 1.17 (d, *J* = 6.9, 3H, 7-CH$_3$); 1.40-1.60 (m, 2H, 5-CH$_2$); 1.85 (d, *J* = 1.5, 3H, 8-CH$_3$); 2.32-2.49 (m, 1H, 4-CH), 6.69 (dd, *J* = 1.5, *J* = 10.0, 1H, 3-CH). **^{13}C-NMR** (CDCl$_3$, 100 MHz): δ 11.9 (6-CH$_3$), 12.6 (7-CH$_3$), 19.7 (8-CH$_3$), 29.7 (5-CH$_2$), 34.9 (4-CH), 126.6 (2-C), 147.9 (3-CH), 168.4 (1-CO). **ES-MS:** *m/z* (%): 143 [M+CH$_3$CN]H$^+$ (100%). [α]$_D$ = +11.0 (CH$_2$Cl$_2$) **IR (ν = cm^{-1}):** 2966 (C-H), 2935 (C-H), 2877 (C-H), 1697 (C=O).[119, 120]

Methyl-6-methylhept-2-enoate (131).[129]
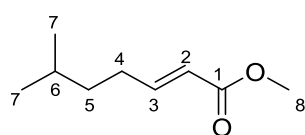
4-Methyl-pentanol (0.5 ml, 3.6 mmol), pyridinium chlorochromate (1.09, 5.0 mmol) and celite (1.31 g) were dissolved in THF (30 ml). The reaction was followed by TLC and after full consumption of the alcohol methyl(triphenylphosphor-anylidene)acetate (2.03 g, 6.1 mmol) was added and the reaction refluxed for 7 hours. Then diethyl ether was added and the mixture was filtered by Florosil. The filtered solution was concentrated *in vacuo* and purified by column chromatography (hexane/ ethyl acetate, 4:1). The obtained product was a colourless oil (0.42 g, 2.6 mmol, 72%) R$_f$: 0.72 (ethyl acetate/ hexane 1:10). **^{1}H-NMR** (CDCl$_3$, 400 MHz): δ 0.89 (d, *J* = 6.5, 6H, 7-CH$_3$); 1.31-1.36 (m, 2H, 5-CH$_2$); 1.53-1.61 (m, 1H, 6-CH$_2$); 2.17-2.23 (m, 2H, 4-CH$_2$); 3.72 (s, 3H, 9-CH$_3$); 5.82 (dt, *J* = 1.7, *J* = 15.6, 1H, 2-CH), 6.97 (dt, *J* = 7.0, *J* = 15.7, 1H, 3-CH). **^{13}C-NMR** (CDCl$_3$, 100 MHz): δ 22.4 (7-2xCH$_3$), 27.5 (6-CH), 30.1 (4-CH$_2$), 37.0 (5-CH$_2$), 51.4 (8-CH$_3$), 120.6 (2-CH), 150.0 (3-CH), 167.2 (1-CO) **ES-MS:** *m/z* (%): 157 [M+CH$_3$CN]H$^+$ (100%).[120]

6-Methylhept-2-enoic acid (132).[129]

To a solution of methyl-6-methylhept-2-enote (0.42 g, 2.60 mmol) in ethanol/water 5:1 (5 mL/ 1 mL) potassium hydroxide (1.22 g, 22.00 mmol) was added to the solution. After stirring under reflux for 3 hours diethyl ether was added. The mixture was washed with $NaHCO_3$ (3 × 10 ml). Then the aqueous layer was acidified with 2 M HCl until pH 1 and extracted with ethyl acetate (3 × 10 mL). The organic layer was dried over $MgSO_4$ and concentrated *in vacuo*. The obtained product was a yellow oil (0.26 g, 1.80 mmol, 70%). **^{1}H-NMR** (CDCl$_3$, 400 MHz): δ 0.89 (d, *J* = 5.5, 6H, 7-CH$_3$); 1.33-1.38 (m, 2H, 5-CH$_2$); 1.53-1.62 (m, 1H, 6-CH$_2$); 2.21-2.27 (m, 2H, 4-CH$_2$); 5.82 (dt, *J* = 1.5, *J* = 15.5, 1H, 2-CH), 6.97 (dt, *J* = 6.9, *J* = 15.5, 1H, 3-CH). **^{13}C-NMR** (CDCl$_3$, 100 MHz): δ 22.4 (7-2xCH$_3$), 27.5 (6-CH), 30.1

(4-CH$_2$), 37.0 (5-CH$_2$), 120.6 (2-CH), 152.7 (3-CH), 171.3 (1-CO). **ES-MS:** m/z (%): 157 [M+CH$_3$CN]H$^+$ (100%). **IR (ν = cm^{-1}):** 2957 (C-H), 2872 (C-H), 1694 (C=O), 1650 (-C=C).[117]

Methyl-7-methyloct-2-enoate (134).[129]
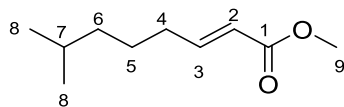
5-Methyl-hexanol (0.5 ml, 3.6 mmol), pyridinium chlorochromate (1.09, 5.0 mmol) and celite (1.30 g) were dissolved in THF (30 mL). The reaction was followed by TLC and after full consumption of the alcohol methyl(triphenylphosphor-anylidene)acetate (2.03 g, 6.1 mmol) was added and the reaction 7 hours refluxed. Then diethyl ether was added and the mixture was filtered through Florosil. The filtered solution was concentrated *in vacuo* and purified by column chromatography (hexane/ ethyl acetate, 4:1). The obtained product was a colourless oil (0.52 g, 3.1 mmol, 86%) R$_f$: 0.75 (ethyl acetate/ hexane 1:10). **^{1}H-NMR** (CDCl$_3$, 400 MHz): δ 0.87 (d, J = 6.6, 6H, 8-CH$_3$); 1.15-1.22 (m, 2H, 5-6-CH$_2$); 1.43-1.58 (m, 1H, 7-CH); 2.18 (dq, J = 1.5, J = 7.2, 2H, 4-CH$_2$); 3.73 (s, 3H, 9-CH$_3$); 5.82 (dt, J = 1.5, J = 15.6, 1H, 2-CH), 6.97 (dt, J = 7.0, J = 15.7, 1H, 3-CH). **^{13}C-NMR** (CDCl$_3$, 100 MHz): δ 22.5 (8-2xCH$_3$), 25.9 (5-CH$_3$), 27.8 (7-CH), 32.5 (4-CH$_2$), 38.4 (6-CH$_2$), 51.4 (9-CH$_3$), 120.8 (2-CH), 149.9 (3-CH), 167.2 (1-CO). **ES-MS:** m/z (%): 171 [M+CH$_3$CN]H$^+$ (100%). **IR (ν = cm^{-1}):** 2954 (C-H), 2870 (C-H), 1725 (C=O), 1658 (-C=C).[120]

7-Methyloct-2-enoic acid (135).[129]

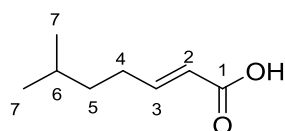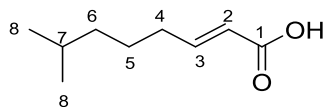To a solution of methyl-7-methyloct-2-enoate (0.42 g, 2.60 mmol) in ethanol/water 5:1 (5 mL/ 1 ml) potassium hydroxide (1.22 g, 22.00 mmol) was added to the solution. After stirring under reflux for 3 hours diethyl ether was added. The mixture was washed with NaHCO$_3$ (3 × 10 mL). Then the aqueous layer was acidified with 2 M HCl until pH 1 and extracted with ethyl acetate (3 × 10 ml). The organic layer was dried over MgSO$_4$ and concentrated *in vacuo*. The obtained product was a yellow oil (0.24 g, 1.50 mmol, 58%). **^{1}H-NMR** (CDCl$_3$, 400 MHz): δ 0.88 (d, J = 5.5, 6H, 8-CH$_3$); 1.17-1.23 (m, 4H, 5-6-CH$_2$); 1.43-1.58 (m, 1H, 7-CH); 2.22 (dq, J = 1.5, J = 7.3, 2H, 4-CH$_2$); 5.82 (dt, J = 1.5, J = 15.5, 1H, 2-CH), 7.09 (dt, J = 6.8, J = 15.5, 1H, 3-CH). **^{13}C-NMR** (CDCl$_3$, 100 MHz): δ 22.4 (8-2xCH$_3$), 25.7 (5 CH$_2$), 27.8 (7-CH), 32.5 (4-CH$_2$), 38.4 (6-CH$_2$), 120.5 (2-CH), 152.3 (3-CH), 171.5 (1-CO) **ES-MS:** m/z (%): 157 [M]H$^+$ (17%), 139 [M-H$_2$O]H$^+$ (70%), 121 [M-2x H$_2$O]H$^+$ (17%). **IR (ν = cm^{-1}):** 2955(C-H), 2930(C-H), 2870 (C-H), 1694 (C=O), 1650 (-C=C).[117]

(4*S*, 6*S*)-Dimethyloct-2-enoic acid (61).[97]
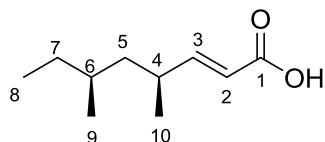
To a solution of squalestatin S1 (1.00 g, 1.40 mmol) in ethanol/water 5:1 (5 mL/ 1 mL) potassium hydroxide (1.22 g, 22.00 mmol) was added to the solution. After stirring under reflux for 3 hours, diethyl ether was added through the solution and washed 3 × with NaHCO$_3$ (3 × 10 mL). The aqueous layer with the (4*S*, 6*S*)-2-4-dimethyloct-2-enoic acid was acidified with 2 M HCl until pH 1 and extracted with ethyl acetate (3 × 10 mL). The organic layer was dried over MgSO$_4$ and concentrated *in vacuo*. The obtained product was a red oil (0.21 g, 0.12 mmol, 86%). **^{1}H-NMR** (CDCl$_3$, 400 MHz): δ 0.88 (t, *J* = 7.4, 6H, 8-9-CH$_3$); 1.07 (d, *J* = 6.2, 3H, 10-CH$_3$); 1.27-1.46 (m, %H, 7-5-CH$_2$-6-CH); 2.41-2.52 (m, 1H, 4-CH), 5.81 (dd, *J* = 1.7, *J* = 16.0, 1H, 2-CH), 6.96 (dd, *J* = 8.8, *J* = 16.0, 1H, 3-CH). **^{13}C-NMR** (CDCl$_3$, 100 MHz): δ 11.1 (8-CH$_3$); 20.2 (9-CH$_3$); 20.7 (10-CH$_3$); 29.8 (7-CH$_2$); 31.9 (6-CH); 34.4 (4-CH); 43.1 (5-CH$_2$), 118.3 (2-CH); 164.6 (3-CH); 176.7 (1-CO). **ES-MS:** *m/z* (%): 171 [M+CH$_3$CN]H$^+$ (100%). **IR (ν = cm^{-1}):** 2960 (C-H), 2914 (C-H), 2873 (C-H), 1693 (C=O), 1649 (-C=C).

6.2.4 Preparation of Acyl Meldrums Acids.

General Procedure: Meldrums acid (2.9 g, 20 mmol) in 50 mL dichloromethane, pyridine (3.3 mL, 40 mmol) stirred under nitrogen for 10 min. After that the temperature of the mixture was settled down to 0 °C and acid chloride (28 mmol) was added slowly to the reaction. The reaction was warmed up to roomtemperature and stirred overnight. The mixture was washed with 2 M HCl and water. After that it was concentrated and purified by column chromatography (hexane/ ethyl acetate 10:1).[166, 167]

Acyl meldrums acid (222a).[166]
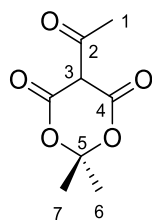
The product was a white solid (2.9 g, 16 mmol, 80%) **^{1}H-NMR** (CDCl$_3$, 400 MHz): δ 1.74 (s, 6H, 6-7-CH$_3$); 2.86 (s, 3H, 1-CH$_3$). **^{13}C-NMR** (CDCl$_3$, 100 MHz): δ 23.5 (1-CH$_3$), 26.8 (6-7-CH$_3$); 91.9 (3-CH); 104.9 (5-C); 170.2 (4-CO); 194.6 (2-CO). **ES-MS:** *m/z* (%): 184 [M]H$^-$ (97%). **IR (ν = cm^{-1}):** 2985 (C-H), 1732 (C=O), 1658 (C=O), 1546 (C-O). **HR-MS:** *m/z* (%): calculated 185.0450, found 185.0453.[166]

Butyryl meldrums acid (222b).[166]
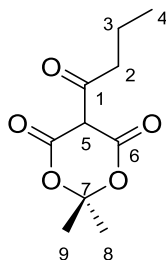
The product was a yellow oil (1.6 g, 7.4 mmol, 78%) **¹H-NMR** (CDCl$_3$, 400 MHz): δ 1.03 (t, J = 8.4, 3H, 4-CH$_3$); 1.74 (s, 6H, 8-9-CH$_3$); 1.72-1.79 (m, 2H, 3-CH$_2$); 3.06 (t, J = 7.3, 2H, 2-CH$_2$). **¹³C-NMR** (CDCl$_3$, 100 MHz): δ 13.9 (4-CH$_3$), 19.6 (3-CH$_2$), 26.6 (8-9-CH$_3$); 37.5 (2-CH$_2$); 91.3 (5-C); 104.8 (7-C); 170.6 (6-CO); 198.2 (1-CO). **ES-MS:** m/z (%): 213 [M]H⁻ (97%). **IR (ν = cm⁻¹):** 2956 (C-H), 2877 (C-H), 1735 (C=O), 1660 (C=O), 1568 (C-O). **HR-MS:** m/z (%): calculated 237.0745, found 237.0739.[166, 167]

6.2.5 Preparation of Pantetheine Dimethyl Ketal Substrates

Pantetheine dimethyl ketal (144).[49]
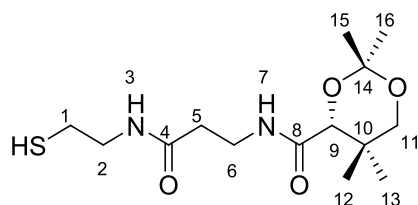
D-pantothenic acid hemicalcium salt (2.50 g, 10.50 mmol), p-toluensulfonic acid (2.30 g, 13.00 mmol) and 5 g molecular sieves were suspended in 125 mL dry acetone and stirred at 25 °C for 12 hours under a nitrogen atmosphere. The suspension was filtered with celite and washed with 200 ml acetone. The filtrate was concentrated to a colourless oil, redissolved in 200 ml ethyl acetate and washed two times with brine (25 mL) and dried over MgSO$_4$. After that the ethyl acetate was removed *in vacuo* and hexane was added to the flask to get a white solid that was dried under high vacuum. The corresponding D-pantothenic dimethyl ketal (1.90 g, 7.00 mmol was dissolved in 40 mL dry THF with CDI (1.70 g, 11.00 mmol) and stirred for one hour at 25 °C. Then cysteamine (1.30 g, 11.00 mmol) was added to the solution and stirred for 12 hours. The solution was concentrated under vacuum and dichloromethane was added. The organic layer were washed with NH$_4$Cl (25 mL) and brine (25 mL), dried over MgSO$_4$ and concentrated *in vacuo*. After that the colourless oil was purified by column chromatography (ethyl acetate) to get a white solid (1.90 g, 6.00 mmol, 86%) R$_f$: 0.1 (ethyl acetate). **¹H-NMR** (CDCl$_3$, 400 MHz): δ 0.98 (s, 3H, 13-CH$_3$); 1.05 (s, 3H, 12-CH$_3$); 1.39 (t, J = 8.6, 1H, SH); 1.43 (s, 3H, 15-CH$_3$); 1.47 (s, 3H, 16-CH$_3$); 2.40 (t, J = 5.8, 2H, 5-CH$_2$); 2.64-2.70 (m, 2H, 1-CH$_2$); 3, 29 (d, J = 12.0, 1H, 11a-C*H*H); 3.37-3.63 (m, 4H, 2-6-CH$_2$); 3, 69 (d, J = 12.0, 1H, 11b-CH*H*); 4.09 (s, 1H, 9-CH); 6.37 (bt, J = 5.2, 1H, 3-NH); 7.03 (bt, J = 5.9, 1H, 7-NH). **¹³C-NMR** (CDCl$_3$, 100 MHz): δ 18.7 (12-CH$_3$); 18.9 (13-CH$_2$); 22.1 (15-CH$_3$); 24.6 (1-CH$_2$); 29.5 (16-CH$_3$); 33.0 (10-C); 34.9 (6-CH$_2$); 36.2 (5-CH$_2$); 42.4 (2-CH$_2$); 71.4 (11-CH$_2$); 77.2 (9-CH); 99.1 (14-C); 170.3 (4-CO); 171.1 (8-CO). **ES-MS:** m/z (%): 319 [M]H⁺ (65%), 261 [M-(CH$_3$)$_2$CO]H⁺ (100%). **IR (ν = cm⁻¹):** 3419 (N-H), 3324 (N-H), 2980 (C-H), 2944 (C-H), 2872 (C-H), 1659 (C=O).

General Procedure Pantetheine Dimethyl Ketal-Compounds.

Acid (1.00 mmol) and pantetheine dimethyl ketal (0.32 g, 1.00 mmol) were dissolved in dichloromethane (9 mL) and the mixture was cooled to 0 °C. Then N, N-dimethylaminopyridine (0.1 g, 0.8 mmol) and N-(3-diethylamino-propyl)-N-ethyl-carbodiimide (N-(3-diethyl-aminopropyl)-N-ethyl-carbodiimide (0.38 g, 2.00 mmol) were added to the reaction. The mixture was warmed to 25 °C and then stirred for three hours. The mixture was quenched with 2 M HCl (10 mL) and extracted with dichloromethane (3 × 15 mL). The organic layer was washed with saturated $NaHCO_3$ and brine. The product was dried over $MgSO_4$ and concentrated *in vacuo*. The crude product was purified by column chromatography (ethyl acetate).[192]

Acyl pantetheine dimethyl ketal (145a).[129]
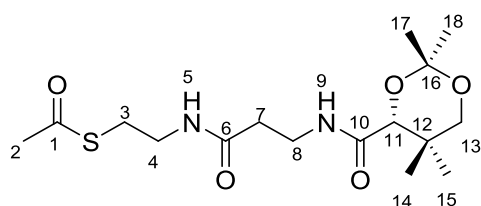
The obtained product was a colourless oil (0.13 g, 0.40 mmol, 40%). R_f: 0.46 (ethyl acetate). **¹H-NMR** (CDCl₃, 400 MHz): δ 0.99 (s, 3H, 14-CH₃); 1.04 (s, 3H, 15-CH₃); 1.44 (s, 3H, 117-CH₃); 1.48 (s, 3H, 18-CH₃); 1.85 (s, 3H, 2-CH₃); 2.44 (t, J = 6.5, 2H, 7-CH₂); 3.08 (t, J = 6.3, 2H, 3-CH₂); 3.28 (d, J = 11.7, 1H, 13a-C*H*H); 3.41-3.62 (m, 4H, 4-8-CH₂); 3.68 (d, J = 11.6, 1H, 13b-CH*H*); 4.08 (s, 1H, 11-CH); 6.13 (bt, J = 5.8, 1H, 5-NH); 7.03 (bt, J = 5.9, 1H, 9-NH). **¹³C-NMR** (CDCl₃, 100 MHz): δ 14.4 (14-CH₃); 18.7 (15-CH₃); 22.1 (17-CH₃); 28.3 (3-CH₂); 29.5 (18-CH₃); 30.6 (2-CH₃); 32.9 (12-C); 34.8 (7-CH₂); 35.9 (8-CH₂); 39.7 (4-CH₂); 71.5 (13-CH₂); 77.2 (11-CH); 99.1 (16-C); 170.1 (6-CO); 171.1 (10-CO); 196.1 (1-CO). **ES-MS:** m/z (%): 383.3 [M]Na⁺ (5%), 361.4 [M]H⁺ (18%), 303.4 [M-C₃H₆O]H⁺ (100%). **HR-MS:** m/z (%): calculated 383.1617, found 383.1619.[192]

2-Bromopropionyl pantetheine dimethyl ketal (145b). [129]
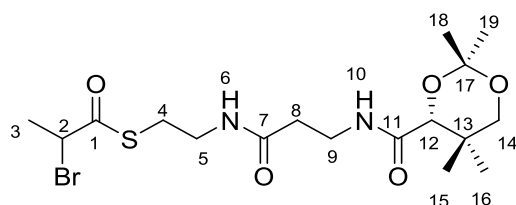
The obtained product was a colourless oil (0.28 g, 0.62 mmol, 62%). R_f: 0.45 (ethyl acetate). **¹H-NMR** (CDCl₃, 400 MHz): δ 0.97 (s, 3H, 15-CH₃); 1.04 (s, 3H, 16-CH₃); 1.41 (s, 3H, 18-CH₃); 1.46 (s, 3H, 19-CH₃); 1.85 (d, J = 6.7, 3H, 3-CH₃); 2.44 (t, J = 6.1, 2H, 8-CH₂); 3.01-3.14 (m, 2H, 4-CH₂); 3.28 (d, J = 11.7, 1H, 14a-C*H*H); 3.40-3.62 (m, 4H, 5-9-CH₂); 3.68 (d, J = 11.8, 1H, 14b-CH*H*); 4.07 (s, 1H, 12-CH); 4.52 (dq, J = 1.1, 7.2, 1H, 2-CH); 6.13 (bt, J = 6.8, 1H, 6-NH); 7.02 (bt, J = 7.4, 1H, 10-NH). **¹³C-NMR** (CDCl₃, 100 MHz): δ 18.7 (15-CH₃); 18.9 (16-CH₃); 21.9 (3-CH₃); 22.1 (18-CH₃); 29.5 (19-CH₃); 29.7 (4-CH₂); 32.9 (13-C); 34.7 (8-CH₂); 36.0 (9-CH₂); 39.1 (5-CH₂); 47.7 (2-CH); 71.5 (14-CH₂); 77.1 (12-CH); 99.1 (17-C); 170.0 (7-CO); 171.2 (11-CO); 196.1 (1-CO). **ES-MS:** m/z (%):

455.7 $[M^{81}Br]H^+$ (60%), 453.3 $[M^{79}Br]H^+$ (46%), 397.5 $[M^{81}Br-(CH_3)_2CO]H^+$ (100%), 395.8 $[M^{79}Br-(CH_3)_2CO]H^+$ (88%). **IR (ν = cm^{-1}):** 3294 (N-H), 2940 (C-H), 1651 (C=O), 1524 (C-O). **HR-MS:** m/z (%): calculated 475.0878, found 475.0872.[192]

2-Methylbutyryl pantetheine dimethyl ketal (145c).[129]
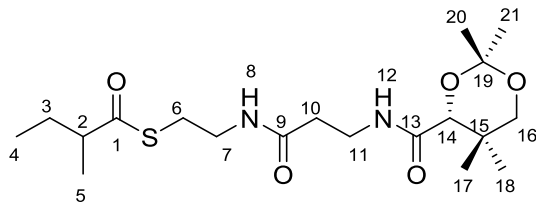
The obtained product was a yellow oil (1.00 g, 2.4 mmol, 88%). R_f: 0.40 (ethyl acetate). **^{1}H-NMR** (CDCl$_3$, 400 MHz): δ 0.90 (t, J = 7.6, 3H, 4-CH$_3$); 0.96 (s, 3H, 17-CH$_3$); 1.03 (s, 3H, 18-CH$_3$); 1.15 (d, J = 6.8, 3H, 5-CH$_3$); 1.41 (s, 3H, 20-CH$_3$); 1.45 (s, 3H, 21-CH$_3$); 1.45-1.77 (m, 2H, 3-CH$_2$); 2.42 (t, J = 6.4, 2H, 10-CH$_2$); 2.52-2.61 (m, 1H, 2-CH); 2.99 (t, J = 6.5, 2H, 6-CH$_2$); 3.27 (d, J = 11.2, 1H, 16a-CHH); 3.36-3.59 (m, 4H, 7-11-CH$_2$); 3.68 (d, J = 11.7, 1H, 16b-CHH); 4.07 (s, 1H, 14-CH); 6.23 (bt, J = 5.7, 1H, 8-NH); 7.03 (bt, J = 5.7, 1H, 12-NH). **^{13}C-NMR (CDCl$_3$, 100 MHz): δ** 13.9 (4-CH$_3$); 17.1 (5-CH$_3$); 18.7 (17-CH$_3$); 18.9 (18-CH$_3$); 22.1 (20-CH$_3$); 27.1 (3-CH$_2$); 28.1 (6-CH$_2$); 29.5 (21-CH$_3$); 32.9 (15-C); 34.8 (10-CH$_2$); 35.9 (11-CH$_2$); 39.7 (7-CH$_2$); 50.2 (2-CH); 71.5 (16-CH$_2$); 77.2 (14-CH); 99.1 (19-C); 170.0 (9-CO); 171.2 (13-CO); 204.8 (1-CO). **ES-MS:** m/z (%): 403.7 [M]H$^-$ (100%). **IR (ν = cm^{-1}):** 3305 (C-H), 2956 (C-H), 2873 (C-H), 1653 (C=O), 1521 (C-O). **HR-MS:** m/z (%): calculated 425.2088, found 425.2086.[192]

Angeloyl pantetheine dimethyl ketal (145d).[129]
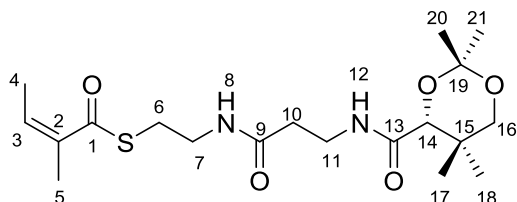
The obtained product was a yellow oil (0.29 g, 0.70 mmol, 70 %). R_f: 0.49 (ethyl acetate). **^{1}H-NMR** (CDCl$_3$, 400 MHz): δ 0.97 (s, 3H, 17-CH$_3$); 1.04 (s, 3H, 18-CH$_3$); 1.41 (s, 3H, 20-CH$_3$); 1.46 (s, 3H, 21-CH$_3$); 1.92-1.97 (m, 3H, 4-CH$_3$); 1.99 (t, J = 1.5, 3H, 5-CH$_3$); 2.42 (t, J = 6.0, 2H, 10-CH$_2$); 3.07 (t, J = 6.7, 2H, 6-CH$_2$); 3.27 (d, J = 11.6, 1H, 16a-CHH); 3.40-3.62 (m, 4H, 7-11-CH$_2$); 3.68 (d, J = 11.6, 1H, 16b-CHH); 4.07 (s, 1H, 14-CH); 5.89 (dt, J = 1.3, 7.3, 1H, 3-CH); 6.11 (bt, J = 5.1, 1H, 8-NH); 7.03 (bt, J = 5.9, 1H, 12-NH). **^{13}C-NMR** (CDCl$_3$, 100 MHz): δ 15.9 (5-CH$_3$); 18.7 (17-CH$_3$); 18.9 (18-CH$_3$); 20.5 (4-CH$_3$); 22.1 (20-CH$_3$); 28.4 (6-CH$_2$); 29.5 (21-CH$_3$); 32.9 (15-C); 34.8 (10-CH$_2$); 35.9 (11-CH$_2$); 39.8 (7-CH$_2$); 71.5 (16-CH$_2$); 77.3 (14-CH); 99.1 (19-C); 134.1 (2-C); 134.9 (3-CH); 170.0 (9-CO); 171.2 (13-CO); 193.9 (1-CO). **ES-MS:** m/z (%): 423.4 [M]Na$^+$ (25%), 401.4 [M]H$^+$ (28%), 343.4 [M-C$_3$H$_6$O$_2$]H$^+$ (100%). **IR (ν = cm^{-1}):** 3260 (N-H), 3078 (C-H), 2924 (C-H), 1651 (C=O). **HR-MS:** m/z (%): calculated 423.1930, found 423.1932.[192]

Tigloyl pantetheine dimethyl ketal (145e).[129]
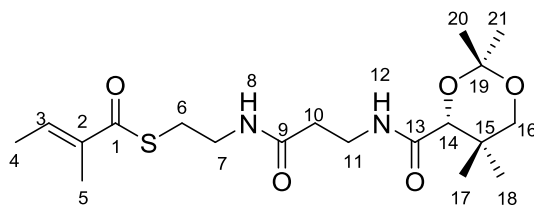
The obtained product was a colourless oil (0.32 g, 0.80 mmol, 80%). R_f: 0.46 (ethyl acetate). **^{1}H-NMR** (CDCl$_3$, 400 MHz): δ 0.99 (s, 3H, 17-CH$_3$); 1.04 (s, 3H, 18-CH$_3$); 1.44 (s, 3H, 21-CH$_3$); 1.48 (s, 3H, 22-CH$_3$); 1.85-1.87 (m, 6H, 4-5-CH$_3$); 2.44 (t, J = 6.5, 2H, 10-CH$_2$); 3.08 (t, J = 6.3, 2H, 6-CH$_2$); 3.28 (d, J = 11.7, 1H, 16a-C*H*H); 3.41-3.62 (m, 4H, 7-11-CH$_2$); 3.68 (d, J = 11.6, 1H, 16b-CH*H*); 4.08 (s, 1H, 14-CH); 6.13 (bt, J = 5.8, 1H, 8-NH); 6.93 (qq, J = 1.4, 6.8, 1H, 3-CH); 7.03 (bt, J = 5.9, 1H, 12-NH). **^{13}C-NMR** (CDCl$_3$, 100 MHz): δ 12.2 (4-CH$_3$); 14.4 (5-CH$_3$); 18.7 (17-CH$_3$); 18.9 (18-CH$_3$); 22.1 (21-CH$_3$); 28.3 (6-CH$_2$); 29.5 (22-CH$_3$); 32.9 (15-C); 34.8 (10-CH$_2$); 35.9 (11-CH$_2$); 39.7 (7-CH$_2$); 71.5 (16-CH$_2$); 77.2 (14-CH); 99.1 (19-C); 136.8 (2-C); 136.9 (3-CH); 170.1 (9-CO); 171.1 (13-CO); 190.2 (1-CO). **ES-MS:** m/z (%): 479.3 [M]Na$^+$ (5%), 457.4 [M]H$^+$ (18%), 399.4 [M-C$_3$H$_6$O]H$^+$(100%). **IR (ν = cm^{-1}):** 3306 (N-H), 2940 (C-H), 1648 (C=O), 1523 (C-O). **HR-MS:** m/z (%): calculated 423.1930, found 423.1929.[192]

2RS-2-Methylhexanoyl pantetheine dimethyl ketal (145f).[129]
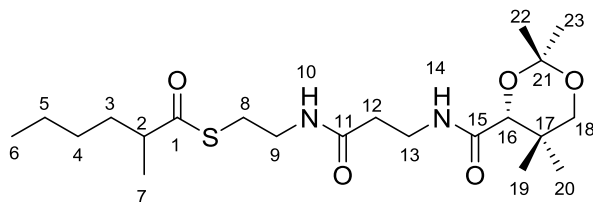
The obtained product was a yellow oil (0.36 g, 0.8 mmol, 88%). R_f: 0.45 (ethyl acetate). **^{1}H-NMR** (CDCl$_3$, 400 MHz): δ 0.88 (t, J = 7.6, 3H, 6-CH$_3$); 0.96 (s, 3H, 19-CH$_3$); 1.03 (s, 3H, 20-CH$_3$); 1.23-1.33 (m, 4H, 4-5-CH$_2$); 1.41 (s, 3H, 22-CH$_3$); 1.46 (s, 3H, 23-CH$_3$); 1.85 (s, 3H, 7-CH$_3$); 1.64-1.74 (m, 2H, 3-CH$_2$); 2.42 (t, J = 6.4, 2H, 12-CH$_2$); 2.60-2.65 (m, 1H, 2-CH); 2.99 (t, J = 6.5, 2H, 8-CH$_2$); 3.27 (d, J = 11.2, 1H, 18a-C*H*H); 3.37-3.60 (m, 4H, 9-13-CH$_2$); 3.68 (d, J = 11.7, 1H, 18b-CH*H*); 4.08 (s, 1H, 16-CH); 6.17 (bt, J = 5.7, 1H, 10-NH); 7.05 (bt, J = 5.7, 1H, 14-NH). **^{13}C-NMR** (CDCl$_3$, 100 MHz): δ 13.9 (6-CH$_3$); 17.6 (7-CH$_3$); 18.7 (19-CH$_3$); 18.9 (20-CH$_3$); 22.1 (22-CH$_3$); 22.6 (5-CH$_2$); 28.1 (8-CH$_2$); 29.3 (4-CH$_2$); 29.5 (23-CH$_3$); 33.3 (3-CH$_2$); 32.9 (17-C); 34.8 (12-CH$_2$); 35.9 (13-CH$_2$); 39.7 (9-CH$_2$); 48.7 (2-CH); 71.5 (18-CH$_2$); 77.2 (16-CH); 99.1 (21-C); 170.0 (11-CO); 171.2 (15-CO); 204.5 (1-CO). **ES-MS:** m/z (%): 429.7 [M]H$^-$ (100%). **IR (ν = cm^{-1}):** 2956 (C-H), 2872 (C-H), 1653 (C=O), 1527 (C-O), 1460 (C=C). **HR-MS:** m/z (%): calculated 453.2406, found 453.2406.[192]

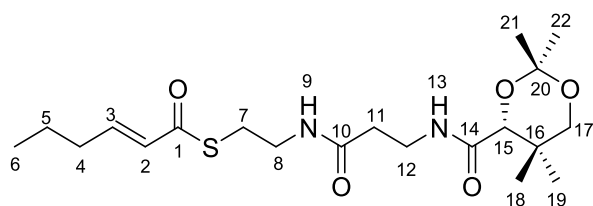**2*E*-Hex-2-enoyl pantetheine dimethyl ketal (145g).**[129]

The obtained product was a yellow oil (0.32 g, 0.70 mmol, 70%). R_f: 0.49 (ethyl acetate). **¹H-NMR** (CDCl₃, 400 MHz): δ 0.92-0.96 (m, 3H, 6-CH₃); 0.97 (s, 3H, 18-CH₃); 1.03 (s, 3H, 19-CH₃); 1.41 (s, 3H, 22-CH₃); 1.46 (s, 3H, 21-CH₃); 1.50 (m, 2H, 5-CH₂); 2.19 (dq, *J* = 1.5, 7.3, 2H, 4-CH₂); 2.42 (t, *J* = 6.3, 2H, 11-CH₂); 3.08 (t, *J* = 6.3, 2H, 7-CH₂); 3.27 (d, *J* = 11.6, 1H, 17a-C*H*H); 3.40-3.62 (m, 4H, 8-12-CH₂); 3.68 (d, *J* = 11.6, 1H, 17b-CH*H*); 4.07 (s, 1H, 15-CH); 6.10 (bt, *J* = 1.6, 1H, 2-CH); 6.14 (bt, *J* = 1.5, 1H, 9-NH); 6.92 (dt, *J* = 6.9, 15.6, 1H, 3-CH); 7.03 (bt, *J* = 5.9, 1H, 13-NH). **¹³C-NMR** (CDCl₃, 100 MHz): δ 13.7 (6-CH₃); 18.7 (18-CH₃); 18.9 (19-CH₃); 21.2 (5-CH₂); 22.1 (21-CH₃); 28.2 (7-CH₂); 29.5 (22-CH₃); 32.9 (16-C); 34.2 (4-CH₂); 34.8 (11-CH₂); 35.9 (12-CH₂); 39.7 (8-CH₂); 71.5 (17-CH₂); 77.3 (15-CH); 99.1 (20-C); 128.4 (2-CH); 146.6 (3-CH); 170.0 (10-CO); 171.2 (14-CO); 190.2 (1-CO). **ES-MS:** *m/z* (%): 415.4 [M]H⁺ (100%). **IR (ν = cm⁻¹):** 3306 (N-H), 2960 (C-H), 2872 (C-H), 1655 (C=O). **HR-MS:** *m/z* (%): calculated 437.2086, found 437.2088.[192]

2*E*-2-Methylhex-2-enoyl pantetheine dimethyl ketal (145h).[129]
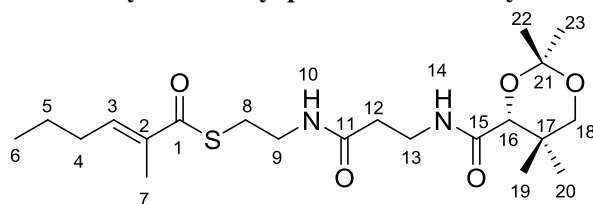
The obtained product was a yellow oil (0.38 g, 0.88 mmol, 88%). R_f: 0.45 (ethyl acetate). **¹H-NMR** (CDCl₃, 400 MHz): δ 0.96 (t, *J* = 7.6, 3H, 6-CH₃); 0.97 (s, 3H, 19-CH₃); 1.04 (s, 3H, 20-CH₃); 1.44-1.55 (m, 2H, 5-CH₂); 1.41 (s, 3H, 22-CH₃); 1.46 (s, 3H, 23-CH₃); 1.87 (s, 3H, 7-CH₃); 2.20 (q, *J* = 7.4, 2H, 4-CH₂); 2.42 (t, *J* = 6.1, 2H, 12-CH₂); 3.05 (t, *J* = 6.5, 2H, 8-CH₂); 3.27 (d, *J* = 11.2, 1H, 18a-C*H*H); 3.39-3.62 (m, 4H, 9-13-CH₂); 3.68 (d, *J* = 11.7, 1H, 18b-CH*H*); 4.07 (s, 1H, 16-CH); 6.10 (bt, *J* = 5.7, 1H, 10-NH); 6.77 (dt, *J* = 1.3, 6.9, 1H, 3-CH); 7.03 (bt, *J* = 5.7, 1H, 14-NH). **¹³C-NMR** (CDCl₃, 100 MHz): δ 12.5 (6-CH₃); 13.9 (7-CH₃); 18.7 (19-CH₃); 18.9 (20-CH₃); 21.8 (5-CH₂); 22.1 (22-CH₃); 28.4 (8-CH₂); 28.8 (4-CH₂); 29.5 (23-CH₃); 32.9 (17-C); 34.8 (12-CH₂); 35.9 (13-CH₂); 39.7 (9-CH₂); 71.5 (18-CH₂); 77.2 (16-CH); 99.1 (21-C); 135.9 (2-C); 142.1 (3-CH); 170.0 (11-CO); 171.2 (15-CO); 193.7 (1-CO). **ES-MS:** *m/z* (%): 429.7 [M]H⁺ (100%). **IR (ν = cm⁻¹):** 3293 (N-H), 2959 (C-H), 2870 (C-H), 1648 (C=O). **HR-MS:** *m/z* (%): calculated 451.2243, found 451.2244.[192]
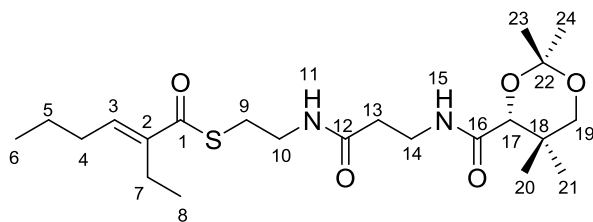
**2*EZ*-2-Ethylhex-2-enoyl pantetheine dimethyl ketal (145i).**[129]

The obtained product was a yellow oil (0.38 g, 0.88 mmol, 88%). R_f: 0.45 (ethyl acetate).
^{1}H-NMR (CDCl$_3$, 400 MHz): δ 0.86-1.08 (m, 12H, 6-8-20-21-CH$_3$); 1.40-1.53 (m, 2H, 5-CH$_2$); 1.41 (s, 3H, 23-CH$_3$); 1.46 (s, 3H, 24-CH$_3$); 2.20 (q, *J* = 7.5, 2H, 4-CH$_2$); 2.31-2.38 (m, 2H, 7-CH$_{2E}$); 2.40-2.44 (m, 2H, 7-CH$_{2Z}$); 3.03-3.09 (m, 2H, 9-CH$_2$); 3.27 (d, *J* = 11.2, 1H, 19a-C*H*H); 3.39-3.64 (m, 4H, 10-14-CH$_2$); 3.68 (d, *J* = 11.7, 1H, 19b-CH*H*); 4.07 (s, 1H, 17-CH); 5.62 (t, *J* = 7.7, 1H, 3-CH$_Z$); 6.12 (bt, *J* = 5.7, 1H, 11-NH); 6.71 (t, *J* = 7.5, 1H, 3-CH$_E$); 7.04 (bt, *J* = 5.7, 1H, 15-NH). **^{13}C-NMR** (CDCl$_3$, 100 MHz): δ 13.9 (6-CH$_3$); 14.1 (8-CH$_3$); 18.7 (20-CH$_3$); 18.9 (21-CH$_3$); 22.2 (5-CH$_2$); 22.1 (23-CH$_3$); 28.4 (9-CH$_2$); 28.8 (7-CH$_2$); 29.5 (24-CH$_3$); 30.9 (4-CH$_2$); 32.9 (18-C); 34.8 (13-CH$_2$); 35.9 (14-CH$_2$); 39.7 (10-CH$_2$); 71.5 (19-CH$_2$); 77.2 (17-CH); 99.1 (22-C); 135.9 (2-C); 142.1 (3-CH); 170.0 (12-CO); 171.2 (16-CO); 193.7 (1-CO). **ES-MS:** *m/z* (%): 465.4 [M]Na$^+$ (51%), 443.7 [M]H$^+$ (28%), 385.4 [M-C$_4$H$_8$]H$^+$ (100%). **HR-MS:** *m/z* (%): calculated 465.2399, found 465.2396.[192]

4*RS*-4-Methylhex-2-enoyl pantetheine dimethyl ketal (145j).[129]
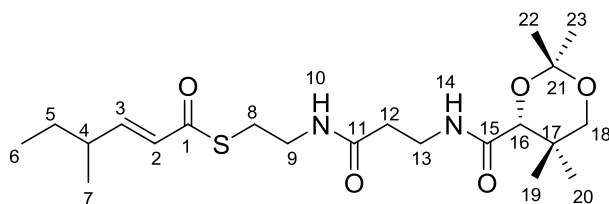
The obtained product was a colourless oil (0.35 g, 0.82 mmol, 82%). R_f: 0.45 (ethyl acetate).
^{1}H-NMR (CDCl$_3$, 400 MHz): δ 0.88 (t, *J* = 7.2, 3H, 6-CH$_3$); 0.97 (s, 3H, 19-CH$_3$); 1.04 (s, 3H, 20-CH$_3$); 1.06 (d, *J* = 6.7, 3H, 7-CH$_3$), 1.40-1.45 (m, 2H, 5-CH$_2$); 1.41 (s, 3H, 22-CH$_3$); 1.46 (s, 3H, 23-CH$_3$); 2.17-2.26 (m, 1H, 4-CH); 2.42 (t, *J* = 6.3, 2H, 12-CH$_2$); 3.05 (t, *J* = 6.3, 2H, 8-CH$_2$); 3.27 (d, *J* = 11.9, 1H, 18a-C*H*H); 3.40-3.62 (m, 4H, 9-13-CH$_2$); 3.68 (d, *J* = 11.7, 1H, 18b-CH*H*); 4.07 (s, 1H, 16-CH); 6.08 (dd, *J* = 1.2, 15.6, 1H, 2-CH); 6.12 (bt, *J* = 5.1, 1H, 10-NH); 6.77 (dd, *J* = 7.5, 15.5, 1H, 3-CH); 7.03 (bt, *J* = 6.0, 1H, 14-NH). **^{13}C-NMR** (CDCl$_3$, 100 MHz): δ 11.6 (6-CH$_3$); 12.2 (7-CH$_3$); 18.7 (19-CH$_3$); 18.9 (20-CH$_3$); 22.1 (22-CH$_3$); 28.3 (5-CH$_2$); 28.4 (8-CH$_2$); 29.5 (23-CH$_3$); 32.9 (17-C); 34.8 (12-CH$_2$); 35.9 (13-CH$_2$); 38.1 (4-CH); 39.7 (9-CH$_2$); 71.5 (18-CH$_2$); 77.2 (16-CH); 99.1 (21-C); 126.7 (2-CH); 151.7 (3-CH); 170.0 (11-CO); 171.2 (15-CO); 190.3 (1-CO). **ES-MS:** *m/z* (%): 429.7 [M]H$^+$ (100%). **IR (ν = cm^{-1}):** 3305 (N-H), 2961 (C-H), 2873 (C-H), 1655 (C=O). **HR-MS:** *m/z* (%): calculated 451.2243, found 451.2243.[192]

4*RS*-2-4-Dimethylhex-2-enoyl pantetheine dimethyl ketal (145k).[129]
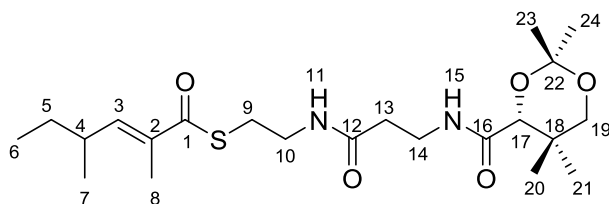
The obtained product was a colourless oil (0.38 g, 0.89 mmol, 89%). R_f: 0.45 (ethyl acetate).
^{1}H-NMR (CDCl$_3$, 400 MHz): δ 0.87 (t, *J* = 7.9, 3H, 6-CH$_3$); 0.97 (s, 3H, 20-CH$_3$); 1.04 (s, 3H, 21-CH$_3$);
1.03 (d, *J* = 7.5, 3H, 7-CH$_3$), 1.24-1.49 (m, 3H, 4-CH, 5-CH$_2$); 1.41 (s, 3H, 23-CH$_3$); 1.46 (s, 3H, 24-CH$_3$); 1.88 (s, 3H, 8-CH$_3$); 2.42 (t, *J* = 5.9, 2H, 13-CH$_2$); 3.05 (t, *J* = 6.4, 2H, 9-CH$_2$); 3.27 (d, *J* = 11.4, 1H, 19a-C*H*H); 3.39-3.64 (m, 4H, 10-14-CH$_2$); 3.68 (d, *J* = 11.7, 1H, 19b-CH*H*); 4.07 (s, 1H, 17-CH); 6.09 (bt, *J* = 5.4, 1H, 11-NH); 6.53 (dd, *J* = 1.4, 9.8, 1H, 3-CH); 7.03 (bt, *J* = 5.8, 1H, 15-NH). **^{13}C-NMR** (CDCl$_3$, 100 MHz): δ 11.9 (6-CH$_3$); 12.2 (7-CH$_3$); 18.7 (20-CH$_3$); 18.9 (21-CH$_3$); 19.9 (8-CH$_3$); 22.1 (23-CH$_3$); 28.5 (9-CH$_2$); 29.5 (24-CH$_3$); 29.6 (5-CH$_2$); 32.9 (18-C); 34.4 (13-CH$_2$); 35.0 (4-CH); 35.9 (14-CH$_2$); 39.7 (10-CH$_2$); 71.5 (19-CH$_2$); 77.2 (17-CH); 99.1 (22-C); 134.5 (2-C); 147.6 (3-CH); 170.0 (12-CO); 171.2 (16-CO); 193.9 (1-CO). **ES-MS:** *m/z* (%): 442.7 [M]H$^+$ (100%). **IR (ν = cm^{-1}):** 3291 (N-H), 2923 (C-H), 2872 (C-H), 1651 (C=O). **HR-MS:** *m/z* (%): calculated 465.2399, found 465.2396.[192]


(2*E*, 4*S*)-Dimethylhex-2-enoyl pantetheine dimethyl ketal (145l).[129]

The obtained product was a colourless oil (0.30 g, 0.68 mmol, 68%). R_f: 0.45 (ethyl acetate). **^{1}H-NMR** (CDCl$_3$, 400 MHz): δ 0.91 (t, *J* = 7.9, 3H, 6-CH$_3$); 0.97 (s, 3H, 20-CH$_3$); 1.04 (s, 3H, 21-CH$_3$); 1.17 (d, *J* = 7.5, 1H, 7-CH$_3$), 1.24-1.49 (m, 2H, 5-CH$_2$); 1.42 (s, 3H, 23-CH$_3$); 1.46 (s, 3H, 24-CH$_3$); 1.88 (s, 3H, 8-CH$_3$); 2.42 (t, *J* = 6.1, 2H, 13-CH$_2$); 2.54-2.62 (m, 1H, 4-CH); 3.05 (t, *J* = 6.5, 2H, 9-CH$_2$); 3.27 (d, *J* = 11.7, 1H, 19a-C*H*H); 3.38-3.62 (m, 4H, 10-14-CH$_2$); 3.68 (d, *J* = 12.1, 1H, 19b-CH*H*); 4.08 (s, 1H, 17-CH); 6.09 (bt, *J* = 5.4, 1H, 11-NH); 6.53 (dd, *J* = 1.5, 10.2, 1H, 3-CH); 7.03 (bt, *J* = 5.8, 1H, 15-NH). **^{13}C-NMR** (CDCl$_3$, 100 MHz): δ 11.6 (6-CH$_3$); 17.2 (7-CH$_3$); 18.7 (20-CH$_3$); 18.9 (21-CH$_3$); 19.9 (8-CH$_3$); 22.1 (23-CH$_3$); 28.5 (9-CH$_2$); 29.5 (24-CH$_3$); 29.6 (5-CH$_2$); 32.9 (18-C); 34.8 (13-CH$_2$); 35.1 (4-CH); 35.9 (14-CH$_2$); 39.7 (10-CH$_2$); 71.5 (19-CH$_2$); 77.2 (17-CH); 99.1 (22-C); 135.6 (2-C); 147.6 (3-CH); 170.1 (12-CO); 171.1 (16-CO); 204.1 (1-CO). **ES-MS:** *m/z* (%): 442.7 [M]H$^+$ (100%). **IR (ν = cm^{-1}):** 3302 (N-H), 2960 (C-H), 2873 (C-H), 1649 (C=O). **HR-MS:** *m/z* (%): calculated 443.2580, found 443.2583.[192]

2*E*-2-Methylhept-2-enoyl pantetheine dimethyl ketal (145m).[129]
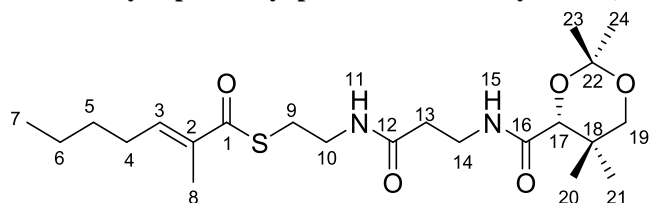
The obtained product was a colourless oil (0.24 g, 0.50 mmol, 54%). R_f: 0.39 (ethyl acetate). **¹H-NMR** (CDCl₃, 400 MHz): δ 0.92 (t, *J* = 7.2, 3H, 7-CH₃); 0.97 (s, 3H, 20-CH₃); 1.04 (s, 3H, 21-CH₃); 1.31-1.49 (m, 4H, 5-6-CH₂); 1.41 (s, 3H, 23-CH₃); 1.46 (s, 3H, 24-CH₃); 1.87 (s, 3H, 8-CH₃); 2.22 (q, *J* = 7.1, 2H, 4-CH₂); 2.42 (t, *J* = 6.3, 2H, 13-CH₂); 3.05 (t, *J* = 6.5, 2H, 9-CH₂); 3.27 (d, *J* = 11.9, 1H, 19a-C*H*H); 3.39-3.62 (m, 4H, 10-14-CH₂); 3.68 (d, *J* = 11.9, 1H, 19b-CH*H*); 4.07 (s, 1H, 17-CH); 6.08 (bt, *J* = 5.0, 1H, 11-NH); 6.77 (dq, *J* = 1.3, 7.1, 1H, 3-CH); 7.03 (bt, *J* = 6.1, 1H, 15-NH). **¹³C-NMR** (CDCl₃, 100 MHz): δ 12.5 (8-CH₃); 13.9 (7-CH₃); 18.7 (20-CH₃); 18.9 (21-CH₃); 22.1 (23-CH₃); 22.5 (6-CH₂); 28.4 (9-CH₂); 28.5 (4-CH₂); 29.5 (24-CH₃); 30.6 (5-CH₂); 32.9 (18-C); 34.8 (13-CH₂); 35.9 (14-CH₂); 39.7 (10-CH₂); 71.5 (19-CH₂); 77.2 (17-CH); 99.1 (22-C); 135.7 (2-C); 142.4 (3-CH); 170.0 (12-CO); 171.1 (16-CO); 193.7 (1-CO). **ES-MS:** *m/z* (%): 465.5 [M]Na⁺ (3%), 443.3 [M]H⁺ (100%). **IR (ν = cm⁻¹):** 3296 (N-H), 2937 (C-H), 2872 (C-H), 1647 (C=O). **HR-MS:** *m/z* (%): calculated 465.2399, found 465.2396.[192]

2*E*-6*RS*-6-Methylhept-2-enoyl pantetheine dimethyl ketal (145n).[129]
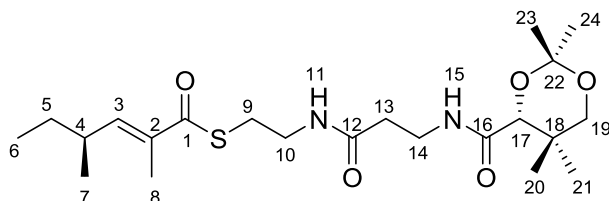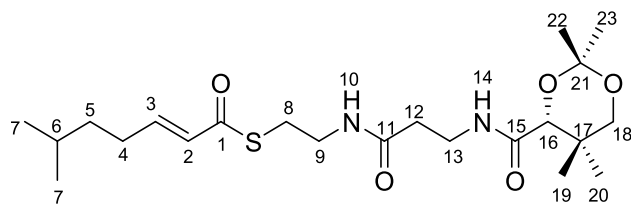

The obtained product was a colourless oil (0.22 g, 0.52 mmol, 52%). R_f: 0.53 (ethyl acetate). **¹H-NMR** (CDCl₃, 400 MHz): δ 0.92 (d, *J* = 6.7, 6H, 7-CH₃); 0.97 (s, 3H, 19-CH₃); 1.04 (s, 3H, 20-CH₃); 1.32-1.38 (m, 3H, 5-6-CH₂); 1.42 (s, 3H, 22-CH₃); 1.46 (s, 3H, 23-CH₃); 2.22 (dq, *J* = 1.9, 7.1, 2H, 4-CH₂); 2.42 (t, *J* = 6.1, 2H, 12-CH₂); 3.08 (t, *J* = 6.4, 2H, 8-CH₂); 3.28 (d, *J* = 11.7, 1H, 18a-C*H*H); 3.40-3.62 (m, 4H, 9-13-CH₂); 3.68 (d, *J* = 11.6, 1H, 18b-CH*H*); 4.07 (s, 1H, 16-CH); 6.10 (bt, *J* = 1.6, 1H, 10-NH); 6.14 (t, *J* = 1.5, 1H, 2-CH); 6.93 (dt, *J* = 7.1, 15.6, 1H, 3-CH); 7.02 (bt, *J* = 6.0, 1H, 14-NH). **¹³C-NMR** (CDCl₃, 100 MHz): δ 18.7 (19-CH₃); 18.9 (20-CH₃); 22.1 (22-CH₃); 22.4 (7-2xCH₃); 27.6 (6-CH); 28.2 (8-CH₂); 29.5 (23-CH₃); 30.1 (4-CH₂); 32.9 (17-C); 34.8 (12-CH₂); 35.9 (13-CH₂); 36.9 (5-CH₂); 39.7 (9-CH₂); 71.5 (18-CH₂); 77.2 (16-CH); 99.1 (21-C); 128.2 (2-CH); 147.1 (3-CH); 170.1 (11-CO); 171.4 (15-CO); 190.2 (1-CO). **ES-MS:** *m/z* (%): 465.3 [M]Na⁺ (28%), 443.3 [M]H⁺ (12%), 385 [M-C₃H₆O]H⁺(100%). **IR (ν = cm⁻¹):** 3303 (N-H), 2953 (C-H), 2870 (C-H), 1655 (C=O). **HR-MS:** *m/z* (%): calculated 465.2399, found 465.2396.[192]

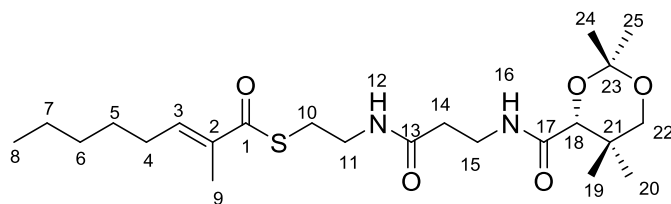## 2*E*-2-Methyloct-2-enoyl pantetheine dimethyl ketal (145o).[129]

The obtained product was a colourless oil (0.27 g, 0.60 mmol, 60%). R_f: 0.47 (ethyl acetate). **^{1}H-NMR** (CDCl$_3$, 400 MHz): δ 0.90 (t, J = 7.4, 3H, 8-CH$_3$); 0.97 (s, 3H, 19-CH$_3$); 1.04 (s, 3H, 20-CH$_3$); 1.31-1.51 (m, 6H, 5-6-7-CH$_2$); 1.41 (s, 3H, 24-CH$_3$); 1.46 (s, 3H, 25-CH$_3$); 1.87 (s, 3H, 9-CH$_3$); 2.21 (g, J = 7.3, 2H, 4-CH$_2$); 2.42 (t, J = 5.8, 2H, 14-CH$_2$); 3.05 (t, J = 6.7, 2H, 10-CH$_2$); 3.27 (d, J = 11.8, 1H, 22a-C*H*H); 3.39-3.62 (m, 4H, 11-15-CH$_2$); 3.68 (d, J = 12.2, 1H, 22b-CH*H*); 4.07 (s, 1H, 18-CH); 6.08 (bt, J = 5.8, 1H, 12-NH); 6.92 (dt, J = 1.5, 7.4, 1H, 3-CH); 7.03 (bt, J = 5.8, 1H, 16-NH). **^{13}C-NMR** (CDCl$_3$, 100 MHz): δ 12.5 (8-CH$_3$); 13.9 (9-CH$_3$); 18.7 (19-CH$_3$); 18.9 (20-CH$_3$); 22.1 (24-CH$_3$); 22.5 (7-CH$_2$); 28.2 (10-CH$_2$); 28.4 (5-CH$_2$); 28.8 (4-CH$_2$); 29.5 (25-CH$_3$); 31.6 (6-CH$_2$); 32.9 (21-C); 34.8 (14-CH$_2$); 35.9 (15-CH$_2$); 39.7 (11-CH$_2$); 71.5 (22-CH$_2$); 77.2 (18-CH); 99.1 (23-C); 135.7 (2-C); 142.4 (3-CH); 170.0 (13-CO); 171.1 (17-CO); 193.7 (1-CO). **ES-MS:** m/z (%): 457.7 [M]H$^+$ (100%). **IR (ν = cm^{-1}):** 3306 (N-H), 2929 (C-H), 2860 (C-H), 1652 (C=O). **HR-MS:** m/z (%): calculated 479.2556, found 479.2552.[192]

2*EZ*-2-Ethyloct-2-enoyl pantetheine dimethyl ketal (145p).[129]
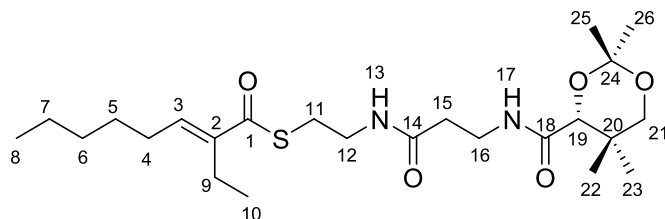
The obtained product was a yellow oil (1.3 g, 2.7 mmol, 45%). R_f: 0.55 (ethyl acetate). **^{1}H-NMR** (CDCl$_3$, 400 MHz): δ 0.86-1.10 (m, 12H, 8-10-22-23-CH$_3$); 1.29-1.53 (m, 6H, 5-6-7-CH$_2$); 1.44 (s, 3H, 25-CH$_3$); 1.48 (s, 3H, 26-CH$_3$); 2.20 (m, 2H, 4-CH$_2$); 2.31-2.38 (m, 2H, 9-CH$_{2E}$); 2.40-2.44 (m, 2H, 9-CH$_{2Z}$); 3.03-3.11 (m, 2H, 11-CH$_2$); 3.30 (d, J = 11.8, 1H, 21a-C*H*H); 3.41-3.64 (m, 4H, 12-16-CH$_2$); 3.70 (d, J = 11.7, 1H, 21b-CH*H*); 4.10 (s, 1H, 19-CH); 5.62 (t, J = 7.4, 1H, 3-CH$_Z$); 6.12 (bt, J = 6.2, 1H, 13-NH); 6.73 (t, J = 7.5, 1H, 3-CH$_E$); 7.06 (bt, J = 6.8, 1H, 17-NH). **^{13}C-NMR** (CDCl$_3$, 100 MHz): δ 12.5 (8-CH$_3$); 13.9 (10-CH$_3$); 18.7 (22-CH$_3$); 18.9 (23-CH$_3$); 21.8 (25-CH$_2$); 22.1 (7-CH$_2$); 28.2 (11-CH$_2$); 28.4 (5-CH$_2$); 28.8 (4-CH$_2$); 29.5 (26-CH$_3$); 30.9 (6-CH$_2$); 32.9 (20-C); 34.8 (15-CH$_2$); 35.9 (16-CH$_2$); 39.7 (12-CH$_2$); 71.5 (19-CH$_2$); 77.2 (21-CH); 99.1 (24-C); 136.3 (2-C); 142.1 (3-CH); 170.1 (14-CO); 171.2 (18-CO); 193.6 (1-CO). **ES-MS:** m/z (%): 493.4 [M]Na$^+$ (12%), 471.7 [M]H$^+$ (56%), 413.4 [M-C$_4$H$_8$]H$^+$ (100%). **IR (ν = cm^{-1}):** 3307 (N-H), 2958 (C-H), 2872 (C-H), 1653 (C=O). **HR-MS:** m/z (%): calculated 493.2712, found 493.2707.[192]

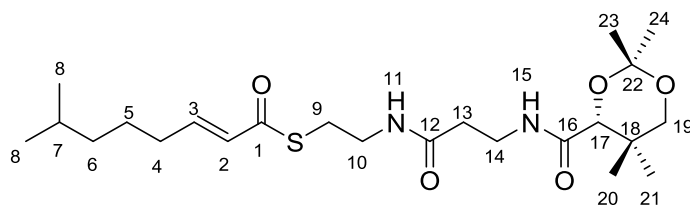**2*E*-7-Methyloct-2-enoyl pantetheine dimethyl ketal (145q).**[129]

The obtained product was a colourless oil (0.18 g, 0.40 mmol, 40%). R_f: 0.43 (ethyl acetate). **¹H-NMR** (CDCl₃, 400 MHz): δ 0.89 (d, *J* = 6.7, 6H, 8-CH₃); 0.97 (s, 3H, 20-CH₃); 1.04 (s, 3H, 21-CH₃); 1.42 (s, 3H, 23-CH₃); 1.46 (s, 3H, 24-CH₃); 1.43-1.62 (m, 5H, 7-CH-5-6-CH₂); 2.22 (dt, *J* = 1.7, 7.3, 2H, 4-CH₂); 2.42 (t, *J* = 6.3, 2H, 13-CH₂); 3.08 (t, *J* = 6.3, 2H, 9-CH₂); 3.28 (d, *J* = 11.7, 1H, 19a-C*H*H); 3.42-3.64 (m, 4H, 10-14-CH₂); 3.68 (d, *J* = 11.6, 1H, 19b-CH*H*); 4.08 (s, 1H, 17-CH); 6.10 (bt, *J* = 1.6, 1H, 11-NH); 6.17 (t, *J* = 15, 1H, 2-CH); 6.93 (dt, *J* = 6.9, 15.4, 1H, 3-CH); 7.02 (bt, *J* = 6.2, 1H, 15-NH). **¹³C-NMR** (CDCl₃, 100 MHz): δ 18.7 (20-CH₃); 18.9 (21-CH₃); 22.1 (23-CH₃); 22.4 (8-2xCH₃); 25.8 (6-CH₂); 27.8 (7-CH); 28.2 (9-CH₂); 28.4 (5-CH₂); 29.5 (24-CH₃); 32.5 (4-CH₂); 32.9 (18-C); 34.8 (13-CH₂); 35.9 (14-CH₂); 39.7 (10-CH₂); 71.5 (19-CH₂); 77.2 (17-CH); 99.1 (22-C); 128.4 (2-CH); 147.1 (3-CH); 170.1 (12-CO); 171.4 (16-CO); 190.2 (1-CO). **ES-MS:** *m/z* (%): 479.3 [M]Na⁺ (5%), 457.4 [M]H⁺ (18%), 399.4 [M-C₃H₆O]H⁺(100%). **IR (ν = cm⁻¹):** 3307 (N-H), 2952 (C-H), 2869 (C-H), 1655 (C=O). **HR-MS:** *m/z* (%): calculated 479.2556, found 479.2557.[192]

6*RS*,4*RS*-2*E*-4,6-Dimethyloct-2-enoyl-pantetheine dimethyl ketal (145r).[129]

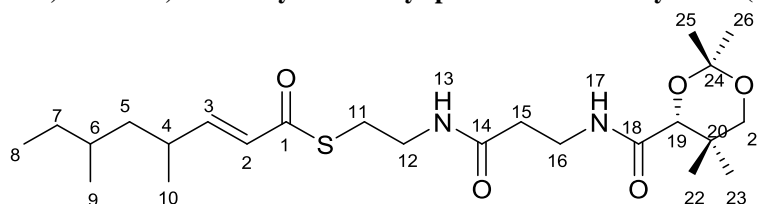The obtained product was a colourless oil (0.32 g, 0.65 mmol, 65%). R_f: 0.46 (ethyl acetate). **¹H-NMR** (CDCl₃, 400 MHz): δ 0.83 (m, 6H, 8-9-CH₃); 0.97 (s, 3H, 22-CH₃); 1.04 (s, 3H, 23-CH₃); 1.14 (m, 3H, 10-CH₃), 1.24-1.49 (m, 5H, 5-6-7-CH₂); 1.42 (s, 3H, 25-CH₃); 1.46 (s, 3H, 26-CH₃); 1.87 (s, 3H, 10-CH₃); 2.42 (t, *J* = 6.1, 2H, 15-CH₂); 2.54-2.62 (m, 1H, 4-CH); 3.05 (t, *J* = 6.5, 2H, 11-CH₂); 3.27 (d, *J* = 11.7, 1H, 21a-C*H*H); 3.38-3.62 (m, 4H, 12-16-CH₂); 3.68 (d, *J* = 12.1, 1H, 21b-CH*H*); 4.07 (s, 1H, 19-CH); 6.05 (m, 1H, 2-CH); 6.12 (bt, *J* = 5.4, 1H, 13-NH); 6.74-6.88 (m, 1H, 3-CH); 7.03 (bt, *J* = 5.8, 1H, 17-NH). **¹³C-NMR** (CDCl₃, 100 MHz): δ 11.1 (8-CH₃); 17.6 (9-CH₃); 18.7 (22-CH₃); 18.9 (23-CH₃); 21.9 (10-CH₃); 22.1 (25-CH₃); 28.2 (11-CH₂); 29.5 (26-CH₃); 29.6 (7-CH₂); 32.1 (6-CH); 32.9 (20-C); 34.7 (15-CH₂) 35.9 (16-CH₂); 39.7 (12-CH₂); 40.8 (4-CH), 46-5 (5-CH₂) 71.5 (21-CH₂); 77.2 (19-CH); 99.1 (24-C); 126.9 (2-CH); 147.6 (3-CH); 170.1 (14-CO); 171.1 (18-CO); 204.1 (1-CO). **ES-MS:** *m/z* (%): 471 [M]H⁺ (100%) **IR (ν = cm⁻¹):** 2958 (C-H), 2927 (C-H), 2872 (C-H), 1654 (C=O), 1629 (C=O). **HR-MS:** *m/z* (%): calculated 471.2893, found 471.2891.[192]

2*E*-4*S*,6*S*-Dimethyloct-2-enoyl-pantetheine dimethyl ketal (145s).[129]
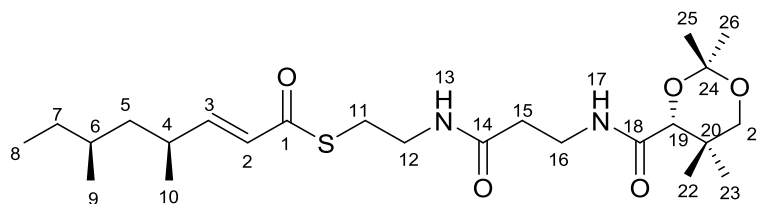
The obtained product was a colourless oil (0.34 g, 0.70 mmol, 70%). R_f: 0.46 (ethyl acetate). **¹H-NMR** (CDCl₃, 400 MHz): δ 0.87 (m, 6H, 8-9-CH₃); 0.97 (s, 3H, 22-CH₃); 1.04 (s, 3H, 23-CH₃); 1.13-1.19 (m, 2H, 7-CH₃), 1.26-1.49 (m, 3H, 5-6-CH₂); 1.44 (s, 3H, 25-CH₃); 1.48 (s, 3H, 26-CH₃); 2.34 (m, 1H, 4-CH); 2.45 (t, J = 5.9, 1H, 14-CH); 3.10 (t, J = 6.5, 2H, 11-CH₂); 3.27 (d, J = 11.7, 1H, 21a-C*H*H); 3.42-3.62 (m, 4H, 12-16-CH₂); 3.70 (d, J = 11.6, 1H, 21b-CH*H*); 4.09 (s, 1H, 19-CH); 6.12 (dd, J = 1.0, 16.0, 1H, 2-CH); 6.28 (bt, J = 6.3, 1H, 13-NH); 6.80 (dd, J = 8.2, 15.8, 1H, 3-CH); 7.06 (bt, J = 5.8, 1H, 17-NH). **¹³C-NMR** (CDCl₃, 100 MHz): δ 11.1 (8-CH₃); 14.2 (9-CH₃); 18.7 (22-CH₃); 18.9 (23-CH₃); 22.1 (25-CH₃); 28.2 (11-CH₂); 29.5 (26-CH₃); 29.7 (7-CH₂); 32.9 (6-CH); 32.9 (18-C); 34.4 (4-CH); 34.7 (15-CH₂) 35.9 (16-CH₂); 39.7 (12-CH₂); 43-5 (5-CH) 71.5 (21-CH₂); 77.2 (19-CH); 99.1 (24-C); 126.6 (2-CH); 152.1 (3-CH); 170.1 (14-CO); 171.1 (18-CO); 190.1 (1-CO). **ES-MS:** *m/z* (%): 471 [M]H⁺ (100%), 413 [M-C₃H₆O₂]H⁺ (12%). **IR (ν = cm⁻¹):** 2958 (C-H), 2927 (C-H), 2872 (C-H), 1654 (C=O), 1629 (C=O). **HR-MS:** *m/z* (%): calculated 493.2712 found 493.2619.[192]

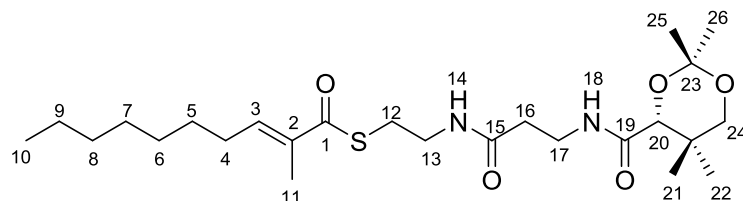**2*E*-2-Methyldec-2-enoyl pantetheine dimethyl ketal (145t).**[129]

The obtained product was a colourless oil (0.28 g, 0.58 mmol, 58%). R_f: 0.45 (ethyl acetate). **¹H-NMR** (CDCl₃, 400 MHz): δ 0.88 (t, J = 7.6, 3H, 10-CH₃); 0.97 (s, 3H, 21-CH₃); 1.04 (s, 3H, 22-CH₃); 1.30-1.47 (m, 10H, 5-6-7-8-9-CH₂); 1.41 (s, 3H, 25-CH₃); 1.46 (s, 3H, 26-CH₃); 1.87 (s, 3H, 11-CH₃); 2.21 (q, J = 7.1, 2H, 4-CH₂); 2.42 (t, J = 6.2, 2H, 16-CH₂); 3.05 (t, J = 6.2, 2H, 12-CH₂); 3.27 (d, J = 12.2, 1H, 24a-C*H*H); 3.39-3.62 (m, 4H, 13-17-CH₂); 3.68 (d, J = 12.2, 1H, 24b-CH*H*); 4.07 (s, 1H, 20-CH); 6.08 (bt, J = 5.0, 1H, 14-NH); 6.77 (dt, J = 1.9, 6.9, 1H, 8-CH); 7.03 (bt, J = 5.5, 1H, 18-NH). **¹³C-NMR** (CDCl₃, 100 MHz): δ 12.5 (11-CH₃); 14.0 (10-CH₃); 18.7 (21-CH₃); 18.9 (22-CH₃); 22.1 (25-CH₃); 22.6 (9-CH₂); 28.4 (5-CH₂); 28.5 (12-CH₂); 28.8 (6-CH₂); 29.1 (7-CH₂); 29.5 (26-CH₃); 31.8 (8-CH₂); 32.9 (C); 33.2 (4-CH₂); 34.8 (16-CH₂); 35.9 (17-CH₂); 39.7 (13-CH₂); 71.5 (24-CH₂); 77.2 (20-CH); 99.1 (23-C); 135.7 (2-C); 142.4 (3-CH); 170.0 (15-CO); 171.2 (19-CO); 193.7 (11-CO). **ES-MS:** *m/z* (%): 485.7 [M]H⁺ (100%). **IR (ν = cm⁻¹):** 3307 (N-H), 2926 (C-H), 2856 (C-H), 1652 (C=O). **HR-MS:** *m/z* (%): calculated 507.2869, found 507.2870.[192]

3-Oxobutanoyl pantetheine dimethyl ketal (145u).[129]
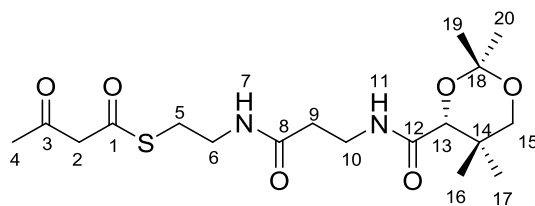
Acetyl meldrums acid (1.60 g, 5.4 mmol) stirred in toluene with pantetheine dimethyl ketal (1.7 g, 5.3 mmol) under nitrogen at 90 °C. After 6 hours the reaction was stopped and the mixture concentrated *in vacuo*. The mixture was purified by flash column chromatography (ethyl acetate) and then concentrated to a colourless oil (1.1 g, 2.7 mmol, 50%). R_f: 0.40 (ethyl acetate). **^{1}H-NMR** (CDCl$_3$, 400 MHz): δ 0.96 (s, 3H, 16-CH$_3$); 1.03 (s, 3H, 17-CH$_3$); 1.41 (s, 3H, 19-CH$_3$); 1.45 (s, 1H, 20-CH$_2$); 1.94 (s, 1H, 4-CH$_3$); 2.26 (s, 2H, 4-CH$_3$); 2.43 (t, *J* = 5.7, 2H, 9-CH$_2$); 2.99 (t, *J* = 6.5, 2H, 5-CH$_2$); 3.27 (d, *J* = 11.2, 1H, 15a-C*H*H); 3.40-3.50 (m, 6H, 6-10-CH$_2$); 3.68 (d, *J* = 11.7, 1H, 15b-CH*H*); 3.70 (s, 2H, 3-CH$_2$); 4.07 (s, 1H, 13-CH); 6.32 (bt, *J* = 5.7, 1H, 7-NH); 7.03 (bt, *J* = 5.9, 1H, 11-NH). **^{13}C-NMR** (CDCl$_3$, 100 MHz): δ 18.7 (16-CH$_3$); 18.9 (17-CH$_3$); 22.4 (19-CH$_3$); 27.8 (5-CH$_2$); 29.5 (20-CH$_3$); 30.1 (4-CH$_3$); 32.9 (14-C); 34.8 (9-CH$_2$); 35.9 (10-CH$_2$); 39.7 (6-CH$_2$); 58.1 (2-CH$_2$); 71.5 (13-CH$_2$); 77.7 (15-CH); 99.1 (18-C); 170.1 (8-CO); 171.4 (12-CO); 192.1 (1-CO); 199.8 (3-CO). **IR (ν = cm⁻¹):** 2989 (C-H), 2872 (C-H), 1720 (C=O), 1654 (C=O). **ES-MS:** *m/z* (%): 425 [M+Na]H⁺ (35%), 403 [M]H⁺ (100%). **HR-MS:** *m/z* (%): calculated 425.1722, found 425.1722.[192]

3-Oxohexanoyl pantetheine dimethyl ketal (145v).[129]
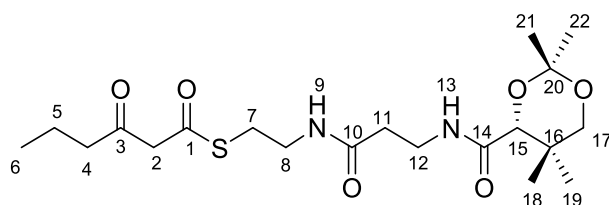
Butyryl meldrums acid (1.6 g, 7.4 mmol) stirred in toluene with pantetheine dimethyl ketal (2.4 g, 7.8 mmol) under nitrogen at 90 °C. After 6 hours the reaction was stopped and the mixture concentrated *in vacuo*. The mixture was purified by flash column chromatography (ethyl acetate) and then concentrated to a colourless oil (1.1 g, 2.4 mmol, 32%). **^{1}H-NMR** (CDCl$_3$, 400 MHz): δ 0.93 (t, *J* = 6.7, 3H, 6-CH$_3$); 1.02 (s, 3H, 18-CH$_3$); 1.08 (s, 3H, 19-CH$_3$); 1.25 (m, 2H, 5-CH$_2$); 1.41 (s, 3H, 21-CH$_3$); 1.45 (s, 3H, 22-CH$_2$); 2.43 (t, *J* = 5.7, 2H, 11-CH$_2$); 3.05-3.16 (m, 2H, 7-CH$_2$); 3.27 (d, *J* = 11.2, 1H, 17a-C*H*H); 3.37-3.59 (m, 6H, 4-9-12-CH$_2$); 3.68 (d, *J* = 11.7, 1H, 17b-CH*H*); 3.73 (s, 2H, 2-CH$_2$); 4.11 (s, 1H, 15-CH); 6.38 (bt, *J* = 5.7, 1H, 9-NH); 7.33 (bt, *J* = 5.9, 1H, 13-NH). **^{13}C-NMR** (CDCl$_3$, 100 MHz): δ 13.5 (6-CH$_3$), 18.8 (5-CH$_2$), 20.4 (18-CH$_3$); 21.7 (19-CH$_3$); 22.1 (21-CH$_3$); 29.0 (22-CH$_3$); 30.6 (7-CH$_2$); 32.6 (16-C); 35.1 (12-CH$_2$); 35.6 (11-CH$_2$); 39.3 (8-CH$_2$); 40.9 (4-CH$_2$); 57.9 (2-CH$_2$); 70.9 (17-CH$_2$); 77.7 (15-CH); 99.9 (20-C); 171.9 (10-CO); 174.3 (14-CO); 192.5 (1-CO); 200.4 (3-CO). **ES-MS:** *m/z* (%): 453 [M+Na]H⁺ (35%), 431 [M]H⁺ (100%). **IR (ν = cm⁻¹):** 2958 (C-H), 2873 (C-H), 1720 (C=O), 1654 (C=O). **HR-MS:** *m/z* (%): calculated 453.2035, found 453.2035.[192]

6.2.6 Synthesis of Pantetheine Substrates.

Acyl pantetheine dimethyl ketal (0.1 g, 0.4 mmol) stirred in a mixture of acetonitrile and water (1:1) and 10% TFA for 20 minutes. The reaction was followed by TLC and LCMS. After that the solvents were liphophilized. 0.03 g of the product were purified by HPLC (acetonitrile).

Acetylpantetheine (249).
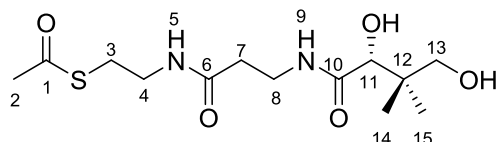
0.03 g of the product were purified by HPLC (acetonitrile). **^{1}H-NMR** (CDCl$_3$, 400 MHz): δ 0.93 (s, 3H, 14-CH$_3$); 1.04 (s, 3H, 15-CH$_3$); 2.37 (s, 3H, 2-CH$_3$); 2.40-2.44 (m, 2H, 7-CH$_2$); 3.02-3.11 (m, 2H, 3-CH$_2$); 3.38-3.41 (m, 2H, 8-CH$_2$); 3.48-3.60 (m, 4H, 4-13-CH$_2$); 3.99 (s, 1H, 11-CH); 6.02 (bt, J = 5.5, 1H, 5-NH); 7.40 (bt, J = 6.1, 1H, 9-NH). **^{13}C-NMR** (CDCl$_3$, 100 MHz): δ 20.4 (14-CH$_3$); 21.5 (15-CH$_3$); 28.2 (3-CH$_2$); 30.7 (2-CH$_3$); 35.2 (7-CH$_2$); 35.6 (8-CH$_2$); 39.4 (12-C); 39.8 (4-CH$_2$); 70.9 (13-CH$_2$); 77.9 (11-CH); 171.5 (6-CO); 173.2 (10-CO); 197.1 (1-COS). **ES-MS:** m/z (%): 343.3 [M]Na$^+$ (4%), 321.4 [M]H$^+$ (22%), 269.4 [M-C$_3$H$_6$O]$^+$ (100%). **HR-MS:** m/z (%): calculated 321.1484, found 321.1485.

Tigloylpantetheine (85).[129]
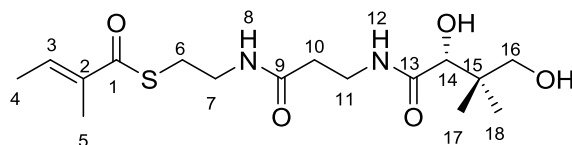
The obtained product was a colourless oil (0.14 g, 0.40 mmol, 50%). **^{1}H-NMR** (CDCl$_3$, 400 MHz): δ 0.92 (s, 3H, 17-CH$_3$); 0.92 (s, 3H, 18-CH$_3$); 1.82-1.87 (m, 6H, 4-5-CH$_3$); 2.41 (t, J = 5.9, 2H, 10-CH$_2$); 3.01-3.10 (m, 2H, 6-CH$_2$); 3.32-3.60 (m, 6H, 7-11-16-CH$_2$); 3.99 (s, 1H, 14-CH); 6.33 (bt, J = 5.8, 1H, 8-NH); 6.86 (qq, J = 1.3, 6.8, 1H, 3-CH); 7.40 (bt, J = 5.6, 1H, 12-NH). **^{13}C-NMR** (CDCl$_3$, 100 MHz): δ 12.2 (5-CH$_3$); 14.5 (4-CH$_3$), 20.4 (17-CH$_3$); 21.5 (18-CH$_3$); 28.2 (6-CH$_2$); 35.2 (11-CH$_2$); 35.6 (10-CH$_2$); 39.3 (15-C); 39.9 (7-CH$_2$); 70.9 (16-CH$_2$); 77.9 (14-CH); 136.8 (3-C); 137.3 (2-CH); 171.8 (9-CO); 173.5 (13-CO); 194.1 (1-COS). **ES-MS:** m/z (%): 383 [M]Na$^+$ (8%), 361 [M]H$^+$ (100%), 343 [M-H$_2$O]H$^+$ (2%), 231 [M -C$_6$H$_{11}$O$_3$]H$^+$ (5%). **HR-MS:** m/z (%): calculated 383.1617, found 383.1621.

Crotonyl-pantetheine (87).[129]
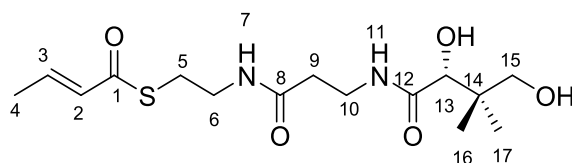
The obtained product was a colourless oil (0.18 g, 0.50 mmol, 34%) **^{1}H-NMR** (CDCl$_3$, 400 MHz): δ 0.92 (s, 3H, 16-CH$_3$); 1.03 (s, 3H, 17-CH$_3$); 1.90 (dd, J = 1.3, 6.8, 3H, 4-CH$_3$); 2.41 (t, J = 5.9, 2H, 9-CH$_2$); 3.02-3.16 (m, 2H, 5-CH$_2$); 3.36-3.60 (m, 6H, 6-10-15-CH$_2$); 3.99 (s, 1H, 13-CH); 6.13 (dd, J = 5.8, 1H, 2-CH); 6.23 (bt, J = 5.8, 1H, 7-NH); 6.95 (dq, J = 1.3, 6.8, 1H, 3-CH); 7.36 (bt, J = 5.6, 1H, 11-NH).

^{13}C-NMR (CDCl$_3$, 100 MHz): δ 18.1 (4-CH$_3$), 20.4 (16-CH$_3$); 21.7 (17-CH$_3$); 28.1 (5-CH$_2$); 35.2 (8-CH$_2$); 35.6 (9-CH$_2$); 39.3 (14-C); 39.9 (6-CH$_2$); 70.9 (15-CH$_2$); 77.9 (13-CH); 129.7 (2-CH); 142.3 (3-CH); 171.8 (8-CO); 173.5 (12-CO); 190.5 (1-COS). **ES-MS:** m/z (%): 716 [M$_2$]Na$^+$ (5%), 693 [M$_2$]H$^+$ (48%), 369 [M]Na$^+$ (2%), 347 [M]H$^+$ (100%), 329 [M-H$_2$O]H$^+$ (2%). **HR-MS:** m/z (%): calculated 369.1460, found 369.1461. **IR (ν = cm^{-1}):** 3308 (O-H), 2932 (C-H), 1645 (C=C), 1530 (-N-H).

2-Methylbutyrylpantetheine (148).[129]
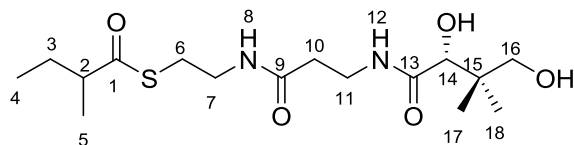
The obtained product was a colourless oil (0.035 g, 0.10 mmol, 36%) **^{1}H-NMR** (CDCl$_3$, 400 MHz): δ 0.90 (t, J = 7.6, 3H, 4-CH$_3$); 0.92 (s, 3H, 17-CH$_3$); 1.01 (s, 3H, 18-CH$_3$); 1.15 (d, J = 7.5, 3H, 5-CH$_3$); 1.36-1.78 (m, 2H, 3-CH$_2$); 2.40 (t, J = 6.1, 2H, 10-CH$_2$); 2.53-2.63 (m, 1H, 2-CH); 2.96-3.05 (m, 2H, 6-CH$_2$); 3.37-3.60 (m, 6H, 7-11-16-CH$_2$); 3.99 (s, 1H, 14-CH$_2$); 6.32 (t, J = 5.4, 1H, 8-NH); 7.44 (bt, J = 5.9, 1H, 12-NH). **^{13}C-NMR** (CDCl$_3$, 100 MHz): δ 11.5 (4-CH$_3$), 17.1 (5-CH$_3$), 20.4 (17-CH$_3$); 21.5 (18-CH$_3$); 27.1 (3-CH$_2$); 27.4 27.9 (6-CH$_2$); 35.1 (10-CH$_2$); 35.6 (11-CH$_2$); 39.3 (15-C); 39.7 (7-CH$_2$); 50.2 (2-CH$_2$); 70.8 (16-CH$_2$); 172.5 (9-CO); 174.5 (13-CO); 205.1 (1-COS). **ES-MS:** m/z (%): 385 [M]Na$^+$ (3%), 363 [M]H$^+$ (100%), 345 [M-H$_2$O]H$^+$ (3%), 233 [M-C$_6$H$_{11}$O$_3$]H$^+$ (8%), 100 [C$_5$H$_{11}$O$_2$] (35%). **HR-MS:** m/z (%): calculated 361.1797, found 361.1796.

Angeloylpantetheine (86).[129]
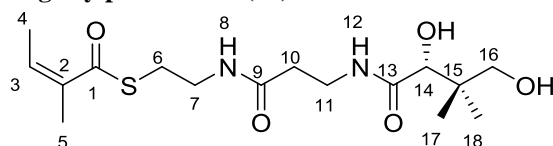

0.03 g of the product were purified by HPLC (acetonitrile). **^{1}H-NMR** (CDCl$_3$, 400 MHz): δ 0.92 (s, 3H, 17-CH$_3$); 1.01 (s, 3H, 18-CH$_3$); 1.83-1.90 (m, 6H, 4-5-CH$_3$); 2.40-2.44 (m, 2H, 10-CH$_2$); 2.99-3.14 (m, 2H, 6-CH$_2$); 3.34-3.59 (m, 6H, 7-11-16-CH$_2$); 3.99 (s, 1H, 14-CH); 5.90 (dq, J = 1.2, 7.3, 1H, 3-CH); 6.35 (bt, J = 5.5, 1H, 8-NH); 7.40 (bt, J = 6.1, 1H, 12-NH). **^{13}C-NMR** (CDCl$_3$, 100 MHz): δ 15.9 (5-CH$_3$), 20.4 (17-CH$_3$); 20.6 (4-CH$_3$); 21.5 (18-CH$_3$); 28.2 (6-CH$_2$); 35.2 (10-CH$_2$); 35.6 (11-CH$_2$); 39.4 (15-C); 39.8 (7-CH$_2$); 70.9 (16-CH$_2$); 77.9 (14-CH); 134.0 (2-C); 135.3 (3-CH); 171.8 (9-CO); 173.5 (13-CO); 194.1 (1-COS). **ES-MS:** m/z (%): 383 [M]Na$^+$ (8%), 361 [M]H$^+$ (58%), 343 [M-H$_2$O]H$^+$ (88%), 231 [M -C$_6$H$_{11}$O$_3$]H$^+$ (100%). **HR-MS:** m/z (%): calculated 383.1617, found 383.1618.

2*RS*-2-Methylhexanoylpantetheine (265).[129]
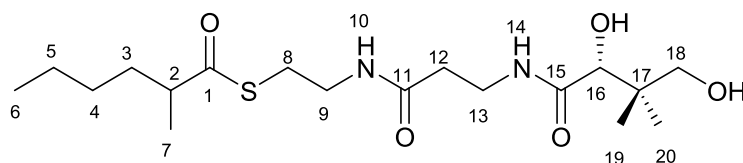
0.13 g of the product were purified by HPLC (acetonitrile). **^{1}H-NMR** (CDCl$_3$, 400 MHz): δ 0.88 (t, J = 7.4, 3H, 6-CH$_3$); 0.93 (s, 3H, 19-CH$_3$); 1.02 (s, 3H, 20-CH$_3$); 1.16 (d, J = 7.6, 3H, 7-CH$_3$); 1.23-1.31 (m,

4H, 4-5-CH$_2$); 1.42 (m, 1H, 3-CH$_2$); 1.64 (m, 1H, 3-CH$_2$); 2.41 (t, J = 5.9, 2H, 12-CH$_2$); 2.65 (q, J = 6.2, 1H, 2-CH); 2.96-3.09 (m, 2H, 8-CH$_2$); 3.33-3.59 (m, 6H, 9-13-18-CH$_2$); 4.00 (s, 1H, 16-CH); 6.20 (bt, J = 5.7, 1H, 10-NH); 7.37 (bt, J = 5.9, 1H, 14-NH). **^{13}C-NMR** (CDCl$_3$, 100 MHz): δ 13.9 (6-CH$_3$), 17.6 (7-CH$_3$), 20.4 (19-CH$_3$); 21.7 (20-CH$_3$); 22.6 (5-CH$_2$); 28.3 (8-CH$_2$); 29.3 (4-CH$_2$); 33.8 (3-CH$_2$); 35.1 (12-CH$_2$); 35.5 (13-CH$_2$); 39.4 (17-C); 39.8 (9-CH$_2$); 48.8 (2-CH); 70.9 (18-CH$_2$); 77.7 (16-CH); 171.6 (11-CO); 173.4 (15-CO); 204.8 (1-COS). **ES-MS:** m/z (%): 389 [M]H$^-$ (38%), 371 [M-H$_2$O]H$^+$ (100%). **HR-MS:** m/z (%): calculated 413.2092, found 413.2093.

2*E*-Hex-2-enoylpantetheine (90).[129]
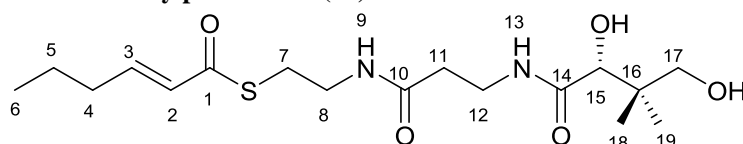
0.003 g of the product were purified by HPLC (acetonitrile). **^{1}H-NMR** (CDCl$_3$, 400 MHz): δ 0.93 (s, 3H, 6-CH$_3$); 0.95 (t, J = 7.8, 3H, 18-CH$_3$); 1.04 (s, 3H, 19-CH$_2$); 1.46-1.56 (m, 2H, 5-CH$_2$); 2.20 (dq, J = 1.3, J = 6.7, 2H, 4-CH$_2$); 2.41 (t, J = 6.1, 2H, 11-CH$_2$); 3.03-3.18 (m, 2H, 7-CH$_2$); 3.36-3.65 (m, 6H, 8-12-17-CH$_2$); 3.99 (s, 1H, 15-CH); 6.13 (m, 1H, 2-CH); 6.17 (dt, J = 1.8, J = 15.7, 1H, 9-NH); 6.93 (dt, J = 6, 7, J = 15.3, 1H, 3-CH); 7.32 (bt, J = 6.^{1}, 1H, 13-NH). **^{13}C-NMR** (CDCl$_3$, 100 MHz): δ 13.7 (6-CH$_3$), 20.4 (18-CH$_3$); 21.1 (19-CH$_3$); 21.7 (5-CH$_2$); 28.1 (7-CH$_2$); 34.3 (4-CH$_2$); 35.1 (11-CH$_2$); 35.5 (12-CH$_2$); 39.4 (16-C); 39.8 (8-CH$_2$); 70.9 (17-CH$_2$); 77.8 (15-CH); 128.3 (2-CH); 147.0 (3-CH); 171.6 (10-CO); 173.3 (14-CO); 190.6 (1-COS). **ES-MS:** m/z (%): 375 [M]H$^+$ (100%), 357 [M-H$_2$O]H$^+$ (32%). **HR-MS:** m/z (%): calculated 397.1773, found 397.1774.

2*E*-2-Methylhex-2-enoylpantethine (91).[129]
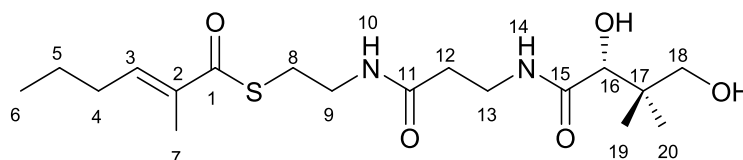
0.02 g of the product were purified by HPLC (acetonitrile). **^{1}H-NMR** (CDCl$_3$, 400 MHz): δ 0.93 (s, 3H, 1-CH$_3$); 0.95 (t, J = 7.4, 3H, 19-CH$_3$); 1.02 (s, 3H, 20-CH$_3$); 1.46-1.55 (m, 2H, 5-CH$_2$); 1.88 (d, J = 1.4, 7-CH$_3$) 2.20 (dq, J = 1.3, J = 7.0, 2H, 4-CH$_2$); 2.41 (t, J = 5.9, 2H, 12-CH$_2$); 3.00-3.13 (m, 2H, 8-CH$_2$); 3.35-3.59 (m, 6H, 9-13-18-CH$_2$); 3.99 (s, 1H, 16-CH); 6.23 (bt, J = 5.7, 1H, 10-NH); 6.77 (tq, J = 1, 4, J = 7.4, 1H, 3-CH); 7.38 (bt, J = 5.9, 1H, 14-NH). **^{13}C-NMR** (CDCl$_3$, 100 MHz): δ 12.5 (6-CH$_3$), 13.9 (7-CH$_3$), 20.4 (19-CH$_3$); 21.7 (20-CH$_3$); 21.8 (5-CH$_2$); 28.3 (8-CH$_2$); 30.8 (4-CH$_2$); 35.1 (12-CH$_2$); 35.5 (13-CH$_2$); 39.4 (17-C); 39.8 (9-CH$_2$); 70.9 (18-CH$_2$); 77.7 (16-CH); 135.7 (2-C); 142.5 (3-CH); 171.6 (11-CO); 173.4 (15-CO); 194.2 (1-COS). **ES-MS:** m/z (%): 411 [M+Na]H$^+$ (28%), 389 [M]H$^+$ (31%), 371 [M-H$_2$O]H$^+$ (88%), 259 [M-C$_6$H$_{11}$O$_3$]H$^+$ (100%). **HR-MS:** m/z (%): calculated 411.1930, found 411.1931.

2*EZ*-2-Ethylhex-2-enoylpantetheine (95).[129]
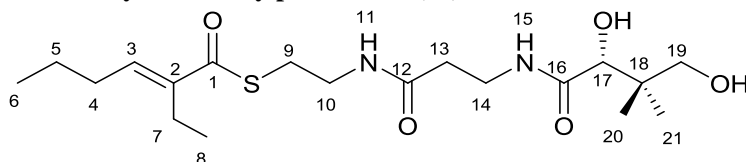
0.027 g of the product were purified by HPLC (acetonitrile). **^{1}H-NMR** (CDCl$_3$, 400 MHz): δ 0.85-0.99 (m, 12H, 6-8-20-21-CH$_3$); 1.38-1.53 (m, 2H, 5-CH$_2$); 2.16-2.35 (m, 4H, 4-7-CH$_2$); 2.41 (t, *J* = 6.4, 2H, 13-CH$_2$); 2.97-3.06 (m, 2H, 9-CH$_2$); 3.33-3.56 (m, 6H, 10-14-19-CH$_2$); 3.98 (s, 1H, 17-CH); 5.63 (t, *J* = 7.6, 1H, 3-CH$_Z$); 6.56 (bt, *J* = 5.7, 1H, 11-NH); 6.70 (t, *J* = 7.6, 1H, 3-CH$_E$); 7.46 (bt, *J* = 5.9, 1H, 15-NH). **^{13}C-NMR** (CDCl$_3$, 100 MHz): δ 13.4 (6-CH$_3$), 13.9 (8-CH$_3$), 20.4 (20-CH$_3$); 21.5 (21-CH$_3$); 22.0 (7-CH$_2$); 22.8 (5-CH$_2$); 28.2 (9-CH$_2$); 30.4 (4-CH$_2$); 35.1 (13-CH$_2$); 35.5 (14-CH$_2$); 39.4 (18-C); 39.8 (10-CH$_2$); 70.9 (19-CH$_2$); 77.7 (17-CH); 136.1 (2-C); 140.5 (2-C); 142.2 (3-CH$_E$); 171.6 (12-CO); 173.4 (16-CO); 193.9 (1-COS). **ES-MS:** *m/z* (%): 425 [M+Na]H$^+$ (78%), 403 [M]H$^+$ (13%), 385 [M-H$_2$O]H$^+$ (56%), 273 [M-C$_6$H$_{11}$O$_3$]H$^+$ (100%). **HR-MS:** *m/z* (%): calculated 425.2086, found 425.2086.

4*RS*-4-Methylhex-2-enoylpantetheine (92).[129]

0.02 g of the product were purified by HPLC (acetonitrile). **^{1}H-NMR** (CDCl$_3$, 400 MHz): δ 0.88 (t, *J* = 7.5, 3H, 6-CH$_3$); 0.98 (s, 3H, 19-CH$_3$); 1.01 (s, 3H, 20-CH$_3$); 1.05 (d, *J* = 6.9, 7-CH$_3$); 1.38-1.47 (m, 2H, 5-CH$_2$); 2.19-2.27 (m, 1H, 4-CH); 2.41 (t, *J* = 5.8, 2H, 12-CH$_2$); 2.94-3.15 (m, 2H, 8-CH$_2$); 3.33-3.58 (m, 6H, 9-13-18-CH$_2$); 4.00 (s, 1H, 16-CH); 6.08 (dd, *J* = 1.4, *J* = 15.4, 1H, 2-CH); 6.40 (bt, *J* = 5.4, 1H, 10-NH); 6.83 (dd, *J* = 7.4, *J* = 15.4, 1H, 3-CH); 7.40 (bt, *J* = 5.4, 1H, 14-NH). **^{13}C-NMR** (CDCl$_3$, 100 MHz): δ 11.6 (6-CH$_3$), 18.7 (7-CH$_3$), 20.4 (19-CH$_3$); 21.7 (20-CH$_3$); 28.2 (5-CH$_2$); 28.8 (8-CH$_2$); 35.1 (12-CH$_2$); 35.8 (13-CH$_2$); 38.2 (4-CH); 39.4 (16-C); 39.7 (9-CH$_2$); 70.8 (18-CH$_2$); 77.6 (16-CH); 126.7 (2-CH); 152.1 (3-CH); 171.7 (11-CO); 173.6 (15-CO); 190.8 (1-COS). **ES-MS:** *m/z* (%): 411 [M+Na]H$^+$ (8%), 389 [M]H$^+$ (65%), 371 [M-H$_2$O]H$^+$ (88%), 259 [M-C$_6$H$_{11}$O$_3$]H$^+$ (100%). **HR-MS:** *m/z* (%): calculated 411.1930, found 411.1930.

4*RS*-2-4-Dimethylhex-2-enoylpantetheine (94).[129]

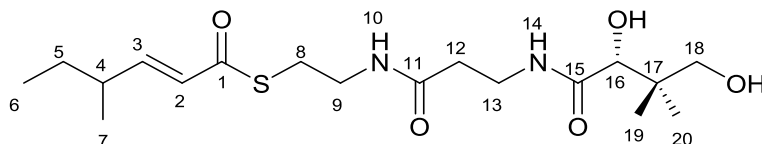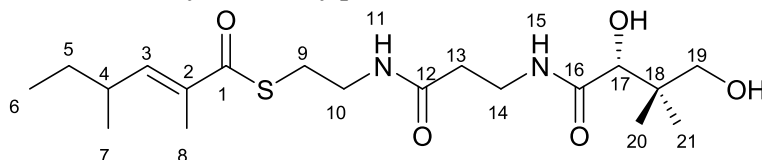0.01 g of the product were purified by HPLC (acetonitrile). **^{1}H-NMR** (CDCl$_3$, 400 MHz): δ 0.86 (t, *J* = 7.4, 3H, 6-CH$_3$); 0.92 (s, 3H, 20-CH$_3$); 1.03 (s, 3H, 21-CH$_3$); 1.03 (d, *J* = 2.3, 3H, 7-CH$_3$); 1.30-1.51 (m, 4H, 5-CH$_2$); 1.88 (d, *J* = 1.1, 8-CH$_3$), 2.41 (t, *J* = 5.6, 2H, 13-CH$_2$); 2.40-2.49 (m, 1H, 4-CH); 2.99-3.14 (m, 2H, 9-CH$_2$); 3.35-3.59 (m, 6H, 10-14-19-CH$_2$); 3.99 (s, 1H, 17-CH); 6.19 (bt, *J* = 5.7, 1H, 11-NH); 6.54 (dq, *J* = 1, 3, *J* = 9.8, 1H, 3-CH); 7.36 (bt, *J* = 5.9, 1H, 15-NH). **^{13}C-NMR** (CDCl$_3$, 100 MHz): δ 11.9 (6-CH$_3$), 12.7 (7-CH$_3$), 19.5 (8-CH$_3$), 20.4 (20-CH$_3$); 21.7 (21-CH$_3$); 28.3 (9-CH$_2$); 29.6 (5-CH);

35.1 (13-CH$_2$); 35.6 (14-CH$_2$); 39.4 (18-C); 39.8 (10-CH$_2$); 71.0 (19-CH$_2$); 77.7 (17-CH); 134.4 (2-C); 147.8 (3-CH); 171.4 (11-CO); 173.3 (15-CO); 194.5 (1-COS). **ES-MS:** *m/z* (%): 425 [M+Na]H$^+$ (12%), 403 [M]H$^+$ (28%), 385 [M-H$_2$O]H$^+$ (88%), 273 [M-C$_6$H$_{11}$O$_3$]H$^+$ (100%). **HR-MS:** *m/z* (%): calculated 425.2086, found 425.2085.

(2*E*, 4*S*)-Dimethylhex-2-enoylpantetheine (93).[129]
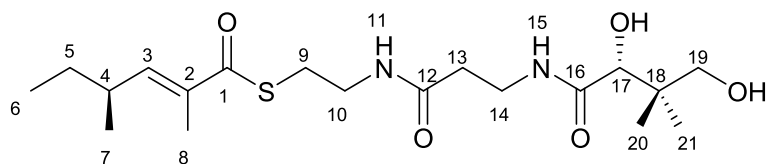
0.01 g of the product were purified by HPLC (acetonitrile). **^{1}H-NMR** (CDCl$_3$, 400 MHz): δ 0.86 (t, *J* = 7.4, 3H, 6-CH$_3$); 0.92 (s, 3H, 20-CH$_3$); 1.03 (s, 3H, 21-CH$_3$); 1.03 (d, *J* = 2.3, 3H, 7-CH$_3$); 1.30-1.51 (m, 2H, 5-CH$_2$); 1.88 (d, *J* = 1.1, 8-CH$_3$), 2.41 (t, *J* = 5.6, 2H, 13-CH$_2$); 2.40-2.49 (m, 1H, 4-CH); 2.99-3.14 (m, 2H, 9-CH$_2$); 3.35-3.59 (m, 6H, 10-14-19-CH$_2$); 3.99 (s, 1H, 17-CH); 6.19 (bt, *J* = 5.7, 1H, 11-NH); 6.54 (dq, *J* = 1, 3, *J* = 9.8, 1H, 3-CH); 7.36 (bt, *J* = 5.9, 1H, 15-NH). **^{13}C-NMR** (CDCl$_3$, 100 MHz): δ 11.9 (6-CH$_3$), 12.7 (7-CH$_3$), 19.5 (8-CH$_3$), 20.4 (20-CH$_3$); 21.7 (21-CH$_3$); 28.3 (9-CH$_2$); 29.6 (5-CH); 35.1 (13-CH$_2$); 35.6 (14-CH$_2$); 39.4 (18-C); 39.8 (10-CH$_2$); 71.0 (19-CH$_2$); 77.7 (17-CH); 134.4 (2-C); 147.8 (3-CH); 171.4 (11-CO); 173.3 (15-CO); 194.5 (1-COS). **ES-MS:** *m/z* (%): 425 [M+Na]H$^+$ (11%), 403 [M]H$^+$ (26%), 385 [M-H$_2$O]H$^+$ (88%), 273 [M-C$_6$H$_{11}$O$_3$]H$^+$ (100%). **HR-MS:** *m/z* (%): calculated 425.2086, found 425.2085.

2*E*-Hept-2-enoylpantetheine (96).[129]
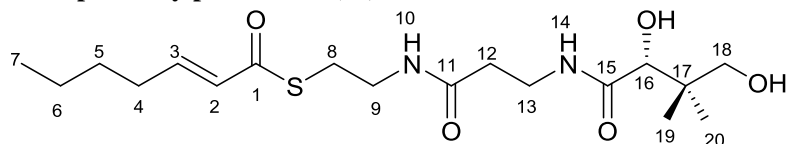
6 mg of the product were purified by HPLC (acetonitrile). **^{1}H-NMR** (CDCl$_3$, 400 MHz): δ 0.94 (t, *J* = 7.1, 3H, 7-CH$_3$); 0.95 (s, 3H, 19-CH$_3$); 1.06 (s, 3H, 20-CH$_3$); 1.28-1.42 (m, 4-H, 5-6-CH$_2$); 2.24 (dq, *J* = 1.6, *J* = 7.2, 2H, 4-CH$_2$); 2.43 (t, *J* = 7.2, 2H, 12-CH$_2$); 3, 05-3.25 (m, 2H, 8-CH$_2$); 3.38-3.62 (m, 6H, 9-13-18-CH$_2$); 4.01 (s, 1H, 16-CH); 6.13 (m, 1H, 2-CH); 6.15 (dt, *J* = 1.5, *J* = 15.4, 1H, 10-NH); 6.96 (dt, *J* = 7, 0, *J* = 15.5, 1H, 3-CH); 7.34 (bt, *J* = 6.0, 1H, 14-NH). **^{13}C-NMR** (CDCl$_3$, 100 MHz): δ 13.8 (7-CH$_3$), 20.4 (19-CH$_3$); 21.7 (20-CH$_3$); 22.3 (6-CH$_2$); 28.1 (8-CH$_2$); 29.9 (5-CH$_2$); 31.9 (4-CH$_2$); 35.1 (12-CH$_2$); 35.6 (13-CH$_2$); 39.3 (17-C); 39.9 (9-CH$_2$); 70.9 (18-CH$_2$); 77.8 (16-CH); 128.1 (2-CH); 147.3 (3-CH); 171.6 (11-CO); 173.2 (15-CO); 190.6 (1-COS). **ES-MS:** *m/z* (%):778 [M$_2$]H$^+$ (28 %), 389 [M]H$^+$ (100 %). **HR-MS:** *m/z* (%): calculated 411.1930, found 411.1929.

2E-2-Methylhept-2-enoylpantetheine (97).[129]
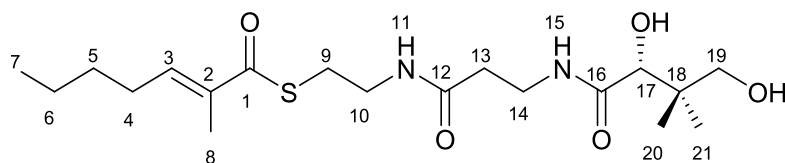
0.01 g of the product were purified by HPLC (acetonitrile). ^{1}**H-NMR** (CDCl$_3$, 400 MHz): δ 0.92 (s, 3H, 1-CH$_3$); 0.93 (t, J = 7.2, 3H, 20-CH$_3$); 1.03 (s, 3H, 21-CH$_3$); 1.31-1.49 (m, 4H, 5-6-CH$_2$); 1.88 (d, J = 1.1, 8-CH$_3$) 2.22 (q, J = 6.8, 2H, 4-CH$_2$); 2.41 (t, J = 5.9, 2H, 13-CH$_2$); 3.00-3.14 (m, 2H, 9-CH$_2$); 3.35-3.59 (m, 6H, 10-14-19-CH$_2$); 3.99 (s, 1H, 17-CH); 6.16 (bt, J = 5.6, 1H, 11-NH); 6.78 (tq, J = 1, 3, J = 7.5, 1H, 3-CH); 7.36 (bt, J = 5.9, 1H, 15-NH). ^{13}**C-NMR** (CDCl$_3$, 100 MHz): δ 12.5 (8-CH$_3$), 13.9 (7-CH$_3$), 20.4 (20-CH$_3$); 21.8 (21-CH$_3$); 22.5 (6-CH$_2$); 28.3 (4-CH$_2$); 28.5 (9-CH$_2$); 30.6 (5-CH$_2$); 35.1 (13-CH$_2$); 35.5 (14-CH$_2$); 39.4 (18-C); 39.8 (10-CH$_2$); 70.9 (19-CH$_2$); 77.7 (17-CH); 135.6 (2-C); 142.5 (3-CH); 171.6 (12-CO); 173.3 (16-CO); 194.2 (1-COS). **ES-MS:** m/z (%): 425 [M+Na]H$^+$ (7%), 403 [M]H$^+$ (81%), 385 [M-H$_2$O]H$^+$ (88%), 273 [M-C$_6$H$_{11}$O$_3$]H$^+$ (100%). **HR-MS:** m/z (%): calculated 425.2086, found 425.2084.

2E-6RS-6-Methylhept-2-enoylpantetheine (98).[129]

0.01 g of the product were purified by HPLC (acetonitrile). ^{1}**H-NMR** (CDCl$_3$, 400 MHz): δ 0.86-0.92 (m, 9H, 7-19-CH$_3$); 1.01 (s, 3H, 20-CH$_3$); 1.14-1.38 (m, 2H, 5-CH$_2$); 1.47-1.62 (m, 1H, 6-CH); 2.22 (q, J = 7.0, 2H, 4-CH$_2$); 2.41 (t, J = 6.2, 2H, 12-CH$_2$); 3.01-3.15 (m, 2H, 8-CH$_2$); 3.35-3.58 (m, 6H, 9-13-18-CH$_2$); 3.99 (s, 1H, 16-CH); 6.13 (dt, J = 1.5, J = 15.2, 1H, 2-CH); 6.39 (bt, J = 5.6, 1H, 10-NH); 6.93 (dt, J = 6.5, J = 15.5, 1H, 3-CH); 7.39 (bt, J = 5.9, 1H, 14-NH). ^{13}**C-NMR** (CDCl$_3$, 100 MHz): δ 20.4 (19-CH$_3$); 21.7 (20-CH$_3$); 22.4 (7-2xCH$_3$); 27.6 (6-CH); 28.1 (8-CH$_2$); 30.2 (4-CH$_2$); 35.1 (12-CH$_2$); 35.6 (13-CH$_2$); 36.9 (5-CH$_2$); 39.4 (17-C); 39.8 (9-CH$_2$); 70.9 (18-CH$_2$); 77.7 (16-CH); 128.0 (2-CH); 147.4 (3-CH); 171.7 (10-CO); 173.5 (14-CO); 190.6 (1-COS). **ES-MS:** m/z (%): 425 [M+Na]H$^+$ (12%), 403 [M]H$^+$ (30%), 385 [M-H$_2$O]H$^+$ (88%), 273 [M-C$_6$H$_{11}$O$_3$]H$^+$ (100%). **HR-MS:** m/z (%): calculated 425.2086, found 425.2089.
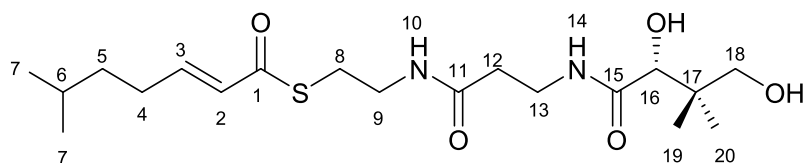
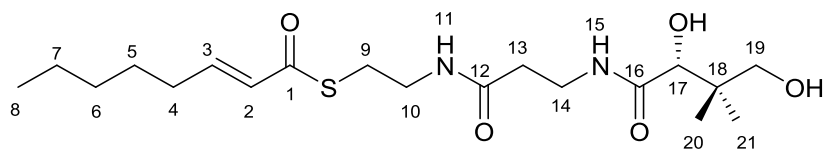### 2E-Oct-2-enoylpantetheine (99).[129]

6 mg of the product were purified by HPLC (acetonitrile). ^{1}**H-NMR** (CDCl$_3$, 400 MHz): δ 0.91 (t, J = 6.7, 3H, 8-CH$_3$); 0.95 (s, 3H, 20-CH$_3$); 1.06 (s, 3H, 21-CH$_3$); 1.28-1.61 (m, 6H, 5-6-7-CH$_2$); 2.21 (dq, J = 1.4, J = 7.3, 2H, 4-CH$_2$); 2.43 (t, J = 6.0, 2H, 13-CH$_2$); 3, 05-3.20 (m, 2H, 9-CH$_2$); 3.38-3.62 (m, 6H, 10-14-19-CH$_2$); 4.01 (s, 1H, 17-CH); 6.13 (t, J= 4.07, 1H, 2-CH); 6.17 (dt, J = 1.4, J= 15.4, 1H, 11-NH);

6.96 (dt, J = 6, 9, J = 15.4, 1H, 3-CH); 7.34 (bt, J = 5.82, 1H, 15-NH). ^{13}**C-NMR** (CDCl$_3$, 100 MHz): δ 13.9 (8-CH$_3$), 20.4 (20-CH$_3$); 21.7 (21-CH$_3$); 22.4 (7-CH$_2$); 27.6 (6-CH$_2$); 28.1 (9-CH$_2$); 31.7 (5-CH$_2$); 32.3 (4-CH$_2$); 35.1 (13-CH$_2$); 35.5 (14-CH$_2$); 39.3 (18-C); 39.9 (10-CH$_2$); 70.9 (19-CH$_2$); 77.8 (17-CH); 128.1 (2-CH); 147.3 (3-CH); 171.6 (12-CO); 173.2 (16-CO); 190.6 (1-COS). **ES-MS:** m/z (%): 806 [M$_2$]H$^+$ (14%), 403 [M]H$^+$ (100%). **HR-MS:** m/z (%): calculated 425.2086, found 425.2089.

2*E*-2-Methyloct-2-enoylpantetheine (100).[129]

0.01 g of the product were purified by HPLC (acetonitrile). ^{1}**H-NMR** (CDCl$_3$, 400 MHz): δ 0.90 (tr, J = 6.9, 3H, 8-CH$_3$); 0.91 (s, 3H, 21-CH$_3$); 1.01 (s, 3H, 22-CH$_3$); 1.25-1.36 (m, 4H, 6-7-CH$_2$); 1.41-1.50 (m, 2H, 5-CH$_2$); 1.85 (s, 3H, 9-CH$_3$); 2.20 (q, J = 7.5, 2H, 4-CH$_2$); 2.41 (t, J = 6.6, 2H, 14-CH$_2$); 2.99-3.12 (m, 2H, 10-CH$_2$); 3.35-3.58 (m, 6H, 11-15-20-CH$_2$); 3.99 (s, 1H, 18-CH); 6.37 (bt, J = 5.7, 1H, 12-NH); 6.77 (tq, J = 1.3, J = 7.6, 1H, 3-CH); 7.41 (bt, J = 6.2, 1H, 16-NH). ^{13}**C-NMR** (CDCl$_3$, 100 MHz): δ 12.5 (9-CH$_3$); 14.1 (8-CH$_3$); 20.4 (21-CH$_3$); 21.6 (22-CH$_3$); 22.5 (7-CH$_2$); 28.1 (5-CH$_2$); 28.2 (4-CH$_2$); 28.8 (10-CH$_2$); 31.6 (6-CH$_2$); 35.1 (14-CH$_2$); 35.6 (15-CH$_2$); 39.4 (19-C); 39.8 (11-CH$_2$); 70.9 (20-CH$_2$); 77.8 (18-CH); 135.6 (2-C); 142.7 (3-CH); 171.7 (13-CO); 173.2 (17-CO); 194.2 (1-COS). **ES-MS:** m/z (%): 439 [M+Na]H$^+$ (2%), 417 [M]H$^+$ (41%), 399 [M-H$_2$O]H$^+$ (85%), 287 [M-C$_6$H$_{11}$O$_3$]H$^+$ (100%). **HR-MS:** m/z (%): calculated 439.2243, found 439.2240.

2*EZ*-2-Ethyloct-2-enoylpantetheine (103).[129]
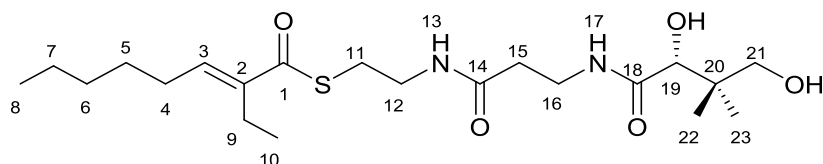
0.027 g of the product were purified by HPLC (acetonitrile). ^{1}**H-NMR** (CDCl$_3$, 400 MHz): δ 0.85-0.99 (m, 12H, 8-10-22-23-CH$_3$); 1.28-1.51 (m, 4H, 5-6-7-CH$_2$); 2.16-2.35 (m, 4H, 4-9-CH$_2$); 2.41 (t, J = 6.4, 2H, 15-CH$_2$); 2.97-3.06 (m, 2H, 11-CH$_2$); 3.33-3.56 (m, 6H, 12-16-21-CH$_2$); 3.98 (s, 1H, 19-CH); 5.63 (t, J = 7.6, 1H, 3-CH$_Z$); 6.56 (bt, J = 5.7, 1H, 13-NH); 6.70 (t, J = 7.6, 1H, 3-CH$_E$); 7.46 (bt, J = 5.9, 1H, 17-NH). ^{13}**C-NMR** (CDCl$_3$, 100 MHz): δ 13.4 (8-CH$_3$), 13.9 (10-CH$_3$), 20.4 (22-CH$_3$); 21.5 (23-CH$_3$); 22.0 (7-CH$_2$); 22.8 (6-CH$_2$); 28.2 (11-CH$_2$), 29.5 (5-CH$_2$); 31.4 (4-CH$_2$); 35.1 (15-CH$_2$); 35.5 (16-CH$_2$); 39.4 (20-C); 39.8 (12-CH$_2$); 70.9 (21-CH$_2$); 77.7 (19-CH); 136.1 (3-CH$_Z$); 140.5 (2-C); 142.2 (3-CH$_E$); 171.6 (14-CO); 173.4 (18-CO); 193.9 (1-COS). **ES-MS:** m/z (%): 453 [M+Na]H$^+$ (8%), 431 [M]H$^+$ (65%), 413 [M-H$_2$O]H$^+$ (88%), 301 [M-C$_6$H$_{11}$O$_3$]H$^+$ (100%). **HR-MS:** m/z (%): calculated 453.2396, found 453.2396.

6*RS*,4*RS*-2*E*-Dimethyloct-2-enoylpantetheine (104).[129]
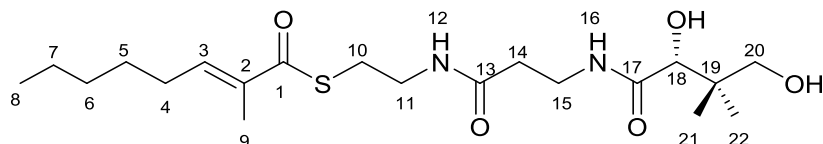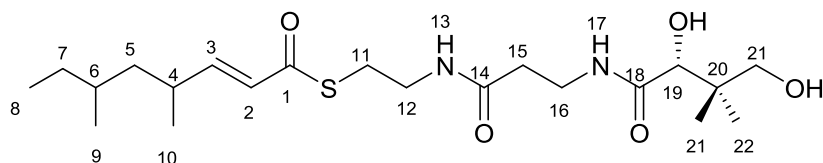

0.027 g of the product were purified by HPLC (acetonitrile). **¹H-NMR** (CDCl₃, 400 MHz): δ 0.81-0.90 (m, 6H, 8-9-CH₃), 0.92 (s, 3H, 22-CH₃), 1.03 (s, 3H, 23-CH₃), 1.00-1.07 (m, 3H, 10-CH₃), 1.07-1.44 (m, 7H, 5-6-7-CH₂), 2.41 (t, 2H, *J* = 6.0, 15-CH₂), 2.34-2.46 (m, 1H, 4-CH), 2.95-3.17 (m, 2H, 11-CH₂), 3.33-3.66 (m, 6H, 12-16-21-CH₂), 3.99 (s, 1H, 19-CH), 6.08 (dt, 1H, *J* = 1.4, *J* = 15.6, 2-CH), 6.23 (bt, *J* = 6.0, 1H, 13-NH), 6.75-6.88 (m, 1H, 3-CH); 7.36 (bt, *J* = 6.0, 1H, 17-NH). **¹³C-NMR** (CDCl₃, 100 MHz): 11.3 (8-9-CH₃), 19.2 (10-CH₃), 20.5 (22-CH₃), 21.9 (23-CH₃), 28.3 (11-CH₂), 29.5 (7-CH₂), 31.9 (6-CH), 34.3 (4-CH), 35.3 (15-CH₂), 35.7 (16-CH₂), 39.5 (20-C), 40.0 (12-CH₂), 71.1 (21-CH₂), 77.9 (19-CH), 126.2 (2-CH), 152.5 (3-CH), 171.8 (14-CO), 173.5 (18-CO), 190.9 (1-CO). **ES-MS:** *m/z* (%): 453 [M+Na]H⁺ (11%), 431 [M]H⁺ (62%), 413 [M-H₂O]H⁺ (85%), 301 [M-C₆H₁₁O₃]H⁺ (100%). **HR-MS:** *m/z* (%): calculated 453.2396, found 453.2396.

6*S*,4*S*-2*E*-Dimethyloct-2-enoylpantetheine (102).[129]
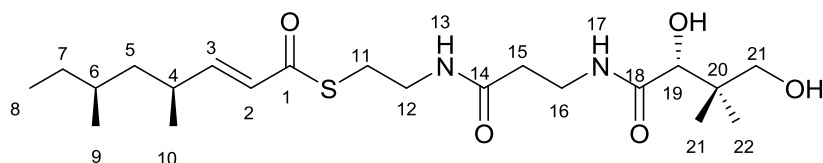
0.027 g of the product were purified by HPLC (acetonitrile). **¹H-NMR** (CDCl₃, 400 MHz): δ 0.81-0.90 (m, 6H, 8-9-CH₃), 0.92 (s, 3H, 21-CH₃), 1.03 (s, 3H, 22-CH₃), 1.05 (m, 3H, 10-CH₃), 1.10-1.44 (m, 6H, 5-7-CH₂, 6-CH), 2.42 (t, 2H, *J* = 6.0, 15-CH₂), 2.37-2.41 (m, 1H, 4-CH), 3.03-3.17 (m, 2H, 11-CH₂), 3.36-3.58 (m, 6H, 12-16-21-CH₂), 3.99 (s, 1H, 19-CH), 6.08 (dd, 1H, *J* = 1.4, *J* = 15.6, 2-CH), 6.23 (bt, *J* = 6.0, 1H, 13-NH), 6.79 (dd, *J* = 7.6, 1H, 3-CH); 7.37 (bt, *J* = 6.0, 1H, 17-NH). **¹³C-NMR** (CDCl₃, 100 MHz): 11.3 (8-CH₃), 18.8 (9-CH₃), 20.2 (10-CH₃), 20.5 (21-CH₃), 21.9 (22-CH₃), 28.3 (11-CH₂), 29.7 (7-CH₂), 31.9 (6-CH₂), 34.3 (4-CH), 35.1 (15-CH₂), 35.9 (16-CH₂), 39.5 (18-C), 39.8 (12-CH₂), 43.3 (5-CH₂), 71.1 (21-CH₂), 77.9 (19-CH), 126.2 (2-CH), 152.5 (3-CH), 171.8 (14-CO), 173.5 (18-CO), 190.9 (1-CO). **ES-MS:** *m/z* (%): 453 [M+Na]H⁺ (8%), 431 [M]H⁺ (65%), 413 [M-H₂O]H⁺ (88%), 301 [M-C₆H₁₁O₃]H⁺ (100%). **HR-MS:** *m/z* (%): calculated 453.2399, found 453.2392.

2*E*-7-Methyloct-2-enoylpantetheine (101).[129]
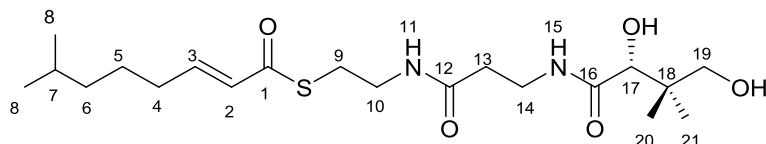
0.01 g of the product were purified by HPLC (acetonitrile). **¹H-NMR** (CDCl₃, 400 MHz): δ 0.86 (d, *J* = 6.6, 6H, 8-CH₃); 0.93 (s, 3H, 20-CH₃); 1.03 (s, 3H, 21-CH₃); 1.14-1.30 (m, 2H, 5-6-CH₂); 1.42-1.60 (m, 1H, 7-CH); 2.22 (q, *J* = 7.4, 2H, 4-CH₂); 2.41 (t, *J* = 5.8, 2H, 13-CH₂); 3.01-3.18 (m, 2H, 9-CH₂); 3.35-3.59 (m, 6H, 10-14-19-CH₂); 3.99 (s, 1H, 17-CH); 6.13 (dt, *J* = 1.5, *J* = 15.5, 1H, 2-CH); 6.18 (bt,

J = 5.8, 1H, 11-NH); 6.93 (dt, J = 6.9, J = 15.5, 1H, 3-CH); 7.34 (bt, J = 5.8, 1H, 15-NH). **^{13}C-NMR** (CDCl$_3$, 100 MHz): δ 20.4 (20-CH$_3$); 21.7 (21-CH$_3$); 22.5 (8-2xCH$_3$); 27.8 (7-CH); 28.1 (9-CH$_2$); 30.1 (5-CH$_2$); 32.6 (4-CH$_2$); 35.1 (13-CH$_2$); 35.6 (14-CH$_2$); 38.5 (6-CH$_2$); 39.4 (18-C); 39.8 (10-CH$_2$); 70.9 (19-CH$_2$); 77.8 (17-CH); 128.1 (2-CH); 147.3 (3-CH); 171.6 (12-CO); 173.3 (16-CO); 190.6 (1-COS). **ES-MS:** *m/z* (%): 417 [M]H$^+$ (15%), 399 [M-H$_2$O]H$^+$ (60%), 287 [M-C$_6$H$_{11}$O$_3$]H$^+$ (100%). **HR-MS:** *m/z* (%): calculated 439.2243, found 439.2242.

2*E*-Dec-2-enoyl-pantetheine (105).[129]
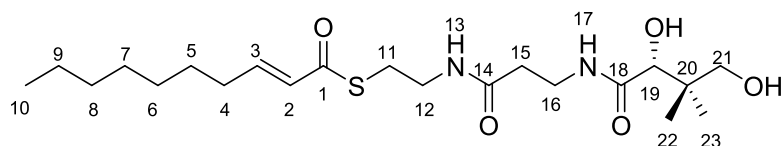
6 mg of the product were purified by HPLC (acetonitrile). **^{1}H-NMR** (CDCl$_3$, 400 MHz): δ 0.91 (t, J = 7.1, 3H, 10-CH$_3$); 0.95 (s, 3H, 22-CH$_3$); 1.06 (s, 3H, 23-CH$_3$); 1.28-1.33 (m, 8H, 6, 7, 8, 9-CH$_2$); 1.45-1.53 (m, 2H, 5-CH$_2$); 2.23 (dq, J = 1.6, J = 7.2, 2H, 4-CH$_2$); 2.43 (t, J = 7.2, 2H, 15-CH$_2$); 3, 05-3.20 (m, 2H, 11-CH$_2$); 3.37-3.62 (m, 6H, 12-16-21-CH$_2$); 4.01 (s, 1H, 19-CH); 6.13 (m, 1H, 2-CH); 6.17 (dt, J = 1.5, J = 15.4, 1H, 13-NH); 6.96 (dt, J = 7, 0, J = 15.5, 1H, 3-CH); 7.34 (bt, J = 6.0, 1H, 17-NH). **^{13}C-NMR** (CDCl$_3$, 100 MHz): δ 14.1 (10-CH$_3$), 20.4 (22-CH$_3$); 21.7 (23-CH$_3$); 22.6 (9-CH$_2$); 27.9 (5-CH$_2$); 28.6 (11-CH$_2$); 29.1 (7-CH$_2$); 29.2 (6-CH$_2$); 31.7 (8-CH$_2$); 32.3 (4-CH$_2$); 35.1 (15-CH$_2$); 35.6 (16-CH$_2$); 39.3 (20-C); 39.9 (12-CH$_2$); 70.9 (21-CH$_2$); 77.8 (19-CH); 128.1 (2-CH); 147.7 (3-CH); 171.6 (14-CO); 173.3 (18-CO); 190.9 (1-COS). **ES-MS:** *m/z* (%): 863 [M$_2$]H$^+$ (28%), 431 [M]H$^+$ (100%), 413 [M-H$_2$O]H$^+$ (1%). **HR-MS:** *m/z* (%): calculated 453.2399, found 453.2399.

2*E*-2-Methyldec-2-enoylpantetheine (106).[129]
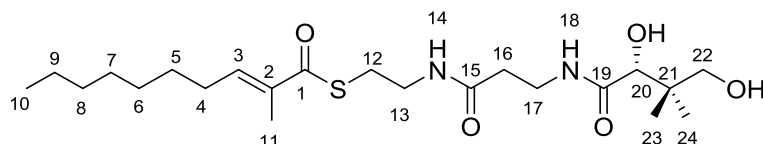
0.01 g of the product were purified by HPLC (acetonitrile). **^{1}H-NMR** (CDCl$_3$, 400 MHz): δ 0.88 (tr, J = 7.2, 3H, 10-CH$_3$); 0.93 (s, 3H, 23-CH$_3$); 1.04 (s, 3H, 24-CH$_3$); 1.28-1.31 (m, 8H, 6-7-8-9-CH$_2$); 1.43-1.48 (m, 2H, 5-CH$_2$); 1.87 (s, 3H, 11-CH$_3$); 2.22 (q, J = 7.2, 2H, 4-CH$_2$); 2.41 (t, J = 6.2, 2H, 16-CH$_2$); 3.00-3.14 (m, 2H, 12-CH$_2$); 3.35-3.63 (m, 6H, 13-17-22-CH$_2$); 3.99 (s, 1H, 20-CH); 6.09 (bt, J = 5.6, 1H, 14-NH); 6.78 (tq, J = 1.3, J = 7.4, 1H, 3-CH); 7.38 (bt, J = 6.6, 1H, 18-NH). **^{13}C-NMR** (CDCl$_3$, 100 MHz): δ 12.5 (11-CH$_3$); 14.1 (10-CH$_3$); 20.4 (23-CH$_3$); 21.7 (24-CH$_3$); 22.6 (9-CH$_2$); 28.3 (5-CH$_2$); 28.5 (12-CH$_2$); 29.1 (7-CH$_2$); 29.4 (6-CH$_2$); 31.8 (8-CH$_2$); 35.1 (16-CH$_2$); 35.6 (17-CH$_2$); 39.4 (21-C); 39.8 (13-CH$_2$); 70.9 (22-CH$_2$); 77.8 (19-CH); 135.6 (2-C); 142.8 (3-CH); 171.7 (15-CO); 173.2 (19-CO); 194.2 (1-COS). **ES-MS:** *m/z* (%): 467 [M+Na]H$^+$ (12%), 445 [M]H$^+$ (27%), 427 [M-H$_2$O]H$^+$ (67%), 315 [M-C$_6$H$_{11}$O$_3$]H$^+$ (100%). **HR-MS:** *m/z* (%): calculated 467.2556, found 467.2556.

3-Oxobutanoylpantetheine (224a).
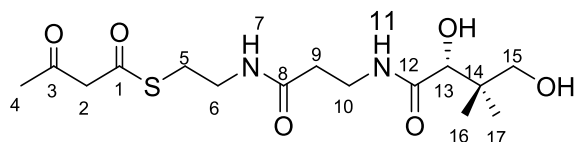
3-oxobutanepantetheine dimethyl ketal (0.96 g, 2.0 mmol was solved in dichloromethane and 10% TFA for 20 minutes. The reaction was followed by TLC and LCMS. After that the solvents were evapurated. The product was purified by HPLC (0.26 g, 0.7 mmol, 30%). **^{1}H-NMR** (CDCl$_3$, 400 MHz): δ 0.92 (s, 3H, 16-CH$_3$); 1.02 (s, 3H, 17-CH$_3$); 1.95 (s, 1H, 4-CH$_3$); 2.27 (s, 2H, 4-CH$_3$); 2.44 (t, J = 5.7, 2H, 9-CH$_2$); 3.09 (t, J = 6.5, 2H, 5-CH$_2$); 3.37-3.65 (m, 6H, 6-10-15-CH$_2$); 3.73 (s, 2H, 2-CH$_2$); 4.00 (s, 1H, 13-CH); 6.49 (bt, J = 5.7, 1H, 7-NH); 7.38 (bt, J = 5.9, 1H, 11-NH). **^{13}C-NMR** (CDCl$_3$, 100 MHz): δ 20.4 (16-CH$_3$); 21.6 (17-CH$_3$); 27.4 (5-CH$_2$); 30.4 (4-CH$_3$), 35.2 (10-CH$_2$); 35.6 (9-CH$_2$); 39.4 (13-C); 39.8 (6-CH$_2$); 57.9 (2-CH$_2$); 70.8 (15-CH$_2$); 77.6 (13-CH); 171.2 (8-CO); 174.2 (12-CO); 192.4 (1-CO); 200.3 (3-CO). **ES-MS:** m/z (%): 385 [M+Na]H$^+$ (65%), 363 [M]H$^+$ (100%). **HR-MS:** m/z (%): calculated 363.1590, found 363.1586.

2-Methyl-3-oxobutanoylpantetheine (225a).
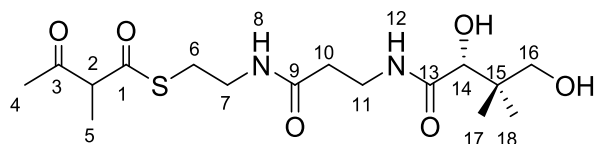
Potassium *tert*-butanolate (0.31 g, 2.8 mmol) in 20 mL THF was added to 3-oxobutanepantetheine dimethyl ketal (1.1 g, 2.4 mmol) and the mixture stirred for further 45 min at room temperature. After that methyliodide (0.39 g, 2.8 mmol) was added and stirred for 5 hours. Ether and water was given to the mixture and the aqueous phase extracted three times with diethyl ether (20 mL). Finally the combined organic layers were washed with brine, dried over MgSO$_4$ and concentrated. The residue was solved in dichloromethane and 10 % TFA for 20 minutes. The reaction was followed by TLC and LCMS. After that the solvents were evapurated. The product was purified by HPLC (0.28 g, 0.7 mmol, 30%). **^{1}H-NMR** (CDCl$_3$, 400 MHz): δ 0.93 (s, 3H, 17-CH$_3$); 1.02 (s, 3H, 18-CH$_3$); 1.40 (d, 3H, J = 7.6, 5-CH$_3$); 2.02 (s, 1H, 4-CH$_3$); 2.25 (s, 2H, 4-CH$_3$); 2.43 (t, J = 5.3, 2H, 10-CH$_2$); 2.99-3.09 (m, 2H, 6-CH$_2$); 3.32-3.59 (m, 6H, 7-11-16-CH$_2$); 3.77 (q, 1H, J = 6.5, 2-CH$_2$); 4.05 (s, 1H, 14-CH); 6.34 (bt, J = 5.7, 1H, 8-NH); 7.36 (bt, J = 5.9, 1H, 12-NH). **^{13}C-NMR** (CDCl$_3$, 100 MHz): δ 13.5 (5-CH$_3$); 20.4 (17-CH$_3$); 21.6 (18-CH$_3$); 28.5 (4-CH$_3$); 28.8 (6-CH$_2$); 30.4 (4-CH$_3$), 35.2 (11-CH$_2$); 35.6 (10-CH$_2$); 39.2 (15-C); 39.4 (7-CH$_2$); 61.8 (2-CH); 70.9 (16-CH$_2$); 77.7 (14-CH); 171.6 (9-CO); 173.6 (13-CO); 197.4 (1-CO); 203.3 (3-CO). **ES-MS:** m/z (%): 399 [M+Na]H$^+$ (5%), 377 [M]H$^+$ (88%), 359 [M-H$_2$O]H$^+$ (73%), 247 [M-C$_6$H$_{11}$O$_3$]H$^+$ (100%). **HR-MS:** m/z (%): calculated 399.1566, found 399.1566.

3-Oxohexanoylpantetheine (224b).
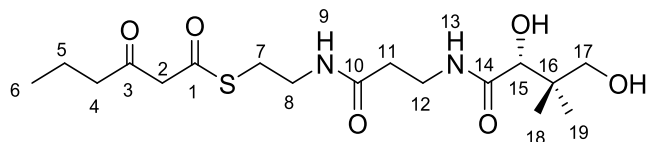
Butanoyl meldrums acid (1.6 g, 7.4 mmol) stirred in toluene with pantetheine dimethyl ketal (2.4 g, 7.8 mmol) under nitrogen at 90 °C. After 6 hours the reaction was stopped and the mixture concentrated under vacuum. The mixture was then solved in 2 M HCl/ MeOH 1:5 and stirred for further 4 hours. After that the product was purified by HPLC to give a yellow oil (0.32 g, 0.7 mmol, 10%). **^{1}H-NMR** (CDCl$_3$, 400 MHz): δ 0.93 (t, J = 7.4, 3H, 6-CH$_3$); 0.95 (s, 3H, 18-CH$_3$); 1.03 (s, 3H, 19-CH$_3$); 1.60-1.65 (m, 2H, 5-CH$_2$); 2.43 (t, J = 5.9, 2H, 11-CH$_2$); 2.51 (t, J = 6.9, 2H, 4-CH$_2$); 3.05-3.15 (m, 2H, 7-CH$_2$); 3.36-3.59 (m, 6H, 8-12-17-CH$_2$); 3.70 (s, 2H, 2-CH$_2$); 4.00 (s, 1H, 15-CH); 6.39 (bt, J = 5.7, 1H, 10-NH); 7.35 (bt, J = 5.9, 1H, 13-NH). **^{13}C-NMR** (CDCl$_3$, 100 MHz): δ 13.5 (6-CH$_3$), 16.9 (5-CH$_2$), 20.4 (18-CH$_3$); 21.7 (19-CH$_3$); 29.0 (7-CH$_2$); 35.1 (11-CH$_2$); 35.6 (12-CH$_2$); 39.1 (16-C); 39.4 (8-CH$_2$); 45.4 (3-CH$_2$); 57.1 (2-CH$_2$); 70.9 (17-CH$_2$); 77.6 (15-CH); 171.9 (11-CO); 173.5 (14-CO); 192.2 (1-CO); 202.9 (3-CO). **ES-MS:** m/z (%): 413 [M+Na]H$^+$ (49%), 391 [M]H$^+$ (98%), 373 [M-H$_2$O]H$^+$ (73%), 261 [M-C$_6$H$_{11}$O$_3$]H$^+$ (100%). **HR-MS:** m/z (%): calculated 413.1720, found 413.1720.

2-Methyl-3-oxohexanoylpantetheine (225b).

Potassium *tert*-butanolate in 20 mL THF was added (0.31 g, 2.8 mmol) to 3-oxohexanepantetheine dimethyl ketal (1.1 g, 2.4 mmol) and the mixture stirred for further 45 min at room temperature. After that methyliodide (0.4 g, 2.8 mmol) was added and stirred for 5 hours. Ether and water was given to the mixture and the aqueous phase extracted three times with diethyl ether (2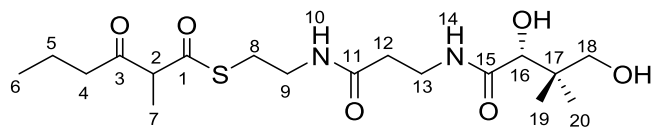0 mL). Finally the combined organic layers were washed with brine, dried over MgSO$_4$ and concentrated. The residue was solved in dichloromethane and 10% TFA for 20 minutes. The reaction was followed by TLC and LCMS. After that the solvents were evapurated. The product was purified by HPLC (0.28 g, 0.7 mmol, 30%). **^{1}H-NMR** (CDCl$_3$, 400 MHz): δ 0.91 (t, J = 6.7, 3H, 6-CH$_3$); 0.93 (s, 3H, 19-CH$_3$); 1.03 (s, 3H, 20-CH$_3$); 1.39 (d, J = 6.7, 3H, 7-CH$_3$); 1.61 (q, J = 7.4, 2H, 5-CH$_2$); 2.43 (t, J = 5.7, 2H, 12-CH$_2$); 2.53 (t, J = 7.1, 2H, 4-CH$_2$); 3.05-3.15 (m, 2H, 8-CH$_2$); 3.36-3.59 (m, 6H, 9-13-178-CH$_2$); 3.79 (q, J = 7.1, 1H, 2-CH); 4.01 (s, 1H, 16-CH); 6.31 (bt, J = 5.7, 1H, 10-NH); 7.37 (bt, J = 5.9, 1H, 15-NH). **^{13}C-NMR** (CDCl$_3$, 100 MHz): δ 13.6 (6-7-CH$_3$), 16.9 (5-CH$_2$), 20.4 (19-CH$_3$); 21.7 (20-CH$_3$); 28.8 (8-CH$_2$); 35.1 (12-CH$_2$); 35.6 (13-CH$_2$); 39.3 (17-C); 39.4 (9-CH$_2$); 43.5 (4-CH$_2$); 61.1 (2-CH$_2$); 70.7 (18-CH$_2$); 77.7 (16-CH); 171.8 (11-CO); 173.5 (15-CO); 197.4 (1-CO); 205.6 (3-CO). **ES-MS:** m/z (%): 427 [M+Na]H$^+$ (65%), 405 [M]H$^+$ (100%), 387 [M-H$_2$O]H$^+$ (68%), 275 [M-C$_6$H$_{11}$O$_3$]H$^+$ (100%). **HR-MS:** m/z (%): calculated 427.1879, found 427.1879.

6.2.7 Synthesis of Pantetheine Glycine Substrates.

General Procedure: Step 1

Corresponding pantetheine and boc-glycine-OH were dissolved in dichloromethane (8 mL). The mixture was cooled to 0 °C. Then *N*, *N*-dimethylaminopyridine and *N*-(3-Diethylaminopropyl)-*N*-ethylcarbodiimide were added. The mixture was warmed to 25 °C and stirred for 8 hours. After that the mixture was quenched with 2 M HCl (10 mL) and extracted with dichloromethane (3 × 25 mL). The organic layer was washed with saturated $NaHCO_3$ (25 ml) and brine (25 mL). The product was dried over $MgSO_4$ and concentrated under vacuo. In the last step dichloromethane and 20% TFA and 10% water was added and stirred for further 20 min. The crude product was purified by HPLC.[192]

3-Oxo-butyrylpantetheine-glycine (210).
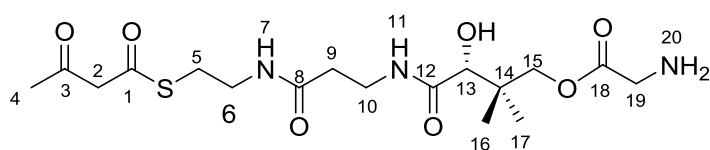
The obtained product was a yellow oil (18 mg, 0.04 mmol, 6%). **^{1}H-NMR** (D_2O, 400 MHz): δ 0.98 (s, 3H, 16-CH$_3$); 0.99 (s, 3H, 17-CH$_3$); 2.23 (s, 1H, 4-CH$_3$); 2.29 (s, 2H, 4-CH$_3$); 2.48 (t, *J* = 6.3, 2H, 9-CH$_2$); 3.10 (t, *J* = 5.9, 2H, 5-CH$_2$); 3.40 (t, *J* = 7.0, 2H, 10-CH$_2$); 3.48-3.52 (m, 2H, 6-CH$_2$); 3.98 (s, 2H, 19-CH$_2$); 4.01 (s, 1H, 13-CH) 4.09 (d, *J* = 11.4, 1H, 15-CH$_2$); 4.19 (d, *J* = 11.4, 1H, 15-CH$_2$). **^{13}C-NMR** (D_2O, 100 MHz): δ 19.4 (16-CH$_3$); 20.3 (17-CH$_3$); 28.5 (5-CH$_2$); 29.9 (4-CH$_3$); 35.1 (13-C); 35.4 (9-CH$_2$); 37.6 (10-CH$_2$); 38.4 (6-CH$_2$); 39.9 (19-CH$_2$); 53.8 (2-CH$_2$); 71.6 (15-CH$_2$); 74.6 (13-CH); 168.0 (18-CO); 174.0 (8-CO); 174.5 (12-CO); 195.8 (1-CO); 206.3 (3-CO). **ES-MS:** *m/z* (%): 442 [M+Na]H$^+$ (16%), 420 [M]H$^+$ (100%), 402 [M-H$_2$O]H$^+$ (6%). **HR-MS:** *m/z* (%): calculated 442.1624, found 442.1628.[192]

3-Oxo-2-methyl-butyrylpantetheine-glycine (211).
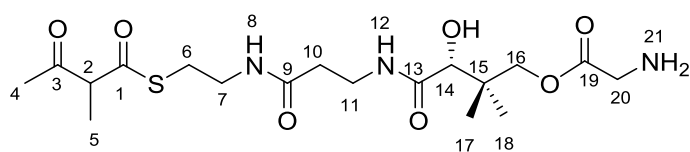
The obtained product was a yellow oil (33 mg, 0.08 mmol, 11%). **^{1}H-NMR** (D_2O, 400 MHz): δ 0.98 (s, 3H, 17-CH$_3$); 0.99 (s, 3H, 18-CH$_3$); 1.35 (s, 3H, 5-CH$_3$); 2.30 (s, 3H, 4-CH$_3$); 2.48 (t, *J* = 6.3, 2H, 10-CH$_2$); 3.10 (t, *J* = 5.9, 2H, 6-CH$_2$); 3.40 (t, *J* = 7.0, 2H, 11-CH$_2$); 3.48-3.52 (m, 2H, 7-CH$_2$); 3.98 (s, 2H, 20-CH$_2$); 4.01 (s, 1H, 14-CH) 4.09 (d, *J* = 11.4, 1H, 16-CH$_2$); 4.19 (d, *J* = 11.4, 1H, 16-CH$_2$). **^{13}C-NMR** (D_2O, 100 MHz): δ 13.1 (5-CH$_3$); 19.4 (17-CH$_3$); 20.3 (18-CH$_3$); 28.4 (4-CH$_3$); 28.5 (6-CH$_2$); 35.1 (15-C); 35.4 (10-CH$_2$); 37.6 (11-CH$_2$); 38.4 (7-CH$_2$); 39.9 (20-CH$_2$); 53.8 (2-CH$_2$); 71.6 (16-CH$_2$); 74.6 (14-CH); 168.0 (19-CO); 173.9 (9-CO); 174.5 (13-CO); 200.1 (1-CO); 208.9 (3-CO). **ES-MS:** *m/z* (%): 462 [M+Na]H$^+$ (31%), 434 [M]H$^+$ (100%), 416 [M-H$_2$O]H$^+$ (2%). **HR-MS:** *m/z* (%): calculated 434.1961, found 434.1960.[192]

3R-Hydroxy-2R-methylbutyrylpantetheine-glycine (212).
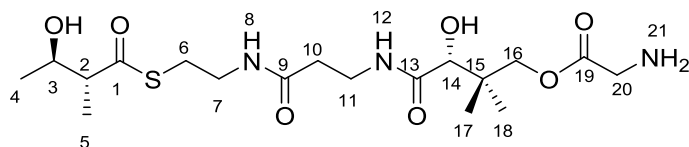
The obtained product was a yellow oil (14 mg, 0.03 mmol, 10%). **^{1}H-NMR** (D$_2$O, 400 MHz): δ 0.98 (s, 3H, 17-CH$_3$); 0.99 (s, 3H, 18-CH$_3$); 1.12 (d, J = 7.1, 3H, 5-CH$_3$); 1.20 (d, J = 6.4, 3H, 4-CH$_3$); 2.47 (t, J = 6.5, 2H, 10-CH$_2$); 2.76-2.83 (m, 1H, 2-CH); 2.98-3.13 (m, 2H, 6-CH$_2$); 3.39 (t, J = 7.0, 2H, 11-CH$_2$); 3.47-3.53 (m, 2H, 7-CH$_2$); 3.95 (m, 1H, 3-CH), 3.98 (s, 2H, 20-CH$_2$); 4.01 (s, 1H, 14-CH) 4.09 (d, J = 11.4, 1H, 16-CH$_2$); 4.19 (d, J = 11.4, 1H, 16-CH$_2$). **^{13}C-NMR** (D$_2$O, 100 MHz): δ 13.8 (5-CH$_3$); 19.3 (4-CH$_3$); 19.4 (17-CH$_3$); 20.3 (18-CH$_3$); 27.9 (6-CH$_2$); 35.1 (15-C); 35.4 (10-CH$_2$); 37.6 (11-CH$_2$); 38.6 (7-CH$_2$); 39.9 (20-CH$_2$); 55.6 (2-CH); 69.4 (3-CH); 71.6 (16-CH$_2$); 74.6 (14-CH); 168.0 (19-CO); 174.0 (9-CO); 174.5 (13-CO); 206.3 (1-CO). **ES-MS:** m/z (%): 458 [M+Na]H$^+$ (12%), 436 [M]H$^+$ (100%). **HR-MS:** m/z (%): calculated 436.2117, found 436.2118

Tigloylpantetheine-glycine (213).
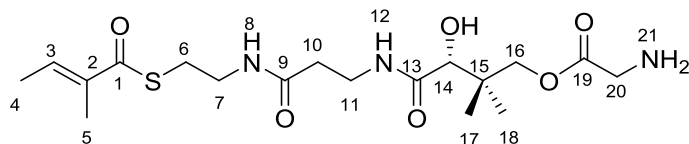
The obtained product was a yellow oil (27 mg, 0.06 mmol, 2%). **^{1}H-NMR** (CDCl$_3$, 400 MHz): δ 0.88 (s, 3H, 17-CH$_3$); 0.97 (s, 3H, 18-CH$_3$); 1.82 (m, 6H, 4-5-CH$_3$); 2.43 (t, J = 5.2, 2H, 10-CH$_2$); 2.99 (t, J = 5.6, 2H, 6-CH$_2$); 3.29-3.56 (m, 4H, 7-11-CH$_2$); 3.80-4.03 (m, 3H, 14-20-CH$_2$); 4.16 (m, 2H, 16-CH$_2$); 6.56 (bt, J = 5.7, 1H, 8-NH); 6.84 (m, 1H, 3-CH); 7.41 (bt, J = 5.7, 1H, 12-NH); 7.71 (bt, J = 7.3, 1H, 21-NH). **^{13}C-NMR** (CDCl$_3$, 100 MHz): δ 12.1 (5-CH$_3$), 14.5 (4-CH$_3$), 19.8 (17-CH$_3$); 21.1 (18-CH$_3$); 27.9 (6-CH$_2$); 35.2 (15-C); 35.6 (10-CH$_2$); 37.4 (101-CH$_2$); 38.5 (7-CH$_2$); 39.9 (20-CH$_2$); 71.6 (14-CH$_2$); 74.6 (14-CH); 136.1 (2-C); 136.8 (3-CH); 167.8 (19-CO); 172.0 (9-CO); 173.7 (13-CO); 193.7 (1-COS). **ES-MS:** m/z (%): 440 [M+Na]H$^+$ (8%), 418 [M]H$^+$ (100%), 400 [M-H$_2$O]H$^+$ (12%), 343 [M-C$_2$H$_4$NO]H$^+$ (100%). **HR-MS:** m/z (%): calculated 440.1831, found 440.1833.[192]

Methylbutyrylpantetheine-glycine (214).
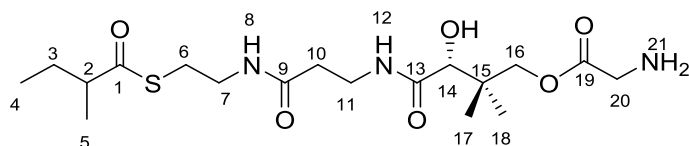
The obtained product was a yellow oil (80 mg, 0.2 mmol, 50%) **^{1}H-NMR** (D$_2$O, 400 MHz): δ 0.87 (t, J = 7.6, 3H, 4-CH$_3$); 0.98 (s, 3H, 17-CH$_3$); 0.99 (s, 3H, 18-CH$_3$); 1.14 (d, J = 7.4, 3H, 5-CH$_3$); 1.44-1.71 (m, 2H, 3-CH$_2$); 2.47 (t, J = 7.0, 2H, 10-CH$_2$); 2.67-2.76 (m, 1H, 2-CH); 3.05 (t, J = 7.6, 2H, 6-CH$_2$); 3.39 (t, J = 7.0, 2H, 11-CH$_2$); 3.47-3.53 (m, 2H, 7-CH$_2$); 3.98 (s, 2H, 20-CH$_2$); 4.01 (s, 1H, 14-CH) 4.09 (d, J = 11.4, 1H, 16-CH$_2$); 4.19 (d, J = 11.4, 1H, 16-CH$_2$). **^{13}C-NMR** (D$_2$O, 100 MHz): δ 10.8 (4-CH$_3$); 16.6 (5-CH$_3$); 19.4 (17-CH$_3$); 20.3 (18-CH$_3$); 26.9 (3-CH$_2$); 27.7 (6-CH$_2$); 35.1 (15-C); 35.4 (10-CH$_2$); 37.6 (11-CH$_2$); 38.5 (7-CH$_2$); 39.8 (20-CH$_2$); 49.9 (2-CH); 71.6 (16-CH$_2$); 74.6 (14-CH); 168.1 (19-CO); 173.8

(9-CO); 174.5 (13-CO); 209.2 (5-CO). **ES-MS:** m/z (%): 442 [M+Na]H$^+$ (23%), 420 [M]H$^+$ (100%), 402 [M-H$_2$O]H$^+$ (4%). **HR-MS:** m/z (%): calculated 442.1988, found 442.1989.[192]

3-Oxohexanoylpantetheine-glycine (215).
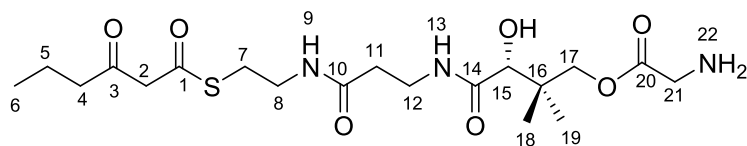
The obtained product was a yellow oil (13 mg, 0.03 mmol, 20%). **^{1}H-NMR** (D$_2$O, 400 MHz): δ 0.87 (t, J = 7.6, 3H, 6-CH$_3$); 0.98 (s, 3H, 18-CH$_3$); 1.00 (s, 3H, 19-CH$_3$); 1.54-1.62 (m, 2H, 5-CH$_2$); 2.48 (t, J = 7.1, 2H, 11-CH$_2$); 2.62 (t, J = 7.3, 2H, 4-CH$_2$); 3.11 (t, J = 6.4, 2H, 7-CH$_2$); 3.40 (t, J = 7.0, 2H, 12-CH$_2$); 3.49-3.52 (m, 2H, 8-CH$_2$); 3.99 (s, 2H, 21-CH$_2$); 4.02 (s, 1H, 15-CH) 4.09 (d, J = 11.4, 1H, 17-CH$_2$); 4.19 (d, J = 11.4, 1H, 17-CH$_2$). **^{13}C-NMR** (D$_2$O, 100 MHz): δ 13.5 (6-CH$_3$); 16.5 (5-CH$_2$); 19.4 (18-CH$_3$); 20.3 (19-CH$_3$); 28.5 (7-CH$_2$); 35.1 (16-C); 35.4 (11-CH$_2$); 37.6 (12-CH$_2$); 38.5 (8-CH$_2$); 39.8 (21-CH$_2$); 46.1 (4-CH$_2$); 71.6 (17-CH$_2$); 74.6 (15-CH); 168.1 (20-CO); 173.9 (10-CO); 174.5 (14-CO); 195.9 (1-COS); 208.8 (3-CO). **ES-MS:** m/z (%): 470 [M+Na]H$^+$ (8%), 448 [M]H$^+$ (100%). **HR-MS:** m/z (%): calculated 484.2093, found 484.2094.

3-Oxo-2-methyl-hexanoyl-pantetheine-glycine (216).
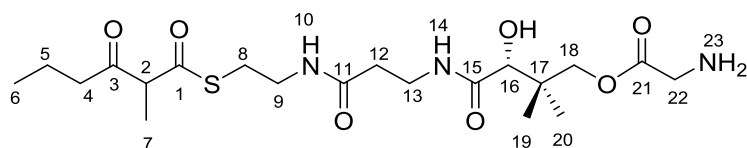
The obtained product was a yellow oil (30 mg, 0.06 mmol, 10%). **^{1}H-NMR** (D$_2$O, 400 MHz): δ 0.87 (t, J = 7.6, 3H, 6-CH$_3$); 0.97 (s, 3H, 19-CH$_3$); 0.99 (s, 3H, 20-CH$_3$); 1.44 (s, 3H, 7-CH$_3$); 1.51-1.60 (m, 2H, 5-CH$_2$); 2.46 (t, J = 7.1, 2H, 12-CH$_2$); 2.66 (t, J = 7.1, 2H, 4-CH$_2$); 3.09 (t, J = 6.2, 2H, 8-CH$_2$); 3.39 (t, J = 6.3, 2H, 13-CH$_2$); 3.47-3.51 (m, 2H, 9-CH$_2$); 3.98 (s, 2H, 22-CH$_2$); 4.01 (s, 1H, 16-CH) 4.09 (d, J = 11.4, 1H, 18-CH$_2$); 4.19 (d, J = 11.4, 1H, 18-CH$_2$). **^{13}C-NMR** (D$_2$O, 100 MHz): δ 12.7 (7-CH$_3$); 13.5 (6-CH$_3$); 16.6 (5-CH$_2$); 19.4 (19-CH$_3$); 20.3 (20-CH$_3$); 27.6 (8-CH$_2$); 35.1 (17-C); 35.4 (12-CH$_2$); 37.6 (13-CH$_2$); 38.5 (9-CH$_2$); 39.8 (22-CH$_2$); 43.7 (4-CH$_2$); 71.6 (18-CH$_2$); 74.6 (16-CH); 168.1 (21-CO); 173.9 (11-CO); 174.5 (15-CO); 199.9 (1-COS); 211.8 (3-CO). **ES-MS:** m/z (%): 484 [M+Na]H$^+$ (9%), 462 [M]H$^+$ (100%). **HR-MS:** m/z (%): calculated 484.2093, found 484.2094.[192]

2E-2-Methylhex-2-enoylpantetheine-glycine (218).
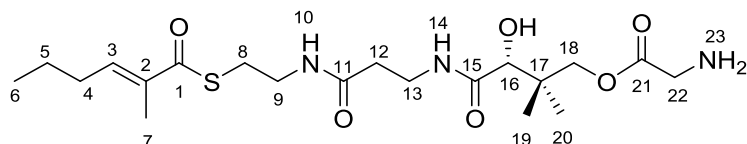
The obtained product was a yellow oil (14 mg, 0.03 mmol, 60%). **^{1}H-NMR** (D$_2$O, 400 MHz): δ 0.91 (t, J = 7.2, 3H, 6-CH$_3$); 0.97 (s, 3H, 19-CH$_3$); 0.98 (s, 3H, 20-CH$_3$); 1.44-1.53 (m, 2H, 5-CH$_2$); 1.86 (s, 3H, 7-CH$_3$); 2.24 (q, J = 7.2, 2H, 4-CH$_2$); 2.46 (t, J = 6.7, 2H, 12-CH$_2$); 3.08 (t, J = 6.1, 2H, 8-CH$_2$); 3.40 (t, J = 6.5, 2H, 13-CH$_2$); 3.44-3.53 (m, 2H, 9-CH$_2$); 3.98 (s, 2H, 22-CH$_2$); 4.00 (s, 1H, 16-CH) 4.09 (d, J =

11.4, 1H, 18-CH$_2$); 4.19 (d, J = 11.4, 1H, 18-CH$_2$); 6.80 (dt, J = 1.4, J = 7.6, 1H, 3-CH). **^{13}C-NMR** (D$_2$O, 100 MHz): δ 11.7 (7-CH$_3$); 13.1 (6-CH$_3$); 19.4 (19-CH$_3$); 20.3 (20-CH$_3$); 21.2 (5-CH$_2$); 27.9 (8-CH$_2$); 30.3 (4-CH$_2$); 35.1 (17-C); 35.4 (12-CH$_2$); 37.6 (13-CH$_2$); 38.7 (9-CH$_2$); 39.8 (22-CH$_2$); 71.6 (18-CH$_2$); 74.6 (16-CH); 135.7 (2-C); 143.9 (3-CH); 168.1 (21-CO); 173.7 (11-CO); 174.3 (15-CO); 197.5 (1-COS). **ES-MS:** m/z (%): 468 [M+Na]H$^+$ (22%), 446 [M]H$^+$ (100%). **HR-MS:** m/z (%): calculated 468.2144, found 468.2144.[192]

2*RS*-2-Methyl-hexanoylpantetheine-glycine (219).
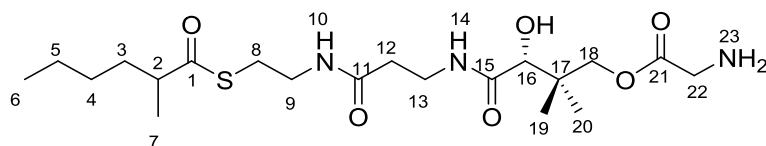
The obtained product was a yellow oil (23 mg, 0.05 mmol, 12%). **^{1}H-NMR** (D$_2$O, 400 MHz): δ 0.86 (t, J = 7.7, 3H, 6-CH$_3$); 0.97 (s, 3H, 19-CH$_3$); 0.99 (s, 3H, 20-CH$_3$); 1.14 (d, J = 6.8, 3H, 7-CH$_3$); 1.26-1.30 (m, 4H, 4-5-CH$_2$); 1.41-1.66 (m, 2H, 3-CH$_2$); 2.47 (t, J = 6.8, 2H, 12-CH$_2$); 2.72-2.78 (m, 1H, 2-CH); 3.04 (t, J = 6.3, 2H, 8-CH$_2$); 3.38 (t, J = 6.5, 2H, 13-CH$_2$); 3.45-3.54 (m, 2H, 9-CH$_2$); 3.98 (s, 2H, 22-CH$_2$); 4.00 (s, 1H, 16-CH) 4.09 (d, J = 11.4, 1H, 18-CH$_2$); 4.19 (d, J = 11.4, 1H, 18-CH$_2$). **^{13}C-NMR** (D$_2$O, 100 MHz): δ 13.1 (6-CH$_3$); 17.2 (7-CH$_3$); 19.4 (197-CH$_3$); 20.3 (20-CH$_3$); 22.2 (5-CH$_2$); 27.9 (8-CH$_2$); 28.7 (4-CH$_2$); 33.4 (3-CH$_2$); 35.1 (17-C); 35.4 (12-CH$_2$); 37.6 (13-CH$_2$); 38.7 (9-CH$_2$); 39.8 (22-CH); 48.3 (2-CH); 71.6 (18-CH$_2$); 74.6 (16-CH); 168.1 (21-CO); 173.6 (11-CO); 174.5 (15-CO); 208.5 (1-COS). **ES-MS:** m/z (%): 470 [M+Na]H$^+$ (13%), 448 [M]H$^+$ (100%). **HR-MS:** m/z (%): calculated 448.2481, found 448.2481.[192]

6.2.8 Synthesis of DH Domain substrates

(2*R*, 3*R*)-3-(*tert*-Butyldimethylsilyloxy)-2-methyl-ethylbutanoate (184).
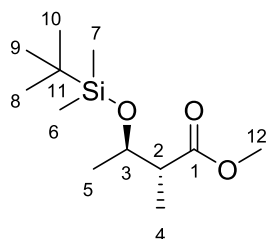
Anhydrous THF (40 mL) was cooled down to -78 °C under nitrogen. Then LDA (21 mL, 2 mol/L) and 3-hydroxy-ethylbutanoate (2.5 g, 18.9 mmol) were added dropwise. The solution stirred for 30 min. Then methyl iodide (50 mL, 2 mol/L) was added dropwise at -78 °C. The reaction stirred for 1.5 h and was then warmed up to 20 °C. It was quenched with 1 M HCl (30 mL). The phaseswere separated and the aqueous phase was adjusted to pH 1 with 1 M HCl and extracted with ethyl acetate (3 × 50 mL). The organic phaseswere combined, dried (MgSO4), filtered and concentrated *in vacuo*. A brown solution was obtained. This was used in the next step without further purification. The resulting residue was dissolved in dry dichloromethane (60 mL) under nitrogen. Then pyridine (3.2 mL, 39.7 mmol) was added and the solution was cooled to 0 °C. *tert*-butyldimethylsilyl triflate (5.2 mL, 22.7 mmol) was added dropwise. A

white solid was precipitated. The reaction stirred at 20 °C for 1 hour. Then it was quenched with $NaHCO_3$ (20 mL). The solid dissolved in the aqueous phase, which was extracted with dichloromethane (2 × 50 mL). The organic phaseswere combined, dried (MgSO4), filtered and concentrated *in vacuo*. The residue was purified two times by flash column chromatography (hexane/ethyl acetate 97/3), which afforded 40 as a yellow oil (0.45 g, 1.8 mmol, 10.7% over two steps). R_f: 0.3 (hexane/ethyl acetate 97/3). **¹H-NMR** (400 M, CDCl₃): δ (ppm) = 0.02 (s, 3H, 6-CH₃), 0.05 (s, 3H, 7-CH₃), 0.85 (s, 9H, 8-9-10-CH₃), 1.08 (d, *J*= 7.05, 3H, 4-CH₃), 1.11 (d, *J*= 6.16, 3H, 5-CH₃), 2.50 (m, 1H, 2-CH), 3.66 (s, 3H, 12-CH₃), 4.00 (m, *J*= 6.15, 1H, 3-CH). **¹³C-NMR** (100 M, CDCl₃): δ (ppm) = −5.1 (6-CH₃), −4.3 (7-CH₃), 12.7 (4-CH₃), 17.9 (11-C), 20.6 (5-CH₃), 25.7 (8-9-10-CH₃), 48.1 (2-CH), 51.4 (12-CH₃), 70.2 (3-CH), 125.6 (1-CO). **ES-MS:** *m/z* (%): 261 [M]H⁺ (60%), 284 [M+Na]H⁺ (10%), 302 [M+CH₃CN]H⁺ (100%), 259 [M]H⁺ (20%).[150]

(2*R*, 3*R*)- (3-(*tert*-Butyldimethylsiloxy)-2-methylbutanoic acid (185).
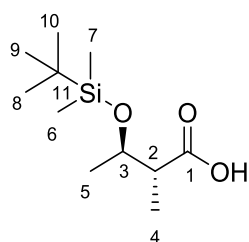
The methyl Ester (0.45 g, 1.8 mmol,) was dissolved in THF (5 mL) and MeOH (12 mL). Then LiOH (0.15 g, 3.6 mmol) in water (2 mL) was added. The reaction mixture was heated to 60 °C overnight. Then it was diluted with water (10 mL). The aqueous phase was extracted with Et_2O (2 × 20 mL). Then it was acidified to pH 3 with H_2SO_4 (6 M) and further extracted with ethyl acetate (3 × 15 mL). The organic layers were combined, dried (MgSO₄), filtered and concentrated *in vacuo*. The yellow residue was purified by column chromatography (10% ethyl acetate/ hexane/ 0.5% acetic acid). A yellow oil was afforded (0.38 g, 1.6 mmol, 89%). R_f: 0.3. **¹H-NMR** (400 M, CDCl₃): δ (ppm) = 0.10 (s, 3H, 6-CH₃), 0.12 (s, 3H, 7-CH₃), 0.9 (s, 9H, 8-9, -10-CH₃), 1.22 (d, *J*= 7.21, 3H, 4-CH₃), 1.24 (d, *J*= 6.24, 3H, 5-CH₃), 2.53 (m, 1H, 2-CH), 3.98 (m, 1H, 3-CH). **¹³C-NMR** (100 M, CDCl₃): δ (ppm) = −5.1 (6-CH₃), −4.4 (7-CH₃), 14.4 (4-CH₃), 17.9 (11-C), 21.5 (5-CH₃), 25.7 (8-9-10-CH₃), 47.4 (2-CH), 70.6 (3-CH). **IR (ν = cm⁻¹):** 2955 (C-H), 2930 (C-H), 2886 (C-H), 2857 (C-H), 1707 (C=O). **ES-MS:** *m/z* (%): 233 [M]H⁺ (90%), 215 [M+H₂O]H⁺ (10%), 256 [M+Na]H⁺ (20%), 231 [M]H⁺ (100%). **HR-MS**: m/z (%): calculated: 231.1407, found: 231.1416.[150]

(2*R*, 3*R*)-3-(*tert*-Butyldimethylsilyloxy)-2-methylbutyl pantetheine dimethyl ketal (186).
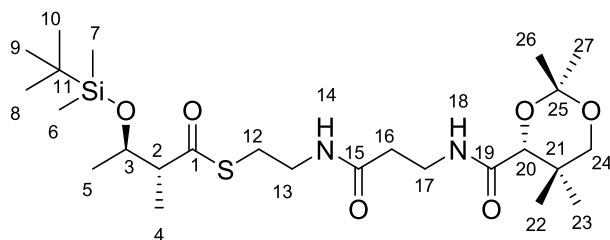
The protected acid (0.38 g, 1.6 mmol) was mixed with EDCI (0.31 g, 1.6 mmol), DMAP (0.1 eq, 11.5 mg, 0.1 mmol) and pantetheine dimethyl ketal (0.51 g, 1.6 mmol) and dissolved in dichloromethane (8 mL). The reaction mixture stirred for 22 hours. It was quenched with 2 M HCl (20 mL). The aqueous phase was extracted with dichloromethane (3 × 25 mL). The organic phaseswere combined, dried (MgSO$_4$), filtered and concentrated *in vacuo*. Flash chromatography (ethyl acetate) afforded a colourless oil (0.64 g, 1.2 mmol, 75%). R$_f$:0.5 (ethyl acetate). **^{1}H-NMR** (400 M, CDCl$_3$): δ (ppm) = 0.00 (s, 3H, 6-CH$_3$), 0.04 (s, 3H, 7-CH$_3$), 0.85 (s, 9H, 8-9-10-CH$_3$), 0.91 (s, 3H, 23-CH$_3$), 0.97 (s, 3H, 22-CH$_3$), 1.09 (m, 3H, 5-CH$_3$), 1.11 (m, 3H, 4-CH$_3$), 1.42 (s, 3H, 27-CH$_3$), 1.46 (s, 3H, 26-CH$_3$), 2.41 (t, 2H, 16-CH$_2$), 2.68 (m, 2H, 12-CH$_2$), 2.95 (m, 1 H, 2-CH), 3.27 (d, *J*= 11.67, 1H, 24b-CH$_2$), 3.42 (m, 2H, 17-CH$_2$), 3.57 (m, 2H, 13-CH$_2$), 3.67 (d, *J*= 11.75, 1H, 24a-CH$_2$), 4.02 (m, 1H, 3-CH), 4.07 (s, 1H, 20-CH), 6.09 (t, *J* = 5.63, 1H, 14-NH), 7.03 (t, *J*= 5.85, 1H, 18-NH). **^{13}C-NMR** (100 M, CDCl$_3$): δ (ppm) = −5.2 (6-CH$_3$), −4.3 (7-CH$_3$), 14.2 (4-CH$_3$), 18.0 (11-C), 18.7 (22-CH$_3$), 19.0 (23-CH$_3$), 21.7 (5-CH$_3$), 25.7 (8-9-10-CH$_3$), 28.3 (12-CH$_2$), 29.5 (27-CH$_3$), 30.0 (26-CH$_3$), 33.0 (17-CH$_2$), 34.8 (16-CH$_2$), 36.0 (21-C), 39.7 (13-CH$_2$), 56.7 (2-CH), 70.1 (3-CH), 71.0 (24-CH$_2$), 77.7 (20-CH), 99.1 (25-C), 170.1 (15-CO), 171.1 (19-CO), 202.7 (1-COS). **IR (ν = cm^{-1}):** 2953 (C-H), 2930 (C-H), 2857 (C-H), 1655 (C=O). **ES-MS:** *m*/*z* (%): 533 [M]H$^+$ (100%), 556 [M+Na]H$^+$ (5%), 531 [M]H$^+$ (10%). **HR-MS**: m/z (%): calculated: 555.2900, found: 555.2897.[150]

(2*R*, 3*R*)- 3-Hydroxy-2-methylbutyrylpantetheine (187).
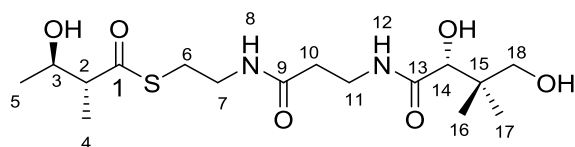
The compound (0.64 g, 1.2 mmol) was dissolved in dichloromethane (1 mL). Then trifluoroacetic acid (0.2 mL) was added and the reaction stirred for 10 min. Water (1 mL) was added and it stirred for further 10 min. The product was purified by HPLC, which afforded a colourless oil (0.13 g, 0.3 mmol, 25%). **^{1}H-NMR** (400 M, CDCl$_3$): δ (ppm) = 0.92 (s, 3H, 17-CH$_3$), 1.02 (s, 3H, 16-CH$_3$), 1.13 (d, *J*= 7.03, 3H, 4-CH$_3$), 1.24 (d, *J*= 6.26, 3H, 5-CH$_3$), 2.40 (m, 2H, 10-CH$_2$), 2.66 (m, 2H, 6-CH$_2$), 2.85 (m, 1H, 2-CH), 3.25 (m, 1H, 18b-CH$_2$), 3.48 (m, 2H, 11-CH$_2$), 3.59 (m, 2H, 7-CH$_2$), 3.73 (m, 2H, 18-CH$_2$), 3.95 (m, 1H, 3-CH), 4.02 (s, 1H, 14-CH), 6.43 (t, *J*= 5.08, 1 H, 8-NH), 7.40 (t, *J*= 6.00, 1 H, 12-NH). **^{13}C-NMR** (100 M, CDCl$_3$): δ (ppm) = 14.9 (4-CH$_3$), 20.3 (5-CH$_3$), 21.2 (17-CH$_3$), 21.7 (16-CH$_3$), 28.8 (6-CH$_2$), 35.4 (11-CH$_2$), 35.7 (10-CH$_2$), 38.8 (15-C), 39.3 (7-CH$_2$), 56.6 (C2), 70.3 (3-CH), 70.9 (18-CH$_2$), 77.7 (14-CH), 171.9 (9-CO), 174.2 (13-CO), 203.8 (1-COS). **HR-MS**: m/z (%): calculated: 401.1722, found: 401.1718.[150]

6.2.9 Synthesis of AT Domain Substrates

[1*S*-[1α(4*R*, 5*S*)3α, 4β, 5α, 6α, 7β]]-1-(4-Hydroxy-5-methyl-3-methylene-6-phenyl-hexyl)-4, 6, 7-trihydroxy-2, 8-dioxabicyclo[3.2.l]octane-3, 4, S-tricarboxylic-acid (Full hydrolysis of Squalestatin S1) (245).[97]
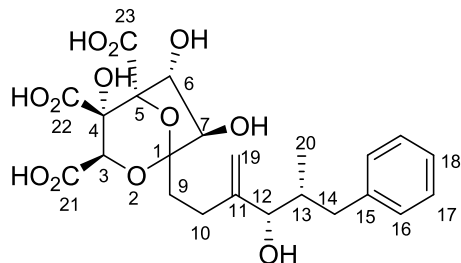
To a solution of Squalestatin S1 (0.10 g, 0.14 mmol) in ethanol/water 5:1 (5 ml/ 1 ml) potassium hydroxide (0.66 g, 11.00 mmol) was added. After stirring under reflux for 3 hours diethyl ether was added. The mixture was washed with $NaHCO_3$ (3x 10 ml). The aqueous layer was acidified with 2M HCl until pH 1 and extracted with ethyl acetate (3x 10 ml). The organic layer was dried over $MgSO_4$ and concentrated under vacuo. 0.01 g (0.02 mmol, 14%) of the product were purified by HPLC. **^{1}H-NMR** (CD$_3$CN, 400 MHz): δ 0.82 (d, 3H, J = 6.9, 20-CH$_3$), 1.98-2.50 (m, 5H, 9-10-14-CH$_2$); 2.75 (m, 1H, dd, *J* = 5, 13, CH$_2$Ph), 3.93 (d, 1H, *J* = 4.9, 12-CH), 4.05 (d, 1H, *J* = 2.0, 7-CH); 4.95-4.99 (m,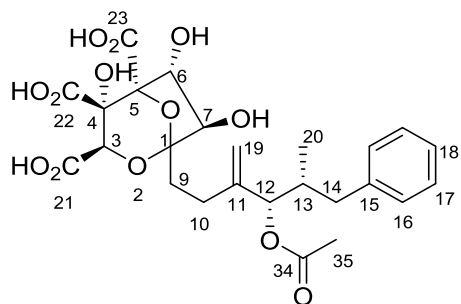 2H, 19-CH$_2$); 5.05-5.09 (m, 1H, 6-CH); 5.12 (s, 1H, 3-CH); 7.10-7.23 (m, 2H, 16-18-CH); 7.27-7.32 (m, 1H, 17-CH). **ES-MS:** *m/z* (%): 519 [M+Na]H$^+$ (12%), 497 [M]H$^+$ (27%).

[1*S*-[1α(4*R*, 5*S*)3α, 4β, 5α, 6α, 7β]]-1-(4-Hydroxy-5-methyl-3-methylene-6-phenyl-hexyl)-4, 6, 7-trihydroxy-2, 8-dioxabicyclo[3.2.l]octane-3, 4, S-tricarboxylic-acid (Full hydrolysis of Squalestatin S1) (244).[97]

To A solution of Squalestatin S1 (0.10 g, 0.14 mmol) in ethanol/water 5:1 (5 ml/ 1 ml) potassium hydroxide (0.044 g, 0.08 mmol) was added. After stirring under reflux for 3 hours diethyl ether was added. The mixture was washed with $NaHCO_3$ (3x 10 ml). The aqueous layer was acidified with 2M HCl until pH 1 and extracted with ethyl acetate (3x 10 ml). The organic layer was dried over $MgSO_4$ and concentrated under vacuo. 0.01 g (0.018 mmol, 13%) of the product were purified by HPLC. **^{1}H-NMR (CD$_3$CN, 400 MHz):** δ 0.85 (d, 3H, *J* = 7.6, 20-CH$_3$), 1.96-2.38 (m, 4H, 9-10-CH$_2$); 2.08 (s, 3H, 35-CH$_3$), 2.48 (dd, 1H, *J* = 5, 13, 14-CH$_2$), 2.68 (dd, 1H, *J* = 5, 13, 14-CH), 4.04 (d, 1H, *J* = 2.1, 7-CH); 4.92-5.11 (m, 3H, 6-12-19-CH/CH$_2$); 5.11 (s, 1H, 1-CH), 7.19-7.22 (m, 2H, 16-18-CH); 7.28-7.32 (m, 1H, 17-CH). **ES-MS:** *m/z* (%): 556 [M+H$_2$O]H$^+$ (12%), 539 [M]H$^+$ (27%), 497 [M-C$_2$H$_3$O] 100%.

[1S-[1α(4R, 5S)3α, 4β, 5α, 6α, 7β]]-1-(4-Hydroxy-5-methyl-3-methylene-6-phenyl-hexyl)-4, 6, 7-trihydroxy-2, 8-dioxabicyclo[3.2.l]octane-3, 4, S-tricarboxylic-acid (Full hydrolysis of Squalestatin S1) (246).[97]
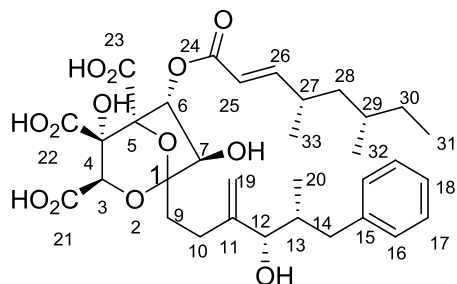

To A solution of Squalestatin S1 (0.10 g, 0.14 mmol) in ethanol/water 5:1 (5 ml/ 1 ml) potassium hydroxide (0.044 g, 0.08 mmol) was added. After stirring under reflux for 3 h diethyl ether was added. The mixture was washed with $NaHCO_3$ (3x 10 ml). The aqueous layer was acidified with 2M HCl until pH 1 and extracted with ethyl acetate (3x 10 ml). The organic layer was dried over $MgSO_4$ and concentrated under vacuo. 0.01 g (0.015 mmol, 11%) of the product were purified by HPLC. **^{1}H-NMR** (CD$_3$CN, 400 MHz): δ 0.85 (m, 9H, 20-31-33-CH$_3$), 1.03 (d, 3H, J = 6.4, 32-CH$_3$), 1.10-1.15 (m, 2H, 28-30-CH$_2$); 1.24-1.42 (m, 3H, 28-29-30-CH$_2$/CH); 1.99-2.23 (m, 4H, 9-10-13-CH$_2$/CH); 2.35-2.51 (m, 3H, 10-14-27-CH$_2$/CH), 2.72 (dd, 1H, J = 5, 13, 14-CH), 3.92 (d, 1H, J = 4.9, 12-CH), 4.12 (d, 1H, J = 2.0, 7-CH), 4.96 (s, 1H, 19- CH$_2$); 5.08 (s, 1H, 19-CH$_2$); 5.75 (dd, 1H, J = 1.0, 16.0, 25-CH); 6.74-6.85 (m, 1H, 26-CH); 7.16-7.22 (m, 2H, 16-18-CH); 7.26-7.30 (m, 1H, 17-CH). **ES-MS:** m/z (%):649 [M]H$^+$ (27%), 631 [M-H$_2$O]H$^+$ (100%), 613 [M-2x H$_2$O]H$^+$ (62%).

Preparation of 4-6-dimethyloct-2-enoyl-CoA (248).
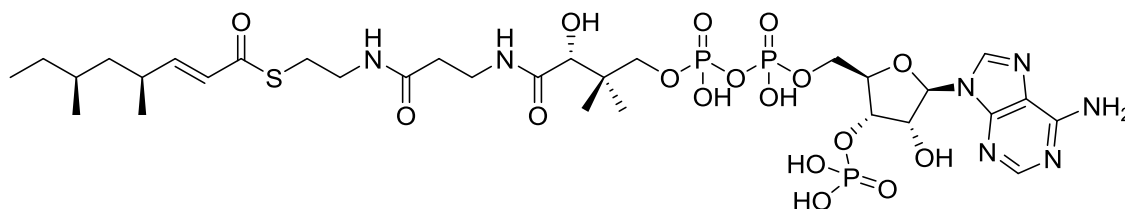
To a solution of (4S, 6S)- Dimethyloctenoic acid (10 mg, 0.05 mmol) in fresh destillated THF (1mL) was added carbonyldiimidazole (10 mg, 0.06 mmol). This solution was controlled by LCMS to a complete activation of the acid (nearly 1 h). After that Coenzyme A (47 mg, 0.06 mmol) in 1 mL water was added to the solution and controlled by LCMS. The product was only analysed by LCMS and directly used reasoned on the instability of the compound.[97]

Preparation of 2-methylhex-2-enoyl-CoA (263).
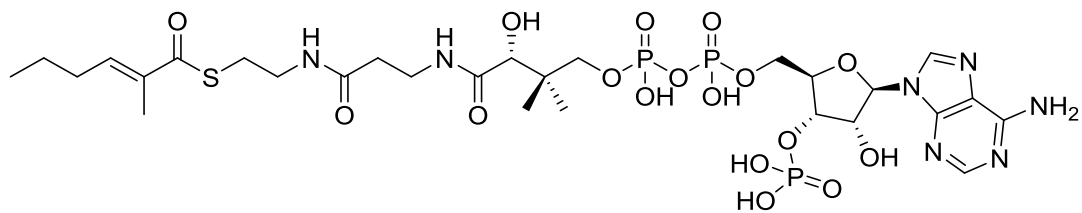
To a solution of 2-methylhexenoic acid (10 mg, 0.07 mmol) in fresh destillated THF (1mL) was added carbonyldiimidazole (12 mg, 0.08 mmol). This solution was controlled by LCMS to a complete activation of the acid (nearly 1 h). After that Coenzyme A (60 mg, 0.08 mmol) in 1 mL water was added to the solution and controlled by LCMS. The product was only analysed by LCMS and directly used reasoned on the instability of the compound.[97]

7.0 Biochemical and Biophysical Investigations

7.1 SQTKS-ER domain

Transformation of pET28-SQTKS-ER into *E. coli* Top10

50 μL chemically competent *E. coli* Top10 cells were thawed on ice and incubated on ice for 30 min with 1 μL of the appropriate vector. For the heat shock transformation, the cells were incubated at 42 °C for 30 s, then immediately chilled on ice for 2 min. 250 μL SOC medium were added. The transformed cells were shaken (200 rpm) for 1 h at 37 °C. Positive clones were selected by plating 50 - 150 μl of the cells on solid LB medium containing the appropriate antibiotic. The cells were grown over night at 37 °C.

Transformation of pET28-SQTKS-ER into *E. coli* BL21

50 μL chemically competent *E. coli* BL 21 cells were thawed on ice and incubated on ice for 30 min with 1 μL of the SQTKS-ER domain. For the heat shock transformation, the cells were incubated at 42 °C for 10 s, then immediately chilled on ice for 2 min. 800 μl SOC medium were added. The transformed cells were shaken (200 rpm) for 1 h at 37 °C. Positive clones were selected by plating 50 - 150 μL of the cells on solid LB medium containing the appropriate antibiotic. The cells were grown over night at 37 °C.

Protein expression and purification

A starter culture was prepared by scraping the surface of a glycerol stock of *E.coli* BL21 transformed with pET28-ER. The cells were grown in LB media with kanamycin (50 mg/mL) and incubated at 37 °C, 200 rpm, over night. 1 ml of the starter culture was added to 100 mL 2TY media. The cells were incubated to an OD_{600} of 0.6, then the flask was cooled down to 16 °C and induced with 50 μl 1M IPTG solution. This solution was incubated over night at 16 °C, 200rpm.

To isolate the protein, the media was centrifuged at 7000 rpm for 15 min and the pellet was collected. The cells could be used immediately or frozen at -80 °C. The cells were suspended in 50 ml of nickel column wash buffer (50 mM Tris pH 8, 150 mM NaCl, 20% glycerol (v/v) and 20 mM imidazole) and sonicated on ice for 6.5 minutes. Every 30 second the sonicator was switched on and of. The rest of the solution was centrifuged at 8500 rpm for 30 min, filtered and purified by a nickel column*. For this a linear gradient of elution buffer (50 mM Tris pH 8, 150 mM NaCl, 20% glycerol (v/v) and 0.5 M imidazole) was used. The fractions were checked by SDS gel and the fractions with the correct mass were combined and concentrated. A second purification was done by a size exclusion column chromatography**. The protein solution was loaded onto the column and eluted with size exclusion elution buffer (Buffer: 50 mM Tris pH 8, 150 mM NaCl, 20% glycerol (v/v)). The fractions were analyzed again by SDS gel and the protein with the correct mass and high purity was combined and concentrated. The concentration of protein was estimated by a calculated absorption coefficient $\varepsilon = 0.69$ at 280 nm. After that the protein was divided into several aliquots and stored at - 80 °C.[104]

*Nickel column Protino Ni-NTA Columns 5 mL
**Size exclusion column- HiLoad 26/600 Superdex 200pg (GE Healthcare), 320 ml.

SQTKS-ER Domain Comparison SNAC/Pantetheine Assays

Assays with acyl-SNAC substrates were performed using stocks of acyl-SNAC (10 mM), NADPH (10 mM), Tris pH 8.5 (1 M), glycerol (50% v/v) and SQTKS-ER (0.2 mU/µl). Assays were conducted at (final concentration, volume of stock): acyl-SNAC (0.5 mM, 10 µl), NADPH (0.75 mM, 15 µl), Tris buffer pH 8.5 (50 mM, 10 µL), glycerol (20% v/v, 80 µL), SQTKS-ER (4 mU, 20 µL) and water (65 µL), to a total volume of 200 µL.

Assays with acyl PANT substrates were performed using stocks of acyl PANT (10 mM), NADPH (10 mM), Tris pH 8.5 (1 M), glycerol (50% v/v) and SQTKS-ER (0.2 mU/µL). Assays were conducted at (final concentration, volume of stock): acyl PANT (0.5 mM, 10 µL), NADPH (0.75 mM, 15 µL), Tris buffer pH 8.5 (50 mM, 10 µL), glycerol (20% v/v, 80 µl), SQTKS-ER (1 mU, 5 µL) and water (80 µL), to a total volume of 200 µL.

SQTKS-ER Domain Kinetic Assays

Assays were run in 500 µL quartz cuvettes with a path length of 1 cm and the absorption was measured at 340 nm against a standard cuvette at 25 ˚C. Assays with acyl PANT substrates were performed using stocks of acyl PANT (5 mM), NADPH (10 mM), Tris pH 8.5 (1 M), glycerol (50% v/v) and SQTKS-ER (0.08 U/µl). Assays were conducted at (final concentration, volume of stock): acyl PANT (62.5 µM – 500 µM, 5 - 40 µl); NADPH (250 µM, 10 µl); SQTKS-ER (20 µL, 4 mU); Buffer (330 - 365 µl) in a total volume 400 µl. Reactions were run in triplicate. Initial rates were plotted vs substrate concentration.*

*10 µLTris pH 8.5 (1 M), 80 µL glycerol (50% v/v), 100 µL water

Polymerase-chain-reaction (PCR)

The successful transformation of BL21 cells was configured by PCR. For standard PCR amplification the Taq DNA polymerase NEB was used according to the manufacturer's instruction. For a colony PCR the template was added by transferring a small part of a single *E.coli* colony into the reaction mixture using a sterile toothpick. For each primer pair the specific annealing temperature was determined in a PCR temperature gradient. For efficient DNA amplification 30 PCR cycles were applied.

Bradford assay

Standard solutions of bovine serum albumin (0.1-2 ml/ml) in size exclusion buffer [50 mM Tris pH 8, 150 mM NaCl, 20% glycerol (v/v)] were prepared by serial dilution. 100 µl of the standards were mixed with Bradford dye reagent (1 ml) and incubated for 15 mins at RT. The absorption of each sample was measured at 595 nm against a standard (size exclusion buffer 100 µl, Bradford dye reagent, 1 ml) to construct a standard concentration curve. A sample of the protein to be quantified (20 µl) was diluted in size exclusion buffer (80 µl) and treated with Bradford dye reagent (1ml). This was incubated at room temperature for 15 mins and then the absorption was measured at 595 nm. This was compared to the previously prepared concentration curve to calculate the amount of protein that had been produced.

7.2   SQTKS-DH Domain

Transformation of pET28-SQTKS-DH into _E. coli_ BL21

50 μL chemically competent _E. coli_ BL 21 cells were thawed on ice and incubated on ice for 30 min with 1 μl of the SQTKS-DH domain. For the heat shock transformation, the cells were incubated at 42 °C for 10 s, then immediately chilled on ice for 2 min. 800 μl SOC medium were added. The transformed cells were shaken (200 rpm) for 1 h at 37 °C. Positive clones were selected by plating 50 - 150 μl of the cells on solid LB medium containing the appropriate antibiotic. The cells were grown over night at 37 °C.

Protein expression and purification

A starter culture was prepared by scraping the surface of a glycerol stock of _E.coli_ BL21 transformed with pET28-DH. The cells were grown in LB media with carbenicillin (stock 50 mg/mL concentration 50 μL / 50 mL) and incubated at 37 °C, 200 rpm, over night. 1 ml of the starter culture was added to 100 mL LB media. The cells were incubated to an OD_{600} of 0.6, then the flask were cooled down to 14 °C and induced with 50 μl 1M IPTG solution. This solution was incubated over night at 14 °C, 200rpm.

To isolate the protein, the media was centrifuged at 7000 rpm for 15 min and the pellet was collected. The cells could be used immediately or frozen at -80 °C. The cells were suspended in 50 ml of nickel column wash buffer (20 mM Tris pH 8, 150 mM NaCl, 10% glycerol (v/v), 5 mM imidazole, 25 mM L-Arginine and L-Glutamic acid) and sonicated on ice for 6.5 minutes. Every 30 second the sonicator was switched on and of. The rest of the solution was centrifuged at 8500 rpm for 30 min, filtered and purified by a nickel column*. For this a linear gradient of elution buffer (20 mM Tris pH 8, 150 mM NaCl, 10% glycerol (v/v), 0.4 M imidazole, 25 mM L-Arginine and L-Glutamic acid) was used. The fractions were checked by SDS gel and the fractions with the correct mass were combined and concentrated to 14 mL. Reasoned on precipitation in the present of imidazole the protein was desalted with a HiPrepTM 26/10 desalting column. One and a half column volumes were used (20 mM Tris-HCl pH 8, 150 mM NaCl, 10 % glycerol, 25 mM L-Arginine and L-Glutamic acid) and collected in fractions. These fractions were analysed by SDS gel and concentrated.

SQTKS-DH Domain Assays: Assays were run in 500 μl quartz cuvettes with a path length of 1 cm and the absorption was measured at 260 nm against a standard cuvette at 25 ˚C. Assays with acyl PANT substrates were performed using stocks of acyl PANT (5 mM), Tris pH 8.5 (1 M), glycerol (50% v/v) and SQTKS-DH (0.01 U/min).

Assays were conducted at (final concentration, volume of stock): acyl PANT (62.5 μM - 500 μM, 5-40 μl); SQTKS-DH (20 μL); Buffer (340– 375 μl) in a total volume 400 μl. Reactions were run in triplicate. Initial rates were plotted vs substrate concentration.*

*10 μLTris pH 8.5 (1 M), 80 μL glycerol (50% v/v), 100 μL water

7.3   SPR investigation

Sensorchip installation

SPR sensor chip HC1000m was installed under a continuous flow of 10 μL/min at 20 °C on the SPR equipment. During this installation, double destilled water was used as standard buffer. After successful installation, the whole system was washed for 20 min with double destilled water. The flow rate was settled to 250 μL/min to remove inpurities and air bubbles out of the system.

Surface modification

Modification of the surface was performed in a 10 mM maleate solution that was calibrated to pH 7. A re-buffering of the system with 250 μL/min was performed at 20 °C.

After that modification of the surface was started with an activation mix that contains 100 mM EDCI. The flow rate was settled down to 10 μL/min and an incubation over 15 min was performed. This step was repeated 3 times. The incubated surface was overflowed with the cross linked material at the same flow rate. This step was repeated 3 times. The concentration of the used cross linkers was 10 mmol. Additionally the whole surface was washed with ethanolamine (25 mmol solution) to block possible active residues of the surface that did not interact with the substrate. Finally, several wash runs with double destilled water were processed to clean the surface from potential residues that could influence the final measuring of the system.

Surface plasmon resonance spectroscopy

A re-buffering was performed for the final investigations. Investigations of the ER domain were executed in 50 mM Tris pH 8, 150 mM NaCl, 20% glycerol (v/v), DH domain in 20 mM Tris-HCl pH 8, 150 mM NaCl, 10 % glycerol, 25 mM L-Arginine and L-Glutamic acid.

An overflow of the surface was performed with different protein concentrations (0.25 mg/mL, 0.5 mg/mL, 1 mg/mL, 2 mg/mL, 4 mg/mL, 6 mg/mL and 10 mg/mL). Constant flow rates were used of 10 μL/min and 25 μL/min at 20 °C. Regeneration of the surface was performed with 1.5 M NaCl solution in the same buffer that was used for the loaded protein. Finally the analysis of the interactions was determined with an internal software of the SPR instrument.

7.4   Isothermal Titration Calorimetry

Reference and sample cell were adjusted to 20 °C. In both cells 150 μL reference 0.1 mM solution of SQTKS-ER was added. For the protein stock solution a buffer of 50 mM Tris pH 8, 150 mM NaCl and 20% glycerol (v/v) was used. Same buffer that showed good properties in stability and activity for the enzyme. The ligand tigloylpantetheine (1.4 M) was titrated in the sample cell. Twenty injections were performed over a time of 7000 seconds. The volume of each injection was 2.69 μL of the ligand tigloylpantetheine. Final results were calculated with internal software of the ITC equipment.

8.0   Literature

1. C. Hertweck, *Angew. Chem. Int. Ed.* **2009**, *48*, 4688.
2. K. J. Weisman, *Methods Enzymol.*, **2009**, *459*, 3.
3. Ulrike Holzgrabe, *Pharmazie*, **2005**, *34*, 258.
4. I. Chopra, M. Roberts, *Microbiol. Mol. Boil. Rev.*, **2001**, *65*, 232.
5. J. Cortes, S. F. Haydock, G. A. Roberts, D. J. Bevitt , P. F. Leadlay, *Nature*, **1990**, *348*, 176.
6. M. Kienitz, Infection, **1977**, *5*, 37.
7. L. Hang, N. Liu, Y. Tang, *ACS Catal.*, **2016**, *6*, 5935.
8. P. F. Leadlay, *Current Opinion in Chemical Biology*, **1997**, *1*, 162.
9. J. M. Winter, G. Chiou, I. R. Bothwell, W. Xu, N. K. Garg, M. Luo, Y. Tang, *Org. Lett.*, **2013**, *15*, 3774.
10. B. J. Rawlings, *Nat. Prod. Rep.*, **1997**, *14*, 523-556.
11. B. Shen, *Current Opinion in Chemical Biology*, **2003**, *7*,285.
12. B. S. Moore, Christian Hertweck, *Nat. Prod. Rep.*, **2002**, *19*, 70.
13. D.A. Hopwood, D.H. Sherman, *Annu. Rev. Genet.* **1990**, *24*, 37.
14. A. Witkowski, A. K. Joshi, S. Smith, *Biochemistry*, **2002**, *41*, 10877.
15. Y. A. Chan, A. M. Podevels, B. M. Kevany, M. G. Thomas, *Nat. Prod. Rep.*, **2009**, *26*, 90.
16. B. Sedgewick, J. W. Cornforth, *Eur. J. Biochem.*, **1977**, *75*, 465.
17. A. T. Keatinge-Clay, *Nat. Prod. Rep.*, **2012**, *29*, 1050.
18. A. T. Keatinge-Clay, *Nat. Prod. Rep.*, **2016**, *33*, 141.
19. J. Zheng, A. T. Keatinge-Clay, *MedChemComm*, **2013**, *4*, 34.
20. Y. Kawai, K. Hida, A. Ohno, *Bioorganic Chemistry*, **1999**, *27*, 3.
21. A. T. Keatinge-Clay, *J. Mol. Biol.*, **2008**, *384*, 941.
22. S. B. Bumpus, N. A. Magarvey, N. L. Kelleher, C. T. Walsh, C. T. J. Calderone, *Am. Chem. Soc*. **2008**, 130, 11614.
23. R. M. Kohli, C. T. Walsh, *Chem. Commun.*, **2003**, *125*, 297.
24. M. Kopp, M. A. Marahiel, *Nat. Prod. Rep.*, **2007**, *24*, 735.
25. C. C. Aldrich, L. Venkatraman, D. H. Sherman, R. A. Fecik, *J. Am. Chem. Soc.*, **2005**, *127*, 8910.
26. Y. Xue, D. H. Sherman, *Metabolic Engineering*, **2001**, *3*, 15.
27. S. C. Tsai, H. Lu, D. E. Cane, C. Khosla and R. M. Stroud, *Biochemistry*, **2002**, *41*, 12598.
28. T. Maier, M. Leibundgut, N. Ban, *Science* **2008**, *321*, 1315.
29. D. I. Chan, H. J. Vogel, *J. Biochem.*, **2010**, *430*, 1.
30. R. J. Cox, *Org. Biomol. Chem.*, **2007**, *5*, 2010.
31. J. Piel, *Nat. Prod. Rep.*, **2010**, *27*, 996.
32. J. Dreier, C. Khosla, *Biochemistry*, **2000**, *39*, 2088.
33. Y. Tang, S. C. Tsai, C. Khosla, *J. Am. Soc.*, **2003**, *125*, 12708.
34. K. K. Burson, C. Khosla, *Tetrahedron.*, **2000**, *56*, 9401.
35. M. B. Austin, J. P. Noel, *Nat. Prod. Rep.*, **2003**, *20*, 79.
36. J. M. Jez, J. P. Noel, *J. Biol. Chem.*, **2000**, *275*, 39640.
37. S. Donadio, L. Katz, *Gene* **1992**, *111*, 51.
38. C. M. Kao, L. Katz, C. Khosla, *Science*, **1994**, *265*, 509.
39. R. Pieper, S. Khosla, D. Cane, C. Khosla, *Biochemistry*, **1996**, *35*, 2054.
40. S. J. Moss, C. J. Martin, B. Wilkinson, *Nat. Prod. Rep.* **2004**, *21*, 575.
41. U. Rix , C. Fischer , L. L. Remsing, J. Rohr, *Nat. Prod. Rep.*, **2002**, *19*, 542.
42. J. Moldenhauer, D. C. G. Götz, C. R. Albert, S. K. Bischof, K. Schneider, R. D. Süssmuth, M. Engeser, H. Gross, G. Bringmann, Jörn Piel, *Angew. Chem. Int. Ed.*, **2010**, *49*, 1465.
43. E. Shelest, N. Heimerl, M. Fichtner, S. Sasso, *BMC Genomics*, **2015**, *16*, 1.
44. J. Schümann, C. Hertweck, *J. Biotechnol.*, **2006**, *124*, 690.
45. J. Staunton, K. J. Weissman, *Nat. Prod. Rep.*, **2001**, *18*, 380.
46. I. Fujii, Y. Ono, H. Tada, K. Gomi, Y. Ebizuka, U. Sankawa, *Mol Gen Genet*, **1996**, *253*, 1.

47. J. M. Crawford, B. C. R. Dancy, E. A. Hill, D. W. Udwary, C. A. Townsend, *Proc. Natl. Acad. Sci. USA*, **2006**, *103*, 16728.

48. J. M. Crawford, A. L. Vagstad, K. P. Whitworth, K. C. Ehrlich, C. A. Townsend, *ChemBioChem* **2008**, *9*, 1019.

49. A. L. Vagstad, A. G. Newman, P. A. Storm, K. Belecki, J. Crawford, C. A. Townsend, *Angew. Chem. Int. Ed.*, **2013**, *52*, 1718.

50. J. F. Sanchez, Y. Chiang, E. Szewczyk, A. D. Davidson, M. Ahuja, C. E. Oakley, J. Woo Bok, N. Keller, B. R. Oakley, C. C. C. Wang, *Mol. BioSyst.*, **2010**, *6*, 587.

51. H. Hajjaj, A. Klaebe, M. O. Loret, G. Goma, P. J. Blanc and J. Francois, *Appl. Environ. Microbiol.*, **1999**, *65*, 311.

52. A. M. Bailey, R. J. Cox, K. Harley, C. M. Lazarus, T. J. Simpson, E. Skellam, *Chem. Commun.*, **2007**, 4053.

53. I. Soehano, L. Yang, F. Ding, H. Sun, Z. J. Low, X. Liub, Z.-X. Liang, *Organic & Biomolecular Chemistry*, **2014**, *12*, 8542.

54. H. Sun, C. L. Ho, F. Ding, I. Soehano, X.-W. Liu, Z. Liang, *J. Am. Chem. Soc.*, **2012**, *134*, 11924.

55. T. Moriguchi, Y. Kezuka, T. Nonaka, Y. Ebizuka and I. Fujii, *J. Biol. Chem.*, **2010**, *285*, 15637

56. H. Kage, E. Riva, J. S. Parascandolo, M. F. Kreutzer, M. Tosin, M. Nett, *Org. Biomol. Chem.*, **2015**, *13*, 11414.

57. T. Ugai, A. Minami, R. Fujii, M. Tanaka, H. Oguri, K. Gomi, H. Oikawa *Chem. Commun.*, **2015**, *51*, 1878.

58. J. Kennedy, K. Auclair, S. G. Kendrew, C. Park, J. C. Vederas, C. R. Hutchinson, *Science*, 1999, **284**, 1368.

59. A. O. Zabala , Y. Chooi, M. Seok Choi, H. Lin , Y. Tang, *ACS Chem. Biol.*, **2014**, *9*, 1576.

60. V. Betina, *Folia Microbiol.* **1992**, *37*, 3.

61. T. Maier, S. Jenni, N. Ban, *Science*, **2006**, *311*, 1258.

62. Y. Tang, C. Kim, I. Mathews, D. E. Cane, C. Khosla, *PNAS*, **2006**, 103, 30, 11124.

63. Y. Tang, A. C. Chen, C. Kim, D. E. Cane, C. Khosla, *Chem. Biol.*, **2007**, *14*, 931.

64. J. L. Martin, F. M. McMillan, *Curr. Opin. Struct. Biol.*, **2002**, *12*, 783.

65. P. Wattana-amorn, C. Williams, E. Płoskoń, R. J. Cox, T. J. Simpson, J. Crosby, M. P. Crump, *Biochemistry*, **2010**, *49* , 2186.

66. A T. Keatinge-Clay, *Chemistry and Biology*, **2007**, *14*, 898.

67. A. T. Keatinge-Clay, R. M. Stroud, *Structure*, **2006**, *14*, 737.

68. S. Tsai, B. Ames, *Methods Enzymol.*, **2009**, *459*, 17.

69. S. Anand, D. Mohanty *BMC Structural Biology*, **2012**, 12:10.

70. W. Xu, K. Qiao, Y. Tang, *Crit Rec Biochem Mol.*, **2013**, *48*, 98.

71. D. L. Akey, J. R. Razelun, J. Tehranisa, D. H. Sherman, W. H. Gerwick, J. L. Smith, *Structure*, **2010**, 18, 94.

72. J. Zheng, D. C. Gay, B. Demmler, M. A. White, A. T. Keatinge-Clay, *Nature chemical Biology*, **2012**, *8*, 615.

73. S. Dutta, J. R. Whicher, D. A. Hannsen, W. A. Hale, J. A. Chemler, G. R. Congdon, A. R. Narayan, K. Hakansson, D. H. Sherman, J. L. Smith, G. Skiniotis, *Nature*, **2014**, *31*, 512.

74. K. J. Weissman, *Nature Chemical Biology*, **2015**, *11*, 660.

75. J. Staunton, P. Caffrey, J. F. Aparicio, G. A. Roberts, S. S. Bethell, P. F. Leadlay, *Nat. Struct. Biol.*, **1996**, *35*, 12363.

76. L. Hendrickson, C. R. Davis, C. Roach, D. K. Nguyen, T. Aldrich, P. C. McAda, C. D. Reeves, *Chemistry & Biology*, **1999**, *6*, 429.

77. A. Endo, *J. Antibiot.*, **1979**, *32*, 852.

78. S. M. Ma, J. W. H. Li, J. W. Choi, H. Zhou, K. K. M. Lee, V. A. Moorthie, X. K. Xie, J. T. Kealey, N. A. Da Silva, J. C. Vederas, Y. Tang, *Science*, **2009**, *326*, 589.

79. K. M. Fisch, *RSC Adv.*, **2013**, *3*, 18228.

80. X. Xie, M. J. Meehan, W. Xu, P. C. Dorrestein, Y. Tang, *J. Am. Chem. Soc.*, **2009**, *131*, 8388.

81. R. A. Cacho, J. Thuss, W. Xu, R. Sanichar, Z. Gao, A. Nguyen, J. C. Vederas, Y. Tang, *J. Am. Chem. Soc*, **2015**, *137*, 15688.

82. K. Auclair, A. Sutherland, J. Kennedy, D. J. Witter, J. P. Van den Heever, C. R. Hutchinson, J. C. Vederas, *J. Am. Chem. Soc.*, **2000**, *122*, 11519.

83. C. D. Campbell, J. C. Vederas, *Biopolymers,* **2010**, *93*, 755.

84. M. N. Heneghan, A. A. Yakasai, K. Williams, K. A. Kadir, Z. Wasil, W. Bakee, K. M. Fisch, A. M. Bailey, T. J. Simpson, R. J. Cox, C. M. Lazarus, *Chem. Sci.*, **2011**, *2*, 972.

85. K. L. Eley, L. M. Halo, Z. Song, H. Powles, R. J. Cox, A. M. Bailey, C. M. Lazarus, T. J.

86. Simpson, *ChemBioChem*, **2007**, *8*, 289.

87. T. J. Simpson, *Nat. Prod. Rep.*, **2014**, *31*, 1247.

88. K. M. Fisch, W. Bakeer, A. A. Yakasai, Z. Song, J. Pedrick, Z. Wasil, A. M. Bailey, C. M. Lazarus, T. J. Simpson and R. J. Cox, *J. Am. Chem. Soc.*, **2011**, *133*, 16635.

89. T. Liu, J. F. Sanchez, Y. Chiang, B. R. Oakley, C. C. C. Wang, *Org. Lett.* **2014**, 16, 1676.

90. M. J. Dawson, J. E. Farthing, P. S. Marshall, R. F. Middelton, M. J. O'Neill, A. Shuttleworth, C. Stylli, R. M. Tait, P. M. Taylor, H. G. Wildman, A. D. Buss, D. Langley, M. V. Hayes, *The Journal of Antibiotics*, **1991**, *45*, 639.

91. P. J. Sidebottom, R. M. Highcock, S. J. Lane, P. A. Procopiou and N. S. Watson, *J. Antibiot.*, **1992**, *45*, 648.

92. J. D. Bergstrom, C. Dufresne, G. F. Bills, M. Nallin-Omstead and K. Byrne; *Annual review of microbiology* **1995**, *49*, 607.

93. K. M. Byme, B. H. Arison, M. Nallin-Olmstead, and Louis Kaplan; *J. Org. Chem.* **1993**, 58, 1019.

94. C. Jones, P. J. Sidebottom, R. J. P. Cannell, D. Noble, B. A. M. Rudd; *J. Antibiot.,* **1992***, 45*, 1492.

95. R. F. Middleton, G. Foster, , R. J. P. Cannell; P. J. Sidebottom, N. L. Taylor, D.Noble; *J. Antibiot.*, **1995**, *48*, 311.

96. C. A. Jones, P. J. Sidebottom, R. J. Cannell, D. Noble and B. A. Rudd, *J. Antibiot.*, **1992**, *45*, 1492.

97. B. Bonsch, V. Belt, C. Bartel, N. Duensing, M. Koziol, C. M. Lazarus, T. J. Simpson and R. J. Cox; **2016,** 52, 6777.

98. R. J. Cox, F. Glod, D. Hurley, C. M. Lazarus, T. P. Nicholson, B. A. M. Rudd, T. J. Simpson, B. Wilkinson, Y. Zhanga, *Chemical communications*, **2004**, 2260.

99. D. Roberts, Ph.D. Thesis, University of Bristol, Investigating the Programming of Type I Highly Reducing Iterative Polyketide Synthases, **2014**, pp. 1-220.

100. D. Ivison, Ph.D. Thesis, University of Bristol, Investigating the Programming of Type I Iterative Polyketide Synthase Enzymes, **2014**, pp. 1-210.

101. J. M. Thorn, J. D. Barton, N. E. Dixon, D. L. Ollis, K. J. Edwards, *Journal of Molecular Biology*, **1995**, *249*, 785.

102. B. Persson, J.S. Zigler, H. Jörnvall, *Eur. J. Biochem.* **1994**, *226*, 15.

103. D. H. Kwan, Y. Sun, F. Schulz, H. Hong, B. Popovic, J. C. Sim-Stark, S. F. Haydock, P. F. Leadlay, *Chem. Biol.* **2008**, *15*, 1231-1240.

104. D. A. Rozwarski, C. Vilcheze, M. Sugantino, R. Bittman, J. C. Sacchettini, *J. Biol. Chem.*, **1999**, *274*, 15582.

105. J. Cortes, K. E. Wiesmann, G. A. Roberts, M. J. Brown, J. Staunton, Leadlay, P. F. *Science*, **1995**, *268*, 1487.

106. L. Kellenberger, I. S. Galloway, G. Sauter, G. Böhm, U. Hanefeld, J. Cortés, J. Staunton, P. F. Leadlay, *ChemBioChem*, **2008**, *9*, 2740.

107. D.H. Kwan, P.F. Leadlay, *ACS Chem. Biol.* **2010**, *5*, 829-838.

108. D. H. Kwan, F. Schulz, *molecules* **2011**, 16, 6092.

109. R. G. Rosenthal, B. V. O. Geli, N. Quade, G. Capitani, P. Kiefer, J. A. Vorholt, M.-O. Ebert, T. J. Erb, *Nat Chem Biol* **2014**, *11*, 398-400.

110. H. Bergler, P. Wallner, A. Ebeling, B. Leitinger, S.Fuchsbichler, H. Aschauer, G. Kollenz, G. Hogenauer, F. Turnowsky, *Journal of Biological Chemistry* **1994**, *269*, 5493.

111. J. Crosby, K. J. Byrom, T. S. Hitchman, R. J.Cox, M. P. Crump, I. Findlow, M. J. Bibb, T. J. Simpson, *FEBS letters*, **1998**, *433*, 132.

112. T. S. Hitchman, J. Crosby, K. J. Byrom, R. J.Cox, T. J. Simpson, *Chemistry & Biology*, **1998**, *5*, 35.

113. M. Kapoor, M. J. Dar, A, Surolia, N. Surolia, *Biochemical and Biophysical Research*, **2001**, *289*, 832.
114. R. Linstead, J. Thomas, W. Mann, *Journal of Chemical Society*, **1930**, 2064.
115. S. Zhang, W. Hu, *Synthetic Communications*, **2010**, *40*, 3093.
116. S. Yadav, R. Nageshwar Rao,B. Prem Kumar,R. Somaiah, K. Ravindar,B. V. Subba Reddy, A. Al Khazim Al Ghamdib, *Synthesis*, **2011**, *19*, 3168.
117. L. Raffier, O. Piva, *J Org Chem.*, **2011**, *7*, 151.
118. K. Motoshima, M. Ishikawa, Y. Hashimoto, K. Sugita *Bioorganic and Medicinal Chemistry*, **2011**, *19*, 3156.
119. H. Akao, H. Kiyota, T. Nakajima, T. Kitahara, *Tetrahedron* **1999**, *55*, 7757.
120. T. Nawrath, K. Gerth, R. Müller, S. Schulz, *ChemBioChem*, **2010**, 1914.
121. A. R. Bressette, L. C. Glover, *Synlett*, **2004**, *4*, 738.
122. M. Morr, V. Wray, J. Fortkamp, R. D. Schmid, *Liebig Ann. Chem.*, **1992**, 433.
123. J. D. White, A. T. Johnson, *Journal of Organic Chemistry*, **1994**, *59*, 12, 3347.
124. A. Kongtso, Masterthesis, Leibniz Universität Hannover, Synthesis and Assay of Pantetheine Substrates of the Squalestatin Acyltransferase Enzymes, **2015**.
125. B. J. Carroll, S. J. Moss, L. Bai, Y. Kato, S. Toelzer, T.-W. Yu, H. G. Floss, *J. Am. Chem. Soc.*, **2002**, *124*, 4176.
126. V. E. Anderson and G. G. Hammes, *Biochemistry,* **1984**, *23*, 2088.
127. C. Fross, W. Boland, *J. Chem. Soc., Chem. Commun.*, **1991**, 1731.
128. B. Sedgwick, C. Morris, *J. Chem. Soc., Chem. Commun.*, **1980**, 96.
129. D. M. Roberts, C. Bartel, A. Scott, D. Ivison, T. J. Simpson, R J. Cox, *Chem. Sci.*, **2016**, 8, 1116.
130. R. Fulwood and D. Parker, *J. Chem. Soc., Perkin Trans. 2*, **1994**, 57.
131. L. Tallorin, K. Finzel, Q. G. Nguyen, J. Beld, J. J. La Clair, M. D. Burkart, *J. Am. Chem. Soc*, **2016**, *138*, 3962.
132. J. S. Yadav, T. S. Rao, N. N. Yadav, Rao, V. R. Kovvuru, B. V. S. Reddy, A. Al Khazim Al Ghamdi, *Synthesis*, **2012** , *44*, 788.
133. K. Tsuji, Y. Terao, K. Achiwa, *Tetrahedron Lett.* **1989**, *30*, 6189.
134. G. Lin, W. Xu, *Tetrahedron*, **1996**, *52*, 5907.
135. J. C. Anderson, S. V. Ley, S. P. Marsden, *Tetrahedron Lett.*, **1994**, 35, 2087.
136. K. Fujita, K. Mori, *Eur. J. Org. Chem.*, **2001**, 493.
137. G. D. McAllister, R. J. K. Taylor, *Tetrahedron Lett.*, **2004**, *45*, 2551.
138. K. Hiyoshizo, K. Isao, O. Masamitsu, *J. Org. Chem.*, **1990**, *55*, 4417.
139. A. K. Ghosh, G. Bilcer, G. Schiltz, *Synthesis*, **2001**, 2203.
140. B. List, C. Castello, *Synlett*, **2001**, 1687.
141. T. Katsuki, K. B. Sharpless, *J. Am. Chem. Soc.*, **1980**, *102*, 5974.
142. K. C. Nicolaou, E. W. Yue, S. la Greca, A. Nadin, Z. Yang, J. E. Leresche, T. Tsuri, Y. Naniwa, F. de Riccardis, *Chem. Eur. J.*, **1995**, 7, 467.
143. A. J. Clark, J. M. Ellard, *Tetrahedron Letters*, **1998**, *39,* 6033.
144. M. G. Organ, Y. V. Bilokin, S. Bratovanov, *J. Org. Chem.*, **2002**, *67*, 5176.
145. Y. Li, G. J. Dodge, W. D. Friers, R. A. Fecik, J. L. Smith, C. C. Aldrich, *J. Chem. Soc.*, **2015**, *137*, 7003.
146. E. Liddle, A. Scott, L. Han, D. Ivison, T. J. Simpson, C. L. Willis, R. J. Cox, *Chem. Commun.*, **2017**, *53*, 1727.
147. G. Frater, U. Muller and W. Gunther, *Tetrahedron*, **1984**, *40*, 1269.
148. G. Fráter, U.Müller, *Tetrahedron*, **1984**, 40, 1269.
149. D. Seebach, D. Wasmuth, *Helvetica Chimica Acta*, **1980**, *1*, 197.
150. S. Johannsen, Bachelor Thesis, Leibniz Universität Hannover, Synthesis of substrates for the SQTKS Dehydratase, **2015**.
151. R. C. Valenzano, Y. You, A. Garg, A. Keatinge-Clay, C. Khosla, D. E. Cane, *J. Am. Chem. Soc.*, **2010**, *132*, 14697.
152. A. Brown , V. Affleck , J. Kroon , A. Slabas *FEBS Lett.*, **2009**, *583*, 363
153. B. Kitir, M. Baldry, H. Ingmer, C. A. Olsen, *Tetrahedron*, **2014**, *70*, 7721.
154. C. Palazzi, L. Colombo, C. Gennari, *Tetrahedron Letters*, **1986**, *27*, 1735.

155. C. Gennari, A. Bernardi, C. Scolastico, D. Potenza, *Tetrahedron Letters*, **1985**, *26*, 4129

156. J. D. Pedelacq, H. B. Nguuyen, S. Cabantous, B. L. Mark, P. Listwan, C. Bell, N. Friedland, M. Lockard, A. Faille, L. Mourey, T. C. Terwilliger, G. S. Waldo*, Nucleic Acids Res*.**, 2011***, 39*, 125.

157. X. Zhou, R. Manjunatha Kini, J. Sivaraman, *Nature Protocols*, **2011**, *6*, 158.

158. X. Guo, *J. Biophotonics.*, **2012**, *7*, 483-501.

159. M. Piliarik, H. Vaisocherová, J. Homola, *Methods Mol. Biol.*, **2009**, 503, 65.

160. S. G. Nelson, K. S. Johnston, S. S. Yee, *Sensors and Actuators*, **1996**, *35*, 187.

161. Gerald Steiner, *Anal. Bioanal. Chem*., **2004**, *379*, 328.

162. T. M. Davis, W. D. Wilson, *Analytical Biochemistry*, **2000**, *284*, 348.

163. J. H. Grassi, R. M. Georgiadis, *Anal. Chem.*, **1999**, *71*, 4392.

164. N. Kanoh, M. Kyo, K. Inamori, A. Ando, A. Asami, A. Nakao, H. Osada, *Analytical Biochemistry*, **2006**, *78*, 2226.

165. B. Johnsson, S. Löfås, G. Lindquist, *Anal. Chem.*, **1991**, *198*, 268.

166. A. Gopalsamy, M. Shi, *Organic Letter*, **2003**, *5*, 3907.

167. Y. Oikawa, O. Sugano, K. Yonemitsu, *Journal of Organic Chemistry*, **1987**, *26*, 2087.

168. P. Lopez-Alvarado, C. Avendaño, J. C. Menéndez, *Synthesis* **1998**, 186.

169. S. Löfås, B. Johnsson, *J. Chem. Soc., Chem. Commun.*, **1990**, 1526.

170. M. Siderius, A. Shanmugham, P. England, T. van der Meer, J. P. Bebelman, A. R. Blaazer, I. J. P. de Esch, R. Leurs, *Analytical Biochemistry*, **2016**, *503*, 41.

171. J. M. Brockman , A. G. Frutos , R. M. Corn, *J. Am. Chem. Soc.*, 1999, *121*, 8044.

172. J. S. Mitchell, Y. Wu, C. J. Cook, L. Main, *Analytical Biochemistry*, **2005**, *343*, 125.

173. D.Nedelkov, R. W. Nelson, *Trends in Biotechnology*, **2003**, *21*, 201.

174. N. J. de Mol, M. J. E. Fischer, *Methods in Molecular Biology*, 2010.

175. C. P. Sönksen, E. Nordhoff , O. Jansson , M. Malmqvist , P. Roepstorff, *Anal Chem.*, **1998**, 70, 2731.

176. C. P. Sönksen, *Eur. J. Mass Spectrom*., **2001**, 7, 385.

177. C. Nguyen, R. W. Haushalter, D. J. Lee, P. R. L. Markwick, J. Bruegger, G. Caldara-Festin, K. Finzel, D. R. Jackson, F. Ishikawa, B. O'Dowd, J. A. McCammon, S. J. Opella, S. C. Tsai, M. D. Burkart, *Nature*, **2014**, *505*, 427.

178. K. J. Weissman, P. F. Leadlay, *Nat. Rev. Microbiol.* **2005**, *3*, 925.

179. P. R. August, L. Tang, Y. J. Yoon, *Chem. Biol.*, 1998, *5*, 69.

180. T. Schupp, C. Toupet, N. Engel, S. Goff, *Amycolatopsis mediterranei. FEMS Microbiol Lett*, **1998**, *159*, 201.

181. T.-W. Yu, Y. Shen, Y. Doi-Katayama, L. Tang, C. Park, B. S. Moore, R. C. Hutchinson, H. G. Floss, *Proc. Natl. Acad. Sci. USA*, **1999**, *96*, 9051.

182. S. J. Admiraal, C. T. Walsh, C. Khosla, *Biochemistry*, **2001**, *40*, 6116.

183. J. Xu, E. Wan, C.-J. Kim, H. G. Floss, T. Mahmud, *Microbiology*, **2005**, *151*, 2515.

184. J. Xu, T. Mahmud, H. G. Floss, *Arch. Biochem. Biophys.*, **2003**, *411*, 277.

185. U. Rix, C. Fischer, L. L. Remsing, J. Rohr, *Nat. Prod. Rep*., **2002**, *19*, 542.

186. X. Xie, K. Watanabe, W. A. Wojcicki, C. C. C. Wang, Y. Tang; *Chemistry & biology*, **2006**, *13*, 1161.

187. W. Xu, K. Qiao, Y. Tang; *Biochem Mol Biol.*, **2013**, *48*, 1161.

188. G. S. Garvey, S. P. McCormick, I. Rayment; *Journal of Biological Chemistry*, **2008**, *283*, 1660.

189. H. E. Gottlieb, V. Kotlyar, A. Nudelman, *J. Org. Chem*., **1997**, *62*, 7513.

190. M. Jenner, S. Frank, A. Kampa, C. Kohlhaas, P. Poeplau, G. Briggs, J. Piel, *Angew. Chem. Int. Ed.*, **2013**, *52*, 1143.

191. A. J. Hughes, A. Keatinge-Clay, *Chem. Biol.*, **2011**, *18*, 165.

192. J. Cronan, A. Klages, *Proc. Natl. Acad. Sci. USA*, **1981**, *78*, 5440.

193. E. Leete, J. A. Bjorklund, S. H. Kim, *Phytochemistry*, **1988**, 21, 8, 2553.

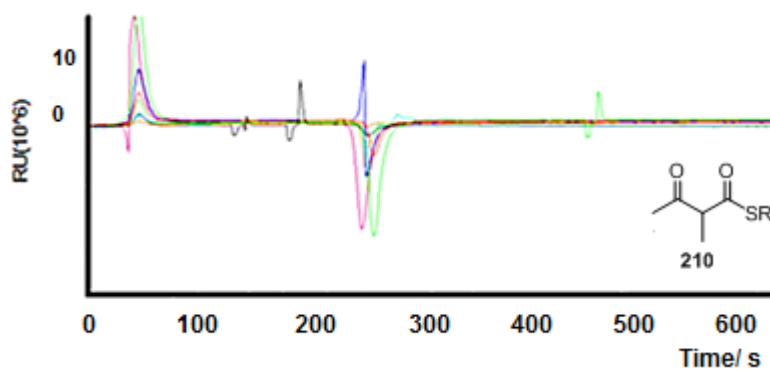194. A. El-Faham, F. Albericio, *Chem. Rev.*, **2011**, *111*, 6557;

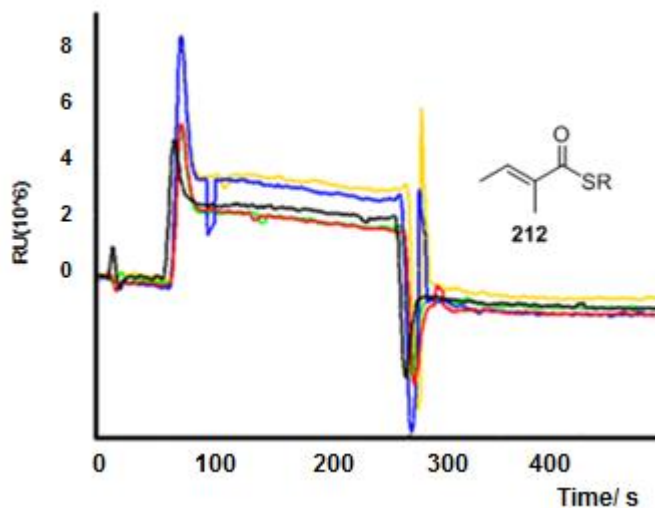## 9.0   Appendix

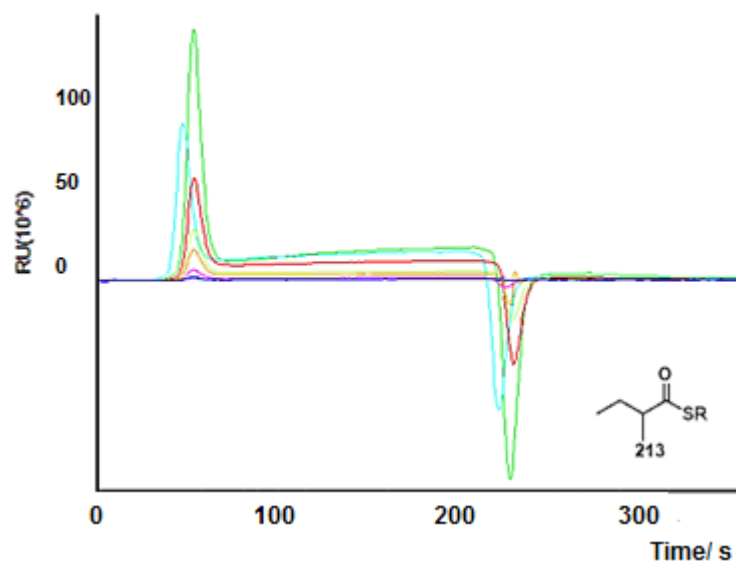## 9.1 DH Domain:

Further SPR results with DH domain
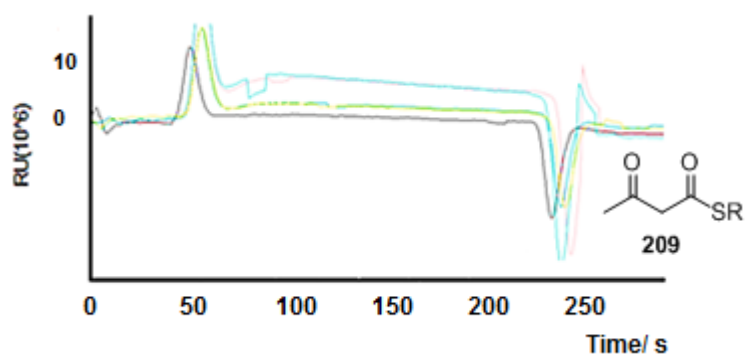
A1: DH overflow of **209**. Protein concentrations are shown by the different colours: 1 mg/ mL, black, 2 mg/ mL, green, 4 mg/ mL, yellow, 6 mg/ mL, purple, 10 mg/ mL, blue.

A2: DH overflow of **210**. Protein concentrations are shown by the different colours: 1 mg/ mL, black, 2 mg/ mL, red, 4 mg/ mL, blue, 6 mg/ mL, purple, 10 mg/ mL, green.
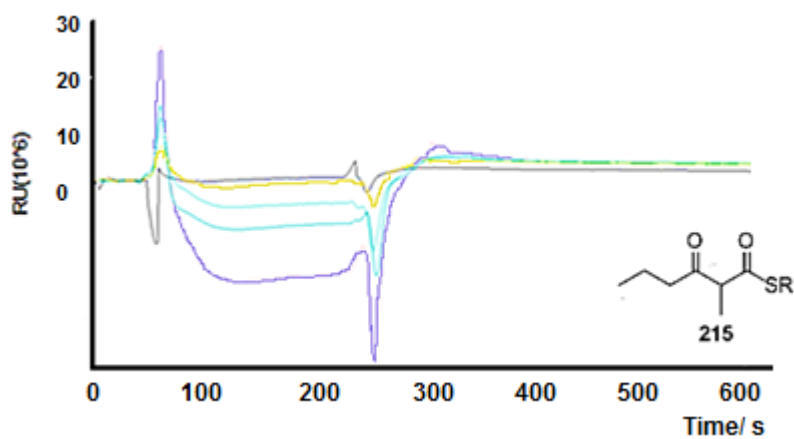

A3: DH overflow of **212**. Protein concentrations are shown by the different colours: 1 mg/ mL, green, 2 mg/ mL, black, 4 mg/ mL, red; 6 mg/ mL, yellow, 10 mg/ mL, blue.
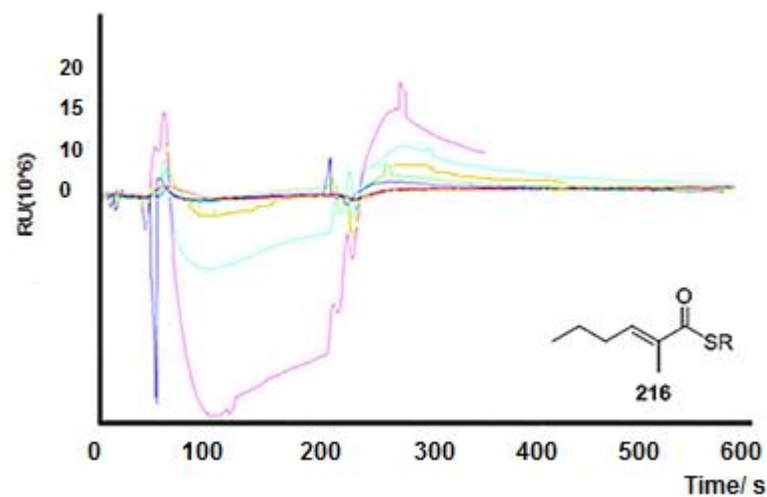
A4: DH overflow of **213**. Protein concentrations are shown by the different colours: 1 mg/ mL, purple, 2 mg/ mL, green, 4 mg/ mL, red; 6 mg/ mL, blue, 10 mg/ mL, green.
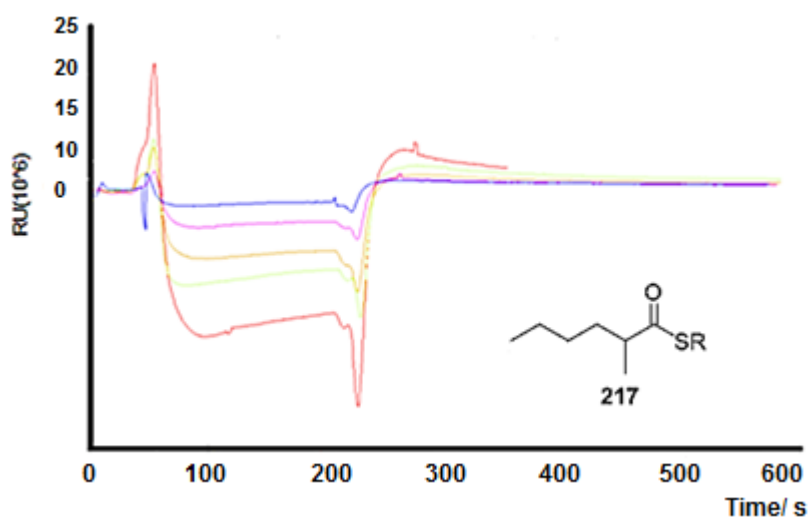
9.2 ER domain:

Further SPR results of ER domain

A5: ER overflow of **215**. Protein concentrations are shown by the different colours: 1 mg/ mL, black, 2 mg/ mL, yellow, 4 mg/ mL, blue; 6 mg/ mL, dark blue, 10 mg/ mL, purple.
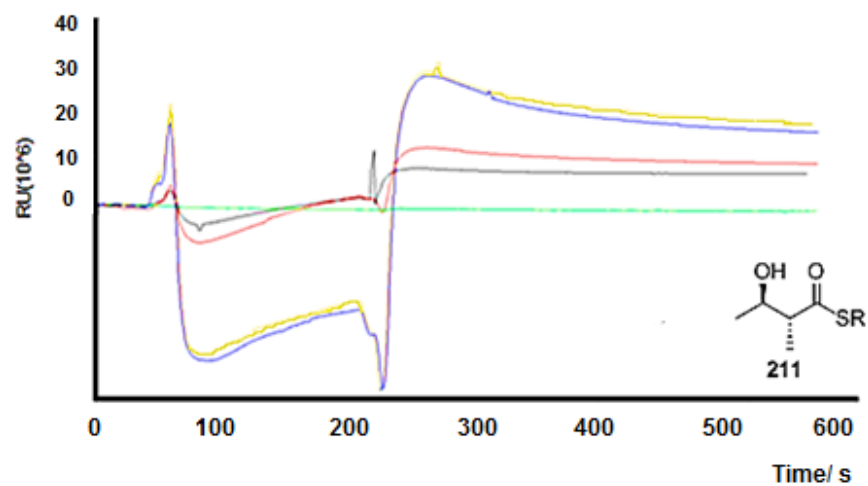
A6: ER overflow of **216**. Protein concentrations are shown by the different colours: 1 mg/ mL, green, 2 mg/ mL, blue, 4 mg/ mL, yellow; 6 mg/ mL, turquoise, 10 mg/ mL, purple.
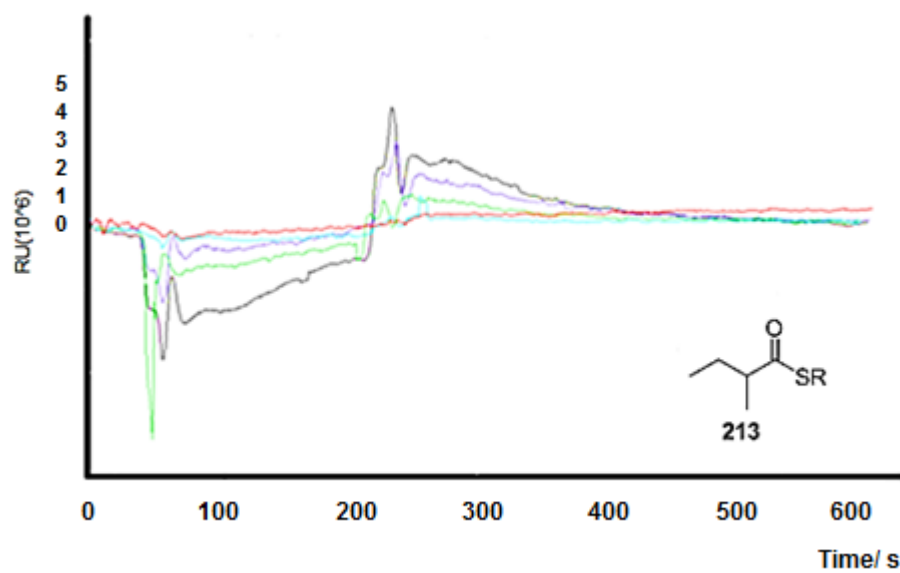

A7: ER overflow of **217**. Protein concentrations are shown by the different colours: 1 mg/ mL, blue, 2 mg/ mL, purple, 4 mg/ mL, brown; 6 mg/ mL, green, 10 mg/ mL, red.
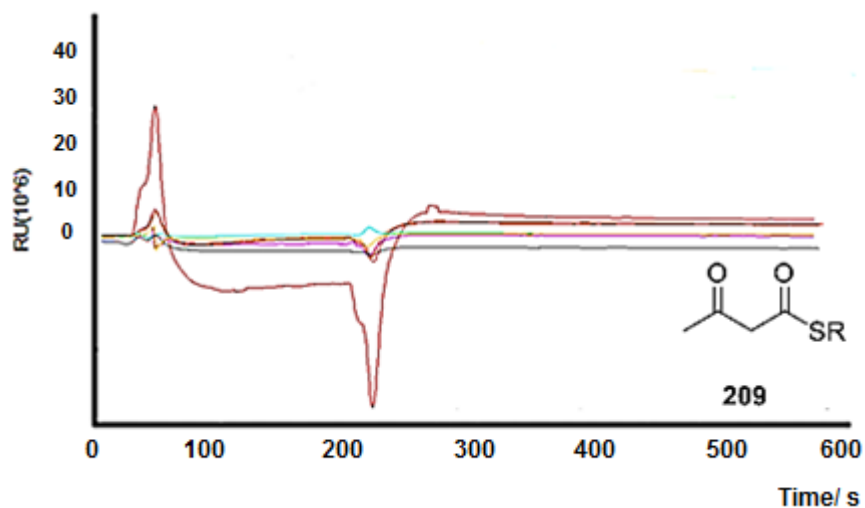
A8: ER overflow of **209**. Protein concentrations are shown by the different colours: 0.5 mg/ mL, green, 1 mg/ mL, yellow, 2 mg/ mL, brown, 4 mg/ mL, purple; 6 mg/ mL, blue, 10 mg/ mL, red.

A9: ER overflow of **211**. Protein concentrations are shown by the different colours: 1 mg/ mL, green, 2 mg/ mL, black, 4 mg/ mL, red; 6 mg/ mL, yellow, 10 mg/ mL, blue.

A10: ER overflow of **213**. Protein concentrations are shown by the different colours: 1 mg/ mL, red, 2 mg/ mL, blue, 4 mg/ mL, purple; 6 mg/ mL, green, 10 mg/ mL, black.

Wissenschaftlicher Werdegang

Christoph Bartel, geboren am 07.04.1986 in Salzgitter-Bad

-Schulbesuch von 1992 bis 2005; Abschluss der allgemeinen Hochschulreife am Gymnasium in Salzgitter Bad im Juni 2005.

-Oktober 2006 bis November 2010; Bachelorstudium der Chemie an der Gottfried Wilhelm Leibniz Universität, Abschlussarbeit im Bereich der Metallorganischen Chemie

-Oktober 2010 bis Dezember 2012; Masterstudium an der Technischen Universität Braunschweig, Vertiefung im Bereich der Biologischen Chemie

-Mai 2013- Februar 2017, Promotionsstudent an der Gottfried Wilhelm Leibniz Universität

Veröffentlichungen, Publikationen

(1) B. Bonsch, V. Belt, C. Bartel, N. Duensing, M. Koziol, C. M. Lazarus, T. J. Simpson and R. J. Cox; *Chem. Commun.*, **2016**, *52*, 6777-6780.

(2) D. M. Roberts, C. Bartel, A. Scott, D. Ivison, T. J. Simpson, R. J. Cox; *Chem. Sci.*, **2017**, *8*, 1116-1126.